

**ENERGY UTILISATION IN
COMMERCIAL BREAD BAKING**

by

JOE BRAMWELL PATON

Submitted in accordance with the requirements for the degree of

Doctor of Philosophy

The University of Leeds

School of Mechanical Engineering

February 2013

Work Formed from Jointly Authored Publications

The candidate confirms that the work submitted is his own, except where work which has formed part of jointly authored publications has been included. The contribution of the candidate and the other authors to this work has been explicitly indicated below. The candidate confirms that appropriate credit has been given within the thesis where reference has been made to the work of others.

Chapter 5 is an extension of a conference paper that was presented at the 2012 EFFoST Annual Meeting (Paton *et al.*, 2012a). The candidate conducted all the experimental and computational analysis of bread provers that is presented in this paper. The work was prepared under the guidance of all co-authors.

Chapter 6 is based on research that formed a journal paper published in Applied Thermal Engineering (Paton *et al.*, 2012b). A similar paper was also presented at the Sustainable Thermal Energy Management International Conference 2011 (Paton *et al.*, 2011). The system-level thermodynamic analysis methodology for a commercial bread baking oven that is described in this paper was designed solely by the candidate. The experiments conducted were also performed solely by the candidate. The computational analysis presented in this paper was conducted by Dr Khatir and forms no part of this thesis. The manuscript was prepared under the guidance of all co-authors.

The oven temperature and velocity profiles presented in Chapter 6 have been published in Applied Energy (Khatir *et al.*, 2012c). This paper was previously presented at the Sustainable Thermal Energy Management Conference 2010 (Khatir *et al.*, 2010). The candidate conducted all the experiments and experimental data processing for this paper. Dr Khatir conducted the computational simulations which are not presented in this thesis. The manuscript was prepared under the guidance of all co-authors.

The experimental work in Chapter 7 has been used in Computational Fluid Dynamics optimisation studies; published in Applied Energy in 2013 (Khatir *et al.*, 2013) and previously presented at the International Conference of Applied Energy 2012 (Khatir *et al.*, 2012b). The candidate conducted all the experimental work contained within these papers, including the graphs showing the optimum heat

transfer coefficient, which is also reproduced in Chapter 7 this thesis. Dr Khatir completed the computational modelling work, none of which forms part of this thesis. Furthermore, these same experimental results have been presented at the 2012 EFFoST Annual Meeting as part of a journal paper discussing oven optimisation (Khatir *et al.*, 2012a). These manuscripts were prepared under the guidance of all co-authors.

This copy has been supplied on the understanding that it is copyright material and that no quotation from the thesis may be published without proper acknowledgement.

© 2013 The University of Leeds and Joe Bramwell Paton

Acknowledgements

Firstly, I would like to acknowledge my academic supervisors, Professor Nik Kapur, Professor Harvey Thompson and Dr Malcolm Lawes. They have been a constant source of encouragement and support and I wish to sincerely thank them for their fantastic supervision and input. Special thanks also go to Dr Zinedine Khatir, for his informal supervision. He has shared his experience and enthusiasm with me throughout this project. I would also like to acknowledge Professor Vassili Toropov for his input over the duration of this project. These colleagues have made this PhD a joy and a privilege to complete.

It would not have been possible to complete this thesis without the help of a great number of supportive industrial partners. From Warburtons: Colin Kelly, Trevor Oakley and Sean Wincote assisted by giving the work a commercial perspective, assisting with experimentation on commercial ovens and supplying historic data. From Spooner Industries: Steve Newell, Dr Andrew Marson and Dan Kirk were able to help me with contributing design details, advice on measurement techniques and generous use of their excellent range of pilot oven facilities. Dr Patrick Horne and Jacque Quinton of SKM Enviros were helpful in extracting and manipulating historic metering data from industrial bakeries.

My parents and family have been a tremendous source of love and support over the years. Their interest in all things bread since I started this project has amused me, as has their commitment to making sure their friends buy Warburtons bread over the past three years. Thank you to each and every one of you.

There are a number of friends, whom I wish to thank for their assistance in preparing this thesis – particularly their thoughts in discussing and proofreading this work, including: Anthony McAndrew, Martin Quinn, Sam O’Sullivan, Richard Mycroft, Gary Beahan and David Dollman.

Finally I would like to thank my partner, Lucy, whose love, patience and motivation has helped me succeed. I especially thank her for putting up with me over the last few years, through the hard times and the good.

Abstract

The aim of this project was to benchmark energy utilisation of bread manufacturing and to provide methodologies and results with the aim of improving efficiency in commercial bakeries. The bread industry is an important provider of staple food products across the world. Owing to the large energy use in bread manufacturing, bakeries have come under increased scrutiny to reduce their environmental impact.

The proving process exposes dough to heat and humidity in order to encourage yeast activation. Provers (responsible for 5 % of carbon emissions in bakeries) are over-engineered to the extent that energy costs impact upon performance. The industry standard practices that use large volumes of airflow to maintain food safety have not been scientifically justified. Experimentally validated Computational Fluid Dynamics (CFD) simulations showed the residence time distribution profiles for different numbers of air changes. The results have indicated that it is possible to reduce airflow by 33 % and electricity demand by over 70 %.

A system-level thermodynamic analysis was developed in order to measure and model heat streams in industrial bread ovens. The model was subjected to a sensitivity analysis to ensure the calculations could be trusted to give suitably accurate results. A number of measurement techniques were employed and the methodology was designed to increase the potential for industry-wide use to assess the efficiency of ovens. The results showed that between 40 and 49 % of heat is wasted in industrial ovens. The model has been successfully distributed to industry.

Experimental measurements of heat transfer for a range of regimes used in baking ovens were undertaken. The results were validated by previous correlations published in literature. Investigation focussed on three particular novel research areas. Firstly, comparisons between nozzle types showed that rows of circular jets could be approximated as slot nozzles for mean heat transfer. Secondly, the ratio of convective to radiative heat transfer was investigated. Thirdly, the prevalence of secondary peaks in local heat flux profiles was compared for two nozzle sets. These unique results can be used to help design baking ovens with energy efficient operating conditions.

Table of Contents

Work Formed from Jointly Authored Publications	2
Acknowledgements.....	ii
Abstract.....	iii
Table of Contents	iv
Figures.....	x
Tables	xvii
Nomenclature.....	xviii
Chapter 1 Introduction.....	1
1.1 The Modern Bread Industry	1
1.2 The Global Energy Setting	3
1.3 Principles of Bread Production.....	5
1.3.1 Formation of Dough	6
1.3.2 Dough Proving.....	7
1.3.3 Bread Baking	8
1.3.4 Cooling	10
1.3.5 Slicing, Packaging and Distribution	11
1.4 Research Aims and Objectives.....	12
1.5 Outline of Thesis.....	13
Chapter 2 Energy Use in the Baking Industry	14
2.1 Previous Studies	14
2.1.1 Bakery Energy Audits.....	15
2.1.2 Life Cycle Assessments	19
2.1.3 Baking Oven Energy Audits.....	21
2.1.4 Other Bakery Equipment	24

Chapter 3	Heat Transfer in the Bread Industry	27
3.1	Heat Transfer Fundamentals	27
3.1.1	Conduction.....	28
3.1.2	Convection.....	29
3.1.3	Thermal Radiation	30
3.2	Jet Impingement Heat Transfer	32
3.2.1	Impingement Nozzles	32
3.2.2	Air Jet Impingement in the Baking Industry	34
3.3	Fluid Flow	37
3.4	Heat Flux Measurement	38
3.4.1	Published Values for Convective Heat Transfer Coefficient	39
3.5	Mass Transfer.....	41
3.5.1	Vaporisation and Evaporation	42
3.6	Thermal Imaging.....	42
Chapter 4	Computational Fluid Dynamics.....	45
4.1	Background.....	46
4.2	CFD in the Food Industry	47
4.2.1	CFD in the Bread Industry.....	48
4.3	CFD Methodology	52
4.4	Discretisation	53
4.4.1	The Finite Element Method	54
4.4.2	The Finite Difference Method	54
4.4.3	The Finite Volume Method	54
4.4.4	Mesh Generation.....	55
4.5	Governing Flow Equations.....	56
4.6	Boundary Conditions	57
4.7	Turbulence Modelling.....	59

4.8	Validation and Verification	61
4.9	Summary	62
Chapter 5 An Experimental and Numerical Investigation of Industrial Bread Proving		
5.1	Industrial Bread Provers	65
5.2	Energy Use of Industrial Provers	67
5.2.1	Gas Consumption Trends	68
5.2.2	Air Handling Unit Electricity Consumption Trends.....	70
5.2.3	Steam Consumption.....	72
5.2.4	Overall Energy Usage.....	73
5.3	Problem Formulation	74
5.4	Computational Fluid Dynamics (CFD) Model Design	75
5.4.1	Geometry	76
5.4.2	Turbulence Model Selection.....	77
5.4.3	Boundary Conditions	77
5.4.4	CFD Solution Process.....	79
5.5	Theory of Residence Time Distribution Analysis	79
5.6	Verification and Validation of Computational Model	82
5.6.1	Verification of Mesh Generation	82
5.6.2	Experimental Validation	83
5.7	Results	84
5.7.1	Plots of Velocity Distribution	84
5.7.2	Numerical Results.....	88
5.8	Residence Time Distribution Curves	89
5.9	Energy Savings	92
5.10	Summary	93

Chapter 6	System-Level Thermodynamic Analysis of Commercial Bread Baking Ovens	95
6.1	Oven Configurations.....	95
6.2	System-Level Energy Modelling	97
6.3	Theory of Energy Audits	98
6.4	System-Level Model of a Commercial Baking Oven	100
6.4.1	Heat in via Gas Burner	102
6.4.2	Heat in via Steam Injection.....	102
6.4.3	Heat Required to Cook the Dough.....	103
6.4.4	Heat Required for Moisture Evaporation	104
6.4.5	Heat Uptake of the Tins and Lids	104
6.4.6	Heat Uptake of the Oven Conveyor.....	105
6.4.7	Heat in the Flue Gas	105
6.4.8	Heat Loss from Oven Walls and Roof.....	106
6.4.9	Total Heat Utilisation	107
6.4.10	System-Level Thermodynamic Analysis Tool	107
6.5	Thermal Imaging.....	109
6.6	Sensitivity Analysis of System-Level Model	111
6.7	Sample Results.....	114
6.8	Opportunities for Energy Savings	115
6.8.1	Oven Insulation.....	116
6.8.2	Conveyors	116
6.8.3	Tins and Lids	116
6.8.4	Heat Recovery	117
6.9	Temperature and Velocity Profiles in a Pilot Oven	118
6.9.1	Temperature Profiles	118
6.9.2	Velocity Profiles	121

6.10 Summary.....	125
Chapter 7 Experimental Measurements of Local and Global Heat Transfer Characteristics	127
7.1 Background.....	127
7.2 Experimental Apparatus	128
7.2.1 The Pilot Oven.....	129
7.2.2 Nozzle Types	131
7.2.3 The Heat Transfer Sensor	133
7.3 Methodology	135
7.4 Validation of Experiments.....	137
7.4.1 Repeatability	137
7.4.2 Heat Flux Symmetry about Nozzle Centre	139
7.4.3 Nusselt Number Correlations Compared with Literature	140
7.5 Mean Heat Transfer Measurements	143
7.5.1 Correlation of Nusselt Number with Reynolds Number	143
7.5.2 Variation of Heat Transfer with Nozzle-to-Surface Distance	144
7.5.3 Mean Proportion of Radiation and Convection	146
7.6 Local Heat Transfer Measurements.....	148
7.6.1 Local Profiles of Nusselt Number with Reynolds Number	148
7.6.2 Local Profiles of Nusselt Number with Dimensionless Nozzle-to-Surface Distance.....	150
7.7 Optimisation of Heat Transfer Coefficient for Energy Savings	152
7.8 Summary.....	154
Chapter 8 Conclusions and Further Work.....	156
8.1 Conclusions and Main Contributions to Scientific Understanding..	156
8.1.1 Computational Fluid Dynamic Analysis of Bread Provers	156
8.1.2 System-Level Modelling of Industrial Bread Baking Ovens	157

8.1.3	Experimental Measurements for Air Jet Impingement Heat Transfer for Regimes Relevant to Bread Baking.....	159
8.2	Future Work.....	160
8.2.1	Prover.....	160
8.2.2	Oven.....	162
8.2.3	Other Bakery Equipment.....	164
8.3	Summary.....	165
	References.....	168

Figures

Figure 1.1 – Bar chart illustrating market segmentation of the worldwide and UK bread industries (Datamonitor, 2011b, Datamonitor, 2011a)	3
Figure 1.2 – Graph of UK GHG emissions by source between 1990 and 2011 (Department of Energy and Climate Change, 2012)	4
Figure 1.3 – Schematic diagram of the bread baking process	6
Figure 1.4 – Photograph of an industrial bread prover located above an industrial oven (Warburtons Limited and Spooner Industries Ltd.)	8
Figure 1.5 – Photographs of an industrial oven: (a) side view along oven length and (b) view showing oven exit (Warburtons Limited and Spooner Industries Ltd.)	9
Figure 1.6 – Photograph of the inside of a spiral bread cooler (Spooner Industries Ltd.)	11
Figure 2.1 – Pie chart showing energy utilisation in a US bakery (Thumann and Mehta, 2008)	18
Figure 2.2 – Graph of heat distribution in commercial ovens from literature (Johnson and Hoover, 1977, Whiteside, 1982)	22
Figure 3.1 – Graph of the thermal conductivity of bread as a function of temperature (Monteau, 2008, Unklesbay et al., 1981, Wong et al., 2007)	29
Figure 3.2 – Diagram of the flow field of an impingement jet	33
Figure 3.3 – Diagram of air impingement nozzles in a baking oven	35
Figure 3.4 – Dimensions of an ASME standard nozzle	37
Figure 4.1 – Diagram of two-dimensional meshes: (a) structured and (b) unstructured	55
Figure 4.2 – Three-dimensional elements commonly used for mesh generation: (a) hexahedra, (b) tetrahedra, (c) extruded triangles and (d) pyramids	56

Figure 5.1 – Diagram showing the shape and dimensions of an L-type prover	66
Figure 5.2 – Screenshot of online energy metering system for an industrial bakery	67
Figure 5.3 – Hourly gas use of a prover over the period of one week with mean hourly gas use (4.1 m ³) shown by red dashed line and the range of values within 1 standard deviation shown by blue dashed line	68
Figure 5.4 – Weekly gas use of an industrial prover over a period of one calendar year with mean weekly gas use (633.4 m ³) shown by red dashed line and the range of values within 1 standard deviation shown by blue dashed line.....	69
Figure 5.5 – Hourly electricity use of a prover AHU over the period of one week with mean hourly electricity use (23.4 kWh) shown by red dashed line and the range of values within 1 standard deviation shown by blue dashed line.....	71
Figure 5.6 – Weekly electricity use of a prover AHU over a period of one calendar year with mean weekly electricity use (3,747 kWh) shown by red dashed line and the range of values within 1 standard deviation shown by blue dashed line.....	71
Figure 5.7 – Energy utilisation profile of an industrial bread prover	73
Figure 5.8 – CO ₂ emissions profile of an industrial bread prover	74
Figure 5.9 – Geometry for prover CFD model generated with assistance from Spooner Industries Ltd. (Kirk, 2011).....	76
Figure 5.10 – Cross section diagram of prover showing the air ducting arrangement, location of straps of tins and blue arrows illustrating the path of airflow.....	77
Figure 5.11 – Partial view of prover CFD solution domain showing boundary conditions and symmetry plane	78
Figure 5.12 – Diagram of a mixing tank showing the concentration of the particles injected at the inlet (A) at the outlet (B) with respect to time	80

Figure 5.13 – C-diagrams as described by Danckwerts (1953) for: (a) piston flow (b) piston flow with longitudinal mixing (c) complete mixing and (d) dead water.	81
Figure 5.14 – Velocity profile across a single prover vent, the second closest to the loading/ unloading end, for five different mesh sizes/ numbers of elements	82
Figure 5.15 – Pearson’s r correlation showing correlation with the finest mesh case (1.39 million cells) for velocity profile across a single prover vent	83
Figure 5.16 – Validation of velocity profile along prover length with error bars representing the experimental error relating to the apparatus used	84
Figure 5.17 – Isometric view contour plot of air velocity illustrating air distribution throughout the prover volume	85
Figure 5.18 – Angled top view contour plot of air velocity showing air distribution down the prover length	86
Figure 5.19 – Velocity vector plot of air velocity showing flow paths of air through a prover vent and around the product for the 13 th plane parallel to a vent from the loading end.....	87
Figure 5.20 – End-on view contour plot of air velocity showing airflow distribution around the tins for (a) the plane closest to the loading end, and (b) the 13 th plane from the loading end.....	88
Figure 5.21 – Prover section view from perpendicular to the xy-plane with red line passing through the centre of the air vents offset in the z-direction by 5 mm.....	89
Figure 5.22 – CFD predictions showing the air velocity profile along the prover length for the red line shown in Figure 5.21.....	89
Figure 5.23 – Residence time distribution for 2,469 particles.....	90
Figure 5.24 – Mean particle residence time as a function of the number of air changes for both analytical and computational solutions	91
Figure 5.25 – Percentage of particles not escaped the prover cavity after 360 s residence time for each case	92

Figure 6.1 – Schematics of two different oven designs: (a) direct-fired forced convection and (b) indirect-fired radiant	96
Figure 6.2 – Diagram showing heat and mass flows within an industrial bread oven, as detailed in Table 6.1	101
Figure 6.3 – Input screenshot of oven thermodynamic energy analysis tool	108
Figure 6.4 – Results screenshot of oven thermodynamic energy analysis tool.....	108
Figure 6.5 – Thermal images of the roofs of two industrial bread baking ovens showing the maximum (white text) and mean (green text) temperatures (°C) for two ovens: (a) oven A and (b) oven B.....	110
Figure 6.6 – Thermal images of the outer walls of two industrial ovens: (a) oven A and (b) oven B	111
Figure 6.7 – Sensitivity analysis showing the effect on outputs based on a 10 % change of each input variable	112
Figure 6.8 – Compound sensitivity analysis based on changing each input variable by the expected precision of the measurement and the instrument accuracy supplied by the manufacturer	113
Figure 6.9 – Sample results of heat distributions obtained by system-level model for two commercial baking ovens.....	115
Figure 6.10 – Location of thermocouples across the oven width for a strap of five tins.....	119
Figure 6.11 – Graph of temperature profile through a pilot oven for different distances underneath the top nozzles: 20, 40, 60, 80 and 100 mm compared with burner set point temperature (solid red line).....	120
Figure 6.12 – Time averaged velocity profile of the top nozzles for three positions: A – closest to the burner and C – furthest from the burner	122
Figure 6.13 – Time averaged velocity profile of the bottom nozzles for three positions: D – closest to the burner and F – furthest from the burner	123

Figure 6.14 – Three-dimensional profile of velocity through a pilot oven for top nozzles: A – closest to the burner and C – furthest from the burner	124
Figure 6.15 – Three-dimensional profile of velocity through a pilot oven for bottom nozzles: D – closest to the burner and F – furthest from the burner.....	124
Figure 7.1 – Partially labelled photograph of the pilot oven used for heat transfer experiments.....	129
Figure 7.2 – Schematic of the pilot oven used for heat transfer experiments	130
Figure 7.3 – ASN arrangement for heat transfer experiments.....	132
Figure 7.4 – ARN arrangement for heat transfer experiments	132
Figure 7.5 – Photograph of Hukseflux RC01 heat flux sensor (Hukseflux Thermal Sensors, c. 2010).....	133
Figure 7.6 – Diagram of heat flux sensor (Hukseflux Thermal Sensors, c. 2010)	134
Figure 7.7 – Diagram showing minimum traverse range (P) of heat flux sensor..	137
Figure 7.8 – Heat transfer graph indicating the degree of repeatability of the heat flux profile measurements	138
Figure 7.9 – Dimensionless heat transfer coefficient of three nozzle profiles overlaid on each other showing the degree of repeatability of the heat flux sensor	139
Figure 7.10 – Graph showing the degree of symmetry of heat flux measurements about the nozzle centre	140
Figure 7.11 – Graph of Reynolds number against mean Nusselt number for ASN experimental results and correlations reported in literature.....	141
Figure 7.12 – Graph of Reynolds number against mean Nusselt number for ARN experimental results and correlations reported in literature.....	142
Figure 7.13 – Graph showing Nusselt number correlations for ASN and ARN ...	143

Figure 7.14 – Regression plot to measure R^2 value of data sets compared with correlation	144
Figure 7.15 – Martin (1977) correlations for dimensionless nozzle-to-surface distance (H/d) against Nusselt number for ASN and ARN	145
Figure 7.16 – Comparison of experimental mean Nusselt number results for ARN at varying H/d ratio with Martin (1977) ASN correlations	146
Figure 7.17 – Graph of Reynolds number against mean percentage of heat transfer due to radiation for ASN.....	147
Figure 7.18 – Graph of Reynolds number against mean percentage of heat transfer due to radiation for ARN	148
Figure 7.19 – Graph of local Nusselt number against dimensionless distance from the centre of the nozzle jet (x/d) for ASN for five different Reynolds numbers between 3,221 and 10,902	149
Figure 7.20 – Graph of local Nusselt number against dimensionless distance from the centre of the nozzle jet (x/d) for ARN for five different Reynolds numbers between 3,771 and 11,801	150
Figure 7.21 – Graph of local Nusselt number against dimensionless distance from the centre of the nozzle jet (x/d) for two different nozzle types and H/d values...	151
Figure 7.22 – Graph of local Nusselt number against dimensionless distance from the centre of the nozzle jet (x/d) for different values of H/d for ARN	151
Figure 7.23 – Predicted specific oven gas and electricity use as a function of heat transfer coefficient	153
Figure 7.24 – Predicted bread baking carbon emissions equivalent per kg as a function of heat transfer coefficient.....	154
Figure 8.1 – Example of a Pareto front showing competing objectives: the objective function, minimising cost (blue) and a critical quality objective (red).....	161

Figure 8.2 – Surface response of CFD optimisation study for optimising airflow in and industrial bread oven (Khatir et al., 2013, Khatir et al., 2012d) 162

Tables

Table 3.1 – Emissivity values for materials relevant to bread manufacturing equipment	31
Table 3.2 – Emissivity values reported for bread from literature over a range of temperatures (* temperature not given).....	31
Table 5.1 – Equivalent carbon impact conversion factors for electricity and natural gas (Carbon Trust, 2009)	73
Table 5.2 – Inlet boundary conditions for prover CFD model	78
Table 6.1 – List and explanation of energy flow streams for a typical commercial baking oven (see Figure 6.2)	101
Table 6.2 – Data statistics showing the variation of temperature in comparison with burner set points for each oven zone	121
Table 7.1 – Description of features of pilot oven	131
Table 7.2 – Dimensions and specifications for the nozzle configurations investigated.....	133
Table 7.3 – Range of conditions for correlations between Reynolds number and Nusselt number	140
Table 7.4 – Changes to dimensions for correlating the asymmetric ARN as an ASN	142

Nomenclature

Abbreviations

AFR	Air-fuel ratio
AHU	Air handling unit
ARN	Array of round nozzles
ASN	Array of slot nozzles
BC	Boundary condition
CAD	Computer-aided design
CBP	Chorleywood Bread Process
CFD	Computational Fluid Dynamics
CIP	Clean-in-place
EPSRC	Engineering and Physical Sciences Research Council
FDM	Finite Difference Method
FEM	Finite Element Method
FVM	Finite Volume Method
GHG	Greenhouse gases
LCA	Life Cycle Assessment
OEM	Original equipment manufacturer
PID	Proportional-integral-derivative
RANS	Reynolds-Averaged Navier-Stokes
RCUK	Research Councils UK
RHM	Rank Hovis McDougall
RKE	Realisable $k-\epsilon$
RNG	Re-normalisation group
SRN	Single round nozzle
SSN	Single slot nozzle
SST	Shear-stress transport
TSB	Technology Strategy Board
VSD	Variable-speed drive

Symbols

A	Area	m^2
c	Concentration	mol/m^3
c_p	Specific heat capacity	$J/(kg \cdot K)$
C	Concentration of injected particles at outlet	-
CV	Calorific value	J/m^3
C_μ	Variable used in the realisable k - ε turbulence model	-
d	Nozzle diameter (holes), nozzle width (slot)	m
D	Diffusion coefficient	m^2/s
E	Energy	J
\dot{E}	Power	W
E_a	Activation energy	J/kg
E_{sen}	Calibration factor of sensor	$V \cdot m^2/W$
$E(t)$	Exit age residence time function	/s
f	Relative nozzle area	-
f_0	Variable used in jet impingement correlations	-
F	Fraction of the fluid flow that is mixed at outlet	-
g	Acceleration due to gravity	m/s^2
h	Heat transfer coefficient	$W/(m^2 \cdot K)$
h	Height	m
H	Nozzle-to-surface distance	m
\dot{H}	Heat flow	W
H_y	Prover thickness in the y -direction	m
J	Diffusion flux	$mol/(m^2 \cdot s)$
k	Turbulence kinetic energy	m^2/s^2
K_0	Pre-exponential factor	/s
K_r	Reaction rate	-
L	Length	m
L_e	Latent heat of evaporation	J/kg
\dot{m}	Mass flow rate	kg/s

N	Number of air changes per hour	/hr
P	Pitch between two sets of nozzles in the x -direction	m
P	Pressure	Pa
q	Heat flux	W/m ²
r	Pearson Product-Moment Correlation	-
R	Universal gas constant	J/(kg·K)
RH	Relative humidity	-
S	Spacing between two round nozzles in the z -direction	m
S	Source term in the Navier-Stokes equations	-
t	Time	s
\bar{t}	Mean residence time	s
T	Temperature	K
\mathbf{u}	Velocity vector	m/s
u, v, w	Velocity in the x, y and z -directions respectively	m/s
V	Volume	m ³
\dot{V}	Volumetric flow rate	m ³ /s
V_{sen}	Voltage signal at sensor	V
W	Width	m
x	Distance from nozzle centre	m

Greek symbols

α	Degree of starch gelatinisation	-
α_k	Thermal diffusivity as a function of temperature	m ² /s
β	Volumetric thermal expansion coefficient	/K
σ	Stefan-Boltzmann constant	W/(m ² ·K ⁴)
σ	Uniformity	-
ε	Rate of dissipation of turbulence kinetic energy	m ² /s ³
ε_A	Emissivity	-
μ	Dynamic viscosity	W/(m ² ·K ⁴)
ω	Turbulence frequency	-

λ	Thermal conductivity	W/(m·K)
ρ	Density	kg/m ³
ν	Kinematic viscosity	m ² /s
ϕ	Interchangeable scalar variable for RANS equation	-
Γ_M	Fluid viscosity	Pa·s
Γ_T	Thermal conductivity in Navier-Stokes equation	W/(m·K)

Subscripts

<i>air</i>	Air
<i>amb</i>	Ambient
<i>atm</i>	Atmospheric
<i>bread</i>	Bread
<i>c</i>	Characteristic
<i>cen</i>	Centre nozzle
<i>crit</i>	Critical value
<i>D</i>	Dynamic
<i>e</i>	Evaporation
<i>elec</i>	Electricity
<i>gel</i>	Gelatinisation
<i>in</i>	Inlet
<i>l</i>	Lids
<i>M_x, M_y, M_z</i>	Momentum equation in the <i>x</i> , <i>y</i> and <i>z</i> directions
<i>noz</i>	Nozzle
<i>P</i>	Constant pressure
<i>s</i>	Surface of oven walls
<i>sen</i>	Sensor
<i>t</i>	Tins
<i>T</i>	Total
<i>w</i>	Water
<i>wall</i>	Oven wall

x, y, z Position in the x, y and z direction
 $z1, z2, z3$ Oven zones 1, 2 and 3

Dimensionless groups

Grashof number: $Gr = \frac{g\beta(\Delta T)L^3}{\nu^2}$ for flat vertical plates

$Gr = \frac{L^3\rho^2g\beta\Delta T}{\mu^2}$ for horizontal flat plates

Nusselt number: $Nu = \frac{hL}{k}$

Prandtl number: $Pr = \frac{c_p\mu}{k}$

Rayleigh number: $Ra = Gr \cdot Pr$

Reynolds number: $Re = \frac{\rho u L}{\mu}$

Chapter 1

Introduction

Bread is one of the oldest known and most important food products, having been consumed worldwide for many millennia. The origins of bread can be traced back as far as the Palaeolithic Period (c. 30,000 BC), as evidence of processing starch has been found on ancient grindstones; it is thought bread was used as a travelling food for wandering nomads and thus helped to populate the earth (Revedin *et al.*, 2010). It is believed that leavened (expanded dough produced by yeast fermentation) bread was probably not consumed until Neolithic times (the ‘New Stone era’, c. 10,000 BC) when the chemical power of yeast was discovered (Kent, 2012). By around 3,000 BC, bread became part an Ancient Egyptian’s staple diet along with beer (Tannahill, 2002), and latterly became ubiquitous across the world in Roman times. In modern times, it is one of few food products consumed across both the developed and developing world and spans almost every culture.

Perhaps the most comprehensive description of the history of bread is given in the book ‘Six Thousand Years of Bread, Its Holy and Unholy History’ that recalls the social and political importance of bread over the years (Jacob *et al.*, 1944). The impact of bread upon society has been diverse; through religion: “Give us today our daily bread”, politics – not least in early 19th century Britain where the abolition of British corn laws made way for an international trade system (Kadish, 1996) – and in everyday colloquialisms: “The best thing since sliced bread”, “Bread and butter”, “Bread-winner”, “Putting bread on the table”, “Dough”, etc.

1.1 The Modern Bread Industry

Commercial bread production occurs on a number of different scales, from artisan bakeries serving the local community, to the large commercial bakeries serving entire nations, as well as in-store/ supermarket bakeries, small chain outlets and other sized bakeries in between. The focus of this thesis is large commercial

bakeries; i.e. bakeries producing bread at a rate of several tonnes of finished product per hour on a continuous production process. The typical distribution range of a commercial bakery of this magnitude can be up to hundreds of miles.

Although the core ingredients of bread are: flour, water, yeast, fat and salt, bread as a product varies vastly depending on the ratio of these ingredients, additional ingredients and production methods. The variations in taste and texture are particularly noticeable across country borders. For example the British standard loaf is largely unavailable in France, where the baguette is the mainstay product, and in Germany (one of the highest consumers per capita); where darker, denser products are often preferred. Further afield, Mediterranean bread is often influenced by olive flavours, Middle-Eastern and Asian cultures typically consume flat-bread type products whilst Latin-American countries consume more corn/tortilla style baked products.

In 2010, the global bread and rolls industry was worth US \$168.9 billion (£106.8 billion) per year and market value has been growing steadily by 2.2 to 2.4 % per year since 2006. Annually, 93 million tonnes of bread are manufactured across the world, of which 38 % is produced on an industrial scale, 48 % by artisan bakers, 9 % in-store and 5 % tortilla production (Datamonitor, 2011b).

The UK bread and rolls industry was worth US \$4.9 billion (£3.1 billion) per year in 2010 and market value has been growing marginally above average when compared with global trends, at 2.4 to 2.6 % per year. Each year over 2.8 million tonnes of baked goods are produced in the UK. Contrary to the global market segmentation, a much higher proportion is produced in industrial bakeries (78 %), with a smaller section of production in-store (16 %), with artisan production (4 %) and tortilla production (2 %) making up the remainder (Datamonitor, 2011a). In terms of the importance of the bread industry to economic prosperity, a 2010 report stated that over 20,000 people are currently employed in UK bakeries (The

Federation of Bakers, 2010). Figure 1.1 shows graphically the difference between the market segmentation of the UK and worldwide bread industries.

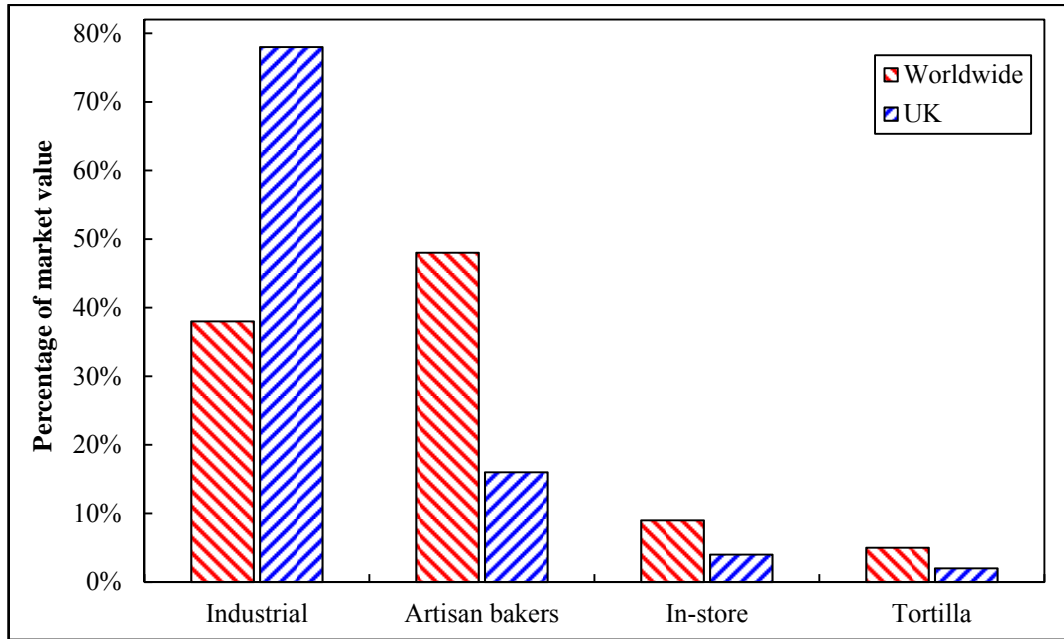


Figure 1.1 – Bar chart illustrating market segmentation of the worldwide and UK bread industries (Datamonitor, 2011b, Datamonitor, 2011a)

The baking industry has historically put little effort into monitoring or reducing energy usage. However, with pressure mounting for industry as a whole to reduce carbon emissions, use of fossil fuels and environmental impact, it is important that commercial bakeries look to improve energy efficiency measures.

1.2 The Global Energy Setting

The global shortage of fossil fuels for energy generation and the harmful effects of greenhouse gas (GHG) emissions on the environment are well documented. This has forced policy-makers worldwide to devise strategies for reducing the environmental impact of the human race. The distribution of GHG emissions across all sectors in the UK is shown by Figure 1.2. Industrial processes have been responsible for between 2.9 and 4.8 % of emissions between 1990 and 2011. In this same period, industry reduced emissions by 47 % from 16.3 to 8.7 MTCO_{2e}, whilst total UK emissions (excluding power generation) have decreased by 19.4 % from 343.5 to 276.7 MTCO_{2e}.

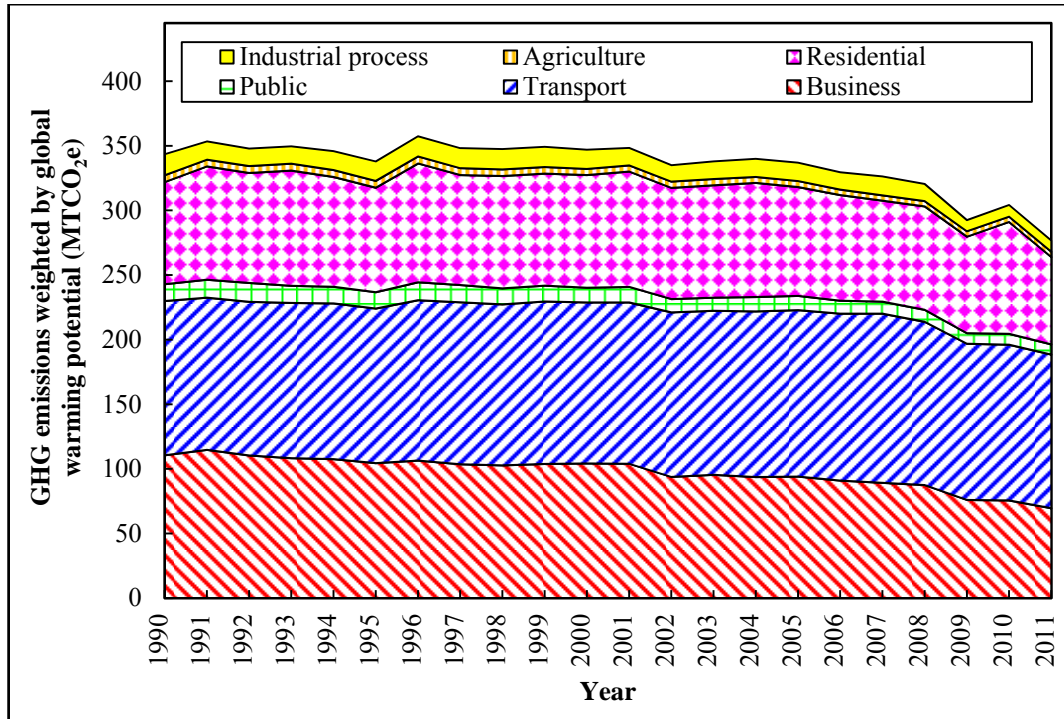


Figure 1.2 – Graph of UK GHG emissions by source between 1990 and 2011 (Department of Energy and Climate Change, 2012)

The member nations of the European Union and a host of other countries worldwide are committed to reducing carbon emissions over the next few decades as part of the Kyoto Protocol. The Kyoto Protocol was agreed in 1997 and is an important addition to the United Nations Framework Convention on Climate Change (UNFCCC) of 1994. As of June 2012, the Kyoto Protocol has been signed and ratified by 191 States worldwide – most notably excluding the United States of America and China. The Kyoto Protocol committed Annex I nations (including the UK) to reduce GHG emissions by 5.2 % before 2012, based on 1990 base levels. Furthermore, the UK Climate Change Act (2008) legally binds the UK government to reduce carbon emissions by 80 % by 2050 based on 1990 base levels. In order for these targets to be met, schemes such as the Climate Change Levy and the EU Emissions Trading Scheme put financial pressure on, or offer incentives to, industrial manufacturing sites to reduce carbon emissions. In addition to legislation, soaring energy prices and diminishing fossil fuel reserves are encouraging industry to reduce the amount of energy they use in order to cut costs and become more environmentally responsible in the medium to long-term future. For these reasons,

bakeries are one area of industry that has recently focussed efforts on energy management.

1.3 Principles of Bread Production

Bread production encompasses a number of fundamental biochemical, chemical and physical processes, such as: evaporation of water, volume expansion, gelatinization of starch, protein denaturation, crust formation, carbon dioxide production, formation of a porous structure and browning reactions (Purlis and Salvadori, 2009a). Bread production on a commercial scale is frequently a continuous manufacturing process, with short shutdown periods occurring on a weekly basis to allow equipment to be cleaned and maintained. Several engineering/ manufacturing issues in a commercial bakery need to be tightly controlled in order for it to be commercially successful. First and foremost, product quality is non-negotiable – this includes food safety, consistency of produce, taste, texture, appearance and shelf-life. Furthermore, other factors such as minimising interruptions to the manufacturing process to avoid wastage and keeping the production time at a minimum are important to keep financial costs low. Energy use is an increasingly important concern for commercial bakeries.

Bread is produced in five key stages:

1. Formation of dough: mixing and binding of raw ingredients and shaping the dough pieces.
2. Proving: supplying the dough with heat and humidity to encourage the yeast to ferment and the dough to rise.
3. Baking: heating the dough at high temperature to evaporate moisture and convert fragile dough to stable bread.
4. Cooling: lowering the temperature of the bread to ambient.
5. Slicing, packaging and distribution: the final preparations are made before the bread is delivered to the customer.

The manufacturing process, which typically takes around 4 hours, is shown diagrammatically by Figure 1.3:

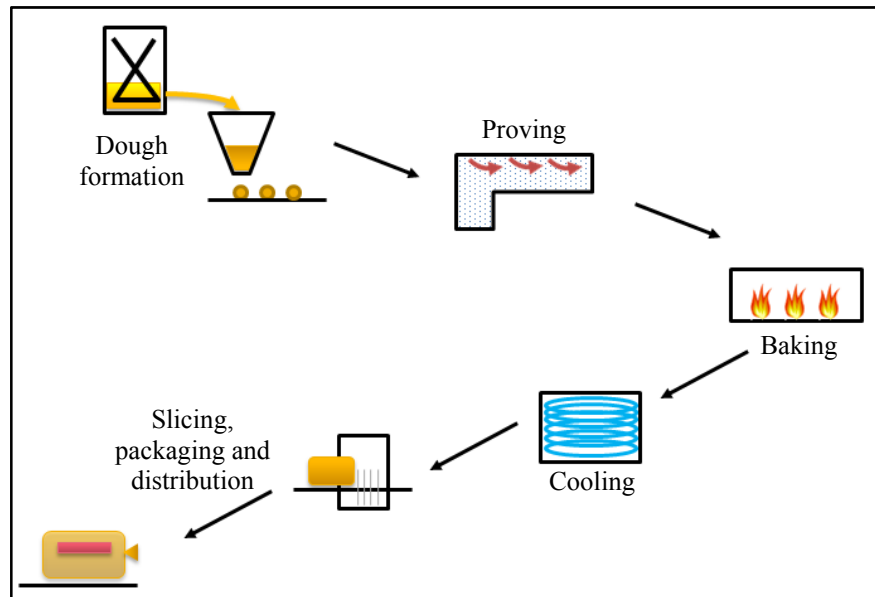


Figure 1.3 – Schematic diagram of the bread baking process

1.3.1 Formation of Dough

A typical bread recipe consists of flour, water, yeast, fat and salt. Mixing forms these raw ingredients together into a dough-piece through the following processes:

- **Moistening**: the surface of the bread is coated in liquid (often brine) to prevent blistering.
- **Solubilisation**: gluten proteins within the bread are dissolved into the dough structure.
- **Swelling**: the starch structure created by the gluten proteins begins to absorb moisture and increase in volume.
- **Gluten formation**: links between the proteins are formed which helps to dictate the crumb structure of the loaf.

At this point the yeast begins to ferment which causes carbon dioxide gas cells to form and creates an aroma (Stear, 1990).

All the major UK bread producers use the Chorleywood Bread Process (CBP) (or the Chorleywood Method), which is a dough preparation technique developed in

1961 by British Baking Industries Research Association (Beech, 1980). The principle of the CBP is to ensure a set amount of mechanical energy is put into each batch of dough in the mixing process at a much higher rate than historically used (Cauvain and Young, 2006); typically this is 44.6 kJ/kg (Stear, 1990). Mechanical energy is forced into the dough using large spiral mixers which allows the chemical binding processes to initiate faster, subsequently causing the dough temperature to increase. This temperature rise is not necessarily desirable in terms of nutrition; therefore some critics favour traditional techniques which allow the dough to develop more naturally with a much reduced energy requirement. Traditional techniques are particularly favourable in terms of reduced salt content (Blanchard, 1965), which has led in part to the recent popularisation of artisan bread-making (Owen, 2012). Two alternatives to the CBP are bulk fermentation and continuous liquid fermentation (Fellows, 2009).

Once mixed, the dough is formed into individual pieces which will eventually form the baked loaf. Depending on the product, the dough is either shaped using '4-piece' or '2-piece' machining which affects product aesthetics, predominantly the position and alignment of the gas cells within the structure and therefore the direction of the crumb pattern – either across the width or height of a slice of bread.

1.3.2 Dough Proving

The proving (occasionally referred to as 'proofing') process prepares the dough for baking by subjecting it to an elevated temperature and a high level of humidity in a controlled environment. This process can take between as little as half an hour and as much as half a day. During proving, yeast in the dough fermentation produces carbon dioxide gas, thus expanding the size of the dough to roughly twice its original size (Stear, 1990). The dough temperature is typically raised from approximately 30 to 40 °C. Enzyme activity within the dough rapidly increases once the temperature reaches 35 °C, therefore it is beneficial to increase the dough temperature relatively rapidly to maximise the initial impact of the proving process.

Industrial provers can be up to 40 m in length. Provers in commercial bakeries are often located in the space above a bread oven in order to use bakery space efficiently and to indirectly recover heat from the oven roof, as indicated by Figure 1.4. Pre-heating technology has been trialled to raise the dough temperature before the bread enters the prover, and thus reduce the energy load of the prover, however the success reported has been limited (Cauvain and Young, 1998).

After proving the dough is in a fragile state as the carbon dioxide gas produced is retained within a skin that forms on the surface of the dough. Until this skin is set to become a crust (in the baking oven), the dough requires careful handling as any disturbance can cause the structure to collapse.



Figure 1.4 – Photograph of an industrial bread prover located above an industrial oven (Warburtons Limited and Spooner Industries Ltd.)

1.3.3 Bread Baking

Baking encompasses a range of complex processes of simultaneous heat, water and water vapour transport within the product as dough is transformed into bread. In addition to dry heat, steam can also be used at the start of the baking process in order to increase glossiness on the bread surface (Altamirano-Fortoul *et al.*, 2012). The main portion of the bake cycle subjects the dough to high temperatures in order to initially deactivate the yeast and form a skin on the product surface. It has been

suggested that the complexity of the process is due to the comparatively high temperature gradient and fast bake time in comparison with other drying processes (Marcotte and Grabowski, 2008). Due to this complexity, there is a careful balance throughout all parts of the manufacturing cycle to ensure that each process occurs in synchronisation in order to produce a consistent and satisfactory loaf of bread.

Commercial bread ovens are typically tunnel-type ovens that can be up to 30 to 40 m long. The oven is often split into three zones so the baker can alter the profile of conditions within the chamber, such as bake time, air velocity, air temperature and steam injection. The baking profiles are dependent on the type of product that the bakery is producing. Anecdotal evidence and experimentation has allowed experienced oven operators to set baking conditions depending on factors such as the ingredients, flavour/ texture required and expected weight loss. Photographs of a commercial oven are shown by Figure 1.5:

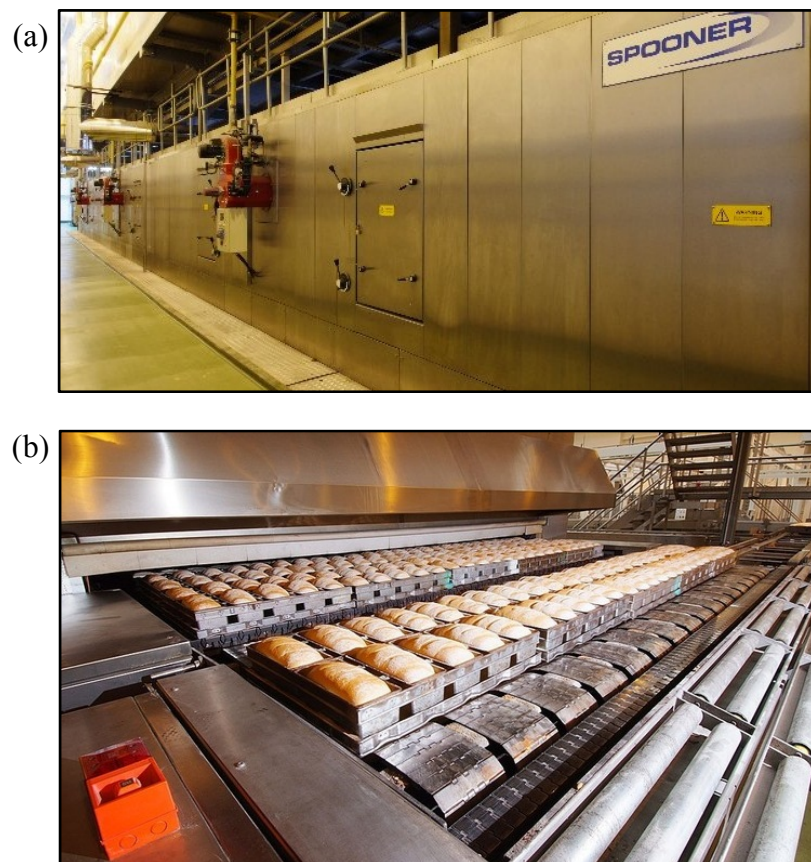


Figure 1.5 – Photographs of an industrial oven: (a) side view along oven length and (b) view showing oven exit (Warburtons Limited and Spooner Industries Ltd.)

The main purpose of baking is to remove moisture from the dough, thus drying the surface and forming a crust, resulting in significant mass transfer in the oven (Klemes *et al.*, 2008). Legislation for weight constraints for bread are tight (typically ± 50 g for an 800 g loaf (Cauvain and Young, 1998)), so control of moisture loss in the oven is critical. Excessive moisture loss from the product is undesirable as this requires an increase in the quantity of raw materials at the start of the manufacturing process and results in a higher energy demand to evaporate the water content in the oven. In addition, decreased moisture loss often results in a softer crumb and increased shelf life – two highly valued product characteristics (Ovadia and Walker, 1998).

Once the dough temperature reaches 74 °C the gluten structure is set, therefore carbon dioxide gas cells are retained in place within the bread, ensuring a porous product (Fellows, 2009). Most academic researchers and industrialists agree that bread is cooked once the core temperature reaches 96 to 98 °C (Ahrne *et al.*, 2007, Price, 2012, Purlis, 2011, Therdthai *et al.*, 2002).

1.3.4 Cooling

The purpose of cooling is to lower the temperature of the bread in preparation for slicing, packaging and distribution. As this is often the most time consuming process in a bakery, coolers require a large quantity of physical space.

Bread is cooled in a humid environment ($RH > 75$ %) to minimise moisture evaporation and the subsequent loss in mass. Due to this high level of humidity, it is critical to monitor the air quality for bacteria to ensure food safety in line with regulations. Product quality dictates that bread is usually cooled at atmospheric temperature using no additional refrigeration or chilling load – this process can take between 2 and 24 hours.

Coolers can be of a tunnel-type or a spiral conveyor; the inside of a spiral conveyor cooler is shown by Figure 1.6. The bread travels on a conveyor in a helical motion,

often from bottom to top with the air flowing from top to bottom. This ensures a more uniform temperature gradient between the bread and the air, thus increasing the efficiency of the cooling process.



Figure 1.6 – Photograph of the inside of a spiral bread cooler (Spooner Industries Ltd.)

Typical conditions within a cooler are air temperature, $T_{air} = 20\text{ }^{\circ}\text{C}$ and air inlet velocity, $u_{in} = 1\text{ m/s}$ (Cauvain and Young, 1998). More radical technologies, such as vacuum cooling and active cooling (where the air temperature is chilled to below ambient) exist in the food industry; however, due to the traditional nature of bread-making bakeries have not widely adopted these to date.

Freezing of bread is possible, though it is well documented that this can have a negative effect on the crumb structure, which can be negated by including additives in the recipe (Ribotta *et al.*, 2001). Food manufacturers are increasingly reluctant to use additives as they are unpopular with consumers and can impact upon other processes within the manufacturing cycle.

1.3.5 Slicing, Packaging and Distribution

The slicing, packaging and distribution phases of bread production make the bread ready for consumption. Mechanical slicing machines ensure uniform width of bread slices, depending on the product type, after which the loaf is placed into a

plastic bag or wax wrapped as appropriate and then it can be stored. Due to the very short shelf-life of many baked products (typically less than 2 weeks), production is very much governed on a supply-demand basis and very short stock is held. Where stock is held it is often for smaller products (for example burger rolls) and held in a freezer in anticipation of a production spike – which can occur on a public holiday or during extreme weather. Distribution networks for commercial bakeries can be vast (up to hundreds of miles), meaning delivery costs are high. These costs can be variable due to fluctuations in oil prices, as the majority of bread is delivered by road. Though this thesis does not address the energy costs of product distribution logistics, it is an area of increasing concern for bakeries for financial cost and environmental reasons.

1.4 Research Aims and Objectives

The aim of this study was to quantify the energy use in the proving and baking processes of bread production and to investigate methods and technologies that could be used to improve energy utilisation in the manufacture of bread on a commercial scale.

The specific objectives of this research project were:

- To understand the fundamental principles of heat and mass transfer, fluid flow, industrial instrumentation and Computational Fluid Dynamics (CFD) so that these analysis methods could be applied to investigate energy use in the bread baking industry.
- To analyse current prover energy consumption and to provide scientific justification for quantifying the minimum number of air changes for a range of provers, thereby directly reducing the energy demand and carbon emissions of commercial bread proving.
- To investigate the thermal energy efficiency of a variety of bread ovens and generate a system-level thermodynamic analysis model that could be

applied to commercial bread ovens by use of non-invasive measurement techniques to visualise opportunities for energy savings.

- To conduct pilot-scale experimental heat transfer experiments to help identify an optimum set of conditions for jet impingement heat transfer with respect to energy usage that are practical for industrial bread baking ovens.

This work has been conducted through the use of both experimental and numerical techniques to influence the engineering design and operational conditions of industrial process equipment, with the overarching aim of reducing the energy consumption and carbon emissions of the bread manufacturing process.

1.5 Outline of Thesis

This thesis addresses a number of key issues relating to energy use in bread baking. The background of energy consumption in relation to bread manufacturing on different scales is addressed in Chapter 2. Heat transfer as a general phenomenon is discussed in Chapter 3, which also goes into detail on how this relates to bread manufacture. Chapter 4 discusses the theoretical background of CFD and identifies how best to utilise these tools in the analysis of process equipment. Chapter 5 presents an experimental and computational analysis of the energy consumption of an industrial bread prover. A system-level thermodynamic analysis model for baking ovens is described in Chapter 6. The methodology for, and results of, heat flux experimentation for conditions relating to industrial baking are carried out in Chapter 7. Finally, Chapter 8 discusses the implications of the work produced in this project and concludes this thesis with some suggestions for further work.

Chapter 2

Energy Use in the Baking Industry

Bread production is considered to be an energy intensive process (Klemes *et al.*, 2008). There are a range of issues that have historically prevented the adoption of energy efficient technologies in the baking industry, including: product quality, hygiene fears, resistance to change, lack of capital investment and insufficient resources to enable technologies to be trialled.

The current global political climate represents an opportunity for bakeries to make step changes to lower the energy demand of baking bread. For instance, there are funding opportunities in the UK through organisations such as: the Carbon Trust, the Technology Strategy Board (TSB), the Engineering and Physical Sciences Research Council (EPSRC) and the Research Councils UK (RCUK) Energy Programme to both develop fundamental understanding and move innovations up the 'technology readiness levels'. Within the EU there are also grants that can address these issues.

2.1 Previous Studies

A number of authors have addressed the issue of energy use in the baking industry. These vary from detailed analyses of process equipment (Carvalho and Nogueira, 1997, Fuhrmann *et al.*, 1984), to more general Life Cycle Assessments (LCAs) of the environmental impact of producing and distributing baked goods (Andersson and Ohlsson, 1999, Braschkat *et al.*, 2003, Holderbeke *et al.*, 2003).

The 1973 oil crisis in the US meant that energy use in process industries was a high priority research area in the 1970s and early 1980s (Johnson and Hoover, 1977), hence, a number of energy audits of bakeries were published between 1977 and 1984 (Beech, 1980, Casper, 1977, Christensen and Singh, 1984, Johnson and Hoover, 1977, Laukkanen, 1984, Whiteside, 1982). After the resolution of the oil

crisis, energy supply had become less of a global concern and research into this field appeared to decline. The recent intensification of research relating to energy use in the process industries is due to environmental concerns and rising energy costs. Bread ovens (and indeed other pieces of bakery equipment) have historically been designed with little regard to energy use, with the main focus being on product quality and production rates (Klemes *et al.*, 2008).

There is a moderate amount of published research in the area of energy use in the bread industry. Sections 2.1.1 to 2.1.4 summarise the findings of this published literature and to critically analyse the contributions and disagreements between authors in this field. As many of the most rigorous published methodologies and datasets are over 20 years old, part of this thesis updates findings previously reported for a modern industrial baking process. Although the principles of baking have not changed significantly, the progressive changes in processing equipment have had an impact on energy usage.

The following literature review categorises the previous research under the general headings of: bakery energy audits, life cycle assessments, baking oven energy audits and other equipment.

2.1.1 Bakery Energy Audits

Johnson and Hoover (1977) conducted an audit of a large industrial bakery in the USA – this paper was published at the height of the oil crisis in the 1970s. The authors gave mean energy use as 7.36 MJ/kg bread; which (in 1977) equated to 3.7 % of the product monetary value (US \$0.0192/kg). As a proportion of the calorific energy content of bread, four times the electricity and heat energy is required in production. The recommendations presented in this report are generic, for example: “unconventional ovens, such as steam and microwave, should be examined”, but no specific improvements to process equipment were proposed. The suggestions for further research of interest included: redesigning the shape of tunnel ovens,

recovering heat from flue gases and further analysis into the dough mixing procedure.

Beech (1980) quantified energy use in three Rank Hovis McDougall (RHM) (Hovis brand – now owned by Premier Foods) UK industrial bread plants, and compared the primary energy use with that of home baking. It was reported the average energy use in the bakeries was 6.99 MJ/kg, though the total energy use was 14.80 MJ/kg when the analysis included all processes from the growing of the wheat to delivery to the consumer – i.e. the bakery processes accounted for 47.2 % of the total energy used to produce a loaf of bread. Home baking with a gas oven used a similar amount of energy, 7.84 MJ/kg, and with an electric oven 20.01 MJ/kg. The figures for home baking depend largely on the method used – for example batch size. This paper was critical of previous reports by Leach (1975) and Chapman (1975), pointing out that there were very large differences in their results due to the generalisations made by averaging out total energy use in the UK rather than conducting a full on-plant energy audits.

Whiteside (1982) conducted energy audits of two bakeries in the USA. The specific energy consumption of each was 1.89 and 4.16 MJ/kg and heat accounted for 80 to 82 % of the total energy. Although this report focussed mainly on the savings possible by optimising process equipment within the bakery, opportunities for energy savings were identified in the transportation of product. It is clear from studying this report that the baking industry has become more automated since 1982 – for example the author makes reference to aligning processes according to operator shift patterns, however due to use of automated machinery, shift patterns no longer dictate production scheduling. The most pertinent energy saving initiative outlined was to recover heat from the oven flue gas for use in the prover via an air-to-air heat exchanger. The heating load of the prover and the amount of heat rejected by the oven is similar and both pieces of equipment are at a fairly constant heat load for the entire year. The idea is particularly feasible because of

the close proximity of the two units; therefore this solution is well suited for heat recovery.

Laukkanen (1984) audited the energy use of 12 bakeries in Finland. The author found that specific energy consumption varied between 3.2 and 11.5 MJ per kg of bread produced (mean energy use was 6.5 MJ/kg). Energy costs in the bakeries were between 1.5 and 3.7 % of turnover (in 1984). The mean production across all bakeries was 1,220 tonnes per year for a range of production rates of between 88 and 7,740 tonnes per year. For each bakery, electricity accounted for approximately a quarter of energy use, whilst the remaining fuel supply was light fuel oil. The author agreed with other publications that ovens accounted for around half the bakery energy use and further investigation on three different types of oven was pursued. The other main energy uses were found to be for boilers and refrigerators. It was reported that combustion in the ovens was inefficient because of air leaks to the burners. The main suggestion for improvement was to recover heat from the exhaust air; the danger of this is that the dust, flour and grease in the air could cause damage to the heat exchanger equipment. Suggested use of the waste heat included preheating supply air, using a heat pump to store the waste energy and heating of service water or domestic hot water. The proposals outlined resulted in potential 10 to 20 % reduction in energy consumption with payback periods of between three and six years.

Probert and Newborough (1985) published an extensive article detailing the thermal performance of a large number of food processing operations, including bakery processes. Much of the paper focusses on relatively small-scale bread production environments – for example in-store style baking ovens. The author reported that the energy demand of bread manufacturing was 25 MJ per kg production. The study largely agreed with the consensus that close to half the primary energy demand of bread manufacture was within the bakery itself, and of this half (i.e. around 6 MJ/kg) was used by the oven.

Kannan and Boie (2003) have outlined management practices for small sized bakeries in Germany to reduce energy usage. Over 80 % of bakery produce is manufactured in small local bakeries in Germany, in contrast with many (particularly English-speaking) nations, where large industrial factories dominate the bread industry – as illustrated by Figure 1.1. The baking process itself accounted for 73 % of the total energy consumption, and 85 % was thermal energy. Hot water generation to 70 °C was possible through heat recovery off the flue gas from the oven, which improved efficiency by 10 to 15 %. It was also possible to pre-heat burner combustion air which saved energy, reduced moisture content of the air and reduced maintenance costs due to less tar build-up in the oil burners. Energy reduction was expected to be 6.5 %, though doubt was raised as to whether these cost savings were worthwhile as the capital cost was much greater than the energy cost, given they are on a small-scale.

As part of a popular guide to energy auditing, an energy study on a US bakery was produced (Thumann and Mehta, 2008). Having surveyed the literature, the numbers presented in this book are in approximate agreement with the consensus, therefore Figure 2.1 shows a graphical breakdown of the data:

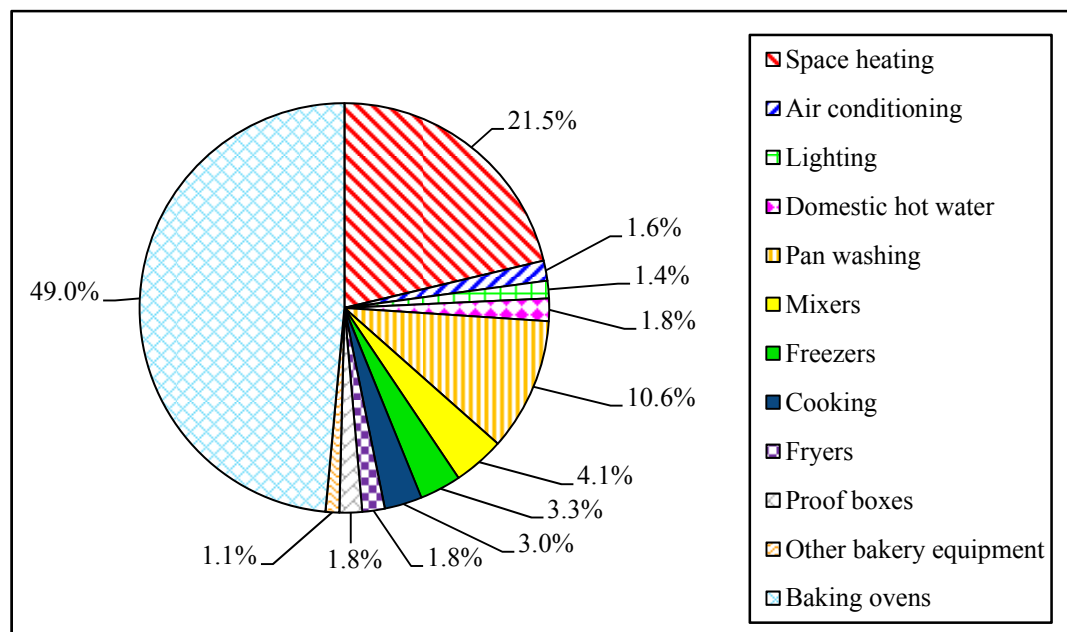


Figure 2.1 – Pie chart showing energy utilisation in a US bakery (Thumann and Mehta, 2008)

Although a full detailed audit is not given, a breakdown of energy consumption shows the primary energy user is the oven, consuming 49.0 % of the total bakery use. Overall process energy totalled 73.7 % and domestic energy 26.3 %. Over a fifth of the domestic energy use was “space heating” – though this is not a large energy requirement in many bakeries located in milder climates.

The UK-based government organisation, the Carbon Trust, initiated a project in 2009 titled “Industrial Energy Efficiency Accelerator” (Carbon Trust, 2010). This project focussed on giving UK bakeries a forum to collaborate on energy savings ideas and to bring together research to improve process efficiency. This project encompassed the three main commercial bakers in the UK: Warburtons, Allied Bakeries (Kingsmill and Allinson brands), and Premier Foods (Hovis brand), alongside smaller bakeries, equipment suppliers, academics and environmental consultants. The initial report gave a solid overview of the UK baking industry. It was reported that the total energy consumption was 2,000 GWh and emissions were 570,000 TCO₂/year. The breakdown of energy supply forms was: 560 GWh electricity, 1,400 GWh natural gas and 40 GWh fuel oil. When the cost differential between the three energy supply forms is taken into account, data for which is supplied by the Department for Energy and Climate Change (DECC) (Carbon Trust, 2012b) in the UK on a quarterly basis, this translates to energy cost of £38.2 million electricity, £44.7 million natural gas and £2.38 million fuel oil. These numbers are in close agreement to the numbers discussed with technical management of industrial bakeries (Oakley, 2009).

2.1.2 Life Cycle Assessments

Life Cycle Assessment (also known as: life cycle analysis, cradle-to-grave analysis, integrated impact assessment or full cycle analysis) is a formal technique that measures the environmental, health and resource impact of the material extraction, production, use, recycle and disposal phases of a product (European Commission Joint Research Centre: Institute for Environment and Sustainability, 2010). The aim

of a LCA is “to enable the incorporation of environmental and social impacts into decision-making processes” (Sørensen, 2011). LCA principles, frameworks, requirements and guidelines are governed by two international standards: ISO 14040 (International Organization for Standardization, 2006b) and ISO 14044 (International Organization for Standardization, 2006a). LCAs typically result in a number of impact measurements, including: energy consumption, hazardous waste, industrial waste, water waste, air emissions, noise, radiation and consumption of raw materials (Rebitzer *et al.*, 2004).

Andersson and Ohlsson (1999) aimed to establish the environmental effects of producing bread on different scales in Sweden by use of LCA, by looking at home baking, a local bakery and baking on an industrial scale. The impact of each has been measured to include all processes from agricultural production, through to flour milling, bakery processes, packaging and distribution. It was found that a ‘large’ industrial bakery (30,800 tonnes/year) had the highest carbon emissions and used the most primary energy, 22 MJ/kg – though it should be noted that a large industrial bakery in the UK may produce upwards of 200,000 tonnes/year. A smaller industrial bakery, producing 12,800 tonnes/year, had similar performance with relation to global warming, acidification and eutrophication as both home baking and a local bakery – the primary energy usage was 14 MJ/kg. The reason provided for the larger bakery using more specific energy was due to the large distribution area – as the analysis included both delivery of raw materials to the bakery and the delivery of the final product to the retail outlets and customers. In terms of the baking processes, the economies of scale allowed the actual baking process to be more efficient for the larger bakery. The authors suggested there was a balance between the size of the bakery and distribution area which would give the smallest possible environmental impact – the model for this would need to consider factors such as population density, transportation method and positioning of bakeries.

Three further LCA based papers were presented at the 4th International Conference on “Life Cycle Assessment in the Agri-food sector” in 2003, and were published in its proceedings (Braschkat *et al.*, 2003, Holderbeke *et al.*, 2003, Rosing and Nielsen, 2003). Braschkat *et al.* (2003) reported that a ‘large’ bread factory used around half the energy requirement of a bakery or home-production, however no definition of ‘large’ was given. Rosing and Nielsen (2003) looked at the environmental impact of different ways of making the holes in French bread for hotdogs – concluding that any environmental concern was less important than retaining the product brand and appearance. The study accounted for global warming, acidification, eutrophication and nature occupation from storage of ingredients to the storage of the finished product – thus, the processing and transport of the ingredients, and the distribution of the finished product is not included. Holderbeke *et al.* (2003), meanwhile reported that in the 19th century the environmental impact of bread production was up to four times worse, due to inefficient processes and the lack of quality fuels.

2.1.3 Baking Oven Energy Audits

As ovens have been shown to be the major energy users in bakeries, conducting an energy audit would be the natural starting point for analysing energy utilisation in the baking industry. Use of a rigorous scientific framework to measure energy streams can help quantify the energy (both heat and electrical) that is useful to the process and the energy wasted. Identifying waste energy streams and considering ways to reduce waste is often a natural starting point for companies to audit industrial equipment such as bread ovens.

Two historical energy audits presented here, from 1977 and 1982, give a good baseline breakdown of heat distribution in industrial bread ovens. Although these reports are not recent, this data is helpful to compare current technology and to give an initial idea of thermal energy utilisation of commercial bread baking ovens. Firstly, Johnson and Hoover (1977) reported that the baking process accounted for

28 % of the total energy usage of the entire manufacturing process. Of the oven heat losses, 27 % was in flue gas and 10 % was through wall conduction. Only 15 % of the heat went into directly heating the bread whilst a large bulk, 40 %, of heat was used to evaporate water from the dough. Whiteside (1982), however, calculated that between 61 and 62 % of the energy use of the two ovens was required for baking processes. Wall losses accounted for just 3 % whereas the largest losses were stack losses (24 %). Figure 2.2 graphically compares these two previous oven audits:

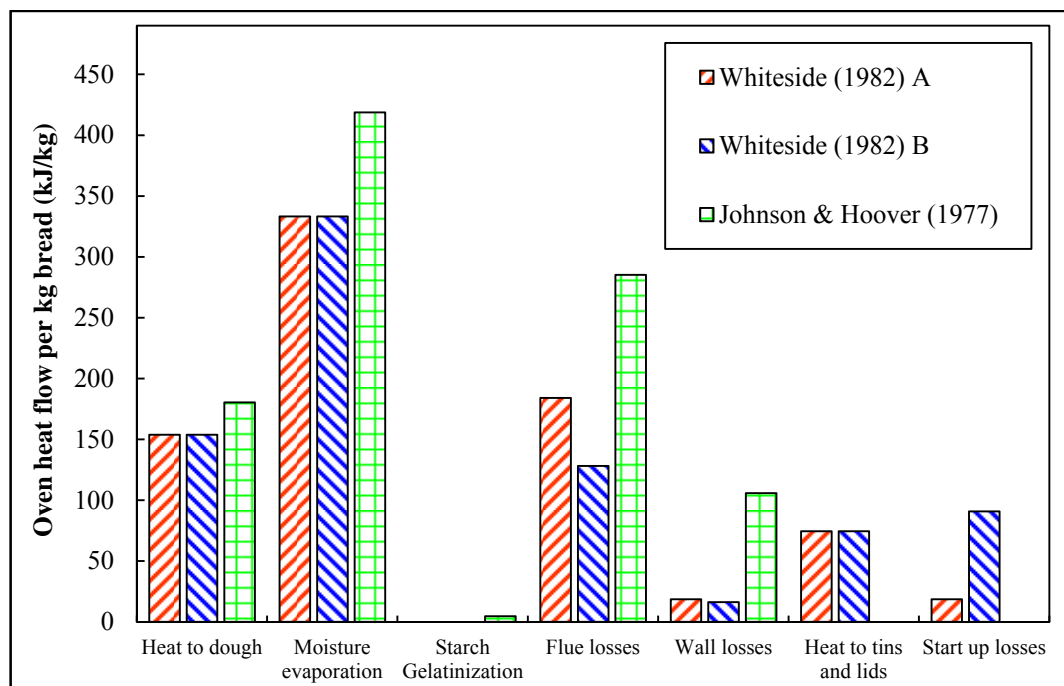


Figure 2.2 – Graph of heat distribution in commercial ovens from literature (Johnson and Hoover, 1977, Whiteside, 1982)

Christensen and Singh (1984) provided a review on advances in energy technologies in the baking industry with reference to ovens manufactured by Werner and Pfleiderer, Germany (now merged with Baker Perkins, UK) and more generally, the Swedish baking industry. For this reason, there is the potential for the report to have bias, particularly since it makes reference to an internal report by the oven manufacturers. Despite this, there is a good explanation of methods used for taking measurements and analysis. Mean specific energy use of the ovens was 0.898 MJ/kg for baking bread without lids, with lids this figure increased to 1.098

MJ/kg. 44 % of heat input is lost through exhaust gas, ventilation and evaporation of moisture from the dough. Only 19 % of the heat was transferred to the bread. Heating of lids and pans was responsible for 17 % of the heat losses. Three main suggestions were made to improve energy efficiency: (i) optimise the ventilation of the ovens, (ii) review the materials used to manufacture pans and lids, and (iii) recover heat from flue gases. No detailed explanation is given on how best to approach realising these improvements.

Fuhrmann *et al.* (1984) reported on energy optimisation of heat streams by recirculating hot air between different processes for a European-style baking process. This research was also commissioned by Werner and Pfleiderer, indicating potential for partiality. The innovation was centred on heat recovery; coupling the high temperature exhaust of the prebaking oven with the lower temperature baking oven. The authors suggested that heat recovery would make the bakery 3.7 % more efficient. There are thorough explanations of methods used and how the improvements were installed. The cost of making these improvements could only be justified if energy costs were suitably high.

Carvalho and Nogueira (1997) analysed energy efficiency of furnaces, kilns and baking ovens. There is a particular focus on free/ forced convection techniques and variation in temperature profiles in these heating processes, thereby measuring heat flux to the bread. Although the title of the paper implies that it is optimising energy efficiency, the research focusses predominantly on global heat flux measurement in baking ovens, a topic that is discussed in further in section 3.4.

Klemes *et al.* (2008) stated that baking is a large energy user in comparison to other similar drying operations, such as preservation of fruit and vegetables. This is because the thermal conductivity of bread is comparatively low and a large amount of heat is needed to evaporate a significant fraction of moisture from the product. The best measurement to gauge performance of baking ovens was reported to be

heat flux, which is dependent on the temperature gradient, air velocity and flow characteristics. Heat flux can be measured with local sensors which are becoming more commercially available and cost effective. Aside from offering opinions on heat recovery, the authors also suggest that significant energy savings can be made by optimising convective heat transfer within the ovens as this would reduce baking time. Design of strategically placed nozzles allows the baker to remove stagnant air from around the product and hence increase the rate of heat transfer. Suggested improvements are low investment and it was suggested that they could result in up to 20 % energy savings, however research is required to experimentally (or otherwise) identify optimum conditions for heat transfer.

2.1.4 Other Bakery Equipment

Aside from general bakery audits and specific investigations on bread ovens, there are other processes in bread manufacturing that have received little attention but which offer the potential for energy savings.

Frank (2009) described recent attempts to reduce the energy consumption of the baking industry in a commercial periodical “Baking Management”. In addition to covering the widely-used industry techniques such as; boiler improvements, new chillers, correctly sized and routed pumps/ pipes, lighting and other domestic opportunities, interesting recent developments in the mixing process have been outlined. An American machinery manufacturer appears to have invested heavily in computational techniques to improve the mixing process by improving the cooling effect and altering the shape of the mixing bowl. The results to show that use of a variable-speed drive (VSD) to better control the mixing process can reduce energy use and improve product quality. Heat recovery was also listed as an area for further research, where a reduction of around 25 % of heat input can be realised.

There has been very little published research relating to energy use in the proving process. Despite this, there is significant scope for reducing the energy use of

commercial bread provers, as shown by Paton *et al.* (2012a) and investigated in Chapter 5. Much of the research into industrial bread proving is focussed on the macroscopic changes to the dough structure as gas cells develop (Chiotellis and Campbell, 2003b, Chiotellis and Campbell, 2003a, Cordoba, 2010, Grenier *et al.*, 2003, Grenier *et al.*, 2010). Considering proving is responsible for upwards of 5 % of the energy consumed in a bakery (Carbon Trust, 2010), the lack of scientific research in this area is deterring bakeries from taking proactive measures to optimise the process.

Cooling of food products can be an energy intensive process, particularly if the temperature of a product needs to be reduced by a large amount, for example in the freeze drying of foods such as ready meals (Pimentel and Pimentel, 2008). The temperature gradient of cooling bread is comparatively large, and thermal conductivity is typically low due to the porous nature of bread, which would normally result in a high energy cost for cooling. However, the energy demand of cooling bread is surprisingly low, since food quality/ safety dictates that there is no requirement to cool bread quickly, nor is there a need to keep bread refrigerated or frozen. For this reason, bread can be cooled over a longer period of time at ambient temperature, resulting in a minimal energy demand. Despite this, in certain circumstances, energy intensive cooling processes can be appealing to bakeries due to the decreased cooling time and therefore potential to increase production rate causing a reduction in the physical space the cooler occupies in a bakery. The two most prominent alternative technologies to conventional methods are refrigerated cooling and vacuum cooling.

Refrigerated cooling can be effective when the temperature difference between the product and the ambient temperature is low (i.e. around 30 to 40 °C). Refrigeration can significantly increase the temperature gradient and thus increase the cooling rate. When the temperature difference between the product and ambient is large, however, refrigeration does not increase the temperature gradient to a level where

the additional energy makes an impact to the cooling time. For this reason, two-stage cooling has been recommended to initially reduce the temperature via ambient cooling and finish the cooling process through refrigeration (James and James, 2011).

Although vacuum cooling has been used since the 1950s in the horticultural industry, much of the food industry has been reluctant to adopt vacuum coolers in a production environment, mainly due to technological barriers (McDonald and Sun, 2000). The main benefits of vacuum cooling are: increased hygiene, improved food safety, low weight loss, quicker cooling times, and the consequent potential benefits of increased energy efficiency and a reduction in the size of machinery required (Wang and Sun, 2001).

Chapter 3

Heat Transfer in the Bread Industry

As with most food production operations, transfer of heat in bread manufacturing is of paramount importance to the success of the production process. Within the bakery, the raw ingredients must be mixed together at ambient temperature, exposed to humid conditions to encourage yeast fermentation, heated to approximately 100 °C, and cooled again to ambient temperature within a confined period of time, often in a continuous manufacturing environment. The major characteristic of bread production, when compared to other heating processes, is the porous nature of the product. Porosity is increased particularly during the proving phase, when the bread expands and density decreases – this means that thermal conductivity within the product is lower than many comparable heating operations involving solids and liquids, meaning control of heat transfer becomes critical. Many other physical changes in bread occur during the manufacturing process that make measuring the heat demand a challenging task, for example during proving the volume expands, during baking and cooling the moisture content decreases and during mixing the dough rheology is constantly evolving.

3.1 Heat Transfer Fundamentals

There are several established textbooks that explain the main aspects of heat transfer (Eckert, 1959, Incropera and DeWitt, 2007, Rohsenow *et al.*, 1998, Russell *et al.*, 2008). The three fundamental forms of heat transfer are conduction, convection and radiation – these are summarised in the following sections 3.1.1 to 3.1.3. Due to the complex nature of heat and mass interactions in real systems, heat transfer is very rarely a result of just one of these three forms, although it is not uncommon to have an overriding mode of heat transfer which deems the other sources negligible. All three aforementioned modes have specific relevance to bread production. For example in a baking oven, heat is transferred to the bread

through a combination of convection and radiation, and then heat is conducted from the surface (crust) to the core of the crumb.

3.1.1 Conduction

Conduction is the transfer of heat from higher temperature to lower temperature through the vibration of molecules. For most simple applications of conduction, Fourier's Law can be used. Fourier's Law defines the rate of heat transfer as being proportional to the temperature gradient across a material, dT/dx , shown in one-dimension by Eq. (3.1):

$$q = -\lambda A \frac{dT}{dx} \quad (3.1)$$

where q is heat flux (W/m^2), λ is thermal conductivity ($\text{W}/(\text{m}\cdot\text{K})$), A is surface area (m^2) and T is temperature (K).

Heat conduction is usually most effective in solids, in particular metals, due to the molecular structure that allows a large number of electrons to vibrate and therefore transfer heat. Thermal conductivity is a material specific property that is dependent on factors such as temperature, phase and material structure.

Midden (1995), described the success of a baking operation as being dependent on "the ability of the product to transfer heat from its outer surface to its center" i.e. the rate at which conduction occurs from crust to crumb. As the temperature at the core of the dough/ bread needs to be raised from ambient to approximately $100\text{ }^\circ\text{C}$, conduction within the bread has a great effect on the energy requirement of both the prover and oven.

Bread is a poor conductor of heat due to the cellular structure of gas cells trapped within the dough/ bread. The thermal conductivity of dough/ bread varies with temperature due physical changes in the material structure, i.e. volume expansion, increase in porosity, decrease in density and moisture loss. Published temperature dependent values of thermal conductivity for white sandwich bread vary between

0.11 and 0.85 W/(m·K) (Monteau, 2008, Unklesbay *et al.*, 1981, Wong *et al.*, 2007). A summary of these studies is shown graphically by Figure 3.1. As with other information presented in literature relating to the bread industry, the variability across different studies means that the reliability of using any of the reported data is compromised, therefore, for this study thermal conductivity values taken from literature have been corroborated with industry to check the reliability.

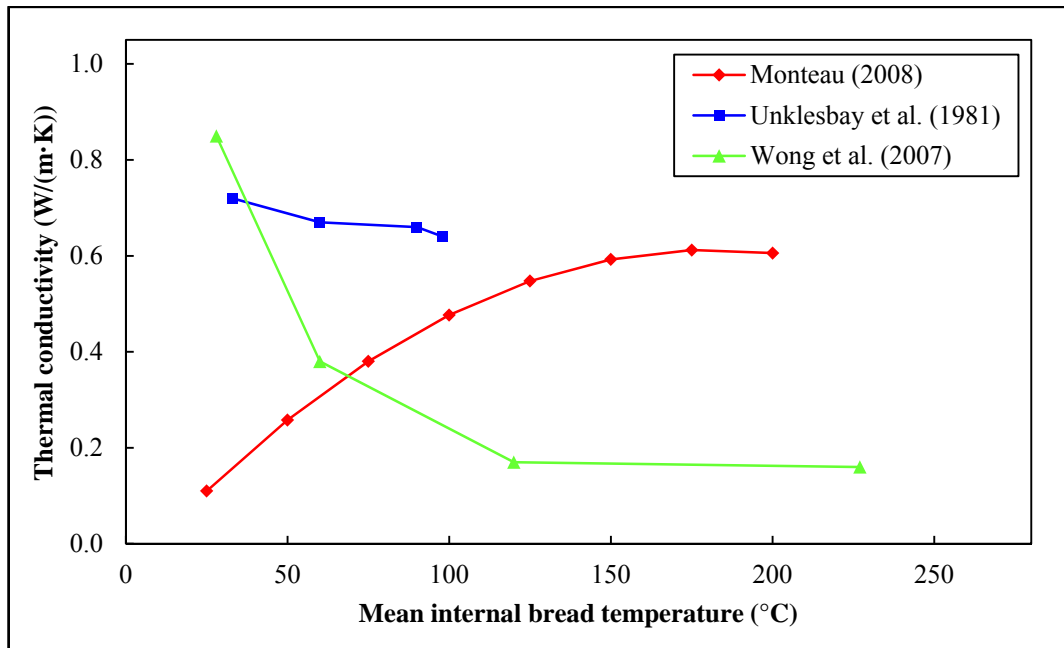


Figure 3.1 – Graph of the thermal conductivity of bread as a function of temperature (Monteau, 2008, Unklesbay *et al.*, 1981, Wong *et al.*, 2007)

3.1.2 Convection

Convective heat transfer occurs when the movement of fluids causes momentum, energy and mass transfer (Bacon, 1989). Two types of convection are frequently discussed: free (or natural) convection and forced convection. Free convection is typically driven by buoyancy forces, for example when hot air molecules rise above cooler air due to temperature and density variations in an enclosed volume. Forced convection requires an external force to encourage the fluid flow, for example a pump forcing fluid to flow through a pipe or duct. The rate of convective heat transfer is given by Newton’s Law of Cooling, Eq. (3.2):

$$q = h_c A dT \quad (3.2)$$

where the convective heat transfer coefficient, h_c , is dependent on a number of physical characteristics of the fluid and flow parameters, thus, it is a difficult value to determine numerically or theoretically. Two methods are frequently used to calculate values – for simple flow problems it may be obtained by solving boundary layer equations, or for complex flow it can be correlated using experimental results (Incropera and DeWitt, 2007).

Values of heat transfer coefficient for gases in free convection regimes are typically between 0.5 and 500 W/(m²·K), and for forced convection between 10 and 700 W/(m²·K). Section 3.4.1 gives a full review of published values for h_c for bread baking applications. For applications that use high velocity fluid flow and fluid temperatures less than 400 °C, convection is often the dominant mode of heat transfer.

3.1.3 Thermal Radiation

Thermal radiation is often considered the most complex mode of heat transfer (Turner, 1993) and occurs when high energy photons are emitted from a hot body in the form of electromagnetic waves. Unlike convection and conduction, no particles are involved in the transfer of heat. Every object that has a temperature greater than absolute zero ($T = 0 \text{ K} = -273.15 \text{ °C}$) will emit thermal radiation. A ‘black body’ is described as an object that will absorb radiation from every wavelength and angle. The Stefan-Boltzmann Law (Eq. (3.3)) describes the heat flux of a black body as the energy being proportional to temperature to the power of four and shows that hotter and object is the more thermal radiation is emitted:

$$q = \sigma T^4 A \quad (3.3)$$

where the Stefan-Boltzmann constant, σ , is equal to $5.670 \times 10^{-8} \text{ W}/(\text{m}^2 \cdot \text{K}^4)$. However, in reality objects will only absorb some of the heat available – these are termed ‘grey bodies’. In order to apply Eq. (3.3) to a grey body, the emissivity, ϵ_A , must be factored in and Eq. (3.4) is used:

$$q = \varepsilon_A \sigma T^4 A \quad (3.4)$$

Earle (2004) used this theory to estimate the heat transfer to a loaf of bread using a value for total radiation as shown by Eq. (3.5):

$$\varepsilon_{AT} = \frac{1}{\left(1/\varepsilon_{A_{bread}} + 1/\varepsilon_{A_{wall}}\right) - 1} \quad (3.5)$$

The results showed that the heat transfer from the oven walls to the surface of the bread was between 67.4 and 68.0 W (Earle, 2004). Table 3.1 shows emissivity values for some relevant metals at bread baking temperatures (200 to 232 °C):

Material	Temperature, T (°C)	Emissivity, ε_A	Reference
Aluminium:			
smooth polished	227	0.05	(Brewster, 1992)
smooth oxidised	227	0.12	(Brewster, 1992)
rough oxidised	227	0.3	(Brewster, 1992)
Gold:			
highly polished	200	0.03	(Aksyutov, 1974)
Stainless steel:			
type 316 polished	232	0.57	(Cverna, 2002)
type 321 polished	149 to 815	0.18 to 0.49	(Cverna, 2002)

Table 3.1 – Emissivity values for materials relevant to bread manufacturing equipment

Values reported in literature generally agree on emissivity values for bread of between 0.74 and 0.9, as shown by Table 3.2:

Temperature, T (°C)	Emissivity, ε_A	Reference
150	0.9	(Yanniotis, 2008)
*	0.9	(Hamdami <i>et al.</i> , 2004)
*	0.9	(Purlis and Salvadori, 2009b)
177	0.85	(Earle, 2004)
*	0.9	(Sablani <i>et al.</i> , 1998)
50 and 70	0.95	(Roberts <i>et al.</i> , 2002)
80, 82 and 84	0.82, 0.79 and 0.76	(Gupta, 2001)
150 to 210	0.8	(Kress-Rogers and Brimelow, 2001)

Table 3.2 – Emissivity values reported for bread from literature over a range of temperatures (temperature not given)*

3.2 Jet Impingement Heat Transfer

Jet impingement heat transfer relies on fluid through an orifice (such as a nozzle) at high velocity onto a surface. Fluid jet impingement is a technique widely used across industry for drying, heating and cooling. Products manufactured using fluid jet impingement include: plasterboard, foodstuffs, metal, paper, thin films, coatings and packaging. High air velocity is used to increase heat and mass transfer rates, often at the expense of increased capital and operating cost of equipment. Due to this, impingement drying is only recommended for operations where a major proportion of moisture is being removed (Mujumdar, 2007).

Jet impingement is an established technology in the food industry and has been used in baking operations worldwide for several decades. The advantage of fluid jet impingement is that the static boundary layer between the fluid and product is reduced in size, which reduces the insulating effect between the hot bulk fluid and cold surface and therefore allows higher rates of heat transfer. Moreira (2002) noted that impingement nozzles ensured that convection is the dominant form of heat transfer at the product surface.

3.2.1 Impingement Nozzles

Temperatures for applications of jet impingement have historically varied from -50 to 400 °C. Air jet impingement is characterised by sets of nozzles discharging air at high velocity, typically between 10 and 50 m/s. It has been proved that for each system there is a limiting velocity beyond which the boundary layer does not decrease further, therefore heat transfer does not increase and using greater fluid velocities would have no effect (Erdoğan and Anderson, 2010).

The development of flow from a jet is of particular importance when designing an impingement heating or cooling device. There are four characteristic regions of flow of an impinging jet of air: the potential core, the free jet region, the impingement region and the wall jet region – see Figure 3.2. There are two

important dimensionless ratios to consider when designing impingement nozzles: dimensionless nozzle-to-surface distance, H/d , and dimensionless distance between the nozzles, P/d and S/d (P is the pitch between two nozzle sets in the x -direction, as shown in Figure 3.3 and S is the spacing between two round nozzles in the z -direction). In addition, other geometric factors such as the nozzle shape contribute to the rate of heat transfer.

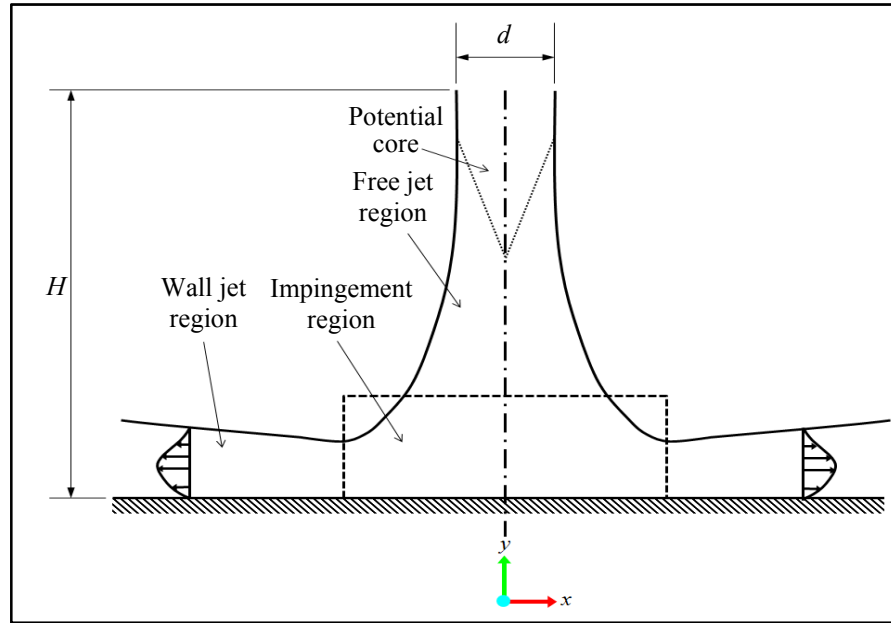


Figure 3.2 – Diagram of the flow field of an impingement jet

Jet impingement nozzles commonly use either arrays of round nozzles (ARN) or arrays of slot nozzles (ASN), although some applications may use a single slot nozzle (SSN) or a single round nozzle (SRN). Martin (1977) developed a universal set of correlations for all the aforementioned types of impingement nozzle. The two important correlations for this study – ASN and ARN, are given by Eq. (3.6) and Eq. (3.8) respectively. These equations use dimensionless numbers to calculate heat transfer from air velocity. Dimensionless heat transfer is displayed as Nusselt number, Nu and dimensionless air velocity is displayed as Reynolds number, Re .

$$\frac{Nu_{ASN}}{Pr^{0.42}} = \frac{2}{3} f_0^{0.75} \left(\frac{2Re}{f/f_0 + f_0/f} \right)^{2/3} \quad (3.6)$$

where f is relative nozzle area the variable f_0 is defined by Eq. (3.7):

$$f_0 = \frac{1}{\sqrt{60 + 4(H/2d - 2)^2}} \quad (3.7)$$

The correlation shown in Eq. (3.6) is valid for the below set of conditions:

- $1,500 \leq Re \leq 40,000$
- $0.008 \leq f \leq 2.5 \cdot f_0$
- $1 \leq H/d \leq 40$

$$\frac{Nu_{ARN}}{Pr^{0.42}} = K(H/d, f) \cdot \sqrt{f} \frac{1 - 2.2\sqrt{f}}{1 + 0.2(H/d) - 6)\sqrt{f}} Re^{2/3} \quad (3.8)$$

where $K(H/d, f)$ is a variable defined by Eq. (3.9):

$$K(H/d, f) = \left[1 + \left(\frac{H/d}{0.6/\sqrt{f}} \right)^6 \right]^{-0.05} \quad (3.9)$$

The above correlation is valid for the below set of conditions:

- $2,000 \leq Re \leq 100,000$
- $0.004 \leq f \leq 0.04$
- $2 \leq H/d \leq 12$

3.2.2 Air Jet Impingement in the Baking Industry

In baking, air jet impingement is generally directed from both the top and the bottom of the oven chamber onto the surface of the bread or tin, see Figure 3.3. Ovadia and Walker (1998) described impingement technology as having “revolutionised certain sectors of the baking industry”. At the time of the study it was estimated that some 100,000 impingement ovens were in use. Two types of impingement nozzles were described; short nozzles (orifices) and long thin nozzles (jet tubes). The advantage of jet tubes is that there is a greater pressure drop across the tube which increases airflow uniformity across an array of nozzles. Short nozzles take up less space so are commonly used in smaller plants, for example restaurants or in-store bakeries. Due to a smaller pressure drop, a more complex design is necessary to maintain uniform air distribution across a bank of nozzles. Yeast activation within the dough causes dough-based products to expand with

time (along the length of the oven). Due to this, the top surface of the bread rises and therefore the distance between the air jets and the top surface of the product, H , decreases. In some cases this is taken into account and the nozzle-to-surface distance down the length of the oven is gradually increased to maintain optimum H/d .

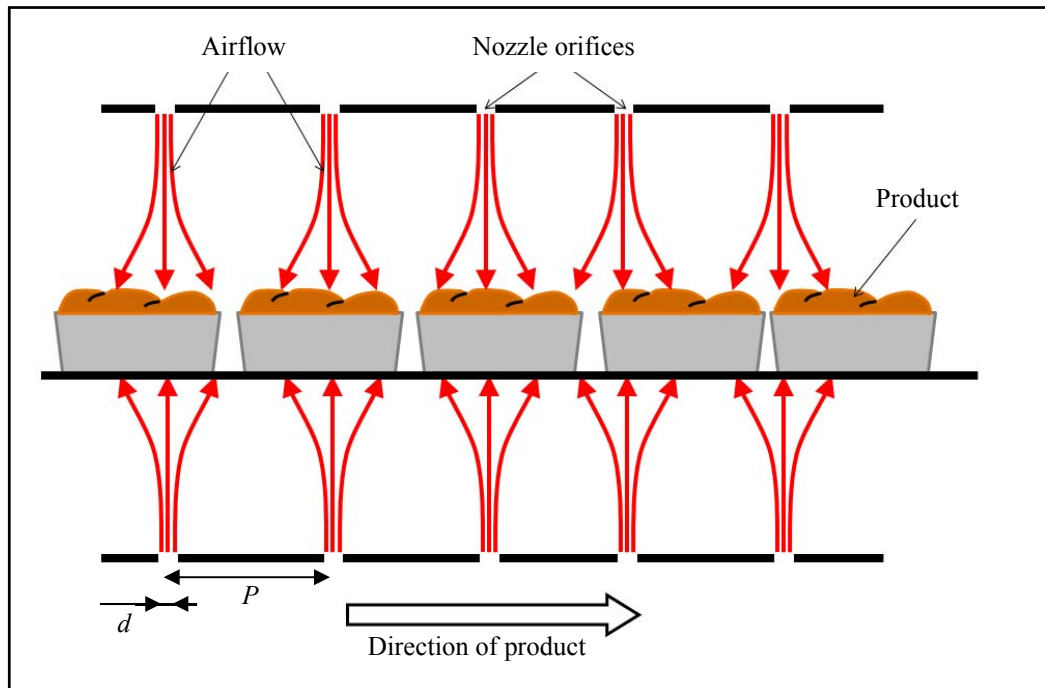


Figure 3.3 – Diagram of air impingement nozzles in a baking oven

A study by Sarkar and Singh (2004) considers factors such as hygiene and product quality when assessing the suitability of jet impingement heat transfer in the food industry. The authors note that jet impingement can often result in hot and cold spots on the food if not correctly designed. In order to avoid this, the H/d ratio must be carefully considered – it must be large enough to give an even distribution of air across the product and small enough to give optimum heat transfer rates for quality and efficiency purposes.

The effect of jet impingement for both heating and cooling of food is investigated by Olsson and Trägårdh (2007), where CFD and experimental results were compared. The importance of ensuring that the interaction between multiple jets is modelled and validated experimentally is emphasised – as this has a significant

effect on the flow field and heat transfer to the product. The same authors presented two further CFD studies on heat transfer from impinging air jets onto cylinders (Olsson *et al.*, 2004, Olsson *et al.*, 2005). The cylinders have a diameter of 35 mm and were given the properties of a generic food product to represent the baking process. The jets investigated were slot jets with a width of 30 mm. The effect of a single jet, two jets and three jets were investigated, by varying the Reynolds number, distance between nozzles and exhaust opening area. It was found that there was a slight increase in heat transfer with a H/d ratio of 2 compared with $H/d = 8$, and there was a significant increase in heat transfer for higher Reynolds numbers – the correlation derived for Nusselt number was in the form of Reynolds number to the exponent 0.59. Larger exhaust openings resulted in significantly lower heat transfer.

A number of authors describe the relation between nozzle parameters and heat transfer in technical detail (Das *et al.*, 1985, Gardon and Akfirat, 1966, Lytle and Webb, 1994, Martin, 1977). Different spatial arrangements of jets, and distances between them can create stagnation points which will negatively affect heat transfer. The key parameters for ensuring efficiency of heat transfer are: fluid flow rate, nozzle diameter, nozzle spacing and the nozzle-to-surface distance. The relevance of this highly academic literature to industry is questioned by Marson (1999), who states that much of the derived correlations are for a single slot nozzle or a single round nozzle, whereas in reality industry uses arrays of nozzles for the vast majority of drying applications.

In addition, ‘ASME Standard’ nozzles are almost always used for these experiments, which use geometries that are specifically designed to give very high discharge coefficients (close to unity) to generate flow streams close to theoretically calculated conditions. However, in reality nozzles can rarely be manufactured cost-effectively to this standard, in which case the flow characteristics used in commercial dryers are significantly different to those

published in theoretical papers. The dimensions of an ASME standard nozzle are shown by Figure 3.4, where the length of the nozzle, L is equal to the nozzle diameter, D .

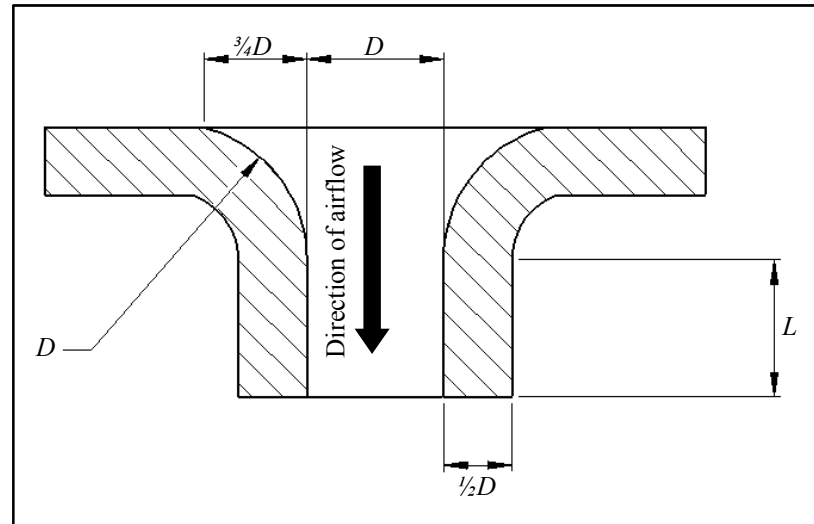


Figure 3.4 – Dimensions of an ASME standard nozzle

3.3 Fluid Flow

A key characteristic of fluid flow is whether it is laminar, turbulent or transitional. Laminar flow at a macroscopic level is orderly. Under transitional flow, the occurrences of fluctuations appear in the flow structure. Once these fluctuations are always present the flow is described as fully turbulent (Falkovich, 2011). The Reynolds number is an indicator of the degree of turbulence in fluid flow. Turbulence occurs when the Reynolds number increases beyond a critical value, Re_{crit} . For example, for highly controlled pipe flow it is universally accepted that $Re_{crit} = 4,000$ (Holman, 2002), although for real applications this value is highly problem dependent. The Reynolds number is affected predominantly by fluid velocities, fluid properties (density and viscosity) and the characteristic length scale – which is related to the flow boundaries.

The type of fluid flow (according to the classification above) greatly affects the way in which it can be analysed. Laminar flow can be both measured and predicted with relative ease. However, the majority of engineering applications of fluid flow

result in some degree of transitional or turbulent flow, which can make measuring or predicting the flow characteristics more challenging. Experimental measurement of turbulent flow can result in unstable readings and whilst numerical predictions can be accurate on an overall basis, they are often unable to convey the degree of instability of the flow.

The Euler equations are used as governing equations for fluid motion. The Bernoulli Equation is a common way to display the momentum part of the Euler equations, and is suitable for analysis of non-viscous, incompressible flow. Derived in the 18th Century by the Swiss scientist Daniel Bernoulli, Bernoulli's Equation is useful for analysing flow as a function of pressure difference. Eq. (3.10) gives Bernoulli's equation in one-dimensional format assuming no frictional losses and for incompressible, smooth fluid flow.

$$P_1 + \frac{1}{2}\rho u_1^2 + \rho g h_1 = P_2 + \frac{1}{2}\rho u_2^2 + \rho g h_2 \quad (3.10)$$

where P is total pressure (Pa), u is fluid velocity (m/s) and h is height (m).

The Navier-Stokes Equations are again derived from the Euler Equations and define mass, momentum and energy conservation of fluid flow, and are used extensively in numerical modelling. Notably difficult to solve analytically, the equations become useful when predicting local properties of fluid within a domain and are discussed further in Chapter 4.

3.4 Heat Flux Measurement

Childs *et al.* (1999) discussed a number of techniques that can be used to determine the heat transfer to an object in a seminal paper on heat flux measurement. The methods vary in ease and intrusiveness to the process. The four methods discussed were: differential temperature, calorimetric methods, energy supply/ removal and mass transfer analogy. Differential temperature is the use of thermopiles to accurately measure the conduction of heat across a material. Calorimetric methods

use time-averaged measurements of temperature to conduct a heat balance by calculating the rate of change of thermal energy of a material. Energy supply or removal is when a known quantity of heat is transferred to or from the sample surface to create a thermal equilibrium to measure the heat flux. Finally, it is possible to measure mass transfer and relate this to heat transfer using mathematical relationships between the two related principles. The most suitable in the scope of this project was the differential temperature method as heat flux sensors using this theory are commercially available. This technique uses principles of Fourier's Law, "temperature differential across a spatial distance within a medium", which can infer heat flux by measuring the temperature gradient across a material with a known thermal conductivity.

Carvalho and Nogueira (1997) analysed heat flux in bread baking ovens. In their study, radiation was found to be more significant as a mode of heat transfer than convection. Radiation was at least 57 % of the heat transfer, but was measured to be as high as 91 % for some sets of conditions. The high degree of radiation can be attributed to the comparatively low air velocity of 0.6 m/s. There were large differences in the heat flux profile between the top, bottom and sides of the loaves. Unfortunately, this report contains little detail on the methodology used to measure heat flux or how the results were obtained. The paper recommended further heat flux measurements, instead of measuring temperature profiles. For this study, there was a difference between experimental and numerical results of less than 15 %.

3.4.1 Published Values for Convective Heat Transfer Coefficient

The convective heat transfer coefficient, h_c , determines the rate of convective heat transfer from the air to the product surface inside a baking oven. Due to the scope for large variations in conditions in which bread is baked, values for h_c vary considerably for different studies. A summary of the values reported in literature is given below.

For the bread industry, the value of $h_c = 10 \text{ W}/(\text{m}^2 \cdot \text{K})$ was first quoted by Rohsenow *et al.* (1998) and subsequently used by Zhang and Datta (2006). A further value of convective heat transfer coefficient of $100 \text{ W}/(\text{m}^2 \cdot \text{K})$ was initially estimated by Therdthai *et al.* (2003) and subsequently quoted by Wong *et al.* (2007). Another study used a value of $14 \text{ W}/(\text{m}^2 \cdot \text{K})$ for forced convection ovens with air velocities between 1.5 and 2.5 m/s (Monteau, 2008). Hamdami *et al.* (2004) and Zanoni *et al.* (1995a) quoted values of 17.53 and $20 \text{ W}/(\text{m}^2 \cdot \text{K})$ respectively for bread baking applications but no details of how these values were obtained were given for either study. Šeruga *et al.* (2007) determined heat transfer coefficients for baking Croatian flat bread by correlating dimensionless Nusselt number, Grashof number and Prandtl number. The value of heat transfer coefficient calculated for free convection was $9.756 \text{ W}/(\text{m}^2 \cdot \text{K})$

A number of authors have measured the convective heat transfer coefficient for the baking of cakes and biscuits, for which similar oven technologies are used for cooking batter, rather than dough. The most thorough of these studies was published by Baik *et al.* (1999), who produced a heat flux profile through a 25 m long oven, which showed heat flux to vary considerably (between 20 and $48 \text{ W}/(\text{m}^2 \cdot \text{K})$ along the length of the oven). Lower values, between 2 and $21 \text{ W}/(\text{m}^2 \cdot \text{K})$, were given for velocities of between 0.5 and 2 m/s (Sato *et al.*, 1987) – this methodology was also used by Shibukawa *et al.* (1989) who reported the value of $29 \text{ W}/(\text{m}^2 \cdot \text{K})$. Further heat transfer coefficient values measured in the cake industry are 20 and $40 \text{ W}/(\text{m}^2 \cdot \text{K})$ for air velocities of 2.5 and 10.0 m/s respectively (Sumnu and Sahin, 2008). Nitin and Karwe (2001) measured heat transfer in a cookie oven and reported much higher values of between 100 and $225 \text{ W}/(\text{m}^2 \cdot \text{K})$ for jet velocities of between 18 and 44 m/s.

Due to the variation of the conditions in which they are measured, the convective heat transfer coefficient values published in relevant literature cannot be reliably applied to this study. This makes it necessary to determine the heat transfer

coefficients for the conditions relevant to this study experimentally, which is discussed in Chapter 7.

3.5 Mass Transfer

Mass transfer is the net movement of matter from one location to another. Mass transfer can occur within a medium or across a boundary – for example in bread baking the evaporation of moisture from within the dough, through the crust, to atmosphere, which dries the crumb of the loaf. As mass transfer is a vast and complex field, only the basic principles are discussed here, but a number of sources discuss the topic in greater detail (Baehr and Stephan, 1998, Eckert, 1959, Incropera and DeWitt, 2007).

The transfer of mass occurs due to a gradient in concentration, pressure or temperature and can be diffusive or convective in nature. Convective mass transfer occurs in moving fluids (Nellis and Klein, 2009), and is synonymous to convective heat transfer in that it can be correlated for different flow regimes (Martin, 1977). Mass diffusion occurs due to concentration gradients and is caused by the macroscopic average movement of fluid molecules. Fick's First Law, Eq. (3.11), describes mass diffusion in one dimension in a similar manner to Fourier's Law of conduction (which is discussed previously in section 3.1.1):

$$J_A = -D_{AB} \frac{dc_A}{dx} \quad (3.11)$$

where J_A is the diffusion flux of A in B ($\text{mol}/(\text{m}^2 \cdot \text{s})$), D_{AB} is the diffusion coefficient (m^2/s) and c_A is the concentration of A (mol/m^3).

Mass transfer and heat transfer often occur simultaneously – indeed many practical heat transfers occur predominantly due to the transfer of mass (and vice versa) and combining the two processes can substantially increase the efficacy of both heat and mass transfer and thus energy efficiency – for example heat pipes which utilise phase changes of fluids to recover heat of flue gas exhausts – heat pipe heat

exchangers are increasingly being used in the process industries. Mass can commonly be transferred by physical processes such as: absorption, evaporation, distillation etc. Of these, moisture evaporation (a form of vaporisation) from the dough surface is the characteristic process required for bread baking.

3.5.1 Vaporisation and Evaporation

Vaporisation is the change in state of a fluid from liquid to gas, which as previously discussed occurs in baking ovens when the loaf is dried. More specifically, evaporation is the vaporisation of fluid from a surface. In order to instigate mass transfer in the form of evaporation, two forms of energy are required – the energy required to increase the fluid temperature to a point at which a phase change can take place, termed sensible heat, and the energy required to cause the phase change of the fluid from liquid to gas, termed latent heat of evaporation/ vaporisation. For water, the latent heat of evaporation at atmospheric pressure, L_{e_w} , is 2,260 kJ/kg at 100 °C (Bird and Ross, 2012). This latent heat, which is required to generate steam at atmospheric pressure, is much larger than the sensible heat required to raise the bulk temperature of water from ambient to boiling point, as the specific heat capacity, c_{p_w} , is between 4.186 and 4.219 kJ/(kg·K) in the temperature region 20 to 100 °C (Serway and Jewett, 2010). This is an important consideration for assessing the energy demand of baking bread. Steam tables and Mollier Diagrams help to calculate the required energy for vaporisation.

3.6 Thermal Imaging

Thermal imaging (or thermography) devices measure the temperature of an object by detecting the amount of infrared radiation being emitted from a surface. Thermal imaging cameras are highly specialist devices that include either cooled or uncooled sensors. These sensors have materials imbedded that are sensitive to infrared radiation. The temperature of the object is then inferred by measurement of the wavelength of the radiation received at the detector (Maldague, 2001).

Uncooled sensors operate at close to the lens temperature, whereas cooled sensors are cryogenically cooled devices that can operate at close to absolute zero. Cooled sensors are typically more expensive but typically have a wider spectral response and due to the large temperature difference are much more efficient at filtering out background noise.

By providing the camera with surface information of the material being analysed (i.e. emissivity), internal software within the camera creates an image which graphically displays temperature distribution through use of isothermal contour lines. Thermal imaging cameras can typically map temperature changes of 0.1 °C and can operate in the temperature region of -40 to 2,000 °C and above (Thumann and Mehta, 2008). Accuracy is variable depending on the device used, but is typically within ± 2 °C.

Thermal imaging is a non-destructive, non-invasive method, which is advantageous in a continuous manufacturing environment since analysis can be conducted without affecting production. Historically, a common use of thermography has been to detect faults, for example cracks in buildings, blockages in pipes and faults in electrical circuits. Additionally it has use for non-engineering tasks, such as marine navigation, security systems and for people or building detection by armed forces or police aircraft.

Since 1970 thermal imaging cameras have become easier to use, more affordable and more precise when giving quantitative results, hence they have become suitable for use in thermodynamic analyses (Ingold, 2008). Ibarra-Castanedo *et al.* (2004) discuss analysis techniques of thermography – focussing on pre-processing and post-processing to ensure that defects in the image are detected. Use of thermal imaging for estimating heat transfer from a surface is described by Stafford *et al.* (2009) where the theory of energy conservation is used to estimate convective heat transfer using a heated thin foil surface. The method resulted in uncertainties in the

accuracy of heat flux measurement, particularly for high values of heat transfer coefficient. However, the results showed good accuracy (within $\pm 13\%$) when secondary heat transfer mechanisms were accounted for – natural convection, conduction and radiation.

Chapter 4

Computational Fluid Dynamics

Assessing the energy efficiency of bakery equipment cannot be tackled by a single approach. The use of both computational methods and experimentation in situations where most appropriate can benefit industrial manufacturing, particularly in analysing energy use of process equipment. This chapter addresses the theory behind an important numerical method, Computational Fluid Dynamics (CFD), which is a computing tool used to predict fluid flow.

CFD creates discretised forms of partial differential equations for fluid flow to solve the governing equations algebraically at a predetermined number of points that are specified by a grid of elements formed within a geometric boundary. CFD is described as “the analysis of systems involving fluid flow, heat transfer and associated phenomena such as chemical reactions by a means of computer-based simulation” (Versteeg and Malalasekera, 2007). It is a technique that has been used across a wide variety of industries since around the 1960s – most notably the aerospace industry.

The advantages of using CFD techniques are numerous. Predominantly, it can result in time and cost savings in engineering design, but it is also used for addressing operational issues with equipment, conducting parametric studies, predicting flow in regions inaccessible to experimental measurements, and visualising flow fields (Donald F. Young *et al.*, 2010). CFD is an analysis mechanism that should be used in conjunction with, rather than instead of experimental measurement.

The proving, baking and cooling stages of commercial bread production all use airflow to transfer heat and/ or mass to/ from the product, making the application of CFD an appropriate method for analysing all three processes with respect to

energy. Bread manufacturing plants are highly automated and therefore access to operating equipment is severely restricted, making it intrinsically difficult to conduct experimental measurements. Strict rules regarding unnecessary use of instrumentation in the vicinity of ingestible food products limit opportunities to conduct experimental measurements on functioning machinery (Kress-Rogers and Brimelow, 2001). These factors, coupled with the reluctance of bakeries to shutdown plants due to the adverse economic impact of doing so, mean that often a non-invasive form of measurement is more suitable for analysis. CFD is a good example of a non-invasive analysis technique.

4.1 Background

The history of CFD can be traced back to the early part of the 20th century, when Richardson (1910) used hand calculations by workers performing up to 2,000 operations per week to analyse the structural integrity of a 6 m high masonry dam. This is the first recorded instance of a scientist/ researcher dividing an object into cells and performing individual calculations at a predefined number of point to estimate local stress distribution properties. The same author went on to later use the same methodology on fluid flow to attempt to predict the weather (Richardson, 1922).

Many consider the first rigorous numerical simulation of fluid flow as the prediction of a flow field around a two-dimensional cylinder for Reynolds numbers of 10 and 20 (Thom, 1933). This study used an iterative series of hand calculations at a set number of points on a square grid to produce a visualisation of streamlines of equal velocity. Kawaguti (1953) notably spent 18 months with a hand calculator for 20 hours per week for a similar study on a cylinder for a higher Reynolds number, $Re = 40$. It was around this time that the early forms of computers were in development and so the prospect of more complex problems (for example three-dimensional flow, non-uniform geometries etc.) could be envisaged.

The next major breakthrough in development of CFD was when the “Marker-and-cell method” was developed in the 1960s. This allowed computers to graphically display fluid simulations – a method that has remained in use since (Harlow and Welch, 1965). The arbitrary Lagrangian-Eulerian methods were developed around the same time and combined the Lagrangian and Eulerian equations to increase the efficiency of the calculations being performed. This also allowed more parameters to be accurately predicted, such as heat transfer and interactions between fluids and solids. A key step in CFD development came with the invention of the $k-\epsilon$ turbulence model (Harlow and Nakayama, 1967); these equations were eventually standardised by Launder and Spalding (1974) and have been widely used since. The influential group of scientists from Imperial College London, which included Professor Brian Spalding, Professor Suhas Patankar and Professor Brian Launder, continued to work on a range of improvements to CFD methods, most notably the Semi-Implicit Method for Pressure-Linked Equations (SIMPLE) algorithm (Patanekar and Spalding, 1972), which has become ubiquitous in commercial software ever since.

Over the past four decades computer hardware has advanced technologically and software has evolved to become more user-friendly and efficient. Thus, the application of computational techniques to engineering challenges has become more widespread in diverse industries such as the food sector and is increasingly being used in the design of machinery, products and processes (Norton and Sun, 2006).

4.2 CFD in the Food Industry

CFD has been successfully applied to many parts of the food industry, for example optimisation of the airflow distribution for chilling meat (Kondjoyan and Daudin, 1997), analysis of airflow in sausage dryers (Mirade and Daudin, 2000), improvement in product quality in sterilisation of canned foods (Ghani *et al.*,

1999b, Ghani *et al.*, 1999a) and controlling the temperature profile in the pasteurisation of beer (Augusto *et al.*, 2010). A number of review papers have summarised recent CFD studies in the food industry (Kaushal and Sharma, 2012, Norton and Sun, 2006, Norton and Sun, 2007, Scott and Richardson, 1997, Sun, 2007, Wang and Sun, 2003).

4.2.1 CFD in the Bread Industry

This section reviews a cross section of papers that utilise CFD methods for problem solving in the bread industry, looking predominantly at airflow distribution and heat transfer characteristics in baking ovens. The main findings are summarised for comparison and critical analysis is given to a number of examples where CFD or experimental validation has been used inappropriately or inadequately. The list is not exhaustive, as there are in excess of 100 papers on the subject, but the most relevant and interesting studies are discussed here.

In the bread industry, CFD has been used predominantly for analysis of airflow within baking ovens. For industrial ovens air distribution, air temperature and air velocity are all important factors to maximise heat transfer. Several CFD studies of baking ovens have been previously published, however there are significant issues affecting the accuracy of the results published in literature. Some of the differences in the results can be attributed to varying oven designs, operating conditions and product types. In addition there is also an issue regarding the type of modelling that has previously been used. Much of the modelling has assumed turbulent flow, however in reality, for these types of problems the flow can be transitional which complicates the set of solving equations. Laminar, turbulent and transitional flow regimes have been discussed in section 3.3. For much of the published material little or no effort is made to experimentally validate the results via accurate experimentation, for example by measurement of physical parameters such as air velocity at predetermined points within the baking chamber and comparison with predicted values.

A single zone batch pilot oven has been analysed using CFD and investigates the effect of inside wall temperature on radiant heat transfer (Boulet *et al.*, 2010). The results were validated by using measurements taken with a commercially available heat transfer monitor and showed good agreement to the numerical predications. The results show that for the geometry analysed with low air velocity, radiation accounts for between 80 to 99 % of the total heat flux. Heat flux to the bread is highest at the start of the process when the temperature difference between the dough and oven is greatest, and at a minimum near the end of the oven cycle when the temperature difference is least.

A study was conducted which investigated the effect of changing the location of the electrical heaters in a buoyancy-driven convection oven, similar to those found within in-store bakeries (Navaneethakrishnan *et al.*, 2007). The aim was to find most efficient heater location for uniformity of temperature distribution and air circulation. It was found that heating from the bottom of the oven provided the highest degree of air circulation, however the most uniform heat distribution occurred with the heaters at the top of the oven.

Two papers were published that study, via use of an experimentally validated CFD model, airflow in an electrically powered forced convection batch-scale oven. The results show the variation in both air velocity and temperature distribution fields for different positions within the oven. Oven velocity was in the region of 0 to 6 m/s and maximum air temperature was less than 240 °C. Validation was conducted through velocity measurement using hot-wire anemometry which gave an average 22 % calculation error (Verboven *et al.*, 2000a, Verboven *et al.*, 2000b).

Wall temperature, air temperature and air velocity profiles were estimated using CFD for a low-velocity industrial biscuit oven. The air temperature in the oven reached a peak of 245 °C towards the centre of the oven. Temperature profile results correlated closely with experimental ones, however velocity profiles were

more difficult to validate as velocity sensors for hot conditions were not easily available (Mirade *et al.*, 2004). Although direct velocity measurement of hot gases is often difficult, it is possible to infer the values through pressure measurements, for example through use of a pitot tube and manometer. It is also possible to use specialised hot-wire anemometers for velocity measurement in baking ovens (Therdthai *et al.*, 2004b).

Time dependent bake and broil (or grill) cycles in domestic ovens were studied, showing temperature profiles and heat distribution after 6 and 15 minutes. Temperatures were in the region of 275 °C and natural convection was dominant for driving airflow. There was a more uniform temperature distribution during the bake cycle due to increased convection. Results were accurate compared to experimental trials – within 4 % for the bake cycle and 10 % for the broil cycle (Mistry *et al.*, 2006).

Two journal papers and a section of a book are dedicated to the analysis of a four zone U-shaped indirect-fired industrial bread oven. The papers used both two-dimensional and three-dimensional geometries to investigate airflow within the oven. The air velocity within the oven was typically less than 1 m/s. The two-dimensional analysis found that by altering the temperature profiles across the zones the shape and colour of the bread could be improved (Therdthai *et al.*, 2003). The three-dimensional studies assessed the impact of the baking load on quality attributes such as weight-loss, core temperature and crust colour (Therdthai *et al.*, 2004a). Whilst these quality attributes were not directly predicted by CFD, a range of empirical relationships were formed from experimental measurements conducted in a baking oven operating under 125 different temperature profiles (Therdthai *et al.*, 2002). The results of the CFD analysis showed that energy use can be reduced by 1.4 % and air velocity increased to generate an improved bake profile (Zhou and Therdthai, 2007). A similar oven configuration was analysed, again in two dimensions, which predicted air temperature and velocity profiles of airflow. The

computational simulations correlated closely with experimental results. The internal product core temperature profile was modelled and was found to be approximately linear, however, an 's-curve' (characterised by a large temperature increase in the middle section of the oven and little temperature change in the first and last portion of the baking process) was measured experimentally (Wong *et al.*, 2007).

Ousegui *et al.* (2010) developed a computational model of the baking process which found that convection was the main source of heat transfer for baking bread – a claim disputed by other authors. This model was able to compute moisture content and temperature. Validation was performed by comparing results with published experimental data collected from other authors. The focus of this study was the heating process of the product itself and the main difference between this paper and other related research papers is the author takes into account the porous nature of the bread. It is not practical to model porous dough/ bread fully as development of pore size and location cannot be predicted due to the random distribution of gas cells as they are generated during yeast fermentation, which is largely dependent on the dough formation stage.

A specialised application of CFD modelling is design optimisation; whereby design variables and constraints are identified and software simulates a series of solutions based on these factors. The best solution that is generated in terms of an objective function can then be used to enhance the design of equipment. CFD optimisation is a rapidly growing research area. Therdthai *et al.* (2002) had previously performed an experimental optimisation of temperature profile for the least amount of weight loss (7.88 %) whilst maintaining other quality attributes, such as crust colour. Design optimisation of bread ovens using CFD has been carried out for temperature uniformity to achieve smaller baking times and minimise energy consumption (Khatir *et al.*, 2012a, Khatir *et al.*, 2010, Khatir *et al.*, 2011a, Khatir *et al.*, 2011b, Khatir *et al.*, 2012d).

4.3 CFD Methodology

In order to formulate a CFD analysis three common steps are used: (i) pre-processing (ii) solving and (iii) post-processing.

Pre-processing allows the user to define a problem for analysis and to design a set of conditions for which computer analysis is required to solve. The first step of pre-processing is to define a geometry, which can be one, two or three-dimensional in nature. Geometries can often be imported from computer-aided design (CAD) tools or generated using specialised pre-processing software. From this, the solution domain can be created – this is the area in which fluid flow occurs and the boundary walls prevent flow outwards. A mesh (or grid) is generated from the solution domain, where the volume is divided into smaller shapes, or elements. The solving parameters are set for the problem which affects both the accuracy and processing time of the solution. Finally, boundary conditions (BCs) are applied at the open faces of the volume. BCs are often applied at inlets, outlets, walls and symmetry planes.

A CFD solver firstly checks the pre-processing steps are compatible with the operations and equations that have been applied. The choice of turbulence model is made – turbulence models are sets of equations that have been devised to estimate flow characteristics of unpredictable three-dimensional fluid flow. Turbulence modelling is described in depth in section 4.7. The solution generated will never be exact – the residuals (degree of error) converge to approach the exact solution with an iterative approach. The computing part of the solving phase can use considerable time and resources, depending on: the parameters selected in the pre-processing stage, the quantity and quality of the processor(s) used and the degree of convergence or stability required for the problem to be considered solved.

Post-processing allows interpretation of results. Due to the magnitude of data that CFD solutions generate, post-processing requires careful thought and

understanding to display results in the most informative format. Results can be displayed in visualised format, numerical results, or graphically. The most common options to display results include:

- Geometry or mesh
- Vector plots
- Contour plots
- Surface or planar plots and x - y plots or graphs
- Particle tracking

Depending upon the problem specified in the pre-processing phase, outputs would usually be flow characteristics such as: pressure, velocity, heat transfer, lift, drag, or many other forces and fluxes.

4.4 Discretisation

Discretisation of the flow domain is necessary to solve the governing equations. Discretisation is used to divide the flow domain into many smaller volumes, which generates a mesh (or grid). Flow domain discretisation and mesh generation is an important part of CFD problem formulation as it determines exactly how many calculation points there will be and therefore the computational demand of the solution process. Mesh refinement at the proximity of the nodes affects the accuracy of the interpolation equations used to approximate the governing differential equations. Generally speaking, regimes of complex flow require fine grids to adequately resolve the large flow gradients associated with rapidly varying flow fields.

Meshes can be one, two or three-dimensional, depending upon the nature of the flow problem. The mesh is made up of cells containing nodes at which the flow variables of interest will be determined. Solving discretised forms of the governing flow equations at each of these nodes allows the flow variables (for example velocity, pressure etc.) to be approximated. Interpolation between each node then allows surface plots of the flow variables to be generated. Depending on the

discretisation method chosen, the governing equations must be expressed in either integral or differential form. The three main discretisation methods are the Finite Difference Method (FDM), the Finite Volume Method (FVM) and the Finite Element Method (FEM).

4.4.1 The Finite Element Method

The FEM is often used in structural engineering or fluid dynamics problems where the fluid is interacting with a solid medium. The method uses shape functions to divide the geometry into a fixed number of elements (Zienkiewicz *et al.*, 2005). The discretised equations of fluid flow are interpolated across each element to approximate a solution for nodes – this approximated solution is in the form of a set of algebraic equations which then require solving to determine the solution across the fluid volume. Commercial analysis software codes that use FEM include COMSOL (COMSOL, 2012).

4.4.2 The Finite Difference Method

The FDM is the oldest discretisation method and is typically best suited to structured meshes where the elements are less irregular. The method uses Taylor series expansion to approximate the finite differences using the governing equations (Tu *et al.*, 2008). The FDM is generally only used for specialist CFD problems and is not frequently used in commercial software.

4.4.3 The Finite Volume Method

The FVM is the most popular method used in general purpose CFD packages. The geometry is divided into a series of cell volumes and the flow variables are applied to the centre of each element (nodal point) (Versteeg and Malalasekera, 2007). Integral forms of the governing flow equations are solved across each element. The FVM is used in software applications such as ANSYS Fluent and OpenFOAM (ANSYS Inc., 2009, OpenCFD Ltd., 2012) and is the most popular discretisation method as it conserves mass, energy and momentum at a cell level, which ensures

that these same three quantities are also consistently conserved for any given control volume.

4.4.4 Mesh Generation

The quality and efficiency of a mesh is highly dependent on the meshing software used and the skill of the operator generating the mesh. Meshes can be broadly categorised as ‘structured’, ‘unstructured’ or ‘hybrid’. Structured meshes, see Figure 4.1 (a), have uniformly-shaped elements applied across a volume, which simplifies the calculation matrices as better approximations to derivative terms in the governing flow equations allow for quicker and more accurate results. Unstructured meshes, see Figure 4.1 (b) are created out of different sized shapes fitted together and can be applied with greater ease to geometries with step changes. Structured meshes are more accurate but less geometrically flexible and vice versa for unstructured meshes. Hybrid meshes combine both structured and unstructured methods to allow the user to select an area to have either uniform or non-uniform elements which are combined together computationally into a single mesh (Thompson *et al.*, 1999).

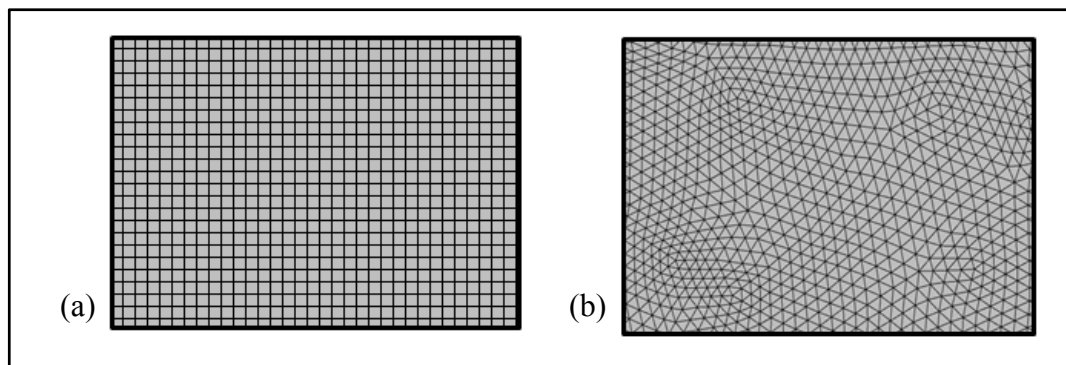


Figure 4.1 – Diagram of two-dimensional meshes: (a) structured and (b) unstructured

Three-dimensional meshes can be created using a variety of different element shapes depending on the relevance to the geometry in question – a selection of the types of shape that could be used are shown by Figure 4.2. Different mesh generation techniques may result in use of any type of polyhedral element.

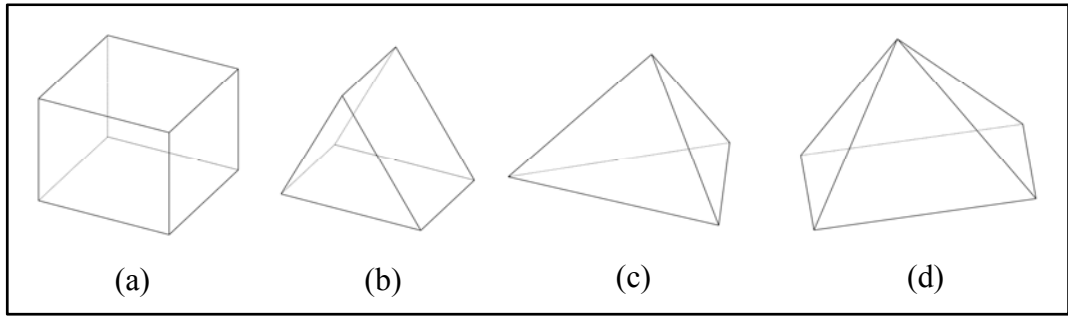


Figure 4.2 – Three-dimensional elements commonly used for mesh generation:
(a) hexahedra, (b) tetrahedra, (c) extruded triangles and (d) pyramids

4.5 Governing Flow Equations

CFD software uses algorithms to solve discretised forms of the governing equations of fluid flow for a designated geometry and set of BCs. The governing equations relate to three fundamental principles of fluid flow:

- Conservation of Mass: states that the rate of change of mass is equal to the net inflow of mass.
- Newton's Second Law: states that momentum is conserved.
- The First Law of Thermodynamics: states that energy is conserved in a closed system.

Explicitly, the Navier-Stokes flow equations for a compressible Newtonian fluid are expressed below in Eq. (4.1) to (4.5) for mass, x , y and z momentum and energy:

Mass:
$$\frac{\partial \rho}{\partial t} + \nabla \rho \mathbf{u} = 0 \quad (4.1)$$

where \mathbf{u} is a velocity vector (m/s).

x -momentum:
$$\frac{\partial(\rho u)}{\partial t} + \nabla(\rho \mathbf{u} u) = \nabla(\Gamma_M \nabla u) + S_{Mx} \quad (4.2)$$

where u is velocity in the x -direction (m/s), Γ_M is fluid viscosity (Pa·s) and S is the source term.

$$\text{y-momentum: } \frac{\partial(\rho v)}{\partial t} + \nabla(\rho v \mathbf{u}) = \nabla(\Gamma_M \nabla v) + S_{My} \quad (4.3)$$

where v is velocity in the y -direction (m/s).

$$\text{z-momentum: } \frac{\partial(\rho w)}{\partial t} + \nabla(\rho w \mathbf{u}) = \nabla(\Gamma_M \nabla w) + S_{Mz} \quad (4.4)$$

where w is velocity in the z -direction (m/s).

$$\text{Energy: } \frac{\partial(\rho T)}{\partial t} + \nabla(\rho T \mathbf{u}) = \nabla(\Gamma_T \nabla T) + S_T \quad (4.5)$$

where Γ_T is thermal conductivity (W/(m·K)).

The conservative form of the Navier-Stokes equations relating to the three fundamental principles of conservation of mass, momentum and energy is shown in vector form by Eq. (4.6), where the application of the scalar variable, ϕ , is interchanged depending on the principle applied.

$$\frac{\partial}{\partial t}(\rho \phi) + \nabla(\rho \phi \mathbf{u}) = \nabla(\Gamma \nabla \phi) + S_\phi \quad (4.6)$$

For application of Eq. (4.6) to Eq. (4.1) to (4.5), ϕ is substituted by 1, u , v , w and T respectively. The conservative transport equation is taken from Versteeg and Malalasekera (2007), who also describe the equation in words:

Rate of increase of ϕ of fluid element	+	Net rate of flow of ϕ out of fluid element	=	Rate of increase of ϕ due to diffusion	+	Rate of increase of ϕ due to sources
---	---	---	---	---	---	---

4.6 Boundary Conditions

BCs are applied at flow domain boundaries to give the solver start and end conditions that are necessary to compute the flow parameters within the computational domain. The importance of setting realistic BCs should not be underestimated – BCs that do not accurately represent the engineering problem

being analysed are highly unlikely to give results that can be experimentally validated.

The standard BCs available in most commercial CFD codes are listed below:

- Inlet: velocity, pressure, mass flow rate
- Outlet: velocity, pressure
- Wall
- Symmetry

The above selection of BCs will be suitable for the vast majority of CFD studies; indeed most problems will only have inlets, outlets and walls, with symmetry planes where applicable.

The magnitude and direction of flow at the inlet are the two key factors when specifying an inlet BC. Inlet BCs should be set so that the profile across a surface or edge is reflective of reality, for example some inlets may have uniform magnitude across a surface, whereas others may vary across a face (2 dimensions) or edge (1 dimension). The level of turbulence should also be quantified at the inlet BC. The presence of an inlet BC suggests mass flux into the fluid domain; therefore for steady state simulations, in order to comply with conservation of mass, an outlet BC must also be located within the fluid domain to expel an equal amount of fluid.

Positioning of outlet BCs can have an important influence on the results of the computational model – this is classically illustrated by “a backward-facing step flow problem” study where a velocity inlet was placed opposite a pressure outlet, the study was repeated for three different distances between the step and the outlet (Tu *et al.*, 2008). The author described the three scenarios, from the outlet being closest to the step to the outlet being furthest from the step: (i) unrealistic (ii) poor accuracy and (iii) good accuracy – where for good accuracy the distance between the step and outlet was greater than 10 times the step height (Tu *et al.*, 2008).

4.7 Turbulence Modelling

Turbulent flow is described as “unsteady irregular, seemingly random and chaotic” (Pope, 2000). Modelling turbulent flow is conducted by application of simplified equations that model the effect of turbulence in an average flow field, which are used in conjunction with the Navier-Stokes governing equations outlined in section 4.5. The choice of turbulence model affects the accuracy of results and processing time.

The majority of turbulence models use the RANS method to investigate turbulent effects on the average flow field. RANS equations are time-averaged (steady state) and are used in conjunction with a turbulence model in order to compute turbulent flow characteristics. Models that use RANS equations and are discussed below are: the standard k - ε model (Launder and Spalding, 1974), the Re-Normalisation Group (RNG) k - ε model (Yakhot *et al.*, 1992), the realisable k - ε (RKE) model (Durbin, 1996), and the k - ω model (Wilcox, 1988), all of which are two-equation models. RANS models can only be used for fully turbulent flow.

The standard k - ε model (Launder and Spalding, 1974) was mentioned in section 4.1 as a breakthrough in CFD development. Turbulence is described with two variables: k (turbulent kinetic energy) and ε (turbulent dissipation rate), which enables computation of both turbulent stress and the turbulent viscosity. The k equation is an exact definition, whereas the equation for turbulent dissipation rate is derived experimentally from correlations. It is the one of the simplest turbulence models to implement and has been widely applied to industrial applications, including instances of both confined and free-flow for low pressure gradients. It is considered by most to be the most established and validated CFD turbulence model. Occasions where this model has been previously found to be lacking in accuracy include unconfined flow with large pressure gradients (such as compressors), and when coarse meshes are specified in the near-wall region (Bardina *et al.*, 1997).

Despite the advantages of the standard $k-\varepsilon$ model, it is not recommended for cases with flow impinging on surfaces, since the turbulence energy may be over-predicted at the stagnation point (Durbin, 1996). An improvement for such flows is the RKE model since it can be used for high Reynolds number flows in complex geometries (Shih *et al.*, 1995). The RKE model can also be used for flow through round jets. There are two key differences between the standard and realisable models: (i) changes to the definition of dissipation rate, ε , which improves the predictions of energy transfer and (ii) a new formulation for variable eddy-viscosity via the addition of a variable, C_μ . The model has been substantially validated for most flow regimes; the main drawback of the RKE model when compared with the standard model is that the solution is considered less stable (Andersson, 2012).

The RNG $k-\varepsilon$ model is a variation of the standard $k-\varepsilon$ model which accounts for the effect of both small and large scale turbulence (Yakhot *et al.*, 1992). The mathematical algorithms incorporated into the RNG method varies the length scale in the turbulent dissipation equation, thus allowing both small and large scale eddies to be predicted, which gives better approximations for swirling flows. The RNG model can also be used for flow regimes with lower Reynolds numbers; however caution is advised when doing so, due to near wall effects. However, unlike the RKE model there is no improvement on the standard model for flow approximation for impinging fluid jets (Andersson, 2012).

For turbulent flow with low Reynolds numbers the $k-\omega$ model is most suited, where ω is turbulence frequency (Wilcox, 1988). This model was predominantly developed as a way to predict shear dominated flows – particularly for fluid jet configurations. The $k-\omega$ model also has good accuracy at high Reynolds numbers and has a similar processing time as the other RANS turbulence models described above. The main disadvantage of this model is that for reliable results the mesh needs to be fine due to the lack of any wall function. The shear-stress transport (SST) $k-\omega$ model, developed by Menter (1994), is similar to the standard $k-\omega$

model but includes elements of the $k-\varepsilon$ model to simulate flow in the free-stream region of the fluid flow. This gives the advantages of both aforementioned methods, however it has a tendency to over-predict turbulence at stagnation regions (Andersson, 2012). This is important for modelling the manufacturing of bread as frequently impinging jets are used to process bread in both the proving and baking phases.

4.8 Validation and Verification

It is important for the user of CFD models to realise that any results obtained contain a degree of error and uncertainty, and a crucial part of CFD is recognising the degree of both error and uncertainty before using or presenting the results. Uncertainty is related to deficiencies due to lack of knowledge, whereas error is not (Versteeg and Malalasekera, 2007). Validation and verification are two techniques that help quantify the error and uncertainty in a computational model, without which results of a CFD study cannot be relied upon for either quantitative or qualitative results. The European Research Community on Flow Turbulence and Combustion (Casey and Wintergerste, 2000) and American Institute of Aeronautics and Astronautics (AIAA, 1998) provide guidelines that are widely accepted standards for verification and validation of computational modelling.

Validation is the process that confirms whether or not the problem identified can be solved by use of the stipulations specified by the user and that the flow model captures the correct physics, this therefore determines the accuracy of the model. Verification addresses the mathematical legitimacy of the model itself and the degree of accuracy of the solution of the governing equations. The difference between validation and verification was described succinctly by Roache (1998), who used the famous phrase that validation is “solving the right equations”, whereas verification is “solving the equations right”. The types of error that can be expected in CFD analysis are generally classified as: numerical (for example

rounding, discretisation), coding or user errors. Uncertainty can be classified by input (for example BCs or fluid properties) or physical model uncertainties (for example simplifying assumptions).

Validation of a model can be conducted by comparing results to an analytical solution or, where this is not possible, comparison with experimental data. As it is not possible to experimentally measure an entire flow field (hence the application of CFD to do this), validation is often conducted by comparing experimental results at particular points in the flow with the equivalent characteristics computed by the model. Often the most logical way to do this is to measure air velocity or pressure at a series of points and compare this with the computational results.

Verification is more difficult to characterise, as each computational model differs with varying geometries, discretisation methods, turbulence modelling equations, BCs etc. Verification should usually be conducted early in the CFD study cycle – in order to ensure that the problem defined is suitable for the accuracy desired (Oberkampf and Trucano, 2002). One essential part of verification is to conduct convergence studies which assess the suitability of assumptions made, for example the difference between different turbulence models or the sensitivity of changing an inlet BC. One such type of convergence study that is almost always applied to CFD models is a mesh sensitivity analysis. Mesh sensitivity allows the user to analyse the effect of coarser or finer meshes on results, with the aim to reduce the number of elements (and therefore the compute time) whilst retaining as much accuracy as possible. The Grid Convergence Index was suggested as a standardised method for ensuring suitability of mesh selection (Roache, 1994).

4.9 Summary

CFD is an increasingly popular method for predicting fluid flow in industrial applications such as bread manufacturing. It is a powerful tool that can be used for both qualitative analysis of airflow distribution and quantitative interpretation of

results to assess performance in terms of engineering efficacy, product quality and energy efficiency.

The range of industries in which CFD has been applied has diversified enormously since the 1960s, when aerospace companies and academics were developing the first useful CFD studies for analysing aircraft design. The increase in efficiency and usability of CFD techniques, combined with the exponential improvement in personal and cluster-based computing capabilities has meant that in many cases it has become easier and cheaper to analyse using CFD modelling than by manual experimentation. CFD techniques have been shown to provide process improvement in the food industry (Norton and Sun, 2007), as CFD makes it possible to investigate a far wider range of design scenarios than is possible with the traditional build-and-test approach, resulting in significant performance gains (Marcotte and Grabowski, 2008).

The outputs of CFD can be used to drive design and/ or operation of engineering systems with potentially significant benefits in: energy efficiency, reliability, manufacturability or operational quality. Despite the obvious advantages of CFD to applications such as energy efficiency in food processing, care must be taken to ensure that the results generated are applicable to the physical problem identified. A level of attention must be exercised during the problem formulation to ensure that the solution methods chosen are suitable for the practical problem identified – this includes correct selection of turbulence model, BCs and convergence criteria. The final stage of CFD is to ensure the results obtained are representative of the solution desired – this is done by thorough experimental validation and verification, which ensure that: (i) the results bear resemblance to what is expected, and (ii) the methodologies used stand up to theoretical scrutiny. Without thorough validation and verification, the results cannot be relied upon.

Chapter 5

An Experimental and Numerical Investigation of Industrial Bread Proving

As discussed in section 1.3.2, proving is the second key process in bread manufacture and occurs after the dough is mixed and shaped. Although bread provers (also known as ‘proofers’ in some regions) come in a variety of configurations, the overall principle of introducing heat and humidity to the air that surrounds the product remains constant across all designs. The British standard loaf is larger and less dense than many of its foreign counterparts; thus, it contains a larger quantity of yeast and requires a higher degree of fermentation (i.e. more time and more energy). Therefore, the scale of the proving process is larger and more critical than elsewhere.

Provers have a heat supply (either by electrical air heaters or gas-fired burners) and a steam supply (either produced by local steam generation units or via a steam ring main and a centralised boiler plant). High flow rates of air are used to distribute heat and humidity to the product, which requires an electrical load to power centrifugal air circulation fans. During the proving process the dough changes in size, density and porosity, although the mass remains approximately constant. The dough temperature increases to approximately 40 °C. The yeast is activated at 35 °C and remains active until the dough temperature reaches 45 to 50 °C in the oven (Gelinas, 2006).

Little research has been published relating to the industrial proving of bread. Of the limited number of publications in existence, the only topics covered address the internal chemical processes within the dough (Chevallier *et al.*, 2012, Chiotellis and Campbell, 2003b, Chiotellis and Campbell, 2003a, Cordoba, 2010, Grenier *et al.*, 2003, Grenier *et al.*, 2006, Grenier *et al.*, 2010, Lucas *et al.*, 2010, Shah *et al.*, 1998). These are almost entirely mathematical models predicting gas cell size

within dough structures. As this project addresses the macroscopic issues concerning energy management of commercial scale provers, these models are of limited use. One reason for the scarcity of research relating to proving technology could be due to the fact that proving processes vary vastly across different regions. Another reason for the lack of scientific research into bread proving technology could be that the prover is a much smaller unit (not necessarily in terms of size but in terms of relative importance, maintenance, capital cost and running cost) than a bread oven – therefore the majority of resource amongst engineers and food scientists has historically been directed towards thermal efficiency of ovens. Despite this, dough proving is still of great significance to the production process as well as being a significant user of energy in an industrial bakery.

This chapter aims to: (i) quantify the energy consumption of a typical industrial bread prover in order that these figures can be used to benchmark energy consumption; (ii) display experimental results of energy use and velocity distribution in an industrial bread prover, and (iii) perform a validated CFD study on a generic prover geometry that is applicable to industrial applications. The results from the CFD study are then used to make recommendations for changes in operating settings for the purpose of reducing the number of air changes per hour, N (/hr), and thus prover energy demand. This study is the first attempt to analyse a prover using CFD and residence time distribution analysis.

5.1 Industrial Bread Provers

Provers can either be ‘L-type’, ‘box type’ or ‘tunnel type’. For large production facilities provers are predominantly L-type. Provers are commonly manufactured with this geometry so that they can fit in the space above an oven to make best use of available space within a bakery. It is assumed in industry that the energy lost through the oven walls and roof is indirectly recovered to provide heat to the prover.

In an L-type prover the bread is initially raised vertically, ①, before travelling horizontally back and forth, ②, before being unloaded opposite the initial start point, ③, as shown in Figure 5.1. Industrial bread provers are typically around 30 to 40 m long (denoted L_x), 4 to 6 m wide in the z -direction (W_z), have loading width (W_x) of between 2 and 5 m and thickness in the y -direction (H_y) of 2 to 4 m.

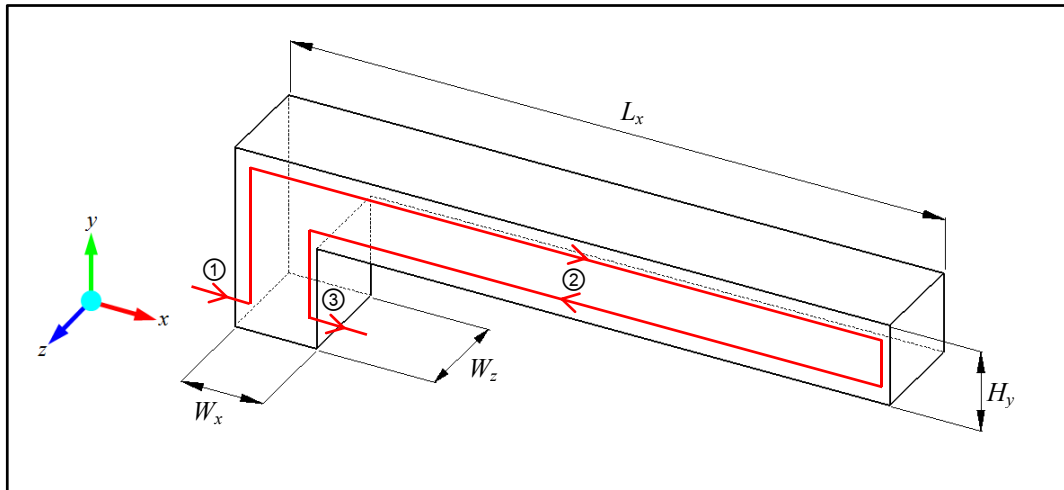


Figure 5.1 – Diagram showing the shape and dimensions of an L-type prover

The air change rate (or number of air changes per hour), N , is the measure that bakeries use to control airflow within the prover. This is a common measurement in building services engineering that defines airflow within a volume – for example to replace the air 10 times per hour ($N = 10/\text{hr}$) in a 1 m^3 box would require a volumetric flow rate of air of $10 \text{ m}^3/\text{hr}$.

Box type provers are cuboid in shape, and have the advantage that the dimensions do not necessarily need to be matched to the oven, although they need to be sized to maintain the same level of throughput. Box type provers are less common in modern bakery environments due to the difficulty of cleaning inside the cavity.

Tunnel type provers describe a system where bread is conveyed through a straight tunnel. These have lower manufacturing costs as they can be positioned without the need to be fixed to a frame above other equipment, but have large footprints as due to their size they are unsuitable to be positioned above an oven. Industrial bakers

have also described them as less energy efficient as indirect heat recovery from heat losses through the oven walls does not automatically occur (Price, 2012).

5.2 Energy Use of Industrial Provers

Proving is one of several important processes for baking bread. It has been previously noted that “proof-boxes” in a large US bakery use around 1.8 % of total site energy usage (Thumann and Mehta, 2008). Moreover, data collected by the Carbon Trust from a number of UK bakeries suggests that 5 % of CO₂ emissions in a bread plant are due to the proving process (Carbon Trust, 2010). Both of these figures represent a substantial impact both environmentally and economically, and so the potential gains by optimising the prover design and operation are of interest to industry. For a typical large UK bakery, consuming 22.5 GWh of electricity and gas and emitting 6,405 TCO₂ per year, the prover is responsible for over 400 MWh and 320 TCO₂ per year. Economically, the yearly cost of this is in the region of £50,000 per prover. In the UK there are more than 90 industrial bakeries and in excess of 100 bread manufacturing lines.

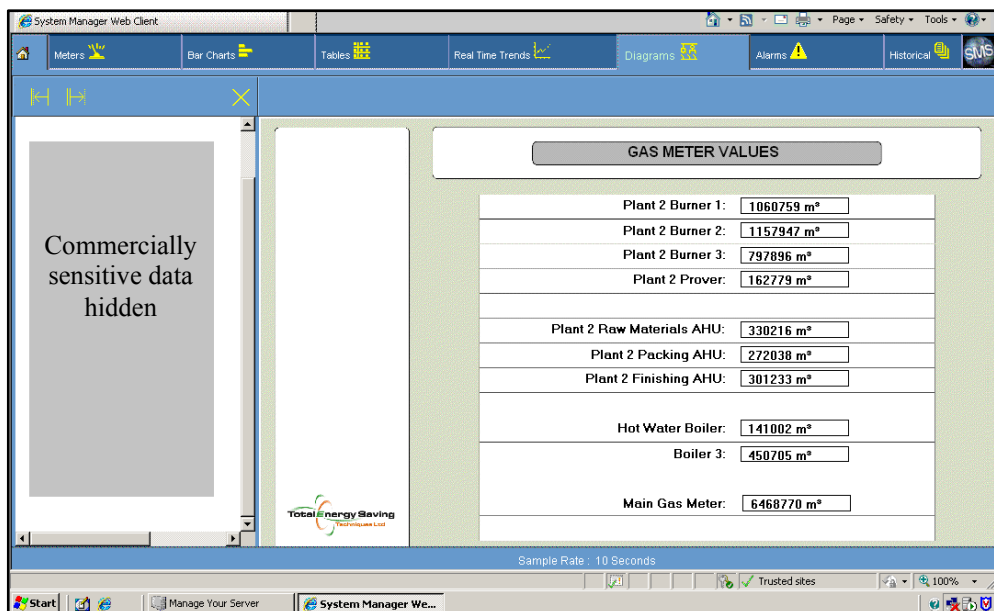


Figure 5.2 – Screenshot of online energy metering system for an industrial bakery

The energy consumption trends of a bread prover presented in sections 5.2.1 and 5.2.2 show new and unique metering data collected from an industrial bakery over

the period of twelve months. The industrial bakery was equipped with online energy monitoring software which read gas and electricity readings at hourly intervals, a screenshot of the software is shown by Figure 5.2 – this data was stored on an online database from which historic data could be extracted and processed – for example to present as weekly totals to show seasonal variations in energy use.

5.2.1 Gas Consumption Trends

Gas-fired burners are used to heat the air within a prover. Figure 5.3 shows the hourly trend for prover gas use over an arbitrary one week period – the week beginning Saturday 1st May 2010.

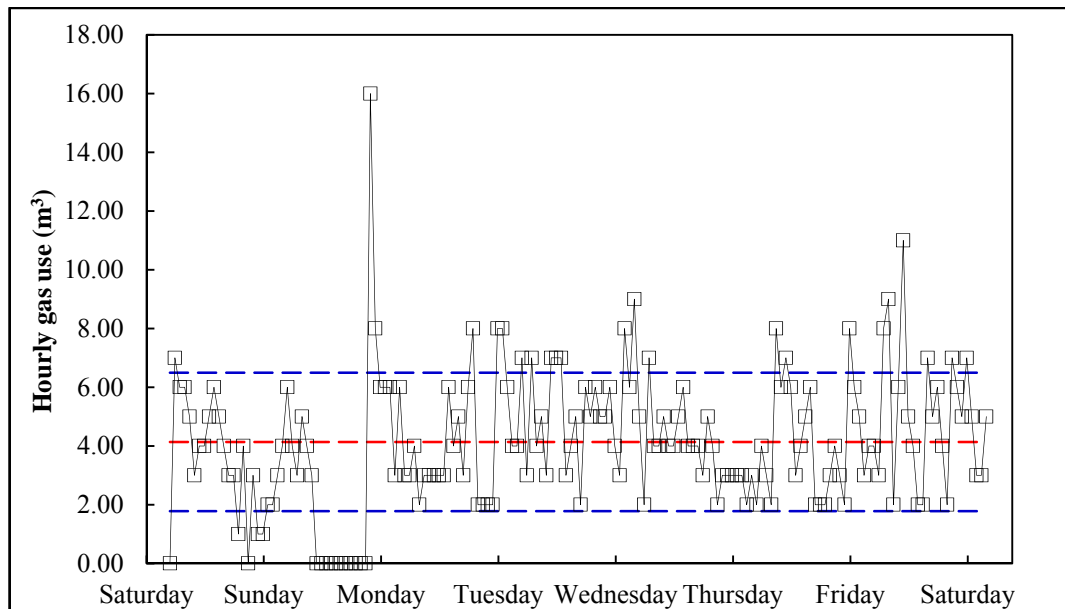


Figure 5.3 – Hourly gas use of a prover over the period of one week with mean hourly gas use (4.1 m^3) shown by red dashed line and the range of values within 1 standard deviation shown by blue dashed line

The most notable peak occurs late on Sunday and comes after a period of shutdown, which had occurred earlier in the day. The heat load required at this time to increase the prover air temperature to operating temperature is three times higher than the mean load; however it is still relatively small compared to other heating processes due to the mild temperature conditions specified in the prover. The graph also shows the range of points within one standard deviation of the mean usage value. The portion of points within one standard deviation of the mean is 77 %

which is a higher percentage than that expected for normal distribution (around 69 %).

Figure 5.4 shows the weekly burner gas consumption over a one year period – between September 2010 and August 2011. The usage trend from week-to-week is erratic, which reflects the flexible nature of the UK bread market. In weeks where supermarket discounts are offered there can often be a production spike. There is no strong trend to suggest that more energy is used in the winter periods, this is due to the bakery internal temperature (and therefore burner air inlet temperature) remaining approximately constant throughout the year largely due to heat losses from the oven.

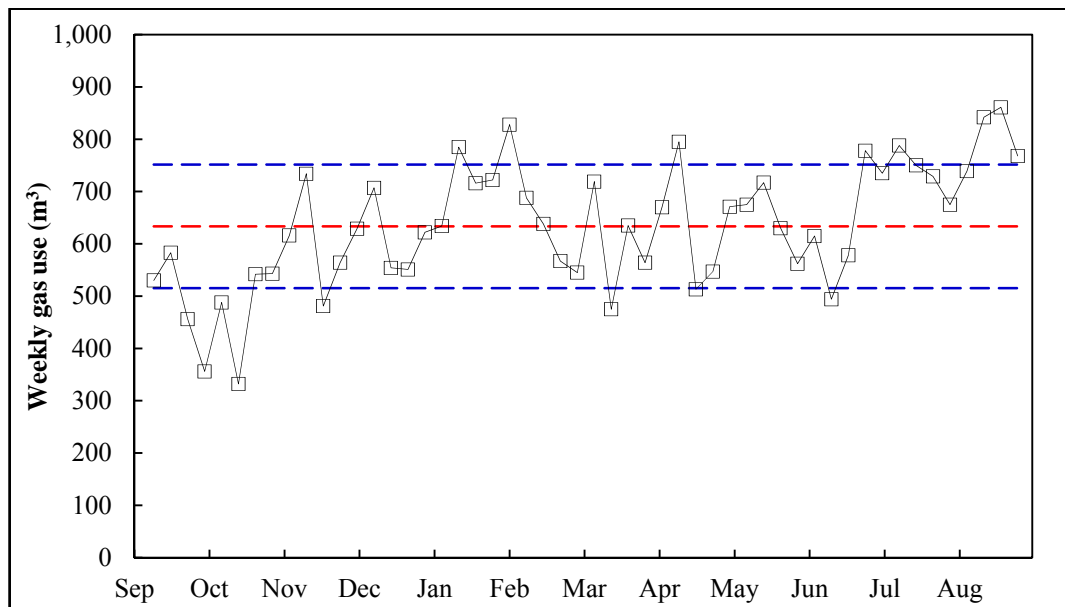


Figure 5.4 – Weekly gas use of an industrial prover over a period of one calendar year with mean weekly gas use (633.4 m^3) shown by red dashed line and the range of values within 1 standard deviation shown by blue dashed line

The mean weekly gas consumption of a prover is $633.4 \text{ m}^3/\text{week}$ and 69 % of values fall within one standard deviation of the mean – indicating normal distribution. When multiplied by the calorific value (or heat of combustion) for gas, $CV_{gas} = 40,000 \text{ kJ/m}^3$, this equates to weekly energy consumption of 25.34 GJ (7,038 kWh). Yearly gas consumption is $33,026 \text{ m}^3$ or 1,321 GJ (367 MWh). The annual financial cost for energy provided to a prover burner is around £9,000 based

on DECC figures of £0.0244/kWh gas (Carbon Trust, 2012b), or in the region of 1% of the capital cost (approximately £1 million). The mean power consumption of the gas burner is 44.0 kW.

5.2.2 Air Handling Unit Electricity Consumption Trends

Distribution of air inside a prover is of critical importance to product quality and the uniformity of the proving profile, particularly across the width of the prover, W_z . Each loaf should be of uniform standard regardless of the position that it enters the prover. If non-uniform air distribution across the prover width were to occur, there would be a difference in product consistency depending on the conditions to which each loaf is exposed. Air handling units (AHUs) are located at the loading end of the prover and supply air via two ducts which run down the prover length, L_x . These ducts are located either side of the centre of the prover, where the warm, humid air is then fed into the inner volume of the prover through vents. The AHUs generate high air pressure in the supply ducts which helps to ensure air is distributed uniformly across the width and length of the prover.

Figure 5.5 shows the constant electricity demand of a prover AHU for the same period as Figure 5.3, with the dip caused by downtime on Sunday when production ceases. It can be seen by comparing Figure 5.3 and Figure 5.5 that the electricity consumed by a prover AHU whilst operational is less variable than burner gas consumption. This is quantified by comparing the distribution of points for electricity consumption and gas consumption, with 95 % of values falling within one standard deviation of the mean for electricity, as opposed to 77 % for gas. The only values that do not fall within one standard deviation are the zero values that occur during the shutdown period.

Figure 5.6 shows weekly electricity consumption of the prover AHU over a twelve-month period. The mean electricity consumption is 3,747 kWh per week with 85 % of values falling within one standard deviation of the mean – again showing the

low degree of weekly change in electricity consumption, which in particular indicates that production fluctuations have little impact upon energy usage. The total yearly consumption is 195 MWh at an annual cost of around £15,000, based on DECC figures of £0.0755/kWh electricity (Carbon Trust, 2012b). This equates to approximately 1.5 % of the capital cost of a prover (~£1,000,000). The mean power consumption of the prover AHU is 23.4 kW.

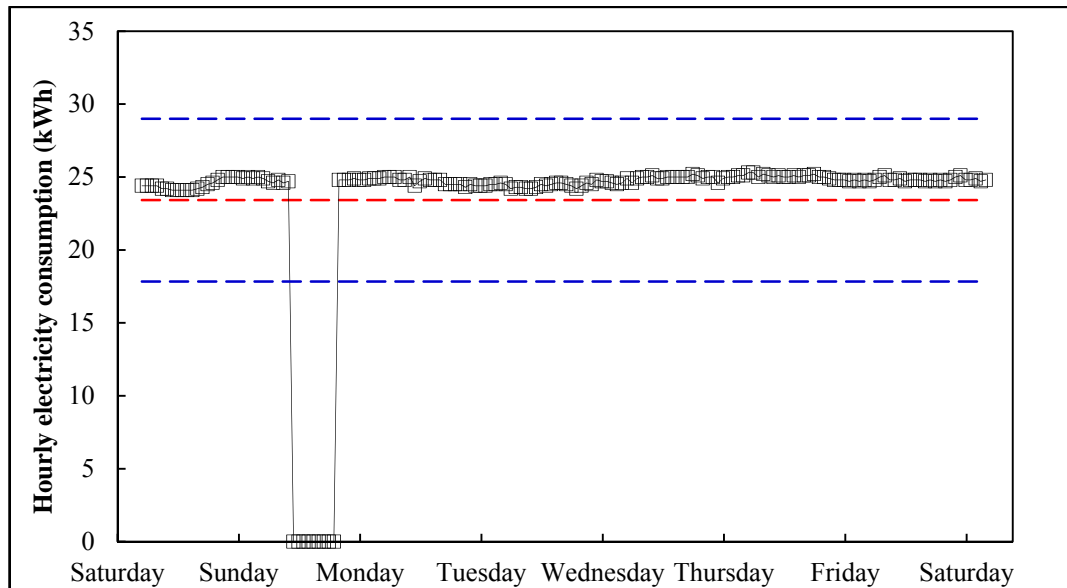


Figure 5.5 – Hourly electricity use of a prover AHU over the period of one week with mean hourly electricity use (23.4 kWh) shown by red dashed line and the range of values within 1 standard deviation shown by blue dashed line

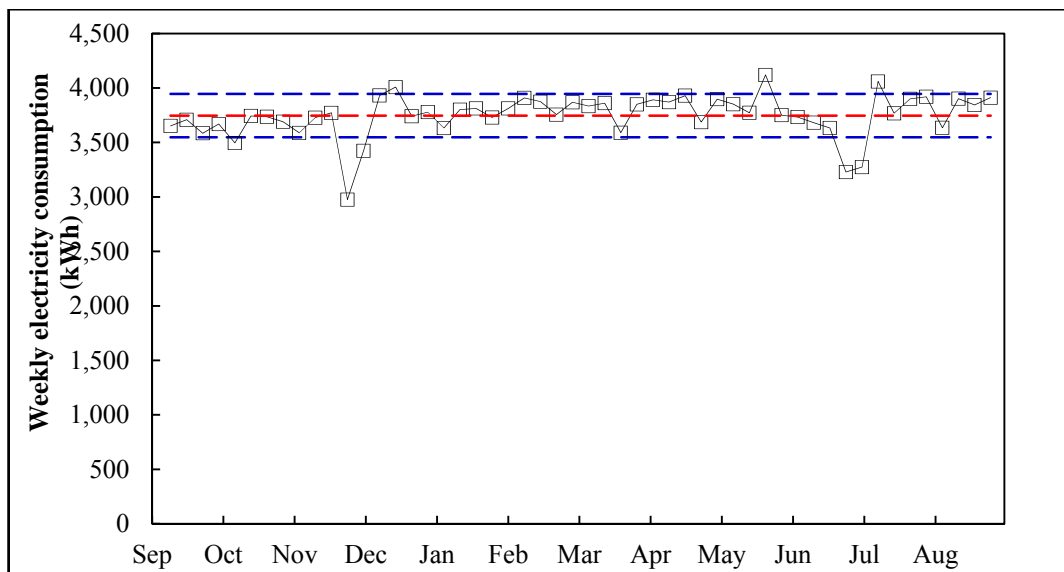


Figure 5.6 – Weekly electricity use of a prover AHU over a period of one calendar year with mean weekly electricity use (3,747 kWh) shown by red dashed line and the range of values within 1 standard deviation shown by blue dashed line

It can be observed that the electricity consumption is constant throughout the year, with two slight drops in late-November and mid-July and peaks in December, May and July. Reasons for the fluctuations in energy consumption have been suggested by industry to be related to production levels (Price, 2012). The drops would be due to production scheduling and/ or maintenance being carried out on the prover at these times. The first peak in electricity consumption, which occurs in December, has been attributed to a peak production period for a bakery due to the Christmas holidays. The other two peaks occur in May and July, which industry suggest could correspond to hot weather weekends during the year, when bread production tends to increase due to more barbeques occurring. Another explanation could be high quantities of produce required for supermarket promotions, causing a substantial short-term increase in production.

5.2.3 Steam Consumption

Steam is injected into the prover air supply duct via a ring-main connected to a centralised steam boiler which also provides steam to other bakery processes, as required. Steam is automatically injected into the prover when relative humidity at the sensor falls below the set point. Manual meter readings taken at the water supply to the boiler over a period of one day at hourly intervals indicate that the steam use of a prover is constant at 0.1 m³/hr of saturated steam at 8 bar (800 kPa) pressure. Therefore, it can be calculated that the quantity of steam supplied to the prover is 100 kg/hour (0.0277 kg/s). Using the industry standard steam tables (Rogers and Mayhew, 1988), it can be seen that the specific enthalpy of saturated steam at 8 bar is 2,759 kJ/kg. Using the resultant specific evaporation enthalpy, the mean steam consumption of the prover was 76.6 kW. Given average rates of shell boiler efficiency of 75 % (Carbon Trust, 2012a), the gas use is approximately 102.1 kW. Again, using DECC figures for cost of natural gas in the UK, £0.0244/kWh (Carbon Trust, 2012b), and operating hours of 159 hours per week all year, the

annual financial cost of the portion of steam generation that is injected into the prover is £21,000.

5.2.4 Overall Energy Usage

The total energy use of the gas burner, AHU and steam consumption is shown by Figure 5.7, which is a culmination of the results presented in previous sections 5.2.1 to 5.2.3. The total energy use is 144.0 kW. The total yearly financial cost of prover operation is in the region of £44,000.

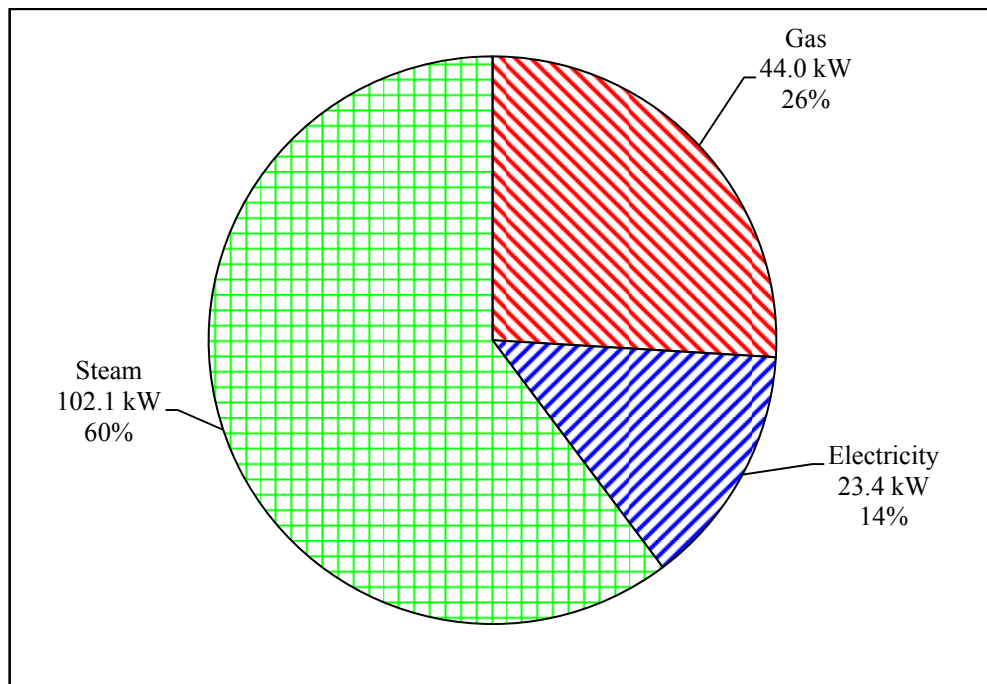


Figure 5.7 – Energy utilisation profile of an industrial bread prover

In terms of CO₂ emissions, the AHU (electricity) energy use has a disproportionately high environmental impact due to the inefficiency of electricity generation and distribution. This is highlighted by the Carbon Trust conversion factors as shown by Table 5.1.

Fuel type	Original unit	Equivalent carbon impact (kgCO ₂ e)
Electricity	kWh	0.544
Natural gas	kWh	0.184

Table 5.1 – Equivalent carbon impact conversion factors for electricity and natural gas (Carbon Trust, 2009)

Figure 5.8 shows the environmental impact of a bread prover, by converting the primary energy use shown by Figure 5.7 into the equivalent mass of carbon dioxide emissions using the conversion factors from Table 5.1. An energy cost profile can provide a financial angle on the impact of energy usage – though this would be mainly of interest to a bakery to analyse the cost efficiency of the process.

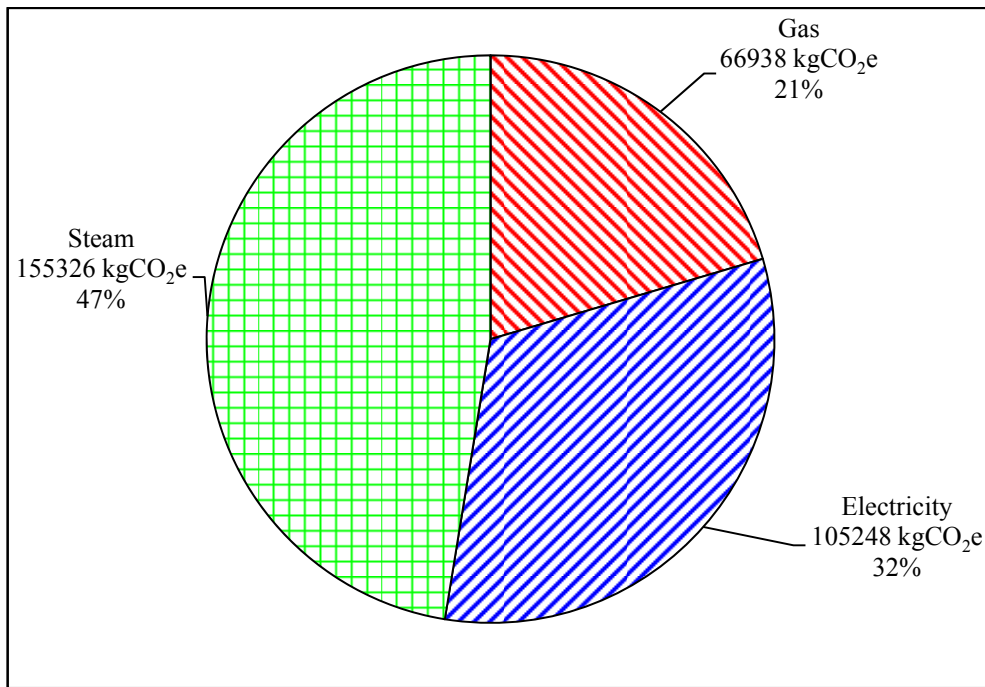


Figure 5.8 – CO₂ emissions profile of an industrial bread prover

5.3 Problem Formulation

The conditions desired within a bread prover are dependent on the type of product. Typically the relative humidity is 65 % and the temperature is 50 °C. Temperature is controlled through modulating the fire rate of the gas burner and humidity is controlled by the amount of steam injection. The key challenge for both prover designers and bakeries alike is to ensure the conditions are constant across the prover width. Currently, to ensure this is the case, provers are over-engineered with large air handing units (AHUs) generating high pressure in the air supply, thereby ensuring airflow is distributed more uniformly. Aside from the energy losses relating to static pressure build-up in the ducts, the high rate of airflow means that a

larger quantity of warm, humid air is expelled to the exhaust resulting in a greater load on the gas burner and higher steam consumption.

5.4 Computational Fluid Dynamics (CFD) Model Design

Balancing temperature, humidity and air velocity distribution in three dimensions in a complex geometry is a difficult task. It is particularly challenging to make measurements and control conditions in a non-invasive and experimental manner. As discussed in Chapter 4, CFD is used to analyse fluid flow numerically and is becoming increasingly popular in the food industry, as it can be a quick, cost-effective and non-invasive form of assessing the operational qualities of a wide variety of food processes (Sun, 2007). Although CFD is a method that has been applied to a wide range of food processes, including both baking and cooling processes in the food industry, the proving of bread is a completely novel application for this type of computational analysis (Paton *et al.*, 2012a). CFD allows bakers an insight into the airflow within a prover which then has the potential to influence more energy efficient prover operation.

The aim of this study is to provide the scientific evidence to encourage the commercial bread manufacturing industry to reduce the number of air changes in provers via use of an experimentally validated computational model. Reducing the number of air changes will reduce prover energy use but will also have an influence on the proving process in terms of product quality and food safety – these factors need to be quantified and offset to provide an energy efficient and quality-friendly solution for industry. This is the first such study to approach prover design and operation from a macroscopic and multi-objective perspective by use of both computational and experimental methodologies.

CFD has been previously used in the baking industry to analyse airflows within ovens for both energy efficiency and process optimisation (Khatir *et al.*, 2012c, Therdthai *et al.*, 2004a, Verboven *et al.*, 2000b). These techniques can be built

upon for the proving process for similar benefit. CFD will be used to study the proving component of industrial bread baking for the first time as there is no previously published work in this field.

5.4.1 Geometry

The prover analysed is a generic geometry developed by working with a commercial prover designer, Spooner Industries Ltd., UK. The box dimensions (refer to Figure 5.1) are: $L_x = 30$ m, $H_y = 5$ m, $W_x = 5$ m and $W_z = 5$ m. The total prover height is 10 m. The internal volume of the prover is 311.2 m³.

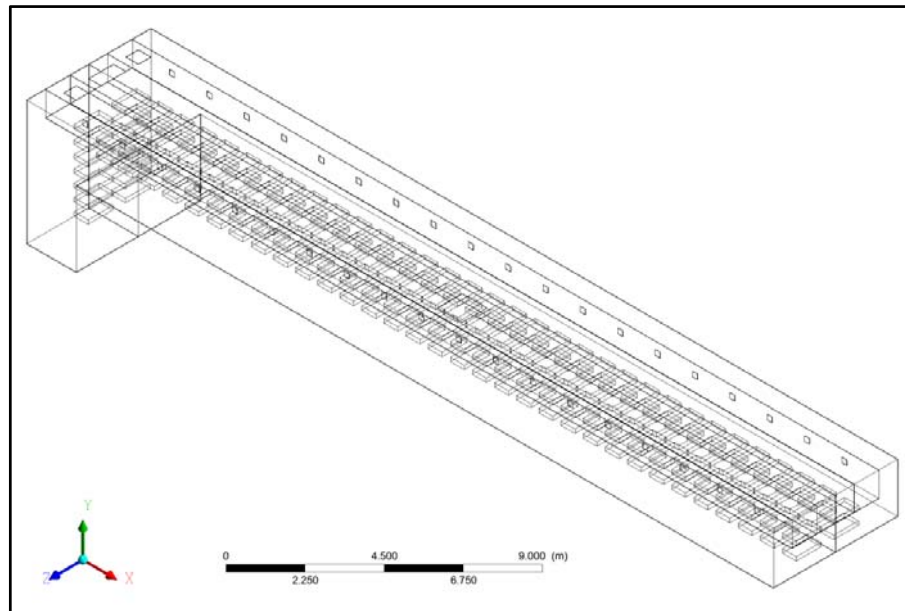


Figure 5.9 – Geometry for prover CFD model generated with assistance from Spooner Industries Ltd. (Kirk, 2011)

A typical throughput for such a prover would be around 8,000 kg/hr with a proof time in the region of 50 minutes. Air is supplied through two full length ducts with 0.2 m x 0.2 m vertical square vents distributed evenly along the prover length at 1.5 m intervals. The bread tins are modelled as solid 0.15 m x 0.56 m x 1 m blocks, and are pitched at 1.5 m intervals. Each block represents 10 tins, referred to as ‘straps’. Straps are attached to swings which are moved by chains to rotate the product around the perimeter of the prover. The computational domain is shown by Figure 5.9. As the swings and chains have a negligible impact on airflow, and the velocity

of the tins is in the region of 0.01 m/s, the assumption is made that the straps are stationary and floating. The arrangement of the three ducts (2 x supply and 1 x return) can be seen by the cross section diagram in Figure 5.10. Also shown in the diagram are the straps of tins and arrows illustrating the intended path of airflow through the prover internal volume.

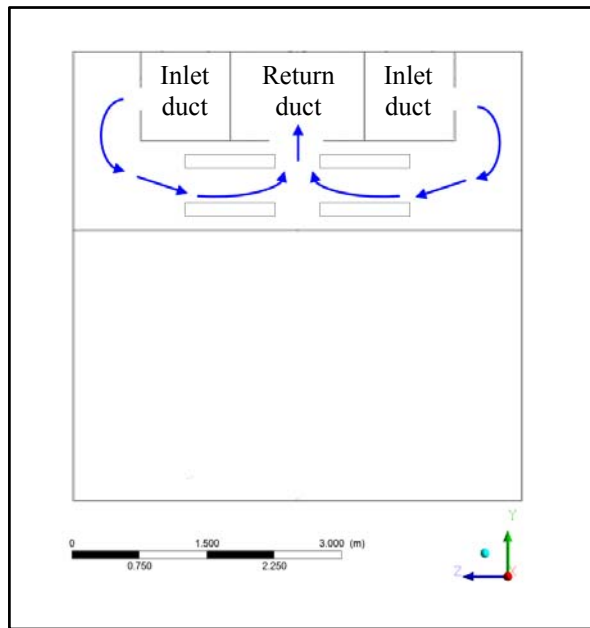


Figure 5.10 – Cross section diagram of prover showing the air ducting arrangement, location of straps of tins and blue arrows illustrating the path of airflow

5.4.2 Turbulence Model Selection

As discussed in section 4.7, selecting a turbulence model is an important part of CFD modelling as it allows the user to generate sufficiently accurate results whilst ensuring that the time to compute is suitable. The intricate geometry of the prover suggests complex flow with impinging jets of air and stagnation points close to the walls and tins. Thus, for this application, the realisable $k-\epsilon$ (RKE) transport model was chosen.

5.4.3 Boundary Conditions

The inlet conditions selected for the model range between a minimum of 10 air changes per hour and a maximum of 100 air changes per hour, as shown in Table

5.2. The Reynolds number for each case is shown, based on characteristic length scale, $L_c = 0.5$ m.

Case number	Number of air changes, N (hr)	Inlet velocity, u_{in} (m/s)	Reynolds number at inlet, Re
1	10	1.73	51,003
2	20	3.46	102,007
3	30	5.19	153,010
4	40	6.92	204,014
5	50	8.64	255,017
6	60	10.37	306,021
7	70	12.10	357,024
8	80	13.83	408,028
9	90	15.56	459,031
10	100	17.29	510,035

Table 5.2 – Inlet boundary conditions for prover CFD model

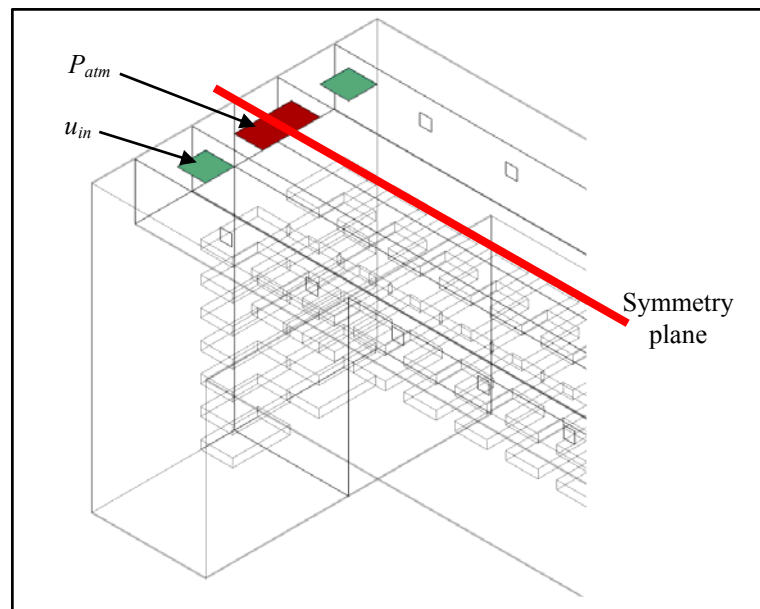


Figure 5.11 – Partial view of prover CFD solution domain showing boundary conditions and symmetry plane

The BCs and symmetry plane can be seen in Figure 5.11. The loading and unloading space is often covered with an air curtain which is brushed aside when tins pass through, and therefore there is no suitable BC to be applied. The model is three-dimensional and utilises a symmetry plane to reduce the processing time. The number of air changes is driven by the inlet air velocity, u_{in} , which is a BC located 0.5 m from the loading end on the top surface of the centre of the supply duct. The

outlet vent, which allows flow into the outlet duct, is in the centre of the return duct. The BC for the pressure outlet, P_{atm} , is located co-planar to the inlet.

5.4.4 CFD Solution Process

The mesh was unstructured and generated using the ANSYS Workbench meshing tool, which uses the Finite Volume Method. Tetrahedral elements were used and the maximum element edge length was set at 0.05 m. Mesh refinement was specified in the areas close to the inlet and outlet at a maximum of half the element size of the rest of the prover, as this is where the highest degree of turbulence was expected. As the temperature was close to ambient and temperature fluctuations within the prover were considered negligible, the solution domain was assumed to be isothermal. Turbulence intensity at the inlet was set at 10 %, assuming a high degree turbulent flow due to the large velocity magnitude and length scale was selected as 0.0175 m based on guidance from the ANSYS User's Guide (ANSYS Inc., 2009). The solution was considered converged once the continuity, $x/ y/ z$ velocity, k and ε residuals reached 10^{-5} , which took approximately 24 hours for each case using a desktop PC.

5.5 Theory of Residence Time Distribution Analysis

Residence time theory was originally developed by chemical engineers to quantify the degree of mixing of fluids inside fluid vessels. The seminal paper on residence time distribution analysis describes flow distribution in mixing tanks through C -diagrams and F -diagrams (Danckwerts, 1953). F -diagrams give the fraction of the fluid flow that is mixed at the outlet with respect to time, whilst C -diagrams display the concentration of injected particles at the outlet with respect to time. For this study, C -diagrams are of more use as humid air is already mixed by the time it enters the prover and more important than the degree of mixing is identification of stagnation regions in the flow. A diagram of a mixing tank for illustration of the physical meaning of a C -diagram is shown by Figure 5.12.

Residence time is important to bread proving as it is directly related to the number of air changes per hour, N , which is the control that industrial bakeries use to ensure the processes meet their own strict criteria as well as important legislative constraints regarding food safety and health, safety and the environment (HSE). It is recommended that bakeries have air changes of at least 20 per hour (Brumbaugh, 2011). The greater the number of air changes, the lower the mean residence time. This results in more energy losses as a result of replacing warm, humid air that has been exhausted to atmosphere and more electricity used by high fan loads.

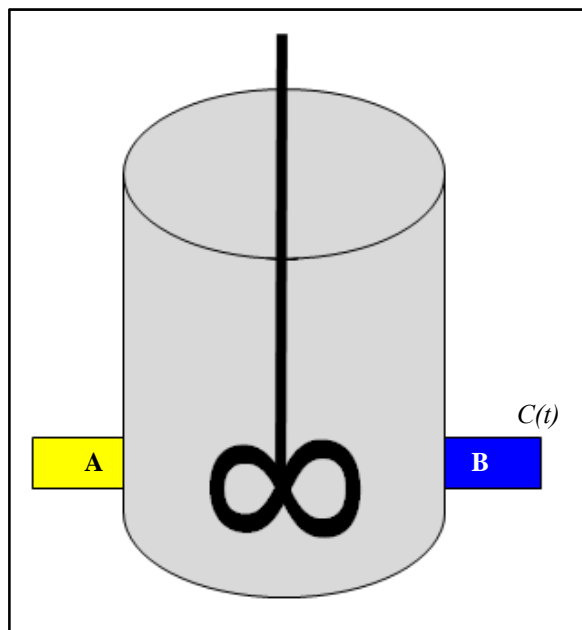


Figure 5.12 – Diagram of a mixing tank showing the concentration of the particles injected at the inlet (A) at the outlet (B) with respect to time

C-diagrams for four representative flow types are shown by Figure 5.13. These four residence time distribution curves can describe most types of regular flow inside a vessel, although in reality fluctuations occur due to irregularities within the fluid domain. Figure 5.13 (a) shows piston flow, which is not possible for Newtonian fluids due to viscosity – for this prover example it would mean that all the flow exits the prover after the same amount of time. Piston flow with some longitudinal mixing, shown by Figure 5.13 (b), is realistically the best case scenario for flow within a prover, as it means all the flow exits the prover within a small space of time. This ensures the flow is well mixed and there are no stagnant zones of

recirculation. Figure 5.13 (c) and (d) show two types dispersed flow. Figure 5.13 (c) is described as perfect-mixing which indicates immediate dispersal of particles upon injection to the volume. Figure 5.13 (d) shows dead water which is undesirable in a food production environment as it causes stagnation regions which can affect both food safety and product uniformity.

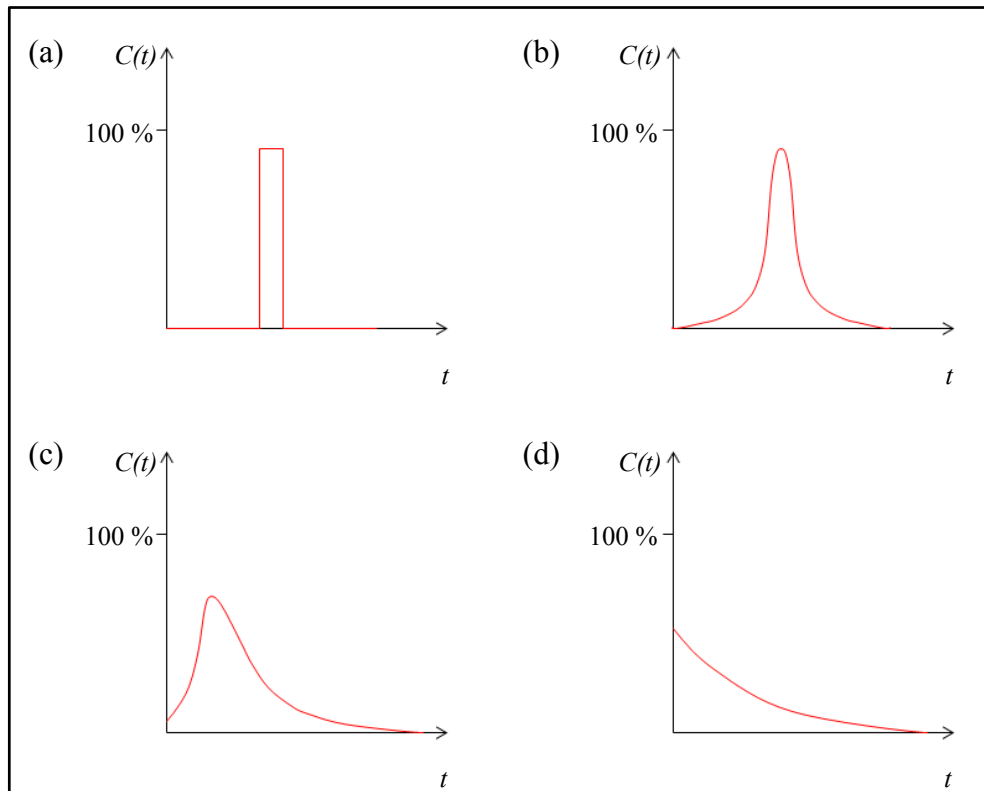


Figure 5.13 – C-diagrams as described by Danckwerts (1953) for: (a) piston flow (b) piston flow with longitudinal mixing (c) complete mixing and (d) dead water

The profile of the residence time distribution curve can be characterised by the exit age residence time function $E(t)$, which is the quantity of fluid that has been in the system for between t and $t + dt$ seconds (Coker, 2001).

In order to generate a residence time distribution curve for airflow using commercial CFD software, ANSYS Fluent has a particle tracking feature which injects a set number of massless, sizeless ‘particles’ into the flow and tracks the path of each one at a set time step and range (ANSYS Inc., 2009). The number of particles passing through the outlet boundary after each time step can be extracted from the software. The time step associated with the particle escaping through the

outlet can be termed ‘residence time’ and therefore a distribution of residence time can be plotted.

5.6 Verification and Validation of Computational Model

Verification of the CFD model is performed via a mesh sensitivity analysis, where the minimum size of the mesh for reliable results is determined. In addition, an experimental validation of the air velocity through the prover air vents is conducted.

5.6.1 Verification of Mesh Generation

The size of mesh (or the number of elements) in a CFD geometry affects the accuracy and processing time of a computational problem. It is important to have a fine enough mesh to achieve sufficient resolution of results without wasting computing resources. Figure 5.14 shows the velocity profile across a prover vent for different numbers of elements.

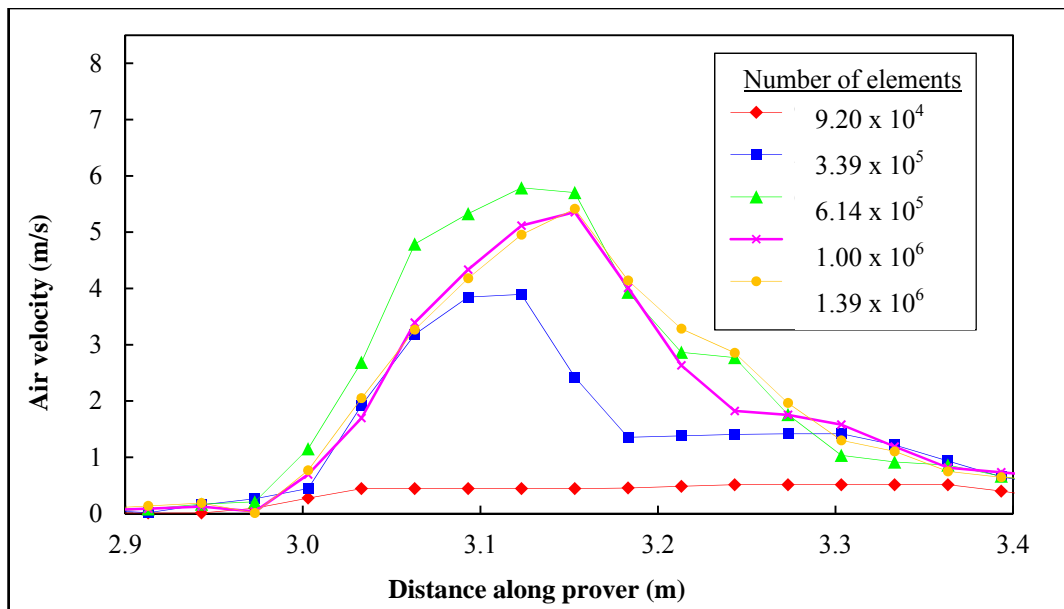


Figure 5.14 – Velocity profile across a single prover vent, the second closest to the loading/ unloading end, for five different mesh sizes/ numbers of elements

It can be observed that the profiles for 9.20×10^4 and 3.39×10^5 elements have qualitatively less accurate velocity profiles when compared to the case with 1.39×10^6 elements, thus implicating strong dependency of the solution on the mesh for

these two cases. The overall correlation between the vent velocity profiles is calculated by Pearson's r coefficient and is shown by Figure 5.15 for the five different mesh sizes. The minimum value of r has been set at 0.975 to ensure quantitative validation. The two coarser meshes shown by Figure 5.14 of 9.20×10^4 and 3.39×10^5 elements had r values of 0.792 and 0.963. Again, it is shown that meshes with more than $\sim 6 \times 10^5$ elements have sufficient statistical correlation ($r = 0.978$) combined with the qualitative agreement shown by Figure 5.14 to be used for analysis. Calculation time for the model with 6.14×10^5 elements was approximately 6 hours. This mesh size has satisfactory velocity profile accuracy and a realistically viable processing time and therefore this mesh was selected.

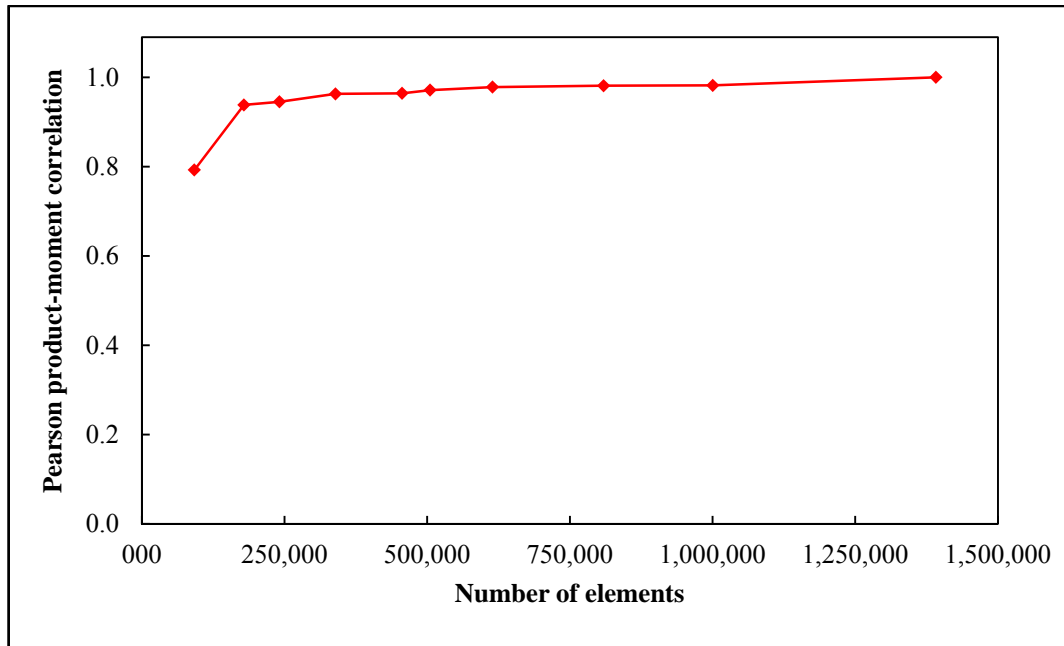


Figure 5.15 – Pearson's r correlation showing correlation with the finest mesh case (1.39 million cells) for velocity profile across a single prover vent

5.6.2 Experimental Validation

Experimental validation of the CFD analyses was carried out by measuring the air velocity at each outlet vent within an industrial prover. The experiments were conducted using a calibrated Testo 405 Thermal Anemometer (Testo Limited, UK). The accuracy given by the original equipment manufacturer (OEM) was ± 0.3 m/s + 5 % of maximum velocity. The velocities measured were in the region of 3.3 to

10.0 m/s therefore the readings could be assumed with an accuracy of within ± 0.8 m/s, giving a percentage error of between 8.00 and 24.24 %.

The experimental measurements of mean air velocity from each duct are compared to the computational predictions in Figure 5.16. A good degree of validation can be inferred from these measurements, with a mean percentage difference of 7.50 % and a Pearson correlation value of $r = 0.798$. The correlation is particularly evident in the half of the prover closest to the loading end, $x < 15$ m, as flow in this region appears to be better predicted by CFD – the mean percentage difference between experimental results and computational predictions was 5.30 %.

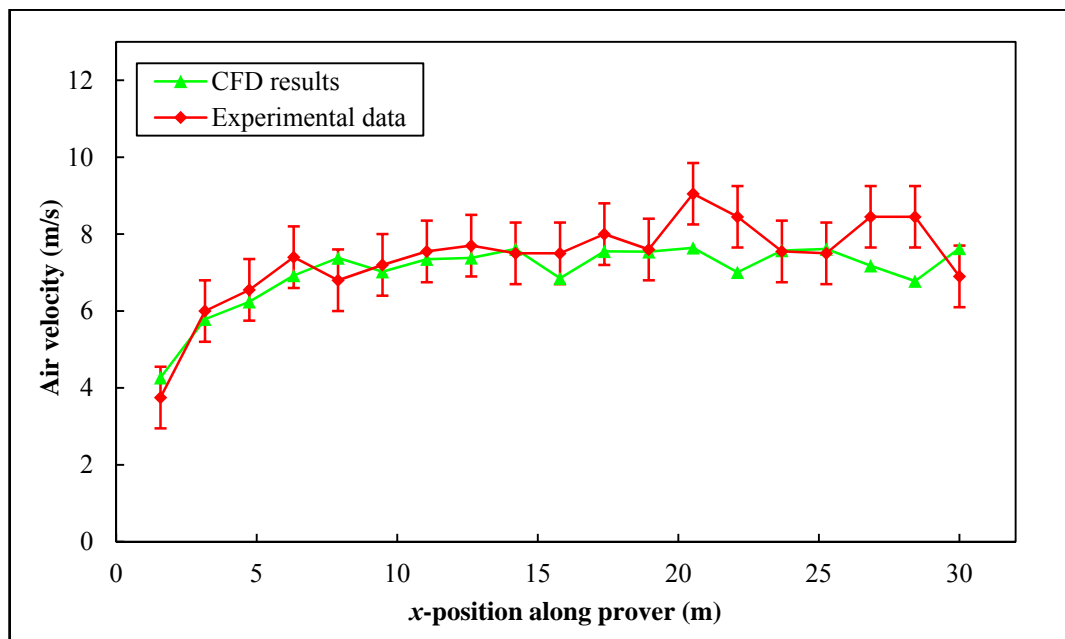


Figure 5.16 – Validation of velocity profile along prover length with error bars representing the experimental error relating to the apparatus used

5.7 Results

The results of CFD can be displayed visually (for example contour plots of air velocity) and numerically (in the form of graphs, tables etc.).

5.7.1 Plots of Velocity Distribution

This section presents results in the form of contour plots and velocity vector plots of air velocity, where yellow/ red colours show high velocity and cyan/ blue

colours represent areas of low velocity. A 3D contour plot of air distribution within the prover volume is shown by Figure 5.17. Nineteen planes normal to the x -axis are shown – one representing each pair of vents on the inlet duct. This plot gives an overall view of velocity distribution through each vent along the length of the prover. High air velocity is evident close to each air vent but especially for the vents in the centre of the prover, whereas low air velocity can be seen towards the loading and unloading areas in the prover and around the straps in the first quarter of the prover. These areas of low air velocity indicate dead regions of stagnant air and can have three particularly adverse effects for bakeries:

- (i) Lower rates of heat transfer to the product as the rate of convective heat transfer is proportional to air velocity.
- (ii) Less uniform air temperature and humidity.
- (iii) Lower air temperature and air velocity, as the stagnant air may cool down and the moisture may condense as it is replaced less often.

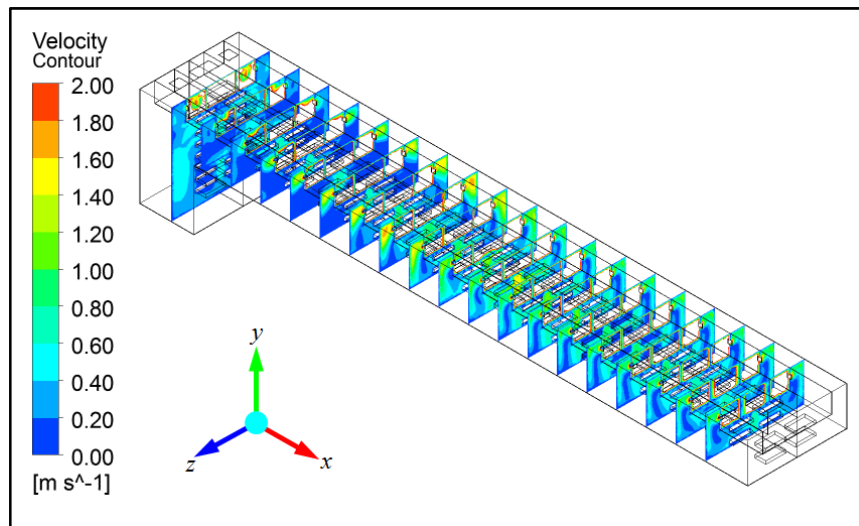


Figure 5.17 – Isometric view contour plot of air velocity illustrating air distribution throughout the prover volume

Figure 5.18 shows the same planes down the prover length from a top view. This contour plot highlights the degree of velocity uniformity at each vent. It can be seen that the air velocity through the central vents in the x -direction are larger than the velocities at both extremities. In addition, the effect of the interaction between

the air jets from the vents and the inside of the prover walls is shown, with air appearing to be artificially steered downwards towards the tins by the right-angled prover geometry. An inner geometry more conducive to directing flow towards the tins could be more applicable in this instance and would make an interesting parametric study with regards to optimising this airflow and assessing the associated additional manufacturing and cleaning costs.

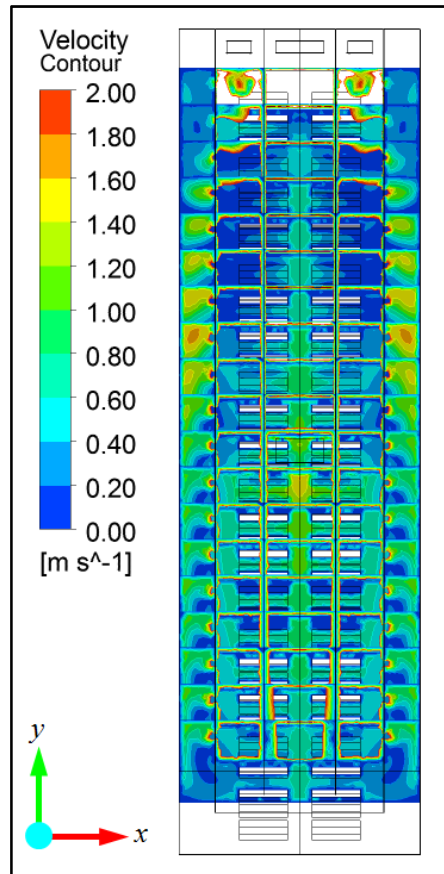


Figure 5.18 – Angled top view contour plot of air velocity showing air distribution down the prover length

The velocity vector plot shown by Figure 5.19 shows the path and magnitude of air through a representative plane parallel to the yz -axis. The high magnitude of air velocity near to the vent illustrates the high degree of turbulence that is present in this area. Furthermore, the comparatively low airflow around the tins that is caused by the prover design with vents facing away from the product. This ensures that the delicate dough is not subjected to high-velocity air jets, which could cause the air cells within the dough to collapse. The vector plot shows that is some substance to

the assumption of prover designers that air deflects off the inside walls of the prover towards the product.

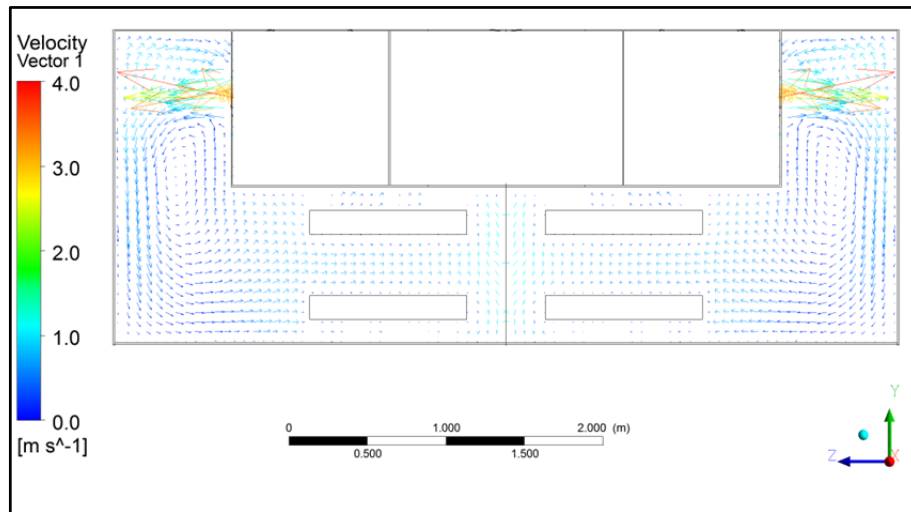


Figure 5.19 – Velocity vector plot of air velocity showing flow paths of air through a prover vent and around the product for the 13th plane parallel to a vent from the loading end

Figure 5.20 shows contour plots of velocity distribution around the tins for two planes perpendicular to the x -axis: (a) parallel to the vent closest to the loading end and (b) parallel to the 13th vent from the loading end. The range of air velocity shown is reduced to $0 < u < 0.8$ m/s allowing further resolution to be shown for areas of low velocity – i.e. to enhance the visualisation of flow around the product. Contour plots of air velocity show similar trends for each of the 19 planes positioned in the centre of an inlet vent down the prover length. Figure 5.20 (a) shows explicitly the regions of low air velocity between the lower tins, indicating stagnation regions at the loading and unloading end of the prover, corroborating the conclusions drawn from Figure 5.17. This will not be a major concern for prover designers, as airflow is deliberately minimised near the loading and unloading ends of the prover to prevent heat and humidity losses to atmosphere. However, it is important to maintain airflow around the tins in the main sections of the prover – in the region shown by Figure 5.20 (b), which demonstrates undesirable stagnation regions above the upper straps and below the lower straps, though this is somewhat mitigated by the uniformity of airflow in between the straps of tins. Both contour

plots also illustrate the interaction between the prover air jets and the wall where prover designers intend to deflect air off the prover wall towards the product.

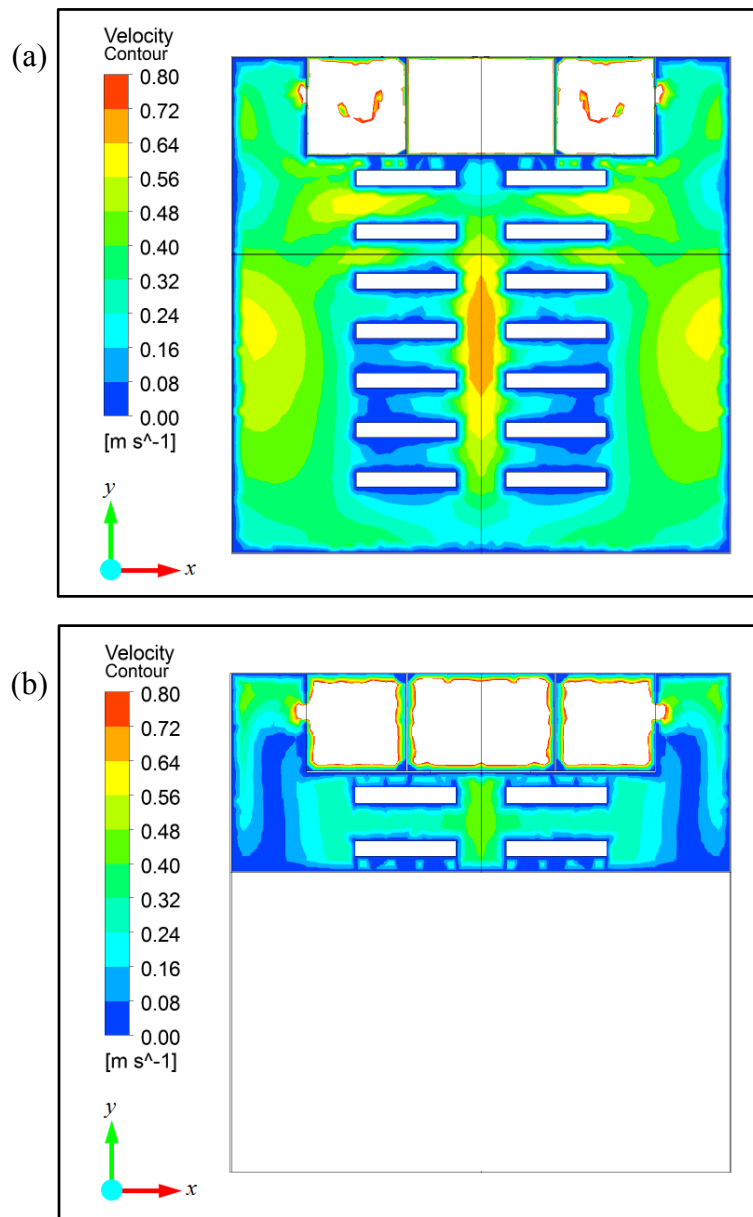


Figure 5.20 – End-on view contour plot of air velocity showing airflow distribution around the tins for (a) the plane closest to the loading end, and (b) the 13th plane from the loading end

5.7.2 Numerical Results

The red line shown by Figure 5.21 is parallel to the xy -axis and in offset from the outlet vents by 5 mm. The air velocity distribution profile down the prover length on this line is shown by Figure 5.22. It is clear to see the peaks of $u > 4$ m/s at for each of the 19 vents 1.5 m intervals along the prover. The peaks are of different

magnitudes due to uneven air distribution through the supply duct. Modifying the internal geometry of the supply duct to force more air through the first three ducts would improve the uniformity of velocity, but may also force more air out of the loading/ unloading areas of the prover and thus contribute towards energy losses. The modification in geometry could be as simple as a decreasing cross section with x which would increase the relative total pressure towards $x = 0$ m and force higher velocities for these vents.

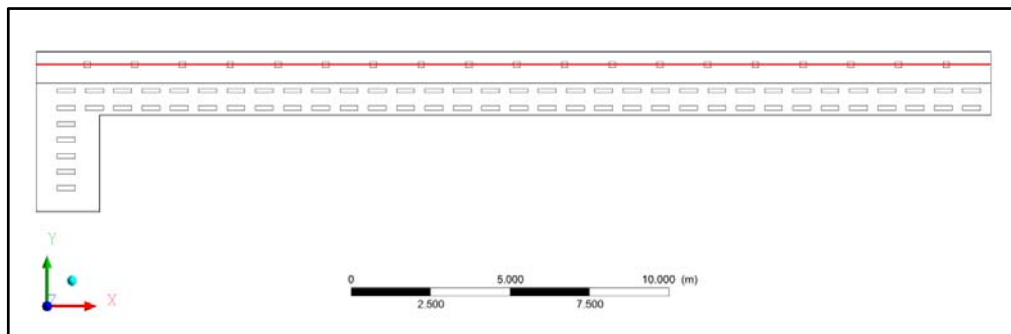


Figure 5.21 – Prover section view from perpendicular to the xy -plane with red line passing through the centre of the air vents offset in the z -direction by 5 mm

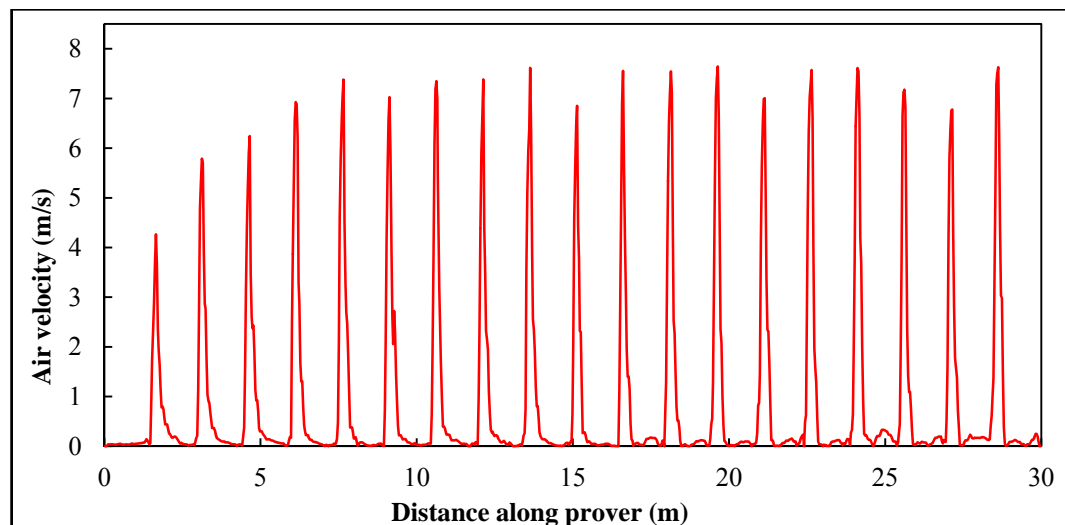


Figure 5.22 – CFD predictions showing the air velocity profile along the prover length for the red line shown in Figure 5.21

5.8 Residence Time Distribution Curves

Residence time distribution curves can be used to verify whether or not the number of air changes is suitable for production purposes. By tracking individual particle flow paths, it is possible to examine overall characteristics of the airflow. If a high

proportion of particles take a long time to escape through the pressure outlet there is a greater chance of a breach in quality standards. The specific standards have not yet been specified quantitatively by a regulatory body; therefore the results of this study could be used to guide future standards for the proving process of bread manufacture.

A typical graph showing the residence time distribution for five cases is shown by Figure 5.23. This illustrates the time taken for each one of 2,469 particles to escape the prover cavity through the outlet after a maximum of 360 seconds. The particles are introduced at the inlet at equally spaced intervals. For all cases, the majority of particles exit the prover within 100 seconds. However, a small proportion of particles have a longer residence time indicating the presence of dead regions and stagnation zones within the flow. More positively skewed residence time distributions will reduce the possibility of mould spores occurring inside the prover, since this shows less proportion of particles stagnating.

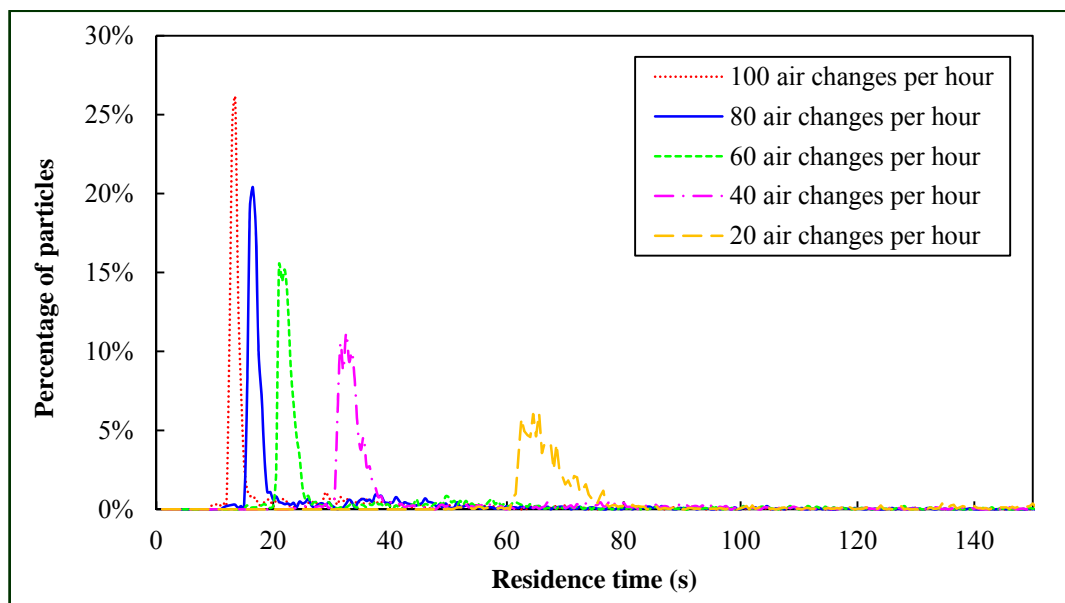


Figure 5.23 – Residence time distribution for 2,469 particles

Mean residence time is of limited use to industry as it does not give an indication as to the residence time distribution spread, which means the prover operator will have little idea as to the portion of air that is stagnant and poses a food quality or

safety risk. Assuming all particles escape the system, there is no change in density and no backflow at the outlet, mean residence time can be calculated analytically by Eq. (5.1).

$$\bar{t} = \frac{V}{\dot{m}_{in}} = \int_0^t t E(t) dt \quad (5.1)$$

A graph showing the analytical calculation of mean residence time alongside the CFD predictions is shown by Figure 5.24. The difference between the two curves, which is greater for lower numbers of air changes, can be attributed to the lower degree of mixing which occurs with lower airflow. The analytical solution will always assume fully mixed airflow. The exponential decrease in mean residence time with the number of air changes illustrates the careful balance of proper airflow which must be tightly controlled to maintain product integrity.

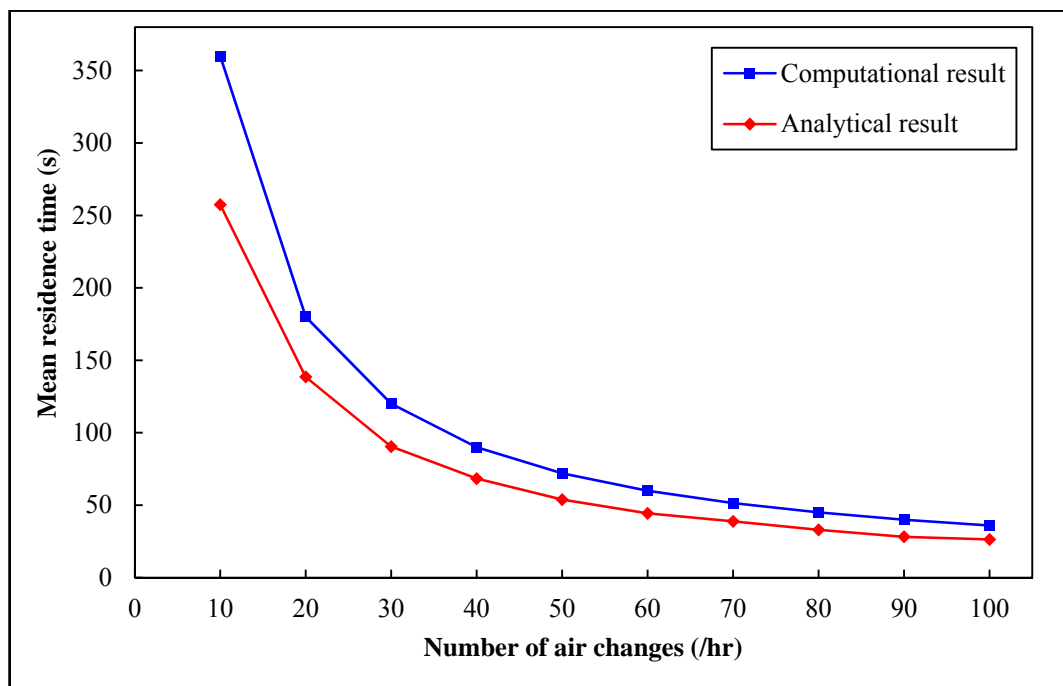


Figure 5.24 – Mean particle residence time as a function of the number of air changes for both analytical and computational solutions

The curve displayed by Figure 5.24 is a typical Pareto front. Pareto fronts are commonly used for analysing trade-offs in optimisation of engineering design to

minimise a particular cost (in this case energy) whilst maintaining minimum standards (in this case product quality and food safety).

5.9 Energy Savings

The stagnation of particles (for example as seen in Figure 5.20 in the loading/unloading area of the prover) is emphasised by the number of particles remaining in the prover after 360 s, as shown by Figure 5.25. Bakers do not typically know the maximum percentage of particles that should have escaped after 360 s, but these results help to give confidence to prover operators when reducing the number of air changes in order to reduce the energy consumption of the prover. It has been suggested by industrialists that less than 1 % of particles remaining inside the prover cavity after 360 s may be an initial estimate to work with, which would immediately enable bakers to initially reduce the number of air changes from 90/hr to 60/hr (Price, 2012).

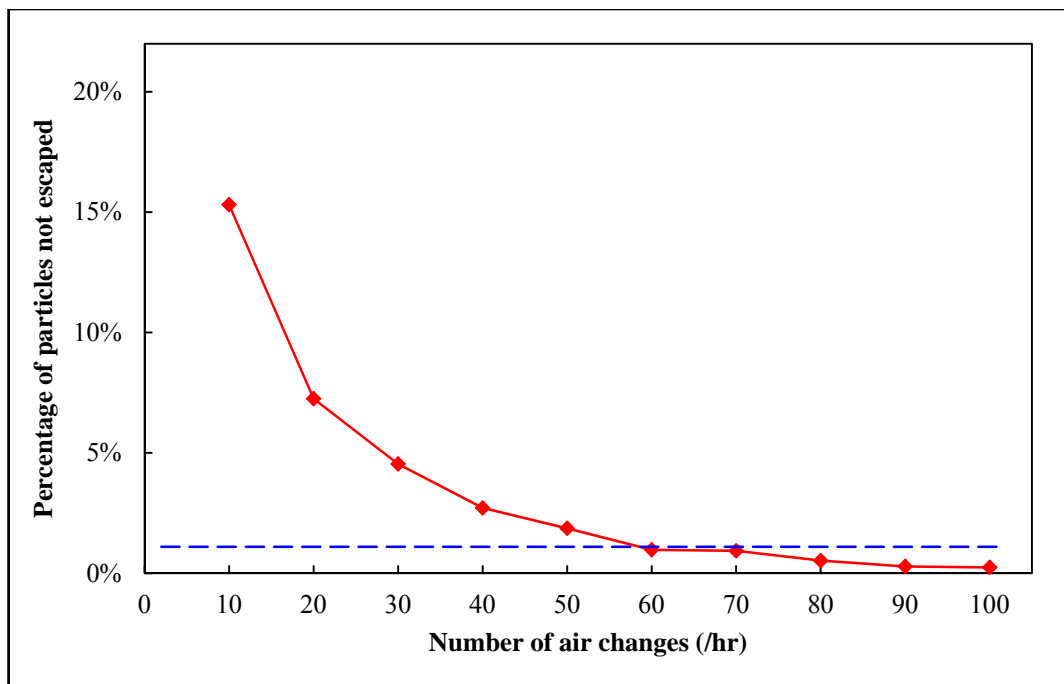


Figure 5.25 – Percentage of particles not escaped the prover cavity after 360 s residence time for each case

With current design, the easiest way to eradicate high residence time is to increase the number of air changes. Equally, for energy savings, adjustment of the AHU to

reduce the number of air changes will reduce the steam, gas and electricity demand of the prover. A reduction in the number of air changes from 90/hr to 60/hr potentially means significant energy savings for the bread industry. Bakeries are trialling this decrease at present as a result of this work and therefore it is too early to prove the year-on-year energy savings based on a full regression analysis. However, engineering estimates of the reduction in electrical load based on theory are possible. Firstly, the quantity of air to be moved by the fans will be 33 % less. By relating this to the power law of fan energy consumption, Eq. (5.2), the required energy can be calculated from the pressure difference between the duct and baking chamber:

$$\dot{E} = \Delta P Q = \Delta P u A \quad (5.2)$$

where the pressure difference, ΔP (Pa), is calculated by the required inlet velocity by using Bernoulli's equation, Eq. (5.3):

$$P_0 = \frac{1}{2} \rho u^2 \quad (5.3)$$

Therefore, if the inlet velocity is reduced by 33 %, the fan power required would be reduced by over 70 %. Gas and steam use will also be lower as a result of a reduction in the number of air changes. However, quantifying these in generic terms is not practical as it depends greatly on the degree of recirculation of air at the return duct specified by individual bakeries.

5.10 Summary

This CFD study has allowed a large amount of quantitative data to be collected without the need for time consuming and expensive experimentation. A generic prover geometry design was developed alongside industrial prover manufacturers to predict isothermal airflow. A parametric study was conducted by varying the number of air changes 10/hr and 100/hr, which are conditions that are realistically feasible for industrial bread proving.

The model has been experimentally validated by measuring air velocity inside an operational prover. The results collected from the CFD model showed strong a correlation with the equivalent measurement points. A mesh sensitivity analysis was performed in order to verify the model, and the element-size beyond which the results converged was identified.

Residence time distribution theory was used to quantify the distribution of number of particles escaped after each time step with respect to the number of air changes which has enabled bakeries to make informed choices about reducing the number of air changes to reduce the energy cost. It has been suggested that the number of particles not escaped after 360 seconds could be used by regulatory bodies to give a quality standard for food safety in the bread proving process to measure the probability of mould spores developing.

The results suggest there is scope to reduce the number of air changes, depending on the product quality specifications dictated by the bakery. The number of particles that remain in the prover after 360 s of being injected is less than 1 % for $N \geq 60$. A reduction from 90 to 60 air changes per hour represents a 33 % reduction in prover airflow. Savings in electricity for this reduction have been estimated at over 70 %. Gas and steam savings are likely to be made possible as a result – a regression analysis would be required to accurately quantify the energy impact of such changes.

Chapter 6

System-Level Thermodynamic Analysis of Commercial Bread Baking Ovens

As shown by previous reports and authors, ovens use half of the energy consumed in the bread manufacturing process (Carbon Trust, 2010, Thumann and Mehta, 2008). It is naturally an area of interest for bakeries to reduce carbon emissions and energy costs. This chapter provides a methodology for modelling baking oven energy use. This system-level model has been widely used in industry to benchmark current ovens, and to identify areas for oven manufacturers to invest in new design in order to improve efficiency of current machinery. The methodology of this system modelling approach has been presented at the Sustainable Thermal Energy Management International Conference 2011 (Paton *et al.*, 2011) and published in Applied Thermal Engineering (Paton *et al.*, 2012b).

The overall aim is to show how a methodology can be developed to drive forward equipment design and influence operating conditions in order to improve energy efficiency of bread baking ovens. The overall methodology enables the most promising opportunities for achieving significant reductions in carbon footprint and financial running cost that can benefit the baking industry to be assessed.

6.1 Oven Configurations

There are two main types of continuous tunnel ovens used in large industrial bakeries; direct-fired and indirect-fired. The important distinction between these two configurations relates to whether combustion products enter the baking chamber. For direct fired ovens the products of combustion do enter the baking chamber, whereas for indirect ovens the products of combustion remain separate from the baking chamber and heat is introduced to the surface of the bread via heat exchangers. Forced convection and ribbon burner are two types of direct-fired ovens. Radiant and turbo-radiant are two types of indirect ovens used in the

commercial baking industry. The differences between direct and indirect ovens are illustrated schematically by Figure 6.1:

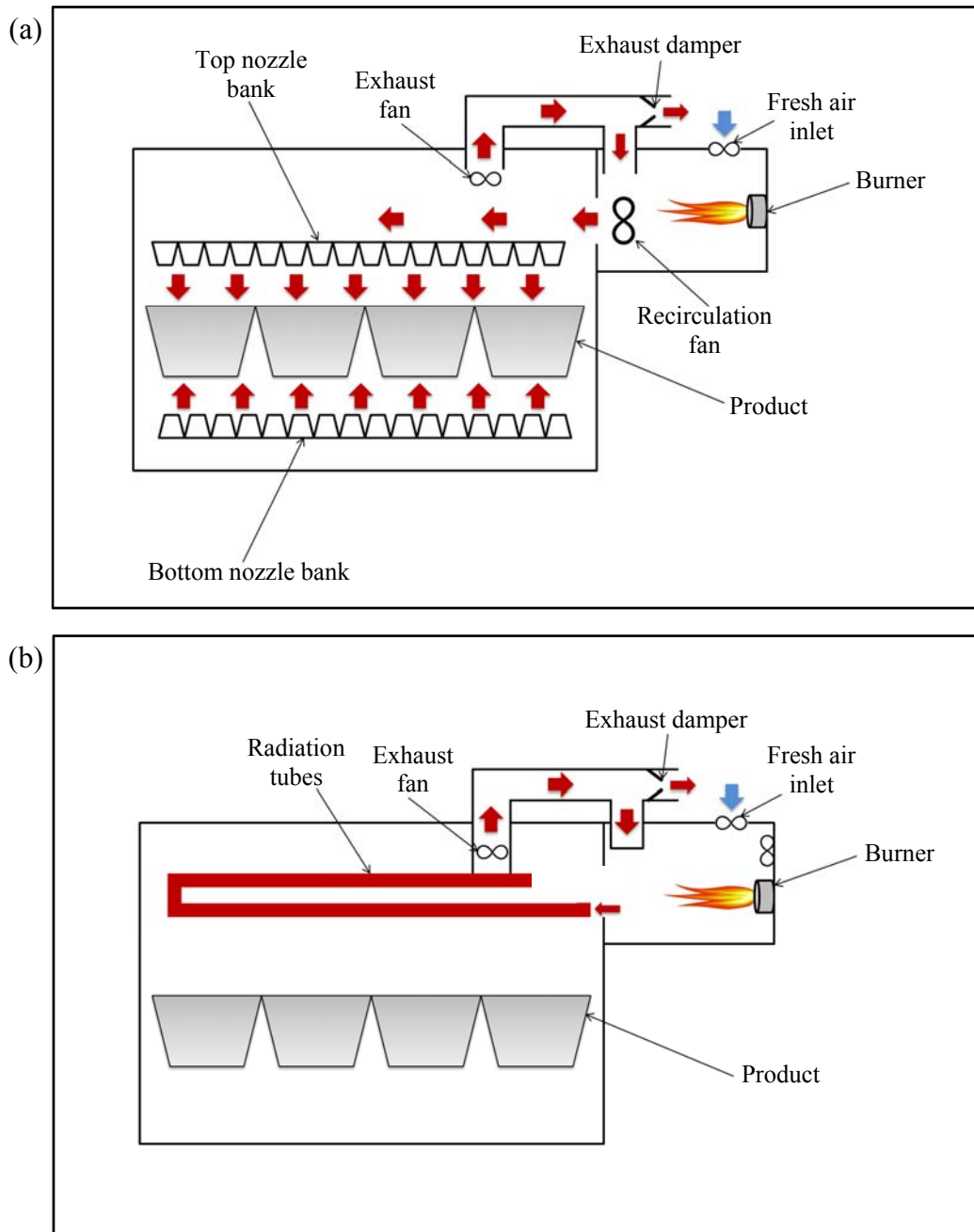


Figure 6.1 – Schematics of two different oven designs: (a) direct-fired forced convection and (b) indirect-fired radiant

Ovens are typically gas, oil or electrically powered. Heat transfer systems include infrared, forced convection, radiation and halogen-lamp. Over the years alternative oven designs have been investigated, such as microwave oven technology (Norris *et al.*, 2002) and hybrid ovens (Li and Walker, 1996).

Innovative oven design has been restricted by the desire of bakeries to use more traditional technologies to maintain product quality. Carbon emissions and cost concerns have forced bakeries and equipment designers to reassess oven design with the aim of baking bread in a more efficient manner.

6.2 System-Level Energy Modelling

System-level energy modelling is a topic identified by the UK Energy Research Centre (UKERC) as key to understanding the interdisciplinary nature of energy challenges that industry faces. When applied to bread baking, system-level thermodynamic modelling provides a methodology for balancing the flow of heat energy within the oven, and includes techniques for estimating the nature of energy losses within the process.

The generic process of designing a whole energy system-level model can be described as follows:

1. Identify the process energy and material flows and fuel supply points.
2. Characterise the essential energy flows to the process and the waste energy streams.
3. Define a system boundary around the system across which energy flows can be established.
4. Devise a generic methodology that can be applied to different types of equipment for measuring or predicting energy use.
5. Put methodologies into a form that can be easily applied by users (for example software).
6. Apply the model to a live process.
7. Perform a sensitivity analysis to evaluate the scope for error.
8. Validate across a number of scenarios to ensure accuracy.
9. Distribute for use.
10. Interpret and present the results.

A full scale energy audit is often useful for industry to identify inefficient processes and make improvements; however these are often time consuming, costly, and give unnecessarily convoluted results in order to analyse a complete system. Although a system-level model will often encompass key components of an energy audit, the main aim is to include flexibility so it can be applicable to a number of scenarios without significant modification. The main benefit of system-level models is that they provide useful results to justify process improvements, whilst remaining cost effective and time efficient.

6.3 Theory of Energy Audits

There are a number of books that describe energy auditing techniques for industrial processes (Beggs, 2002, Gottschalk, 1996, Hansen and Brown, 2004, Kreith and Goswami, 2008, Marcotte and Grabowski, 2008, Mattsson and Sonesson, 2003, Thumann and Mehta, 2008, Thumann and Younger, 2003, Turner, 1993). These authors all outline practical techniques for quantifying energy streams in manufacturing processes, buildings and transportation systems. Turner (1993) describes the drivers for energy auditing as “to ensure survival, maximise profits, and enhance competitive positions”.

Thumann and Mehta (2008) give a comprehensive description of industrial energy audits with a focus on site services and process optimisation, including: HVAC, lighting, electricity co-generation, heat recovery, control systems and thermal storage. In addition, transportation and envelope audits were discussed. Two phases are listed; “acquisition” and “analysis of data”, the results are then used to develop savings opportunities. There are a number of methods for analysing energy savings proposals over the life time of an installation. Such models are sensitive to changing fuel prices and economic circumstances giving an overall value to a business in terms of payback time. If the payback is deemed economically beneficial and installation is practical, priorities for investment proposals can be

made. It is important to continuously monitor and record energy consumption through use of submetering after changes have been introduced, in order to ensure performance is improved to the levels predicted.

A large focus of Thumann and Mehta (2008) is on the worldwide legislation that has been brought into effect over recent years. There is a detailed analysis of different system measurement techniques and devices, of particular interest was the use of infrared thermal imaging to analyse heat losses. Heat recovery options are assessed – the process of directing waste heat streams through a heat exchanger, or otherwise, to reduce the energy losses in flue gases. For heat recovery purposes, heat from oven exhaust gasses can be categorised as within the low temperature range, i.e. less than 232 °C. This means heat recovery would not typically involve conversion of heat to mechanical power (for example Stirling engines), due to inefficiencies involved with low grade heat, but instead pre-heating fluid streams such as feed water. There are a variety of commercially available heat exchangers, which are explained and analysed for their functionalities.

Beggs (2002) described the audit process in four stages:

- (i) collation of data
- (ii) analysis of data
- (iii) presentation of energy consumption
- (iv) assess priorities for energy efficiency savings

The first three stages are the main processes necessary to establish the basic framework and strategy for energy usage and reduction. The fourth stage can be used to make necessary recommendations for detailed energy savings proposals. This is followed by a financial appraisal, using two different valuation techniques: “net present value” and “internal rate of return”. A cautious approach is advised for new installations; the author warns that the cost of running ancillary equipment, such as fans and pumps, could outweigh the financial and environmental benefit

gained through recovering waste heat. There is a comprehensive guide to heat exchangers and heat pumps, covering all the main flow types used in industry. Much of the book is relevant to supply of site services, cogeneration and building design. Overall, this book is a reliable reference from which to conduct an energy audit.

6.4 System-Level Model of a Commercial Baking Oven

The methodology presented here is generic; therefore it can be applied to any type of large production oven. The analysis was illustrated and validated for a standard 800 g white loaf, though when applying this model practically the type of product being manufactured makes very little difference to the overall results of the model. The quantity of ingredients as a percentage of the weight of the while loaf recipe is (as a percentage of initial dough mass): 55.7 % flour, 1.1 % salt, 4.2 % yeast, 2.8 % sugar, 30.6 % water and 5.6 % other ingredients (Monteau, 2008). The model generated assumes steady-state operating conditions – an assumption that is justified given the continuous nature of bread baking operations.

Several methodologies have been proposed for analysing the thermodynamic energy flows in processing equipment, according to the First Law of Thermodynamics. These methods combine a number of techniques outlined by energy audit books and aspects of pinch analysis as well as offering some novel approaches for quantifying heat losses (Wu *et al.*, 2010, Wu *et al.*, 2012).

After surveying a number of industrial bread ovens and bakeries, it was possible to summarise the energy functions of a bread oven into ten key heat flows. There are two heat supply methods: heat in via the gas burner and steam injection. There are seven areas where the thermal energy is utilised or dissipated: cooking of the dough, evaporation of water from the product, starch gelatinisation, heat uptake of tins and lids, heat in exhaust gases, heat uptake of the conveyor and losses through the oven walls and roof. These are summarised in Figure 6.2 and Table 6.1.

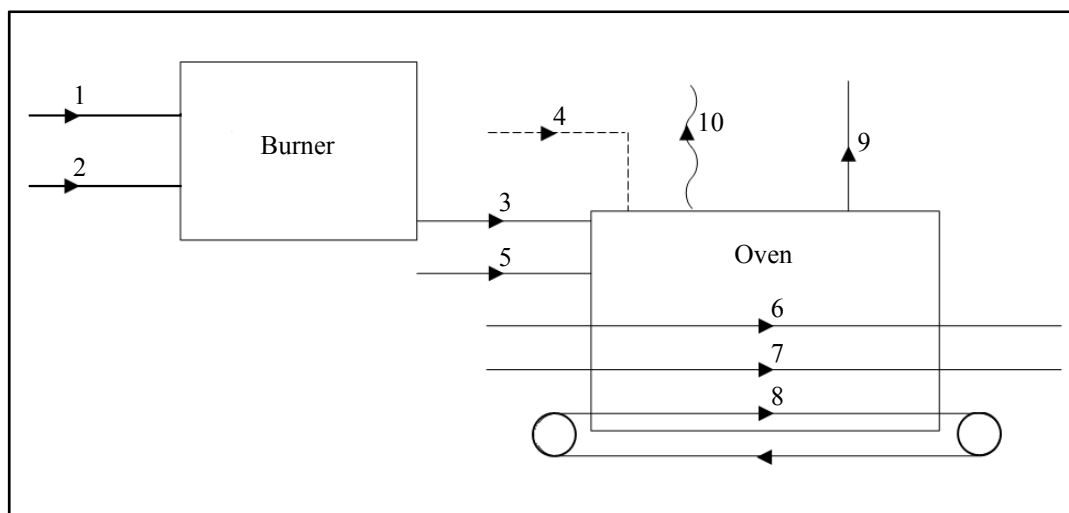


Figure 6.2 – Diagram showing heat and mass flows within an industrial bread oven, as detailed in Table 6.1

#	Energy stream	Remarks
1	Fuel in	Typically a natural gas burner, larger ovens have three or more burners.
2	Air supply to the burner	Burners in industrial ovens will operate with excess air, in order to remove moisture, dust and other unwanted products of combustion.
3	Combustion products	Hot air and products of combustion.
4	Steam supply	Static steam sections are used typically on some unglazed products to give the bread surface a glossy finish.
5	Air drawn in from the oven ends	Ovens are typically run at negative pressure, thus drawing ambient air in to the baking chamber.
6	Bread	Energy required to bake the bread. Larger bread plants can produce upwards of 5,000 kg/hr.
7	Baking tins and lids	Tins are heated to oven temperature during the bake cycle, only to be cooled in order to be recycled.
8	Conveyor	Heat losses occur when the conveyor protrudes out of the oven ends.
9	Exhaust gases	Contains air, combustion products, alcohols, flour dust and steam.
10	Heat loss from oven walls	Convective losses due to airflow around the oven and a temperature differential between the oven surface and ambient.

Table 6.1 – List and explanation of energy flow streams for a typical commercial baking oven (see Figure 6.2)

The governing methodology, measurement techniques and related equations used to define the heat flows into and out of a bread oven are summarised in sections 6.4.1 to 6.4.8.

6.4.1 Heat in via Gas Burner

The amount of energy supplied to the oven from the burner (Figure 6.2, flow 3) is calculated from the volumetric flow rate of fuel used in each of the three burners, multiplied by the calorific value of the natural gas. Because the supply air for oven gas burners is not typically preheated, the heat injected to the baking chamber through the gas burner is shown by Eq. (6.1).

$$\dot{H}_3 = CV_{gas} \cdot \dot{V}_1 \quad (6.1)$$

where \dot{H} is the heat flow (kW) and \dot{V} is volumetric flow rate (m³/s). The heat of combustion for natural gas, CV_{gas} (J/m³), is supplied at 25 °C. The average temperature in a bakery is typically between 24 and 30 °C. In this temperature range, CV_{gas} varies by less than 0.03 %; therefore the assumption that burner inlet air is temperature is 25 °C is suitable for this model.

6.4.2 Heat in via Steam Injection

Some baking processes require the injection of steam at the start of baking (flow 3), as bakers believe the condensed moisture on the top surface of the bread gives it a glossy (or glazed) finish (Altamirano-Fortoul *et al.*, 2012). For these particular products, energy in via steam injection can be represented by Eq. (6.2). This equation takes into account the mass flow rate of steam and the evaporation enthalpy of water.

$$\dot{H}_4 = \dot{m}_3(c_{p_w} \cdot (T_3 - T_{amb}) + L_{e_w}) \quad (6.2)$$

where \dot{m} is mass flow rate (kg/s) and c_p is specific heat at constant pressure (J/(kg·K)) and the subscript w represents water. The latent heat of evaporation for water, L_{e_w} , at atmospheric pressure is 2,260 kJ/kg at 100 °C (Bird and Ross, 2012).

6.4.3 Heat Required to Cook the Dough

The heat required to cook the dough is given by the difference between the heat in the product at the end and at the beginning of the baking process (flow 6). This is calculated using Eq. (6.3):

$$\dot{H}_6 = \dot{m}_6 \cdot c_{p_{bread}} \cdot (T_{bread_{out}} - T_{bread_{in}}) \quad (6.3)$$

In addition, heat is required to gelatinise the starch within the dough, an irreversible process that is characterised by starch molecules absorbing water and setting the dough to create bread – thereby essentially defining the baking process (Fessas and Schiraldi, 2000). Starch gelatinisation is important for three reasons:

- (i) it provides an indication of when the bread is cooked
- (ii) it forms the dough together to create the crumb structure inside the loaf, and
- (iii) it controls the rate of the staling process of the bread (Yasunaga *et al.*, 1968).

The heat required for starch gelatinisation is calculated by Eq. (6.4):

$$\dot{H}_{gel} = \dot{m}_6 \cdot c_{gel} \quad (6.4)$$

where specific heat of starch gelatinisation, $c_{gel} = 1.2$ kJ/kg baked product (Le-Bail *et al.*, 2010).

Assuming a constant temperature on the bread surface at the start of the baking process, the rate of temperature increase inside the dough/ bread can be modelled in a simplified manner by Eq. (6.5):

$$\Delta T = \frac{1}{\alpha_k(T)} \frac{\partial T}{\partial t} \quad (6.5)$$

Thermal diffusivity is given as a function of temperature (α_k), assuming a constant dough/ bread density as obtained from Wong *et al.* (2007) – this is also shown in Figure 3.1. Zanoni *et al.* (1995b) developed a model to evaluate the degree of starch gelatinisation to predict the rate at which the bread is baked, Eq. (6.6):

$$\alpha(t) = 1 - e^{-K_r t} \quad (6.6)$$

where $\alpha(t)$ is the degree of gelatinisation. The reaction rate constant, K_r , is calculated in terms of the Arrhenius equation:

$$K_r = K_0 e^{-E_a/RT} \quad (6.7)$$

where the pre-exponential factor, K_0 , is $2.8 \times 10^{18}/s$ and the activation energy, $E_a = 139$ kJ/mol. These equations have been used to develop a computational model for the prediction of bread temperature and the degree of starch gelatinization with respect to bake time (Khatir *et al.*, 2012b).

6.4.4 Heat Required for Moisture Evaporation

The mass of moisture evaporated from the dough (flow 9) during baking is highly dependent on the product type, oven type and baking process. The heat required for evaporation is mostly due to the latent heat, as discussed in section 3.5. The system model uses Eq. (6.8) to calculate this energy load:

$$\dot{H}_{9,v} = (\dot{m}_8 - \dot{m}_6) [c_{p,w} \cdot (T_9 - T_{amb}) + L_{e,w}] \quad (6.8)$$

6.4.5 Heat Uptake of the Tins and Lids

When the dough is transferred to the tin it is in a delicate state so recycled tins are often cooled to ambient temperature after the bake cycle to prevent scorching of the dough. Additionally, many products use lids which are useful to create a microclimate of moist air within the tins. The lids also control the shape of the top of the loaf as the dough expands. The energy required to heat the tins and lids (flow 7) is given by Eq. (6.9):

$$\dot{H}_7 = \left[\underbrace{\dot{m}_{7,t}(T_{7,t,in} - T_{7,t,out})}_{\text{tins}} + \underbrace{\dot{m}_{7,l}(T_{7,l,in} - T_{7,l,out})}_{\text{lids}} \right] \cdot c_{p,steel} \quad (6.9)$$

6.4.6 Heat Uptake of the Oven Conveyor

Conveyors in industrial ovens (flow 8) are typically large steel slats covered in a steel mesh to support the bread travelling through the oven. The mass flow rate of the slats is typically comparable to that of the mass flow rate of bread travelling through the oven, although feed and return temperatures are closer to the set point of the oven, due to the high thermal conductivity of steel – approximately 30 to 40 W/(m·K), depending upon the exact grade (Kreith *et al.*, 2011). The heat loss of the conveyor is calculated by Eq. (6.10):

$$\dot{H}_8 = \dot{m}_8 \cdot c_{P_{steel}}(T_{8_{out}} - T_{8_{in}}) \quad (6.10)$$

6.4.7 Heat in the Flue Gas

The exhaust flue (flow 9) mostly consists of hot air, water vapour and combustion products removed from the baking chamber. Other components such as grease and flour are neglected for the purposes of calculations. The flow rate of flue gas was measured using a pitot tube inserted into the exhaust duct. Measurements ideally should be completed at traverse points located at equal increments across the duct and averaged to obtain the most stable value. The mass flow rate is then used to calculate the heat losses from flue gases by using Eq. (6.11):

$$\dot{H}_{9,a} = (\dot{m}_9 - \dot{m}_{9,v})c_{P_{air}} \cdot (T_9 - T_{amb}) \quad (6.11)$$

where the simplification that specific heat of the exhaust gases is the same as the specific heat of air, $c_{P_{air}}$, as oven burners are purposely set to operate with large amounts of excess air (typically greater than 50 %).

Hood exhausts are often positioned at the oven entrance and exit to extract hot air and combustion product to prevent these gases entering the bakery atmosphere. Hood exhaust gases are much lower in temperature than exhaust gases. Where relevant, these gases should also be included in flue gas energy loss calculation. In

order to do this, the quantity of fresh air and air that has over spilled from the oven should be quantified – which can be estimated by analysing the comparative temperature between ambient and the baking chamber. The fresh air that is exhausted from the oven should then be deducted from the total mass flow rate. The lower exhaust gas temperature can then be used in Eq. (6.11).

6.4.8 Heat Loss from Oven Walls and Roof

Heat losses from the surface of an oven (flow 10) are dependent on the surface temperature, ambient air temperature and airflow near the surface of the oven. To estimate the surface temperature, a thermal imaging camera was used (ThermaCAM™ SC640, FLIR Systems Ltd, UK), and validated using a surface thermocouple probe – more details are given in section 6.5. The convective heat losses through the vertical stainless steel oven walls were estimated using Eq. (6.12):

$$\dot{H}_{10} = \sum hA(T_s - T_{amb}) \quad (6.12)$$

where heat transfer coefficient, h (W/(m²·K)), is calculated from the Nusselt number:

$$h = \frac{Nu \cdot \lambda}{L_c} \quad (6.13)$$

where λ is thermal conductivity (W/(m·K)). The Nusselt number, Nu , is highly dependent on the atmospheric conditions around a flat surface. Therefore, the Nusselt number is different for the vertical oven wall panels and the horizontal pressure relief panels situated on the oven roof.

A correlation for heat transfer from the surface of vertical walls has been outlined by Incropera and DeWitt (2007) and is given by Eq. (6.14):

$$Nu = \frac{4}{3} \cdot \left(\frac{Gr}{4}\right)^{0.25} gPr \quad (6.14)$$

where the Grashof number and the Prandtl number are both commonly defined dimensionless numbers used in a range of fluid dynamics and heat transfer problems. The Grashof number is the ratio of buoyancy to viscous forces in a fluid and the Prandtl number is ratio of kinematic viscosity to thermal diffusivity in a fluid.

Heat transfer from the surface of horizontal pressure relief panels located on the oven roof can be estimated using the McAdams (1954) correlations – Eq. (6.15):

$$Nu = 0.15 \cdot Ra^{\frac{1}{3}} \quad (6.15)$$

for Rayleigh numbers in the region of $10^7 < Ra < 10^{11}$. The Rayleigh number for bakery conditions is typically 5×10^8 for roof panels.

6.4.9 Total Heat Utilisation

This analysis can be validated in a straight-forward manner since according to the First Law of Thermodynamics, the sum of energy flows into the oven must be equal to the sum of energy flows out of the oven, confirmed by Eq. (6.16):

$$\dot{H}_4 + \dot{H}_3 \equiv \dot{H}_6 + \dot{H}_7 + \dot{H}_8 + \dot{H}_{9,v} + \dot{H}_{9,a} + \dot{H}_{10} \quad (6.16)$$

In most practical cases Eq. (6.16) will not balance exactly, but the expectation is that both sides of the equation will be within $\pm 10\%$ of each other. The remaining balance, which is likely to be on the right hand side of the equation, can be attributed to ‘other’ heat streams that are not quantified. Depending on the oven this may be in one of several places.

6.4.10 System-Level Thermodynamic Analysis Tool

The equations presented above (Eq. (6.1) to (6.16)) are the fundamental building blocks for the system-level thermodynamic analysis tool that has been distributed for use in the baking industry. Screenshots of the interface with approximate values to protect commercial sensitivities are shown by Figure 6.3 and Figure 6.4.

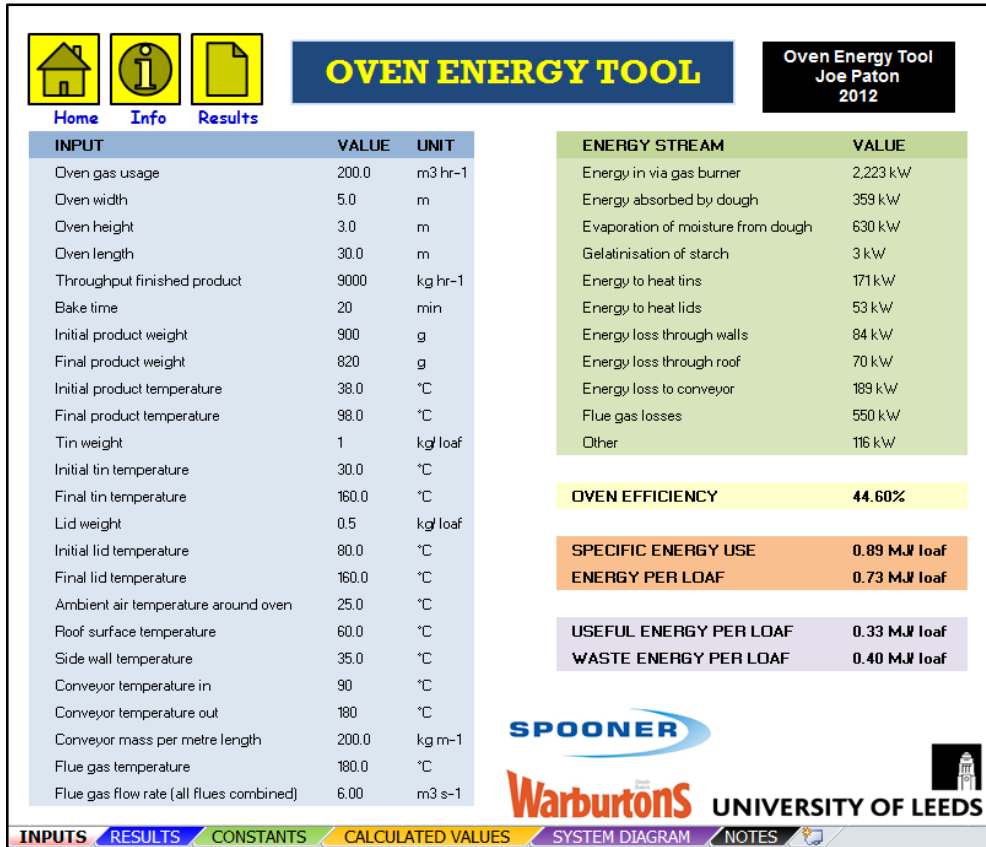


Figure 6.3 – Input screenshot of oven thermodynamic energy analysis tool

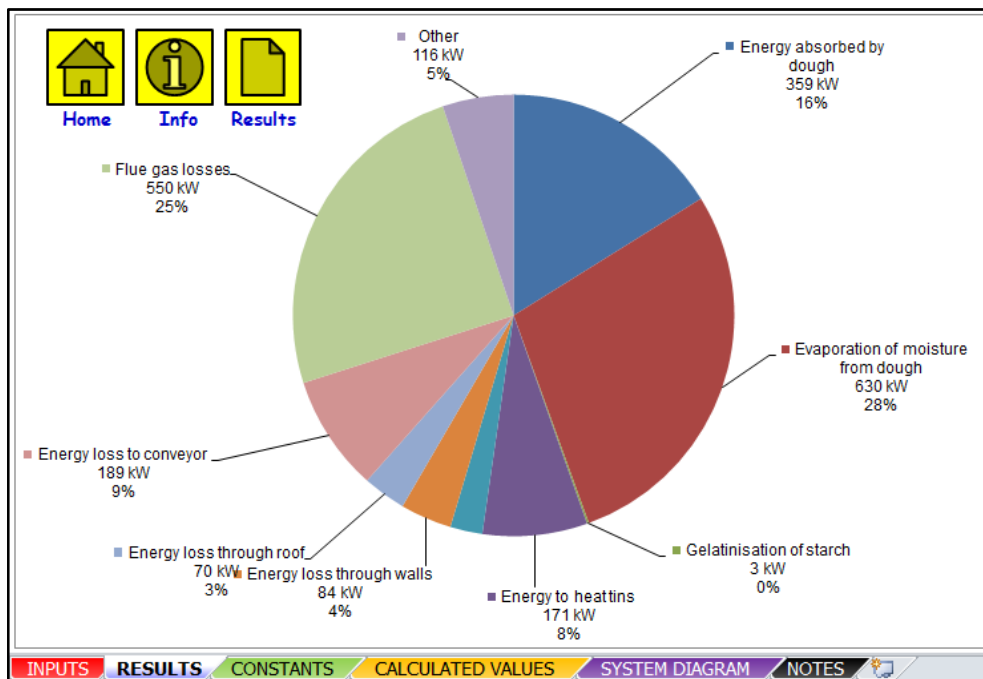


Figure 6.4 – Results screenshot of oven thermodynamic energy analysis tool

The home screen, where the user inputs the values that have been measured from the baking oven, is shown by Figure 6.3. The results in tabular form are also

(instantaneously) displayed here. The results screen, shown by Figure 6.4 , gives a pie chart showing the breakdown of heat losses from the oven. The model also incorporates notes for the user to use as reference and shows the list of assumptions.

6.5 Thermal Imaging

Thermal imaging, the theory for which is discussed in section 3.6 of this thesis, is a useful tool for measuring temperature in a non-invasive manner. Whilst not formally required for the system-level model described in section 6.4, thermography techniques have been used to help estimate wall heat losses and to identify cost savings.

The thermal imaging camera used in this study was a ThermaCAM™ SC640 (FLIR Systems Ltd, UK), which has an accuracy of ± 2 °C in the range -40 to 1,500 °C. Thermal imaging was used to measure surface temperature of the vertical oven walls and horizontal roofs in order to estimate heat losses using the methodology described in section 6.4.8. In order to quantitatively validate the surface temperature measurements, a number of validation checks were taken using a surface thermocouple – this was especially important given the large range of values for emissivity, as seen in Table 3.1. A direct temperature measurement at a set point on the oven surface could be compared with the indirect measurement given from the thermal imaging camera. The emissivity setting that the camera uses to adjust the temperature scale could then be altered to ensure the two temperature values are the same, within the range of emissivity values expected.

Figure 6.5 shows thermal images imbedded in regular photographs for two different ovens; oven A and oven B. The mean and maximum temperatures are displayed and it can be seen that the mean surface temperature of oven B is 4.2 °C greater than that of oven A, and the deviation of the maximum temperature from the mean is higher, 3.3 °C compared with 0.4 °C. This indicates that there were

more ‘hotspots’ on the roof of oven B – potentially resulting from gaps in the mineral wool insulation. Another explanation is that the different insulation on the roof of oven A, which has a covering of metallic foil, thereby lowering the radiative emissivity of the roof and reflecting heat back towards the internals of the oven and providing another form of insulation – this can be observed in the photograph section of Figure 6.5 (a).

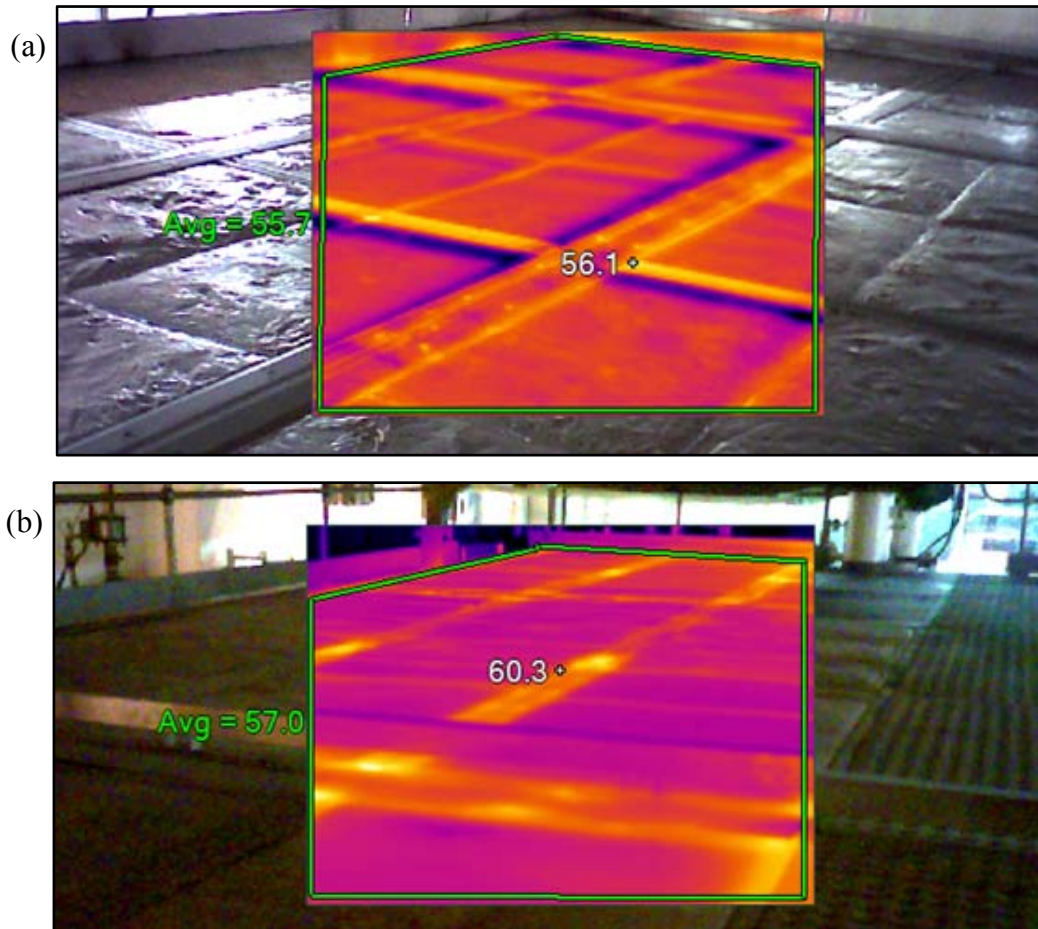


Figure 6.5 – Thermal images of the roofs of two industrial bread baking ovens showing the maximum (white text) and mean (green text) temperatures (°C) for two ovens: (a) oven A and (b) oven B

Thermal images of the vertical oven walls for the same two industrial ovens are shown by Figure 6.6. The mean surface temperature for oven A is 36.1 °C and for oven B it is 39.3 °C. The difference in wall material can again be seen by the photographs – resulting in the mean surface temperature of oven B being 3.2 °C hotter than oven A.

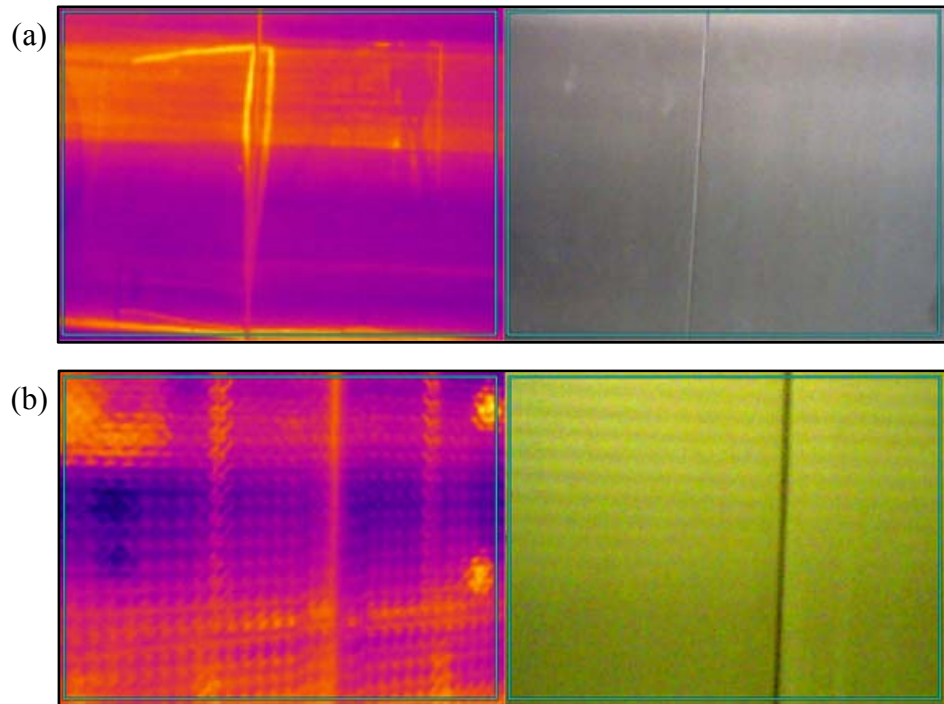


Figure 6.6 – Thermal images of the outer walls of two industrial ovens: (a) oven A and (b) oven B

6.6 Sensitivity Analysis of System-Level Model

As with any model aiming to approximate the behaviour of a real system, it is essential to verify the applicability of the methodologies used in order to check the outputs can be relied upon. For this system model of heat energy use of bread ovens, the sensitivity of outputs is measured with respect to changes in input variables. In this case, two separate sensitivity analyses have been conducted which aim to quantify the consistency of the model generated.

Firstly, as shown by Figure 6.7, each input variable was changed by $\pm 10\%$ and the resultant change on the output was recorded. The figure of 10% was subjectively chosen as a value within which most measurements can be performed with little cost or specialist equipment.

It can be seen that for changes in gas metering measurements, an equivalent change in the output is noted – therefore it is important that the gas metering values can be relied upon. As a safety and billing accuracy measure, gas meters are annually inspected by registered professionals to ensure the integrity of the readings. In

addition, a simple check is conducted by adding the sum of gas sub meters to ensure they equal the total of the main gas supply meter (the meter that energy supply companies use to formulate energy bills) will show any discrepancy in the metering data.

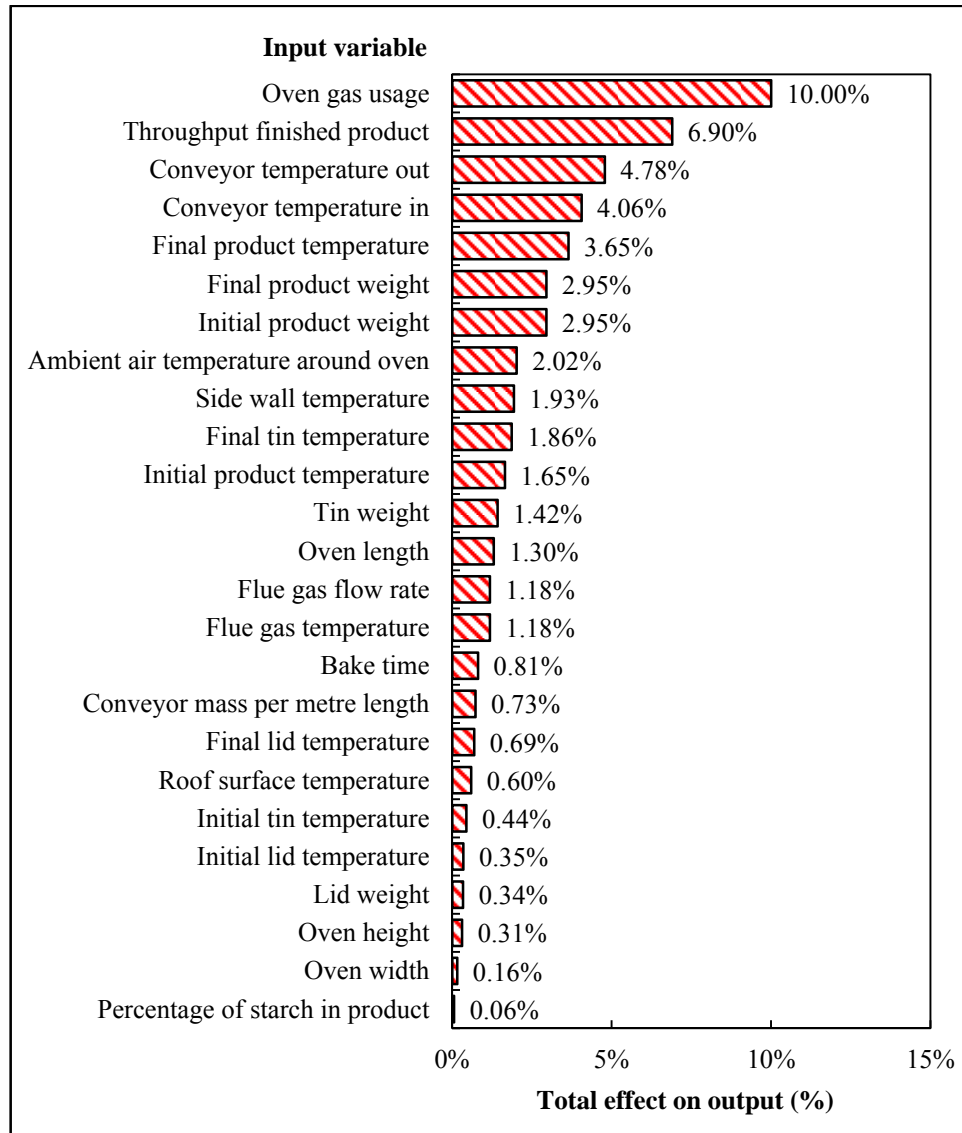


Figure 6.7 – Sensitivity analysis showing the effect on outputs based on a 10 % change of each input variable

Other input measurements that have a significant influence on the results (over 3 %) are throughput, conveyor temperature (in and out) and final product temperature. Of these, throughput is calculated exactly by the bakery, as all produce and wastage is accounted for and the final product temperature as a quality

requirement is kept within ± 1 °C (< 1.05 %). Conveyor temperature is more difficult to accurately measure due to the inaccessibility of the slats due to the dangers of the chain mechanisms that drive the rotation, however the accuracy of measurement is still well within the 10 % boundary, resulting in a potential error accuracy of less than 5 %. Input variables that have little effect on the outputs include the oven dimensions (width and height), the percentage of starch in the product and the tin specifications/ temperatures. Although an increase in the oven width would result in a larger cavity to fill with hot air, the overall throughput of the oven would increase so a large increase in energy is not necessarily inevitable. The effect of the increase in oven height has little effect on the energy use as it is assumed that the volume of the baking chamber would be unaffected, therefore it is only the wall losses that are increased.

Secondly, as shown by Figure 6.8, a compound sensitivity analysis was conducted. This analysis considered the maximum expected degree of error for each of the inputs – taking into account both procedural error and the accuracy of equipment given by the OEM – usually gathered from the technical manual provided.

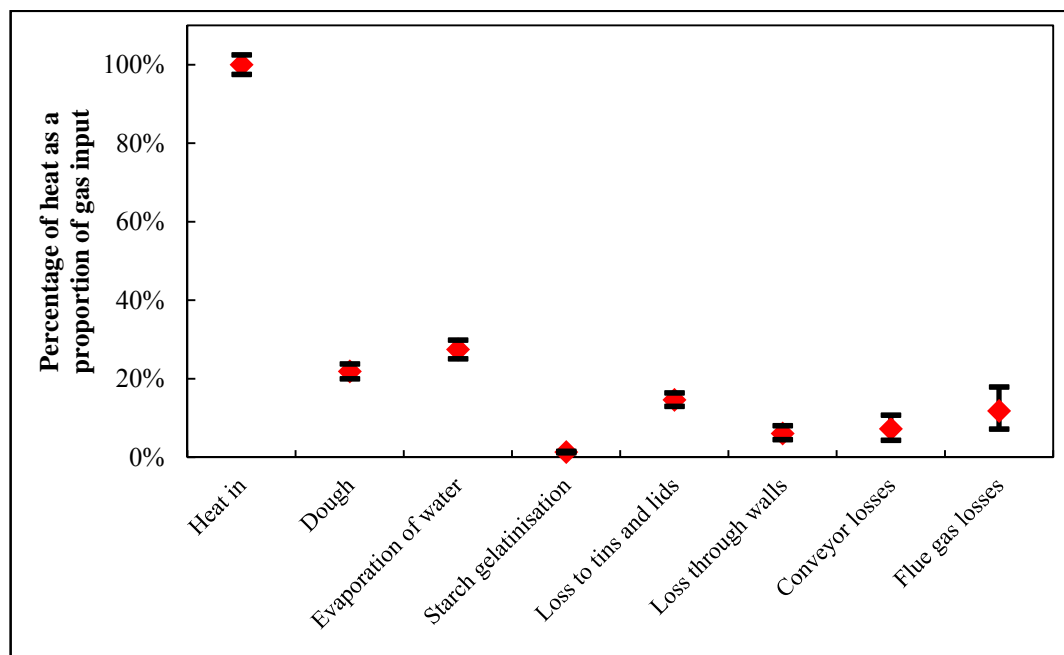


Figure 6.8 – Compound sensitivity analysis based on changing each input variable by the expected precision of the measurement and the instrument accuracy supplied by the manufacturer

In this case, the most sensitive outputs were the flue gas losses and conveyor losses. As experimental measurement of these two energy losses involved indirect measurements due to the harsh environment in which bread ovens operate, scope for error can be expected. Improvements to the measurement of conveyor temperature could be improved by permanently soldering a thermocouple to the conveyor slats and mounting a temperature-resistant wireless data logger to the conveyor. This would, however, require a significant amount of downtime for a bakery and would therefore damage the ease and applicability of the system model. Measuring the flue gas flow rate has historically been done by use of pitot tubes, a technique that can be less accurate than direct measurement of air velocity, as the flow rate is inferred from pressure. Other techniques for predicting flow include CFD modelling, acoustic velocimetry, laser anemometry or hot-wire measurement (Jahnke, 2000). However, due to the complexities and expense of these methods (which also rely on inference), it is doubtful that industry would adopt them for the purpose of system modelling of bread oven energy efficiency.

6.7 Sample Results

Two commercial bread ovens at separate sites have been analysed for energy efficiency for the purposes of this report in order to demonstrate the applicability of the system model. Oven A was installed in c. 2009 and oven B c. 2006, with product throughputs of 6,500 kg/hr and 9,000 kg/hr respectively. At the time of analysis both ovens were operating at steady state producing the same product recipe.

The specific energy consumption of ovens A and B were 804 and 920 kJ/kg respectively. The minimum theoretical energy required to bake the bread that comes in three forms (heat the dough, evaporate moisture and gelatinise starch) is 476 kJ/kg, which is equivalent to 59.2 % of the oven gas supply for oven A and 51.7 % for oven B, making oven A significantly more efficient. Figure 6.9 shows

the distribution of energy losses, illustrating the main difference is the losses through the walls and roof, whilst the other losses are comparable. ‘Other’ losses are the remaining heat flows deduced from Eq. (6.16) – and can be predominantly attributed to hot air leaks from the oven. Ovens are designed with inner and outer walls, where hot air can flow in the volume between the two. This air has a tendency to escape from leaking joints, particularly in the roof area of the oven, where pressure-relief panels are joined to the solid frame structure. Hot air leaks can also occur around the access doors. Access doors and pressure-relief panels are both regulatory requirements.

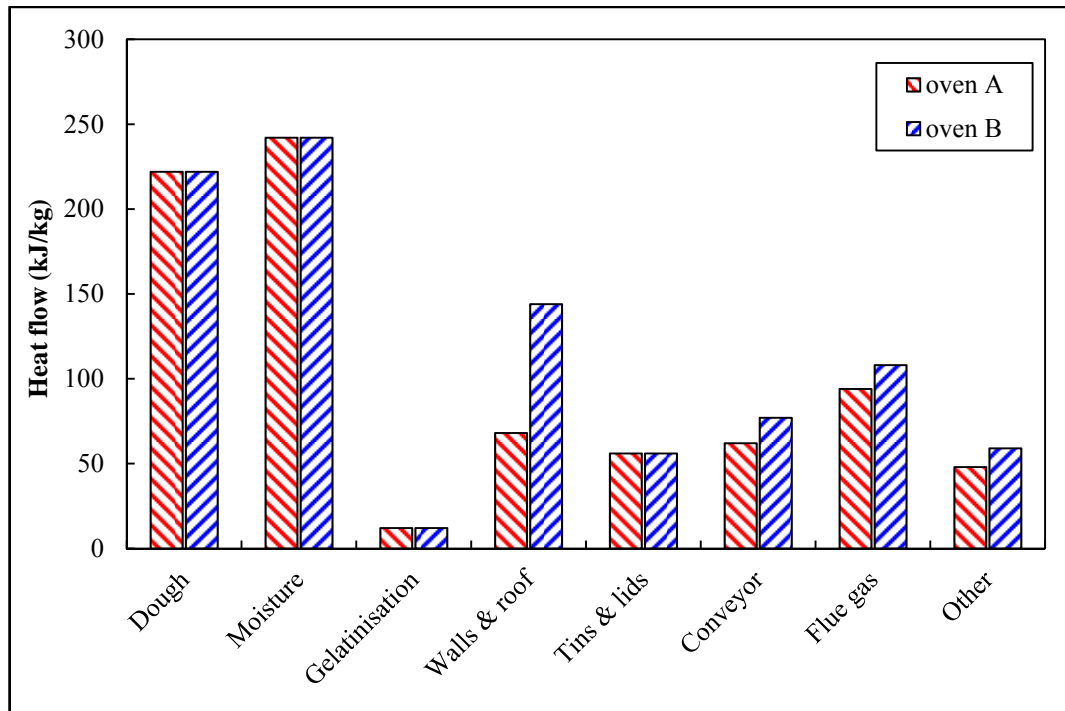


Figure 6.9 – Sample results of heat distributions obtained by system-level model for two commercial baking ovens

6.8 Opportunities for Energy Savings

Having assessed the distribution of heat loads for the oven, bakeries have looked to analyse where energy savings can be made for financial benefit and carbon reductions. The two focusses are on: (i) reducing the energy into the oven by reducing the losses to ambient, and (ii) recovering heat from the oven in order to provide energy for other processes.

6.8.1 Oven Insulation

One outcome based on this system model was to quantify the heat losses through the walls and roof – and it was found that the most significant heat loss from the oven surfaces for industrial ovens was through the roof. Whilst regulatory restrictions for pressure relief panels to be placed on the roof make it prohibitive to have the same level of insulation as the oven walls, it was found that for new designs of oven the insulation thickness for the whole oven could be increased by 50 mm from 150 to 200 mm for minimal additional capital cost. Further investigation will be required to assess the efficiency gains as a result of this improvement.

6.8.2 Conveyors

Due to the thermal mass of the conveyors, energy losses are significant. One solution that is currently being trialled on a new generation of commercial ovens is to have ‘enclosed terminal ends’. This solution will help to ensure that the heat losses from the conveyor are recovered into the oven recirculation ducts. The technology provides an extension to the hoods that already cover the entrance and exit, and will completely eliminate the conveyor losses from the oven – though a full regression analysis over a prolonged period would need to be conducted to investigate whether the overall energy efficiency of the oven is improved. The disadvantage of this technology is that the oven internal volume is larger, requiring a greater quantity of hot air.

6.8.3 Tins and Lids

Due to the nature of square-edged loaves of bread, tins and lids are a necessary energy load. Since they are cycled through the baking process several times per day, they are required to be robust. Reduction to the mass or specific heat capacity of bread tins and lids with the aim to reduce energy losses has been an interest for bakers for many years. Although increasingly commonplace in home-baking, silicone tins have been deemed too weak to withstand long term use in a

commercial bakery. Furthermore, there is a perceived risk of product contamination from silicone coming into contact with food products. Efforts have already been made to reduce the mass of the current design of steel tins, though for full replacement there is a significant capital cost associated.

6.8.4 Heat Recovery

Heat recovery is an established way to reuse energy from waste heat streams for the same or another process – historic suggestions of ways to recover waste heat in bread baking are discussed in section 2.1.3. Heat recovery from flue gases is the most obvious form of recuperating energy for an industrial oven. There is a large quantity of heat being exhausted directly to atmosphere which does not require treating. Whilst the flue gas temperature is considered ‘low grade’, at temperatures less than 200 °C (Bending and Eden, 1984), there are still possibilities to recover heat.

Processes that require heat in a bakery need to be identified before a heat recovery system can be designed. One use of waste heat can be to pre-heat burner inlet air – this is logical, as the flue is naturally located close to the burner fresh air supply. The main challenge is to ensure the burner is suitable to run off pre-heated air, though retrofitting or replacement of unsuitable burners can allow this. Washing systems; both industrial pan washing machines and Clean-In-Place (CIP) require heat and depending on the location, this can be feasible. Office and warehouse heating demand is seasonal and weather dependent, so is not an ideal heat recovery option. Finally, a study by the Campden & Chorleywood Food Research Association (CCFRA) and Bristol University (2008) analysed the opportunities in the food industry (including bread baking) to use waste heat to power Stirling engines thereby generating electricity for the factory. This was deemed unfeasible at the time due to insufficient technology to make the engines commercially viable. Furthermore, as the maximum theoretical efficiency was calculated to be 40 %

(excluding frictional losses), the majority of heat recovered mechanically in this way would still be wasted.

Turner (1993) warns of the dangers of exploiting waste energy from a process to recover to a secondary process, advising the first process may suffer if the heat streams are not managed properly. In the 1990s a large plant bakery in the UK suffered a potentially dangerous explosion when trying to recover heat off an oven to supply heat to the prover. This was due to mismanagement of waste heat streams (Ward, 2010).

6.9 Temperature and Velocity Profiles in a Pilot Oven

Temperature and velocity profiling gives the local value down an oven length. In common with section 6.8, temperature and velocity measurements in commercial ovens are not strictly necessary for the system-level model described. However, these measurements can result in important diagnostic data that help bakers and oven designers to understand the effects of changes to plant equipment in their search for energy savings.

This section presents profiles of temperature and velocity through a 9 m long pilot oven used by oven manufacturers to trial bake profiles of new products and experiment on new heating technologies. The oven is a scaled-down replica of an industrial oven and is approximately 30 % the size. The significance of temperature and velocity profiles in relation to energy is that there is an energy cost associated with increasing the airflow necessary to achieve greater airflow uniformity.

6.9.1 Temperature Profiles

Temperature profiling is a common technique used by chain bakeries and their oven manufacturers or installation engineers to benchmark baking characteristics in order to maintain product consistency between different ovens or sites. The advantage of measuring temperature, rather than other flow characteristics such as

air velocity, heat transfer coefficient etc., is that the cost of equipment is low and the sensor technology is well established, robust and reliable.

For this study, temperature was logged using K-type thermocouples connected to a TCLink 6 Channel Wireless Thermocouple Node (Microstrain, Inc.). Thermocouples are subject to common measurement errors, including: reference junction inaccuracies, electrical noise, manufacturing imperfections and linearization approximations (Park and Mackay, 2003). These were minimised through calibration by placing thermocouples in boiling water and adjusting to check the instantaneous readout. K-type thermocouples specifically have a typical operating range of -50 to 300 °C and have accuracy of $\pm 0.3 \% + 2 \text{ }^\circ\text{C}$ in the operating range used for this study (RS Components Ltd.), which is an acceptable level of accuracy. Once the oven reached set-point temperature a C9001 Thermometer (Comark Ltd.) displayed an instantaneous temperature reading for the location of the thermocouple. Air temperature was logged at 5 positions (see Figure 6.10) on a strap of tins travelling through the oven.

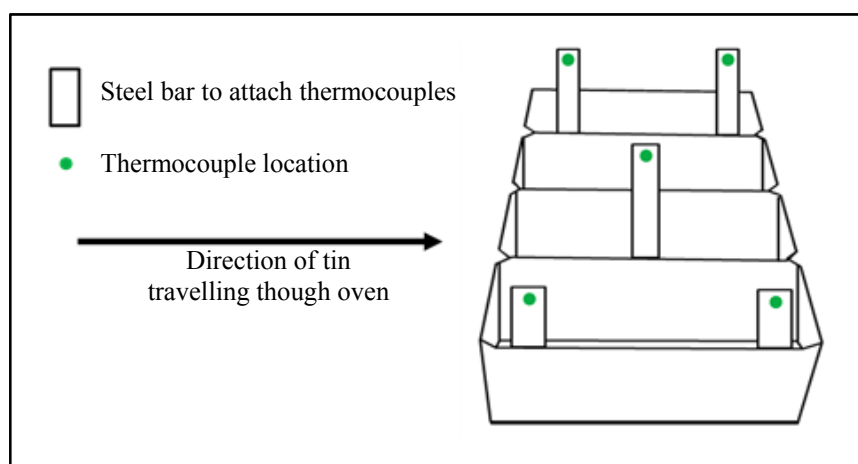


Figure 6.10 – Location of thermocouples across the oven width for a strap of five tins

The air temperature at each of the five locations was recorded at 10 s intervals and the mean temperature at all five locations was used to plot temperature profile graphs. The distance between the thermocouples and the nozzles was changed to investigate whether the temperature varied with distance from the nozzle.

Figure 6.11 shows air temperature underneath the nozzles compared with the burner set point profile through the length of the pilot oven. The three zones are clearly recognizable by the temperature profiles, where $T_{z1} = 240\text{ }^{\circ}\text{C}$, $T_{z2} = 275\text{ }^{\circ}\text{C}$ and $T_{z3} = 265\text{ }^{\circ}\text{C}$. Actual air temperature through the oven is consistently lower than the burner set point. Although there is a defined shape, there are local temperature variations, particularly further away from the nozzles. Fluctuations in temperature are to be expected for turbulent flow, though it can be observed that these fluctuations are localised, meaning the overall heat profile experienced by a loaf of bread is likely to be uniform down the length of the oven. The reason for these variations being slightly more noticeable further from the nozzle plates, i.e. for $H = 80$ and 100 mm , is that there is more mixing with the surrounding air and greater interaction with other nozzle jets. Also noticeable from Figure 6.11 is the temperature at the entrance and exit of the oven, which is significantly below set point temperature. This is caused by a negative pressure gradient which draws ambient air into the oven from the ends. There is little dependence on air temperature with relation to distance beneath the nozzles due to the strong turbulent mixing within the oven.

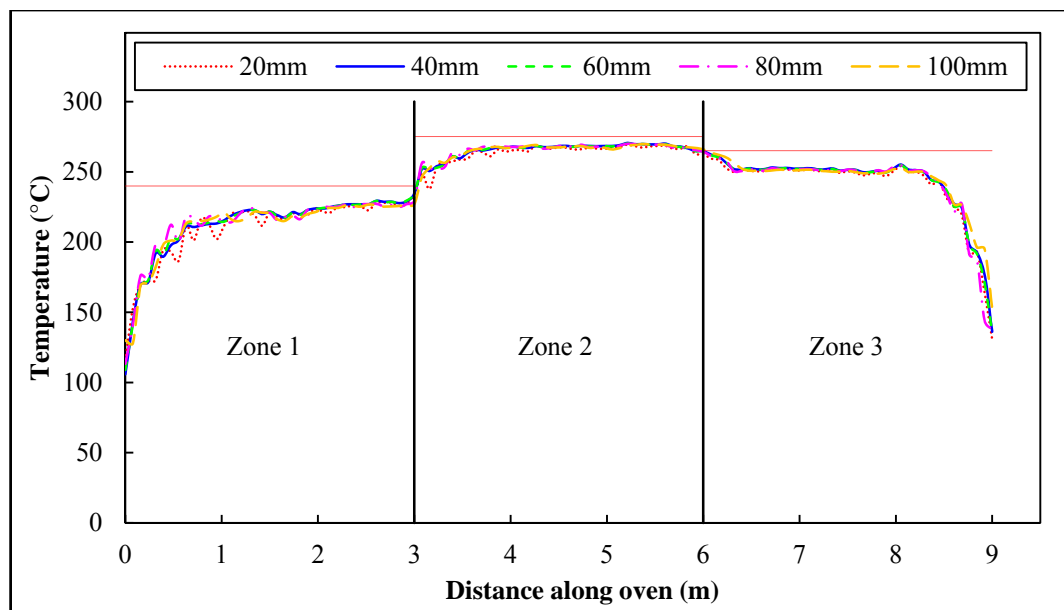


Figure 6.11 – Graph of temperature profile through a pilot oven for different distances underneath the top nozzles: 20, 40, 60, 80 and 100 mm compared with burner set point temperature (solid red line)

The statistics for the temperature distribution profiles given in Table 6.2 show the degree of variation for each zone. As expected, the middle zone remains hotter than 227 °C for the entire oven length, whereas the temperature in zones 1 and 3, which are exposed to the ambient air at the oven entrance and exit, drops to below 140 °C in both cases. The mean temperature for zones 1, 2 and 3 as a proportion of the burner set points are 88.3, 96.4 and 91.6 % respectively – consistently below the set point temperatures. The reason for this is because the thermocouple that controls the burner firing rate is located in the plenum above the nozzles, where the flow is not cross-mixed with other zones or ambient air and consequently the air temperature has not decreased.

Zone	Maximum temperature (°C)	Minimum temperature (°C)	Mean temperature (°C)	Mean temperature as a proportion of set-point temperature (%)
1	234.5	105.9	211.9	88.3
2	270.6	227.0	265.0	96.4
3	266.0	130.7	242.6	91.6

Table 6.2 – Data statistics showing the variation of temperature in comparison with burner set points for each oven zone

In an energy context, temperature uniformity throughout the volume of the oven is driven by the flow of air. For high airflow, temperature uniformity is increased due to a high degree of mixing, whereas for low airflow the opposite is true. Increasing air velocity has an associated energy cost which is discussed in section 6.9.2.

6.9.2 Velocity Profiles

Velocity profiles of commercial ovens are not routinely conducted on new installations, unlike temperature profiling. Equipment for velocity measurement in hot environments is expensive and often prohibitive due to manufacturing schedules and the delicate nature of the baking process. Measurements are therefore frequently made in cold ovens with recirculation and exhaust fans

running to imitate production conditions – the results presented in this section are velocity profiles for a cold oven.

Velocity magnitude was inferred from dynamic pressure readings obtained using a pitot tube connected to a handheld 922 Airflow Meter Micromanometer (Fluke Corporation). The pressure measurement was taken at the nozzle exit and it was ensured that the measurement position was replicated for each nozzle as the pitot tube was fitted with a washer welded into place to guide it into place. Instantaneous dynamic pressures, P_D , at the nozzle exit were converted to air velocity using Eq. (6.17):

$$u = \sqrt{\frac{2P_D}{\rho}} \quad (6.17)$$

Figure 6.12 and Figure 6.13 show the velocity profiles down the oven length for three positions for top and bottom nozzles; two at the extreme x -positions from the centre: A and C (top), and D and F (bottom) and one at the centre of the oven B (top), and E (bottom). The two peaks for each section for the top nozzles (Figure 6.12) is due to the ducting arrangement where recirculation occurs between at the midpoint of each zone (i.e. $y = 1.5, 4.5$ and 7.5 m).

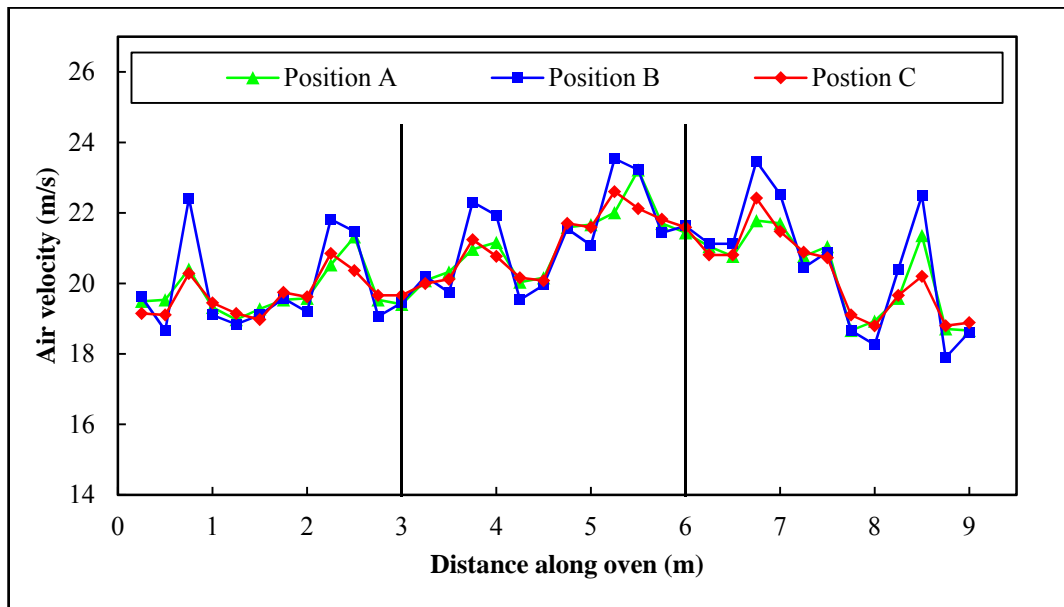


Figure 6.12 – Time averaged velocity profile of the top nozzles for three positions: A – closest to the burner and C – furthest from the burner

Slightly more variable flow can be observed in the first and final sixth of the pilot oven ($y < 1.5$ m and $y > 7.5$ m), which can be attributed to the increase in mixing between the jets and the ambient air. The decrease in air velocity in the same regions for the bottom nozzles (Figure 6.13) is another feature of the design of the pilot oven – the plenum below the bottom nozzles is designed with ducting located nearer to the oven centre, which reduces the quantity of air escaping from the oven entrance and exit.

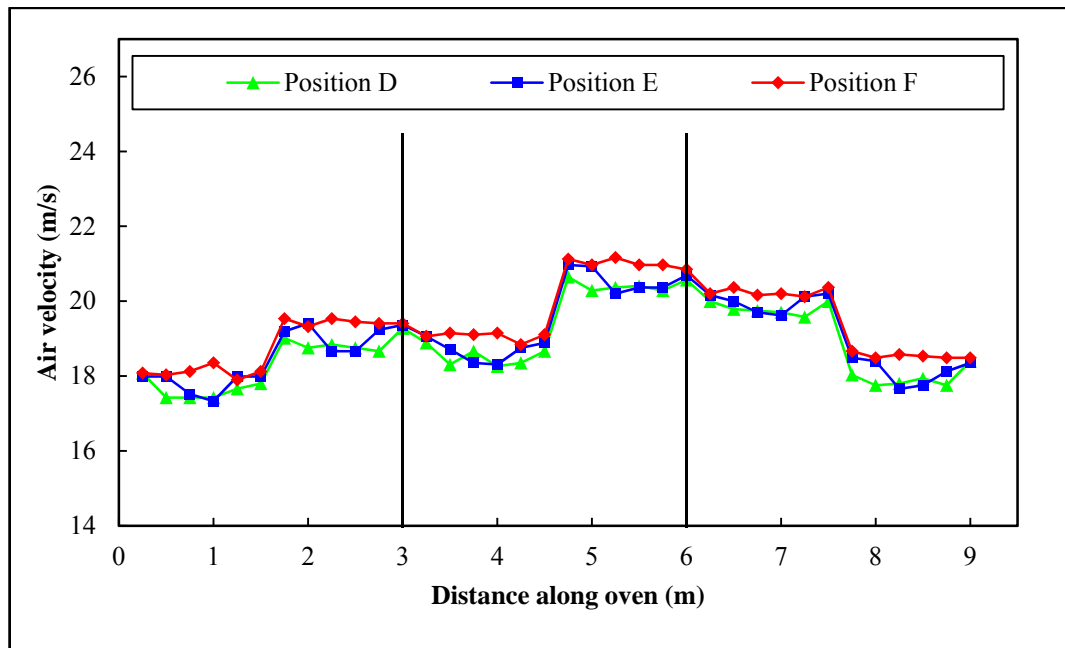


Figure 6.13 – Time averaged velocity profile of the bottom nozzles for three positions: D – closest to the burner and F – furthest from the burner

Figure 6.14 and Figure 6.15 show three-dimensional plots of velocity distribution for top and bottom nozzles respectively. Figure 6.14 further illustrates the non-uniformity of velocity across the width for the top nozzles – where the velocity at the centre of the oven is consistently greater than that at the outer edges. Conversely, Figure 6.15 illustrates the large degree of uniformity across the width of the oven for the bottom nozzles, which occurs due to the plenum design. The uniformity of the velocity profiles can be expressed in terms of deviation from the centre nozzle velocity; for the top nozzles: $-9\% < u_B < 11\%$ and for the bottom nozzles $-6\% < u_E < 2\%$.

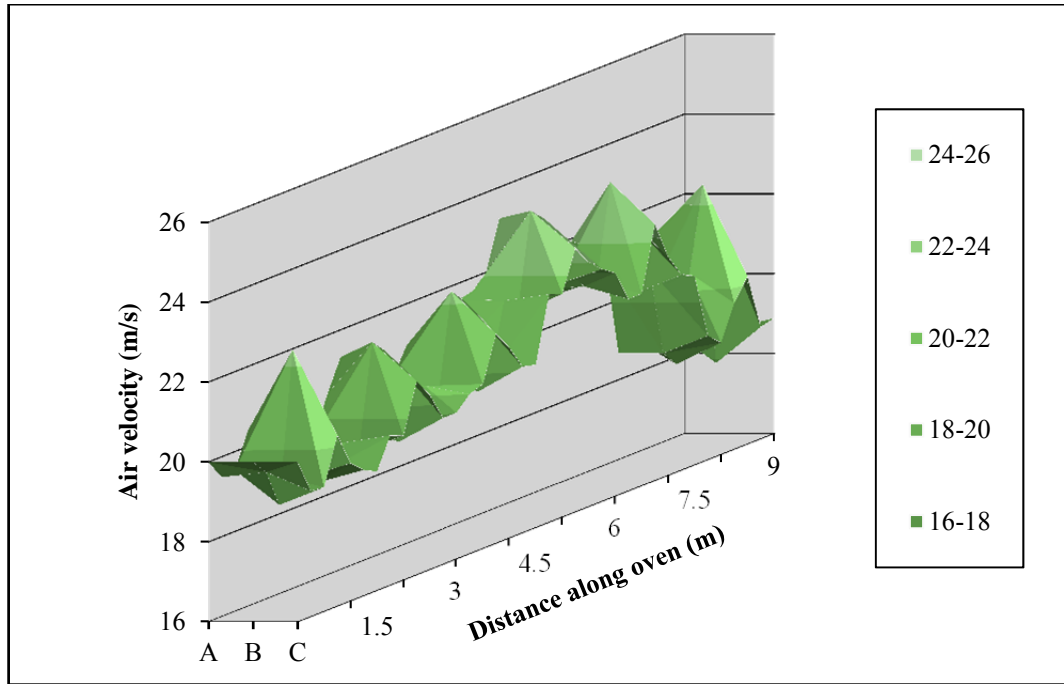


Figure 6.14 – Three-dimensional profile of velocity through a pilot oven for top nozzles: A – closest to the burner and C – furthest from the burner

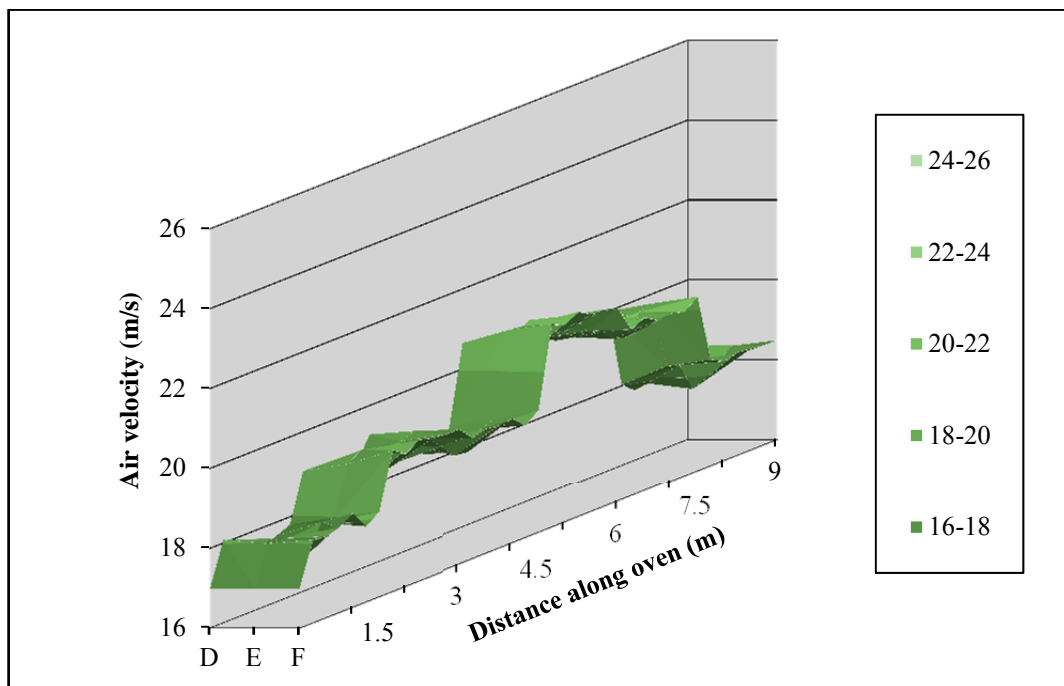


Figure 6.15 – Three-dimensional profile of velocity through a pilot oven for bottom nozzles: D – closest to the burner and F – furthest from the burner

In order to increase the velocity uniformity of impingement jets, a more uniform pressure drop across the nozzle bank is necessary. The way this is usually controlled is by increasing the static pressure in the plenum above the nozzle orifices. The additional energy cost associated with this pressure increase is

dictated by the electricity load required to operate the recirculation fans at a higher speed. The balance between the additional electricity load required for increased air distribution and the heat savings made possible as a result of a faster bake time are discussed further in Chapter 7.

6.10 Summary

The system-level thermodynamic analysis methodology presented here has been used to assess the energy performance of bread ovens. This is a rigorous scientific framework that has been developed via systematic research and has been widely used by bread manufacturers to measure, predict and reduce the energy demand of current ovens. Furthermore, oven designers have used the findings to influence the future design of the next generation of ovens. This work has been combined with a CFD optimisation to estimate annual savings of over £0.5 million and 5,000 TCO_{2e} for the UK (Paton *et al.*, 2011, Paton *et al.*, 2012b).

The use of thermal imaging to help determine surface temperature and thus calculate heat losses from the oven walls provides a new, non-invasive approach to quantify convective losses to atmosphere. Temperature and velocity profiles on a pilot oven provide an example of measurement techniques that can be used to pragmatically benchmark bread oven heat and airflow characteristics. Temperature and velocity uniformity are not only important quality constraints that dictate the consistency of products, but are also factors that have an impact on energy use of bread ovens, due to the increase in fan power required increase air distribution and the pressure drop across the plenum. The energy cost of this is investigated further in Chapter 7.

A sensitivity analysis indicates the equations and methodologies used in the model are suitable, provided appropriately accurate instrumentation is used and careful experimental procedures are executed. The sample results show the validity of the model, and give an idea of the scale of the energy demand of bread ovens. The

widely reported figure that half the heat in a bread oven is wasted has been corroborated to an extent and uniquely, the losses to ambient have been quantified and incorporated into a flexible model that has been extensively used in industry.

Chapter 7

Experimental Measurements of Local and Global Heat Transfer Characteristics

In the previous chapter, the methodology for a system-level thermodynamic analysis of industrial bread baking ovens was outlined. In addition to this, experimentation on the heat transfer characteristics inside commercial ovens is necessary to gain an appreciation of how airflow can affect product quality and energy efficiency. Experimental results allow equipment designers to develop ovens with optimum heat transfer rates. Optimum heat transfer means an improvement in energy efficiency whilst maintaining the essential product characteristics required by bakeries.

This chapter describes experimental methods and presents novel results that are intended to be used by oven designers and bakery operators to influence both oven design and operating conditions to increase energy efficiency of commercial baking ovens. The aim of this chapter is to measure the radiative and convective heat transfer coefficient for jet impingement nozzle designs relevant to bread baking ovens. The heat transfer coefficient is directly linked to factors such as jet velocity and nozzle-to-surface distance – these relationships can be converted into an cost to determine an optimum heat transfer coefficient, which can then be translated into a set of operating conditions for an oven.

7.1 Background

According to Ovadia and Walker (1998) there are at least nine different ways to heat food; the three conventional methods outlined in section 3.1: conduction, convection and radiation, and four further modes: microwave, capacitive heating, electrical resistance heating and intense visible light. In general (and studied here), the bread baking process uses hot air to transfer heat to the dough surface through convection. Thermal radiation is also used to transfer heat between the internal

oven surfaces and the bread. Heat is then transferred to the centre of the dough via conduction.

Relatively high rates of heat transfer can be achieved with comparatively low air temperatures through jet impingement heat transfer, which is discussed in detail in section 3.2. Although jet impingement heat transfer is a well understood phenomenon, little work has been published relating to local heat transfer characteristics specific to bread-baking regimes. As discussed in section 3.2, much of the previously published work on jet impingement heat transfer has focussed on generating correlations for ASME standard nozzles. Whereas in practice, baking ovens are designed in the most cost-effective manner, meaning the nozzles are, in reality, sharp-edged punched holes in sheets of metal. These sheets are attached to pressure plenums above and below the product surface. Due to this, the heat transfer characteristics of jet impingement nozzles in industrial applications can differ somewhat to those reported in literature.

7.2 Experimental Apparatus

In order to measure mean and local heat transfer rates in the regimes relevant to the baking industry, experiments on a scaled down baking oven were carried out. The pilot oven, named the ‘hand sampling machine’, located at Spooner Industries Ltd., Ilkley, was designed to carry out small scale experiments using jet impingement for the food, coating, paper, thin-film, and other drying industries. One of the main advantages of being able to use this specialised drying apparatus was the ability to reproduce a wide range of conditions that are relevant to bread baking. This included the use of different nozzle designs, air velocities and dimensions of important geometries such as nozzle-to-surface distance.

Improvements in heat flux measurement technology over the past two decades have meant commercial sensors are now available that can measure and log heat transfer rates locally underneath nozzle orifices. The experimentation discussed in this

section makes use of these sensors to give correlations and results that are useful to oven designers and operators when assessing heat transfer in commercial ovens.

7.2.1 The Pilot Oven

A photograph of the oven used for the heat transfer experimentation is shown in Figure 7.1:



Figure 7.1 – Partially labelled photograph of the pilot oven used for heat transfer experiments

A labelled schematic of the pilot oven is shown by Figure 7.2, and the features are explained in Table 7.1. The overall dimensions of the oven were 2.5 m (height) x 4 m (width) x 4 m (length). 100 mm thick insulation panels cover each face of the machine, ①. Banks of nozzles were attached to the baking chamber above and/ or below the sensor position by sliding plates into mounting slots and bolting into place, ② and ③. Heat was supplied from a natural gas burner (Comtherm Limited) (up to 500 kW), which was further insulated for health and safety reasons, ④. K-type thermocouples located inside the oven plenum chamber fed into a PID controller which maintained consistent nozzle jet temperatures of up to 400 °C. The oven could reach steady set-point temperature within 30 minutes.

Combustion air was circulated to the top and bottom nozzle banks via a centrifugal recirculation fan which used a VSD to control air velocity, ⑤. This system allowed

nozzle exit velocities of between 10 and 60 m/s to be achieved. Manual dampers were located in the ducting between the recirculation fan and the nozzles which gave further control of air velocity to top and bottom nozzle banks, ⑥ and ⑦. For this study, only the top set of nozzles were used to give heat transfer rates of one set of impingement jets. An exhaust duct was located above the oven, which removed a proportion of the air to atmosphere to expel the products of combustion. The remainder of the air was recirculated in order to maintain oven temperature and airflow, ⑧. An integrated centrifugal exhaust fan was located in the exhaust duct, ⑨. The proportion of recirculated/ exhausted air was controlled by a manual air damper, ⑩. The proportion of recirculated/ exhausted air was controlled by a manual air damper, ⑩.

A heat flux sensor was used to measure and log the heat transfer characteristics created by the oven conditions, ⑪. The sensor was reciprocated below the top nozzle set by a specialised rig which used a motor, gearbox and extension arm to oscillate the sensor at a set frequency and displacement range, ⑫.

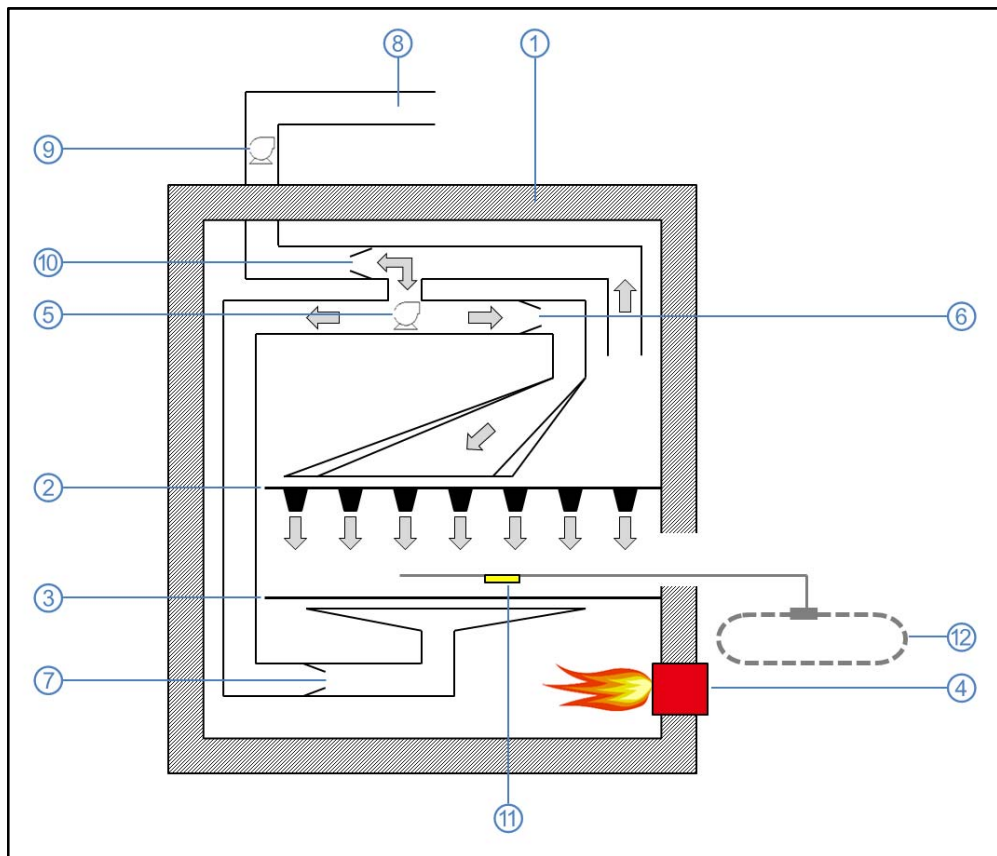


Figure 7.2 – Schematic of the pilot oven used for heat transfer experiments

#	Equipment	Description
①	Outer insulation:	100 mm thick outer insulation panels were used to maintain oven temperature and keep the operation of the pilot oven safe.
②	Top nozzle plate:	Different nozzle banks could be attached to supply airflow above the product.
③	Bottom nozzle plate:	Different nozzle banks could be attached to supply airflow below the product.
④	Burner:	Natural gas was supplied to the burner and combustion air was regulated to maintain a constant quantity of excess air (typical AFR ~ 2).
⑤	Recirculation fan and ducting:	A 22 kW fan was used to distribute air to the top and bottom nozzle plenums.
⑥	Top nozzle recirculation dampers:	Manual dampers were used to control the flow rate of air to the top nozzle banks, and thus jet velocity.
⑦	Bottom nozzle recirculation dampers:	Manual dampers were used to control the flow rate of air to the bottom nozzle banks, and thus jet velocity.
⑧	Exhaust duct:	Hot flue gases were exhausted to a centralised duct to be safely released to atmosphere.
⑨	Exhaust fan:	A 7.5 kW fan was used to expel exhaust air and maintain the oven at negative pressure. This ensured there were no hot air leaks out of the oven entrance.
⑩	Exhaust damper:	A manual damper was adjusted to determine the ratio of air that was recirculated and air that was exhausted to atmosphere.
⑪	Heat flux sensor:	Commercially available sensor used to measure local heat flux profiles and deduce values for heat transfer coefficient.
⑫	Reciprocating arm:	A motor and gearbox connected to a VSD allowed the sensor to be oscillated at a set velocity and traverse range. An arm was attached to the gearbox drive chain at one end and the heat flux sensor at the other.

Table 7.1 – Description of features of pilot oven

7.2.2 Nozzle Types

Two nozzle sets were used for comparison, an array of slot nozzles (ASN), consisting of rows of thin slots (or slits) and an array of round nozzles (ARN), consisting of rows of round holes. Both sets of nozzles were formed from 1.8 mm thick mild steel sheets.

The ASN arrangement, shown by Figure 7.3, consisted of a long array of 5 mm slots (more than 10 rows) pitched 230 mm apart in the x -direction. To maintain the slot width the folded metal sheets were welded together at a 5 mm gap at 200 mm intervals in the z -direction. ASNs are typically used for drying of food, paper, plastic film or metallic sheets (Wimberger, 1999). The reason for selecting this arrangement is that a number of correlations for heat transfer already existed for ASNs, meaning experimental results can be compared with the correlations reported in literature.

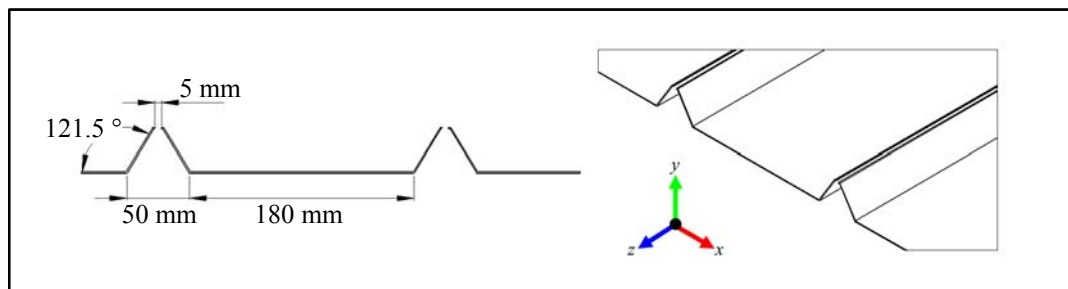


Figure 7.3 – ASN arrangement for heat transfer experiments

The ARN arrangement, shown by Figure 7.4, consisted of 36 x 12 mm diameter round holes spaced 22 mm apart across the width (z -direction), and pitched 230 mm along the length of the oven (x -direction). The ARN arrangement used is typical of those used in bread baking and differs from many studies reported in literature as the distance between the holes were asymmetrically distributed (i.e. the distance between holes down the length of the oven, x -direction, 230 mm, was more than ten times the distance across the width of the oven, z -direction, 22 mm). The holes for this nozzle arrangement were made using a CNC (computer numerical control) laser cutting machine.

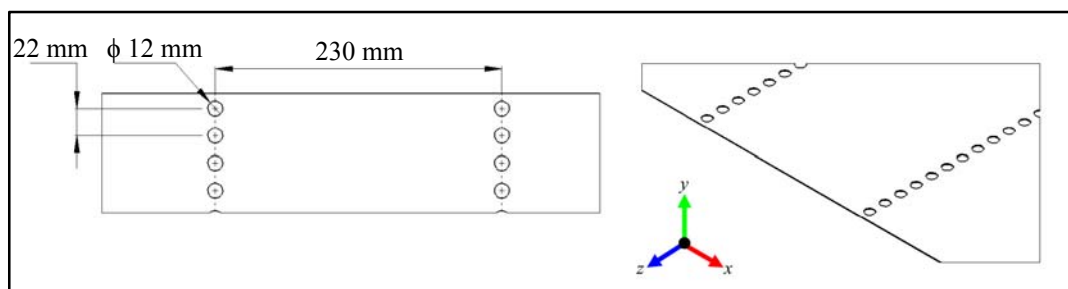


Figure 7.4 – ARN arrangement for heat transfer experiments

For the ARN, relative nozzle area, f , was calculated using Eq. (7.1), which has been altered to incorporate the asymmetry of the nozzle set used:

$$f = \frac{\pi d^2}{(4P \cdot S)} \quad (7.1)$$

The relative nozzle area for the ASN was calculated by Eq. (7.2):

$$f = \frac{d}{P} \quad (7.2)$$

The specifications for the two types of nozzle under investigation are shown by Table 7.2:

Nozzle type	ASN	ARN
Nozzle diameter/ width, d (mm)	5	12
Characteristic length, L_c (mm)	10 (= $2d$)	12 (= d)
Nozzle pitch, P (mm)	230	200
Ratio of pitch to diameter, P/d	46.00	16.67
Hole spacing, S (mm)	n/a	22
Relative nozzle area, f	2.174 %	2.235 %

Table 7.2 – Dimensions and specifications for the nozzle configurations investigated

7.2.3 The Heat Transfer Sensor

The heat transfer sensor used in this study is a commercially available RC01 heat flux sensor (Hukseflux Thermal Sensors, c. 2010), see Figure 7.5:

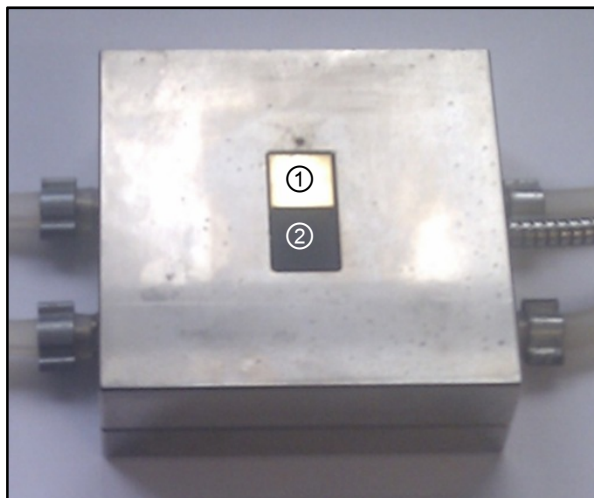


Figure 7.5 – Photograph of Hukseflux RC01 heat flux sensor (Hukseflux Thermal Sensors, c. 2010)

This sensor converts convective and radiative heat transfer into conductive heat transfer. Heat from the hot air jets heats two surfaces, one gold, ①, and one black, ②. This heat is then transferred across a thin layer of filling material that has a known value for thermal conductivity across a wide range of temperatures, usually a plastic is used, such as Kapton (Azar *et al.*, 2009). A thermopile accurately measures the temperature gradient across the filling material by locating alternate joints at the hot and cold faces of the material. A voltage output is generated which is directly proportional to the heat flux, Q , see Eq. (7.3):

$$Q = \frac{V_{sen}}{E_{sen}} \quad (7.3)$$

The sensor measured both convective heat flux and total heat flux; therefore radiative heat flux could be inferred. A diagram of the heat flux sensor is shown by Figure 7.6. Convective heat flux was measured by a gold-plated sensor, ①, which reflects the vast majority of thermal radiation as the emissivity of the surface in this regime is very low, $\epsilon_A < 0.05$ (Aksyutov, 1974). Total heat flux was measured by a black sensor, ②, which absorbs radiation, $\epsilon_A = 0.85$. The two calibration values, E_{sen} , were determined experimentally by the manufacturer on 17/01/2011. In addition, two K-type thermocouples; one located above the sensors, ③, and one located below the gold sensor, ④, were used to log ambient air temperature and internal sensor temperature.

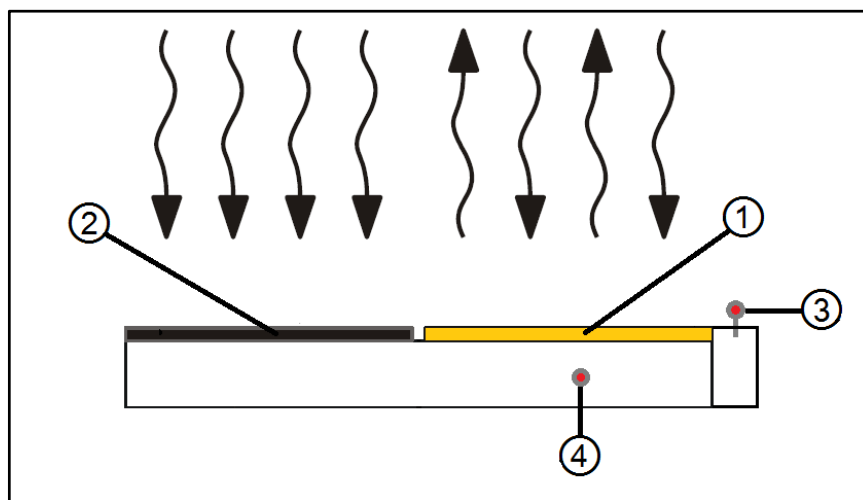


Figure 7.6 – Diagram of heat flux sensor (Hukseflux Thermal Sensors, c. 2010)

The sensor was mounted onto a nickel heat sink to ensure high thermal conductivity away from the filling material to prevent both surfaces reaching thermal equilibrium. Underneath the heat sink was a water-cooled block which dissipated heat away from the system.

The maximum temperature for measurement for this type of sensor is 250 °C, and the maximum flux that the sensor could be exposed to was experimentally determined for each particular regime. The accuracy of the heat flux sensor was given by the manufacturer as $\pm 10\%$ for total heat flux.

The sensor was connected to a TL01 Heavy Duty Data Logger (Hukseflux, The Netherlands), which logged results at 2 second intervals from four separate channels: ambient air temperature, ①, internal sensor temperature, ②, heat flux at black plate, ③ and heat flux at gold plate, ④ (see Figure 7.6). The logger could store up to 47,662 readings (equivalent of 26 hours of data), which was sufficient for this study. Live readings and the status of the sensor could be viewed via specialised 'TL01 Ovenlogger Application' software connected via USB to a PC.

Heat transfer sensors and the accuracy of their readings are discussed in detail by other authors: (Childs *et al.*, 1999, Diller, 1993). For the purposes of this report, the heat transfer results are compared with literature to validate their accuracy.

7.3 Methodology

In order to conduct heat transfer experiments the conditions within the oven had to be carefully prepared. The exhaust fan on the pilot oven was turned on to ensure any unburned gas was expelled from the oven before the burners were ignited. This was done with all dampers fully open and the recirculation fan running to circulate air throughout the ducts and oven plenum chambers. Once the purge cycle was complete, the burners were ignited. Hot air and combustion products were recirculated until set temperature was reached. The oven was then left for approximately 30 minutes for the internal temperature to stabilise.

Nozzle exit velocity was calculated from two temperature corrected static pressure readings from the oven plenum. The first reading was from a mounted pressure gauge which was connected directly to the plenum chamber above the top nozzles. The second reading was taken from a P200UL Digital Manometer (Digitron Instrumentation Limited, UK) attached to a tapping point connected directly to the top nozzles. Mounted pressure gauges and tapping points were also located at the bottom nozzle plenum chamber. The velocity values inferred were corroborated by pitot tube measurements taken at the nozzle exit. The accuracy of the manometer measurements is given in the P200UL manual as $\pm 0.1 \% \text{ FS} + 1 \text{ digit}$, i.e. 0.02 mbar. Measurements were between 0.13 and 2.00 mbar, giving potential percentage error in nozzle jet air velocity readings, u_{noz} , of between 1.00 and 15.38 %.

The heat flux sensor was housed in a square-shaped aluminium holding rig, with dimensions of 0.5 m x 0.5 m, made out of 1.8 mm thick aluminium sheet. This ensured the sensor was flush to the surface of the aluminium rig, thus not affecting the airflow field around the sensor. An adjustable bracket on the back of the sheet fixed the sensor in place. This rig was fixed to a steel frame which prevented the rig from bending under the high-velocity air jets and maintained consistent nozzle-to-surface distances, H .

The sensor and holding rig were reciprocated in the x -direction (the length of the oven) via a gearbox and motor configuration housed outside the pilot oven entrance. The velocity of the reciprocator could be altered using a VSD which controlled the motor speed. The minimum velocity of the reciprocating arm was 0.1 mm/s and maximum velocity was 40 mm/s. For this study, a velocity of 0.25 mm/s was chosen, which gave a good balance of measurement profile resolution whilst being able to conduct a complete traverse of a standard nozzle arrangement (230 mm pitch with a safety margin of at least 50 mm either side) in less than 30 minutes. Taking into account the time required to set up the equipment and to adjust the rig between experiments, around six to eight experiments could be

conducted per day, which allowed time for the quantity of results presented here to be collected.

In order for the sensor to remain functional during the tests, water cooling to the bottom surface of the sensor was necessary. Tests were conducted to show that the effect of using different water flow rates did not affect the results. Mains water was supplied, and warm cooling water (around 30 °C) was discharged to drain, via two 5 m long, 5 mm inner diameter high-temperature flexible hoses. The volumetric flow rate of cooling water through the sensor was nominally $1 \times 10^{-5} \text{ m}^3/\text{s}$.

When the heat flux sensor entered the pilot oven, it was left for approximately 5 minutes to allow output readings to stabilise. The sensor traversed across more than one full nozzle pitch length in all cases. One nozzle pitch length, P , is shown diagrammatically by Figure 7.7:

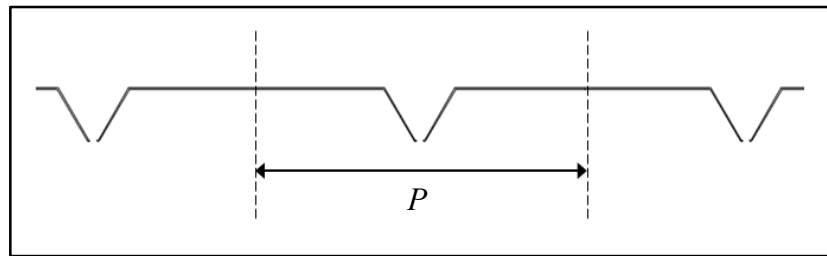


Figure 7.7 – Diagram showing minimum traverse range (P) of heat flux sensor

7.4 Validation of Experiments

An important part of this project was to validate the results of the sensor in terms of repeatability, symmetry about a nozzle orifice and correlation of results with those reported in literature. These issues are addressed in the following sections 7.4.1 to 7.4.3.

7.4.1 Repeatability

In order to investigate the repeatability of the experiments, the sensor was traversed across the width of more than two complete pitch lengths of 5 mm slot nozzles (i.e. centre-to-centre of three nozzle sets). The conditions for the repeatability study

were: Temperature, $T = 200\text{ }^{\circ}\text{C}$, Reynolds number, $Re = 4,541$ and ratio of nozzle-to-surface distance over nozzle diameter, $H/d = 6$. The heat flux profile measurements for both convective and radiative heat fluxes have been shown to be repeatable by Figure 7.8:

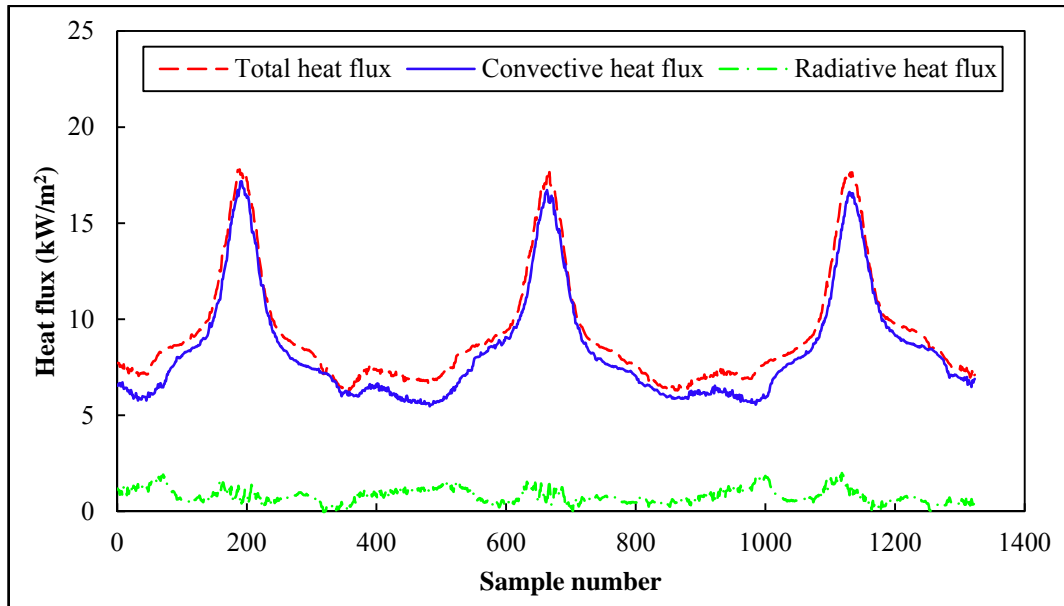


Figure 7.8 – Heat transfer graph indicating the degree of repeatability of the heat flux profile measurements

It is standard practice in the field of jet impingement heat transfer to display results in dimensionless form, therefore the following results are given using this format, meaning h_c and u_{noz} are expressed as Nu and Re respectively.

The Nusselt number profiles of the three nozzles traversed for Figure 7.8 are shown overlaid on each other in Figure 7.9, where x/d is the dimensionless distance from the nozzle centre. Again, it can be seen that in the region $-13 < x/d < 13$ the measurements are very similar, however in the regions $x/d > 13$ and $x/d < -13$ the Nusselt number profiles of the three nozzle sets are unsteady. This is because in this region the flow is interacting with the adjacent jets. Jet interaction can give unpredictable results depending on the internal ducting and fan arrangements in the pilot oven. It is important to note that the correlation between the three nozzle peaks is extremely high; the Pearson product-moment correlation coefficient

(Pearson's r value) is between 0.972 and 0.991 for the three data sets. The mean Nusselt number values in the region $-18 < x/d < 18$ (the only region where all three data sets could be equally compared) were 16.46, 17.12 and 16.72 for nozzles sets 1, 2 and 3 respectively. These values are all within 4 % error margin of each other indicating a high degree of repeatability.

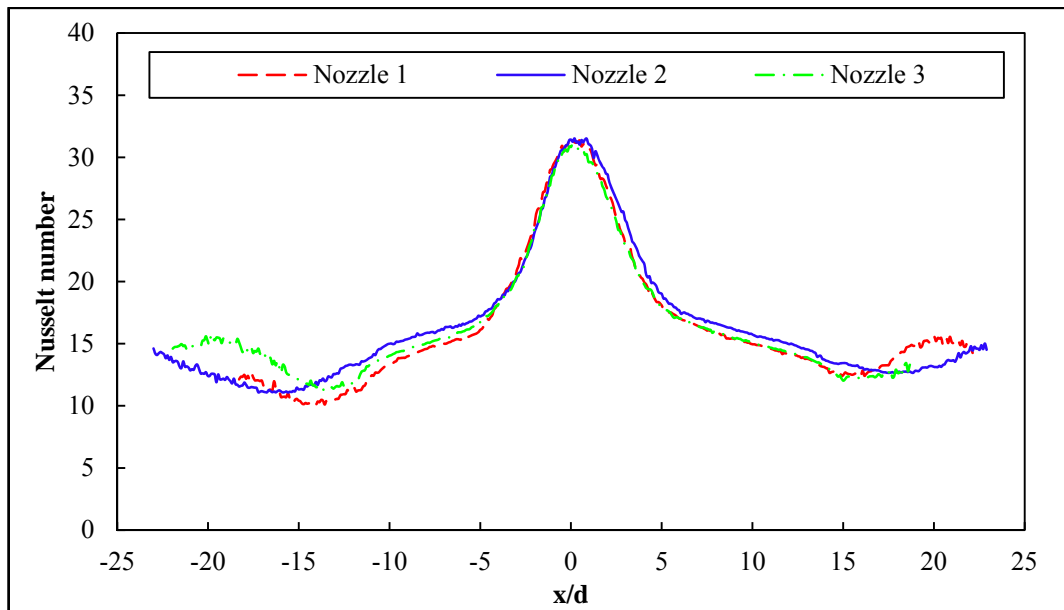


Figure 7.9 – Dimensionless heat transfer coefficient of three nozzle profiles overlaid on each other showing the degree of repeatability of the heat flux sensor

7.4.2 Heat Flux Symmetry about Nozzle Centre

The Nusselt number profiles presented in this chapter can be slightly asymmetric due to local flux fluctuations, particularly in the region between two sets of nozzles where external factors such as jet interaction, ducting arrangements and exhaust fan positioning can have a greater effect on heat transfer. In small scale experiments, these effects can be minimised by locating fans at the optimum position, however it is important to gather an appreciation of these effects for industrial applications using the pilot oven arrangement discussed here.

For the nozzles studied in Figure 7.8 and Figure 7.9, the asymmetry of heat flux of nozzles 1, 2 and 3 in the region $-18 < x/d < 18$ is 6.54, 15.27 and 5.96 % respectively. This level of asymmetry is typical for heat transfer measurements of

arrays of jets due to the effect of interaction between jets (Geers *et al.*, 2004). The values of Nu for $x/d > 0$ and $x/d < 0$ are shown graphically by Figure 7.10. It can be seen that in general slightly higher values are typically obtained for $x/d > 0$ than those obtained for $x/d < 0$.

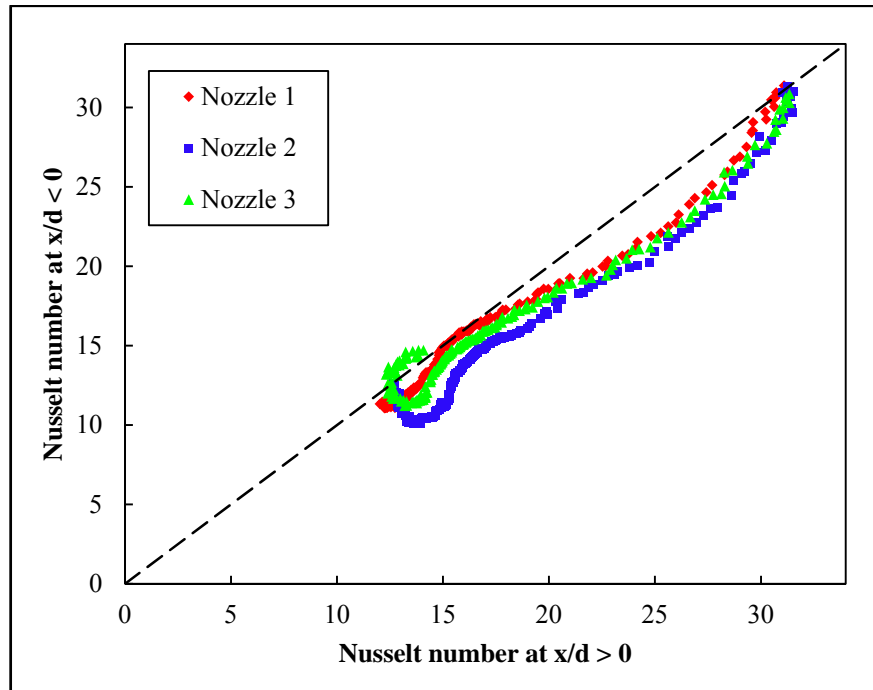


Figure 7.10 – Graph showing the degree of symmetry of heat flux measurements about the nozzle centre

7.4.3 Nusselt Number Correlations Compared with Literature

The effect of air velocity (Reynolds number) on mean heat transfer coefficient (mean Nusselt number) was investigated for ASN and ARN for the set of conditions outlined in Table 7.3. The purpose of measuring these values was to compare the results with literature.

Nozzle type	ASN	ARN
Jet temperature, T , (°C)	184 to 204	192 to 200
Nozzle-to-surface distance, H (mm)	25	25
Ratio of nozzle-to-surface distance over diameter, H/d	5.000	2.083
Reynolds number, Re	3,221 to 10,902	3,711 to 13,129

Table 7.3 – Range of conditions for correlations between Reynolds number and Nusselt number

Heat transfer correlations for ASNs are widely available. Since their profile is constant across the width of the oven they can be considered two-dimensional. In addition, the nozzle profiles can be easily and consistently manufactured from sheet metal making experimental measurements on different facilities comparable.

Experimental values for mean Nusselt number, shown in Figure 7.11, match closely with the correlations in literature (Das *et al.*, 1985, Hardisty and Can, 1983, Martin, 1977). The results particularly corresponded with Das *et al.* (1985), comparison with this data shows their correlation over predicted Nusselt number by a mean percentage error of 6.7 % and a maximum percentage error of 10.2 %, and Martin (1977), who under predicted Nu by a mean percentage error of 8.8 % and a maximum percentage error of 13.4 %. The correlation of Hardisty and Can (1983) was less applicable; it over predicted the Nusselt number by a mean of 30.2 % and a maximum of 40.7 %. The wide range of correlations highlights the need for experimental correlations to be made for the specific nozzle types under investigation.

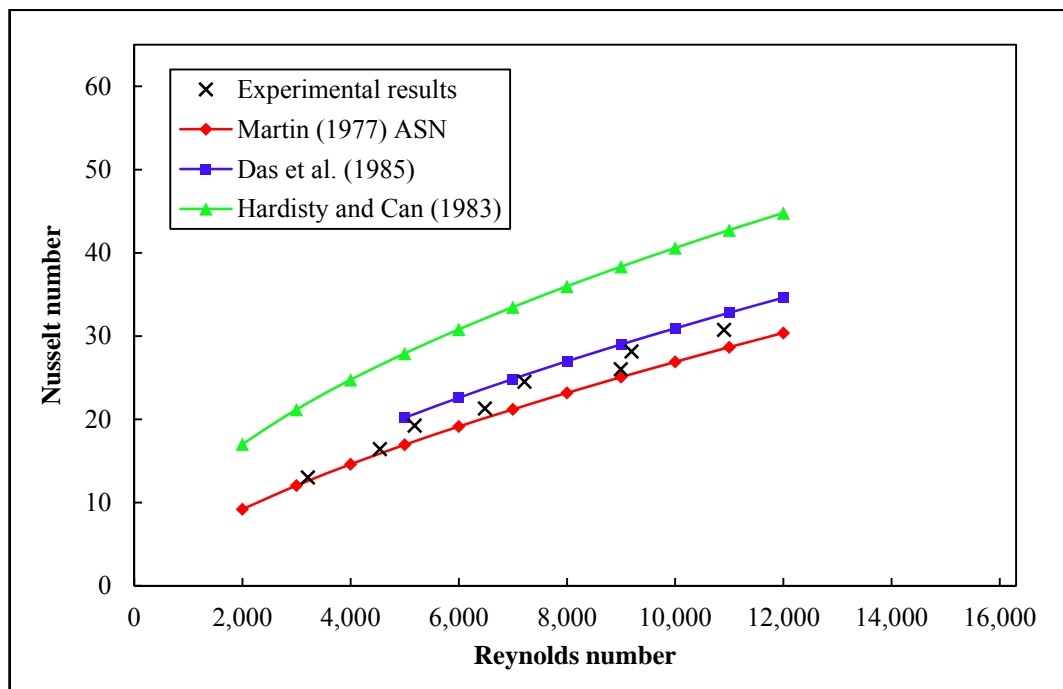


Figure 7.11 – Graph of Reynolds number against mean Nusselt number for ASN experimental results and correlations reported in literature

For the ARN used, there are no correlations in literature which capture the asymmetric nature of the hole distribution. For this reason, the results were compared with two of the Martin (1977) correlations; ARN and ASN. This was to test the assumption within industry that rows of closely spaced rows of round nozzles approximate ASNs. Table 7.4 shows the alterations to the dimensions that were necessary to approximate the correlation for ARNs as ASNs:

Nozzle type	ARN	ARN as ASN
Nozzle diameter/ width, d (mm)	12	5.141
Characteristic length, L_c (mm)	12 (= d)	10.282 (= $2 d$)
Ratio of nozzle-to-surface distance over diameter, H/d	2.083	4.863
Relative nozzle area, f	2.235 %	2.235 %

Table 7.4 – Changes to dimensions for correlating the asymmetric ARN as an ASN

Figure 7.12 shows that the non-symmetrical ARN behaves closer to the Martin (1977) ASN correlation than it does to the ARN correlation, particularly at lower Reynolds numbers ($Re < 10,000$). The mean difference between experimental results and the ASN correlation is 9.0 % and the maximum difference is 13.5 %, whilst the mean difference when compared to the ARN correlations is 28.3 % and the maximum difference is 33.2 %.

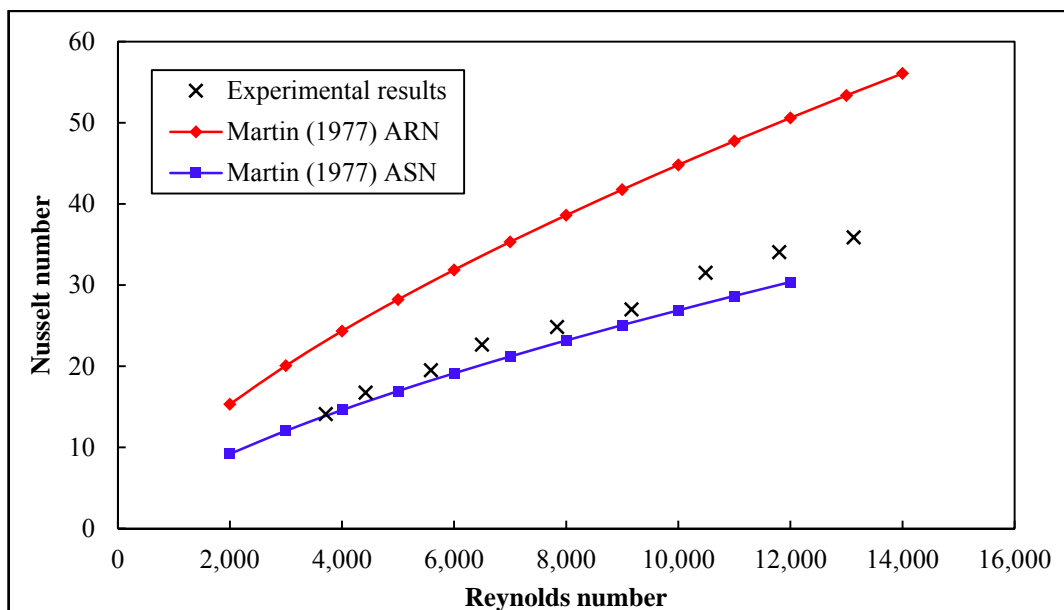


Figure 7.12 – Graph of Reynolds number against mean Nusselt number for ARN experimental results and correlations reported in literature

7.5 Mean Heat Transfer Measurements

Mean heat transfer correlations are useful to industry as they give an overall value to benchmark differences between heat transfer characteristics for a range of nozzle configurations.

7.5.1 Correlation of Nusselt Number with Reynolds Number

The results showing how the rate of heat transfer varies with air velocity (Re versus Nu) are shown in the previous section by Figure 7.11 and Figure 7.12. These results are reproduced below in Figure 7.13, with a correlation that represents a good fit when compared to both aforementioned data sets. For simplicity, the correlation to predict the Nusselt number from the Reynolds number is given by the power relation:

$$Nu = mRe^n \quad (7.4)$$

where, for the set of conditions used, $m = 0.047$ and $n = 0.7$.

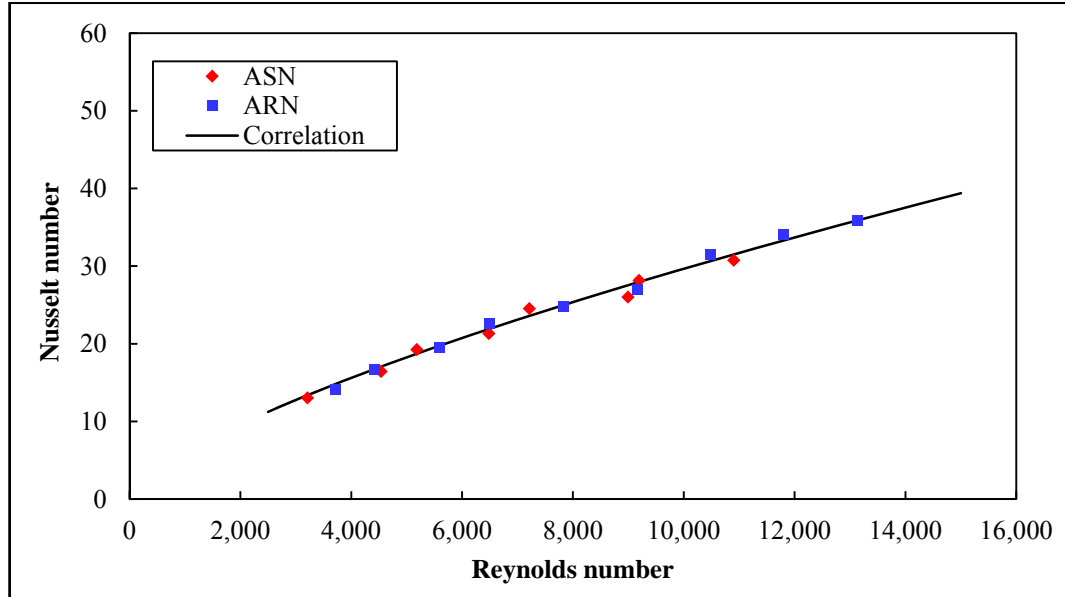


Figure 7.13 – Graph showing Nusselt number correlations for ASN and ARN

The Coefficient of Determination (R^2) value for these two sets of data when compared to Eq. (7.4) is shown by the regression plot, Figure 7.14. R^2 values of 0.9838 and 0.9928 for ARN and ASN respectively show the very high degree of

validity of the proposed correlation of Reynolds number and Nusselt number. The correlation developed is valid for the following range of conditions, which are relevant to bread baking applications:

- $3,200 < Re < 13,200$
- $H/d = 5, d = 5 \text{ mm}, f = 2.17 \%$ for ASN
- $H/d = 2.083, d = 12 \text{ mm}, f = 2.24 \%$ for ARN
- $T = 200 \text{ }^\circ\text{C}$

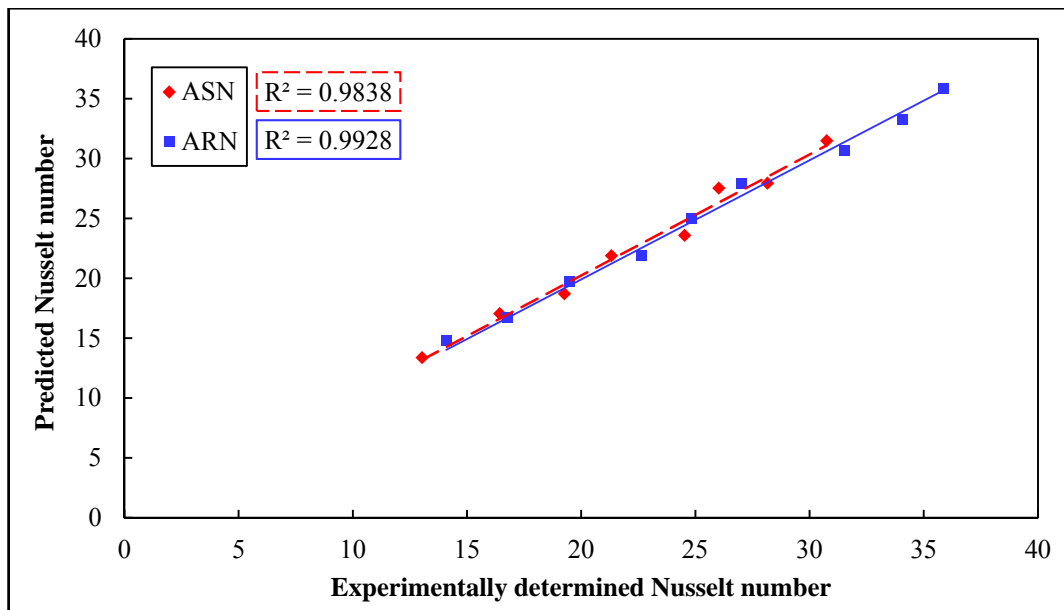


Figure 7.14 – Regression plot to measure R^2 value of data sets compared with correlation

The correlation presented, predicts the Nusselt number as a function of Reynolds number. This enables commercial oven designers to balance the energy flows in a new design of oven. Heat transfer rates at greater air jet velocities will inevitably increase production rates and therefore reduce the gas consumption of the oven. However, this should be balanced against the additional electrical energy required for air distribution and product quality concerns, as discussed further in section 7.7.

7.5.2 Variation of Heat Transfer with Nozzle-to-Surface Distance

It has been widely reported that maximum heat transfer rates are achieved when H/d is between 2 and 8 (Mujumdar, 2007, Stephan, 1993), and that heat transfer

rates can be increased by 20 % by optimising H/d (Zuckerman and Lior, 2006). Figure 7.15 shows the Martin (1977) correlations for Nusselt number compared with H/d for $Re = 5,000$. The correlations show that for both ASN and ARN, heat transfer decreases when $H/d > 2$.

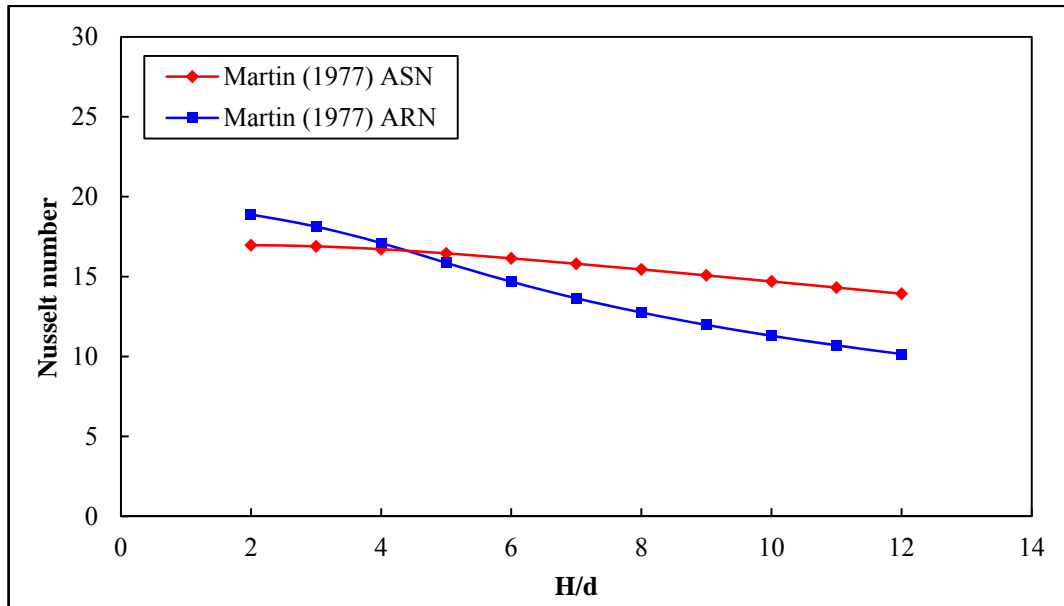


Figure 7.15 – Martin (1977) correlations for dimensionless nozzle-to-surface distance (H/d) against Nusselt number for ASN and ARN

Experimental results of Nusselt number using the ARN for $1.33 < H/d < 7.83$ are shown by Figure 7.16. It can be seen again that these results align well with correlations from literature, in this case Martin (1977) ASN. The degree of accuracy of the approximation of the asymmetric ARN as ASN can be observed for a range of H/d ratios. The experimental results have a mean percentage difference in comparison with literature of 2.06 % and a maximum difference of 6.99 %. The trend of slightly decreasing Nusselt number with increasing H/d is observed. This trend is relevant to bread baking as decreasing the nozzle-to-surface distance would be desirable to achieve higher heat transfer rates whilst maintaining the same nozzle velocity, indicating the opportunity to decrease the baking time whilst using the same amount of energy. Decreasing the nozzle-to-surface distance presents a number of practical problems for bread baking; as the nozzles are closer to the conveyor, cleaning can be made more difficult and blockages in the oven can

become more frequent when two dough-pieces are accidentally stacked above one another. In order to manufacture ovens with optimum H/d ratios, these issues require addressing.

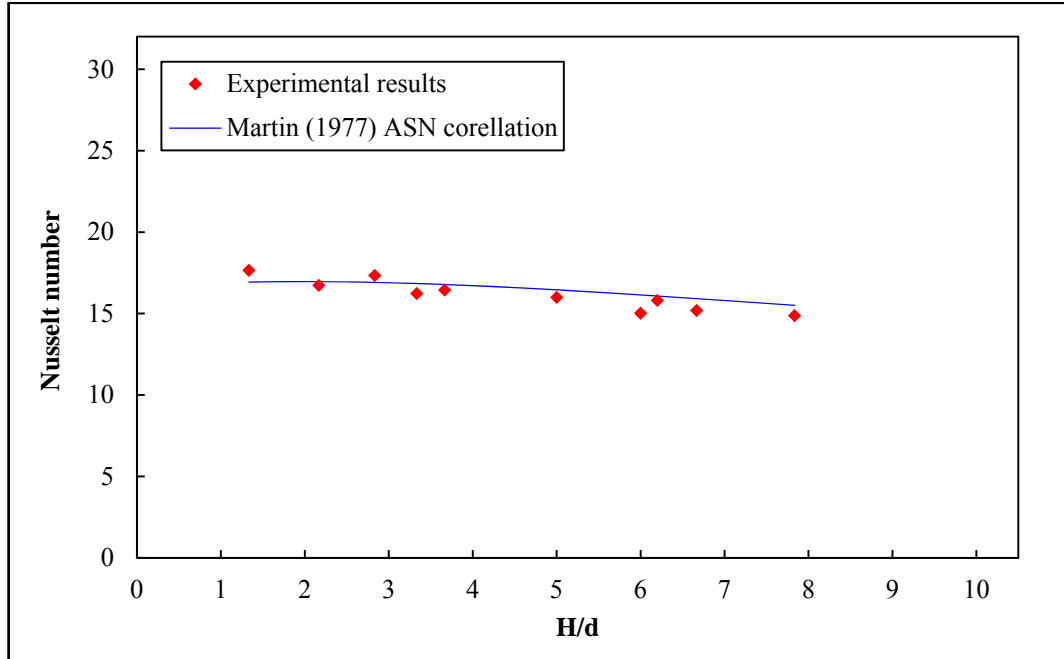


Figure 7.16 – Comparison of experimental mean Nusselt number results for ARN at varying H/d ratio with Martin (1977) ASN correlations

7.5.3 Mean Proportion of Radiation and Convection

The quality parameters of bread are partially determined by the balance of heat transfer to the surface of the bread through radiation and convection in the oven (Williamson and Wilson, 2009). For a bakery chain with multiple ovens it is important to ensure that each oven produces the same product. This can be standardised by profiling the percentage of radiation and convection for different operating regimes. It is known that baking cookies with a higher proportion of radiative heat transfer results in a darker coloured product (Shibukawa *et al.*, 1989), and it is believed, though it is not reported in literature, that the same phenomena applies to bread baking (Kirk, 2011). Other quality factors that are thought to be determined by the degree of radiation include taste and density.

As the Reynolds number increases, the proportion of heat transfer due to convection increases and radiation decreases, as shown by Figure 7.17 and Figure

7.18, for ASN and ARN respectively. This is consistent with theory, as values of radiative heat transfer are unaffected by air velocity, whereas the convective heat transfer increases, therefore the relative proportion convection increases and radiation decreases.

For both sets of nozzles, the proportion of radiation decreased linearly with increasing Reynolds number. Both graphs exhibit a strong trend, with R^2 values of 0.998 and 0.978 for ASN and ARN respectively.

The linear trend line equations given for ASN and ARN give y-intercept values as 11.428 and 10.271 % respectively. This implies that for regimes with very low airflow ($Re < 500$), only 10 to 12 % of heat transfer would be due to radiation – this seems unlikely. The proportion of heat transfer due to radiation for low Reynolds numbers would require validation, therefore the linear trends in Figure 7.17 and Figure 7.18 can only be valid for the set of conditions that have been tested in this study, the same as those in Table 7.3. The gradient of both trend lines is roughly equal, further indicating that closely spaced rows of round holes can be approximated as ASN.

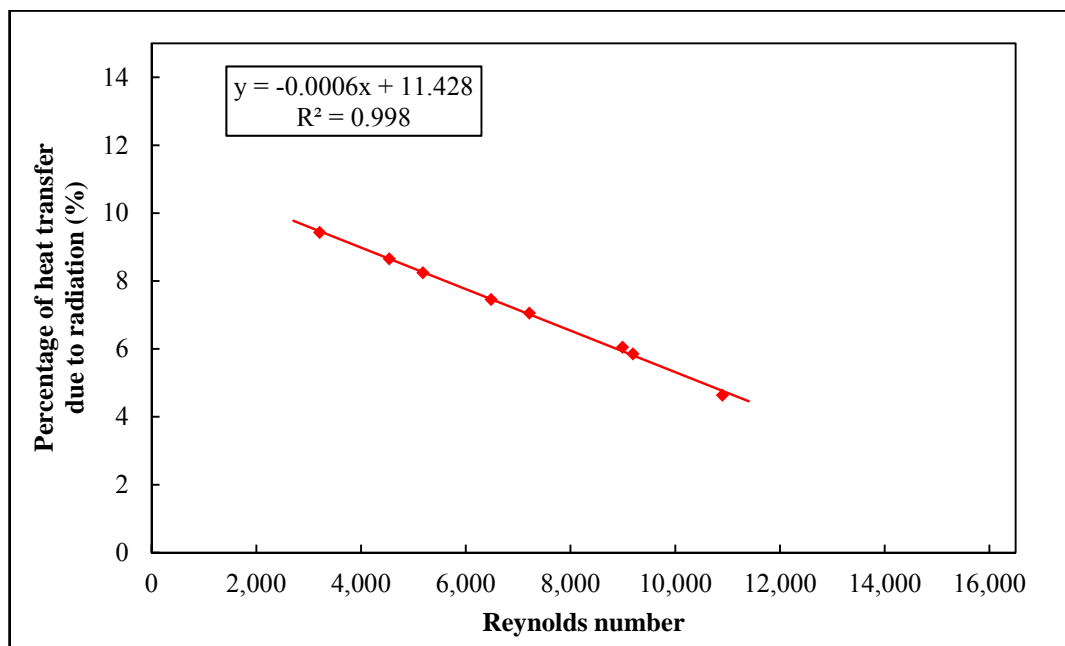


Figure 7.17 – Graph of Reynolds number against mean percentage of heat transfer due to radiation for ASN

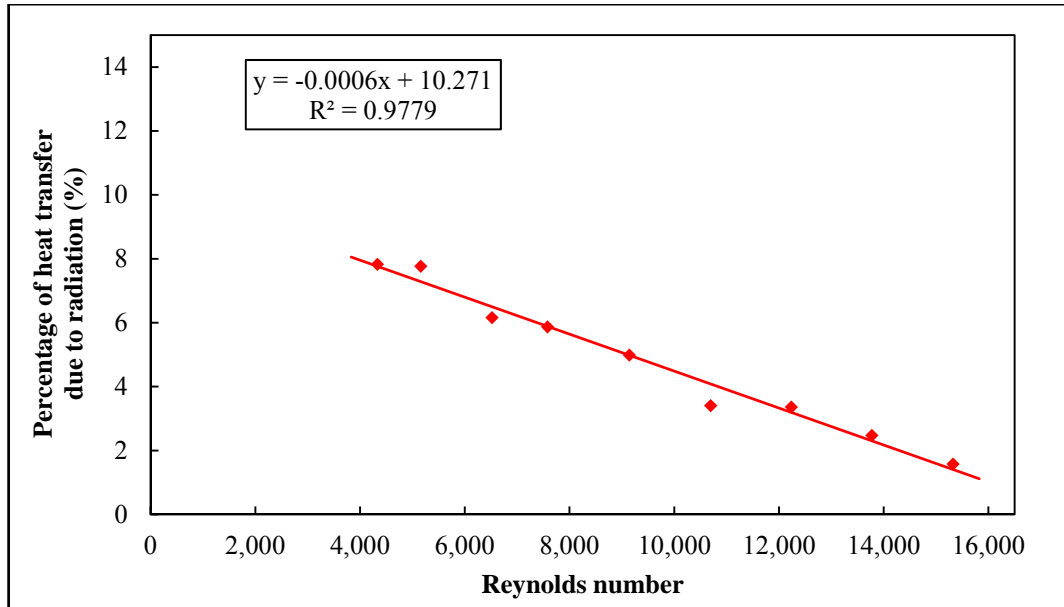


Figure 7.18 – Graph of Reynolds number against mean percentage of heat transfer due to radiation for ARN

7.6 Local Heat Transfer Measurements

Local heat transfer measurements show the locations of maximum and minimum heat transfer rates and detailed profiles of heat transfer across the nozzle pitch can be observed. Local heat transfer profiles are particularly useful for oven designers to assess the difference between maxima and minima, thus indicating the degree of non-uniformity of the bake profile. For nozzles that are close together, or where H/d is small, interactions between flow fields can be identified, these can have positive or negative effects on local and mean heat transfer rates.

As the heat flux profiles have been shown to be greater than 90 % symmetric about the nozzle centre, standard practice is followed for displaying local jet impingement heat transfer results and the local profiles are shown for half of the nozzle pitch (i.e. Nu only displayed for $x/d \geq 0$).

7.6.1 Local Profiles of Nusselt Number with Reynolds Number

Figure 7.19 shows local dimensionless heat transfer coefficient distribution across the ASN configuration for Reynolds numbers in the range of $3,221 \leq Re \leq 10,902$, for $H/d = 5$ and $T = 200$ °C. There is one primary peak at $x/d = 0$. Either side of this

peak the Nusselt number decays exponentially until the middle point of two nozzle banks ($x/d = \pm 23$), where the minimum value is reached. Subtle secondary peaks in Nusselt number can be identified at $x/d \approx \pm 14$, indicating a small amount of turbulence in the wall jet region; the insignificance of these peaks can be attributed to the H/d value (5), which is around the upper limit at which secondary peaks occur (Colucci and Viskanta, 1996).

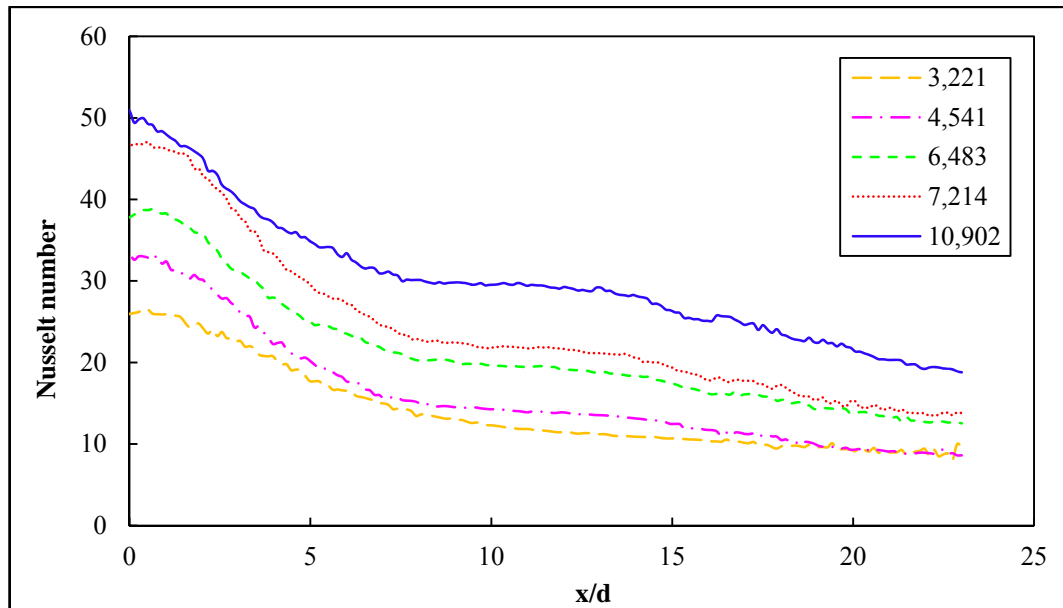


Figure 7.19 – Graph of local Nusselt number against dimensionless distance from the centre of the nozzle jet (x/d) for ASN for five different Reynolds numbers between 3,221 and 10,902

The H/d ratio has a dominant effect on the occurrence of secondary peaks, as they only appear for low values ($H/d < 5$) (O'Donovan and Murray, 2007). This is due to a thinning effect of confining the airflow which causes a change from transitional to turbulent flow in the wall jet boundary layer. This increase in turbulence causes a peak in heat transfer (Fitzgerald and Garimella, 1998). The effect of air velocity on the appearance of secondary peaks is also well documented in literature – and is due to the illusion that higher Reynolds number has on reducing H/d . The potential core of the jet is longer for higher jet velocities due to an increase in turbulent intensity, meaning the interaction between the jet and the surface behaves as if the H/d ratio were lower. This results in a further recirculation zone between the nozzle

centres and thus, the development of secondary peaks (O'Donovan and Murray, 2007). It can be seen that for both Figure 7.19 and Figure 7.20 secondary peaks are more prevalent at higher Reynolds numbers.

Figure 7.20 shows local dimensionless heat transfer coefficient distribution across the ARN configuration for Reynolds numbers in the range of $3,711 \leq Re \leq 11,801$, for $H/d = 2.083$ and $T = 200$ °C. Aside from the primary peak in the Nusselt number at $x/d = 0$, there are two distinct secondary peaks at $x/d \approx \pm 7$. Minimum heat transfer occurs at $x/d \approx \pm 5$ and 10. The three maxima at the centre of the nozzle exit and the locations of the two secondary peaks either side of the jet centre are clearly identified for the ARN. This is due to the effective 58.3 % reduction in H/d (5 to 2.083) from the ASN results shown by Figure 7.19.

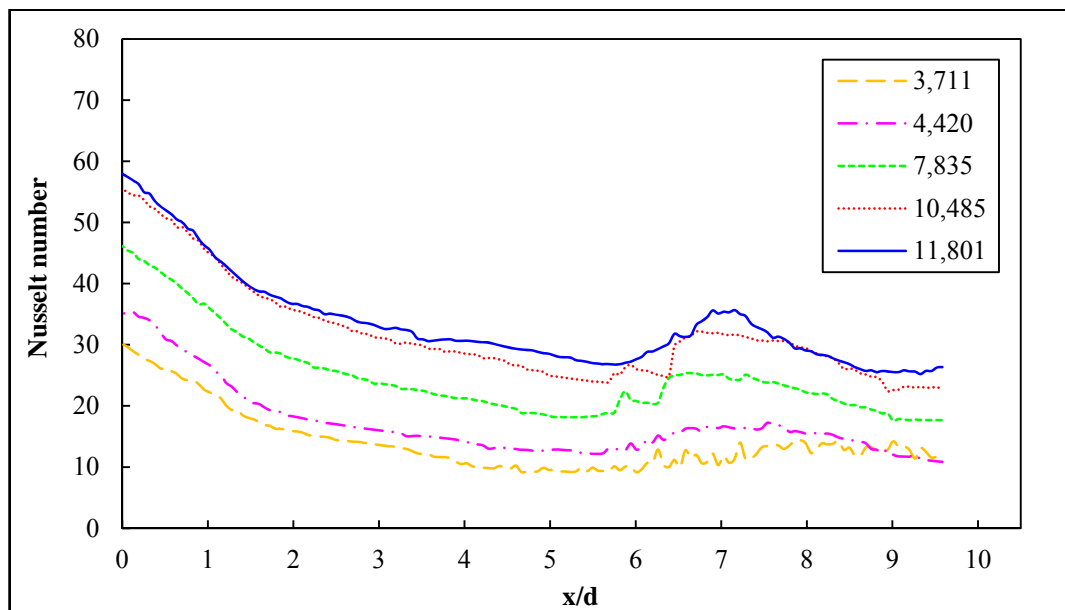


Figure 7.20 – Graph of local Nusselt number against dimensionless distance from the centre of the nozzle jet (x/d) for ARN for five different Reynolds numbers between 3,771 and 11,801

7.6.2 Local Profiles of Nusselt Number with Dimensionless Nozzle-to-Surface Distance

By combining the closest comparable results from Figure 7.19 and Figure 7.20 ($Re = 6,483$ and $6,496$ respectively) a rudimentary comparison between local heat flux measurements at different nozzle heights can be seen, as shown by Figure 7.21. As

these results are from differing nozzle arrangements, they are not directly comparable, but the clarity of the secondary peaks is improved when H/d is decreased from 5 to 2.083.

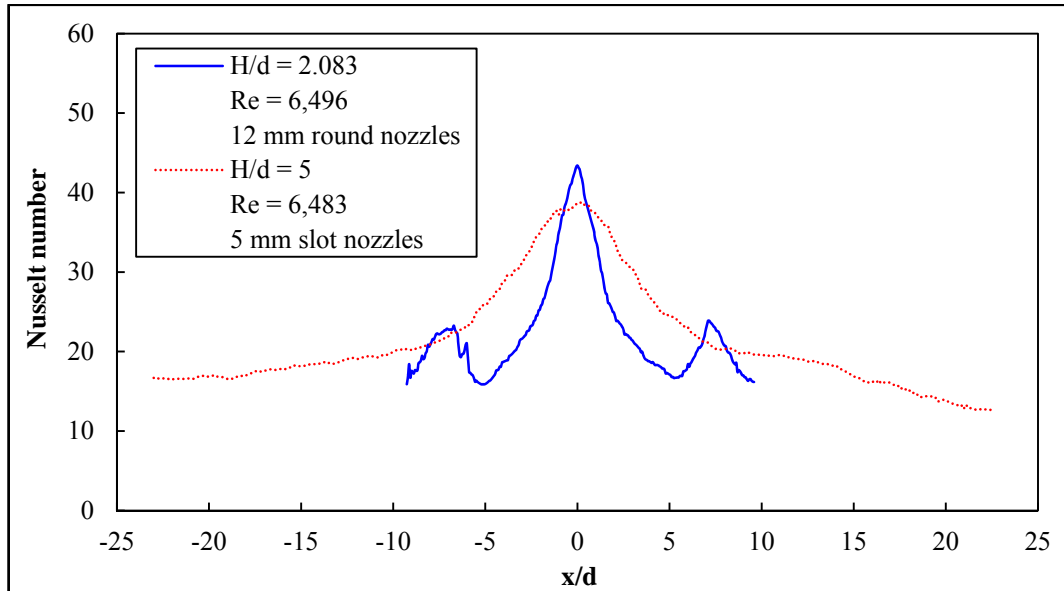


Figure 7.21 – Graph of local Nusselt number against dimensionless distance from the centre of the nozzle jet (x/d) for two different nozzle types and H/d values

The local variation of Nusselt number for values $1.33 \leq H/d \leq 7.83$ is shown by Figure 7.22. The constant conditions for these experiments were: $Re = 3,211$, $T = 200$ °C and the set of nozzles used was the ARN.

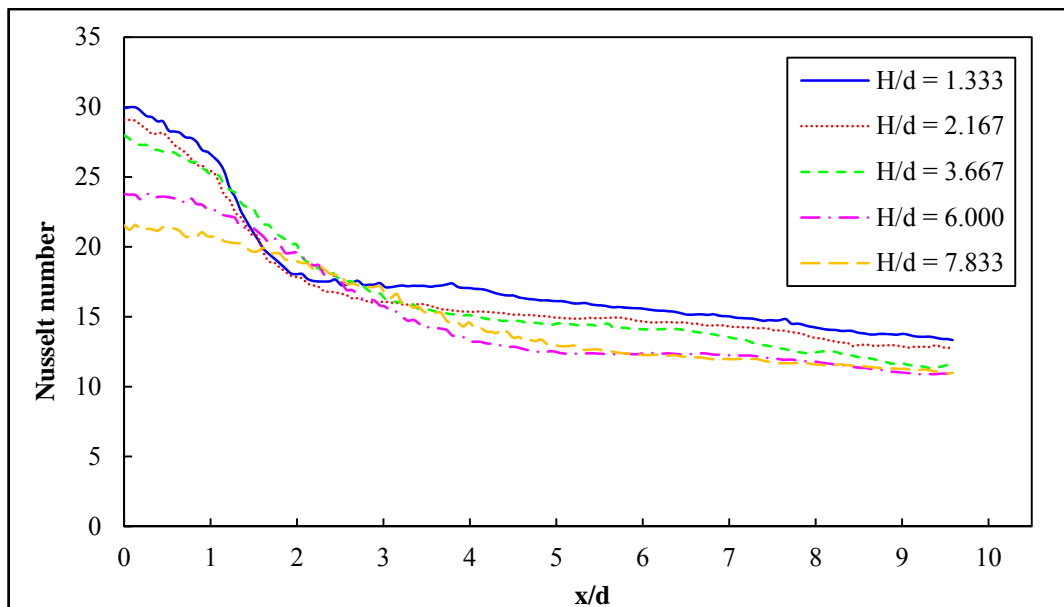


Figure 7.22 – Graph of local Nusselt number against dimensionless distance from the centre of the nozzle jet (x/d) for different values of H/d for ARN

It can be seen that for lower nozzle-to-surface distances, the Nusselt number has a higher peak at $x/d = 0$, but these decrease more rapidly with increasing x/d . At $x/d \approx 2.5$ all the profiles converge and secondary peaks can be observed for x/d values of between 4 and 6.

7.7 Optimisation of Heat Transfer Coefficient for Energy Savings

Heat flux correlations can be used to model oven energy use by using a three-dimensional conduction model to predict the bake time for a range of heat transfer coefficients. The model used makes use of finite element analysis software, COMSOL Multiphysics (COMSOL, 2012), to predict bake time and is described fully in Khatir *et al.* (2012b).

Once bake time is deduced, the throughput of product can be predicted if the capacity of the oven is known – for example if the bake time was 30 minutes (1,800 s) for an oven with a capacity of 5,000 kg the throughput would be $5,000/1,800 = 2.78$ kg/s. If the bake time were halved, the throughput would double whilst the oven will require the same amount of energy per kg of product to heat the dough, tins and conveyor, to gelatinise the starch and to evaporate the moisture from the product. The other heat losses – such as those through the roof, walls and exhaust, remain constant regardless of the oven throughput. The thermal energy efficiency saving can be calculated by assuming that approximately 19 % of oven heat is lost to ambient, using the methodology described by in Chapter 6. Therefore for a faster bake time the specific energy loss is reduced linearly with bake time.

Whilst a faster bake allows throughput to increase, and thus thermal efficiency to increase, the higher air velocity required to increase convective heat transfer results in a larger electricity load to power recirculation fans to increase the pressure in the air supply ducts. The energy required to operate the fans given a certain required velocity can be estimated using Eq. (7.5):

$$\dot{E}_{elec} = \Delta P Q \quad (7.5)$$

where ΔP is calculated using Bernoulli's equation for a range of air velocities.

The relationship between air velocity and heat transfer coefficient is given by the dimensionless correlation, Eq. (7.5). By balancing the heat saving (gas) with the additional energy load to power the fans (electricity), the optimum convective heat transfer coefficient for energy efficiency can be calculated – this graph is shown by Figure 7.23. It can be seen that when the heat transfer coefficient increases above 40 W/(m²·K), there is a marked rise in electricity required to distribute the air. Conversely, with small values for heat transfer coefficient, the heat losses to ambient are more significant.

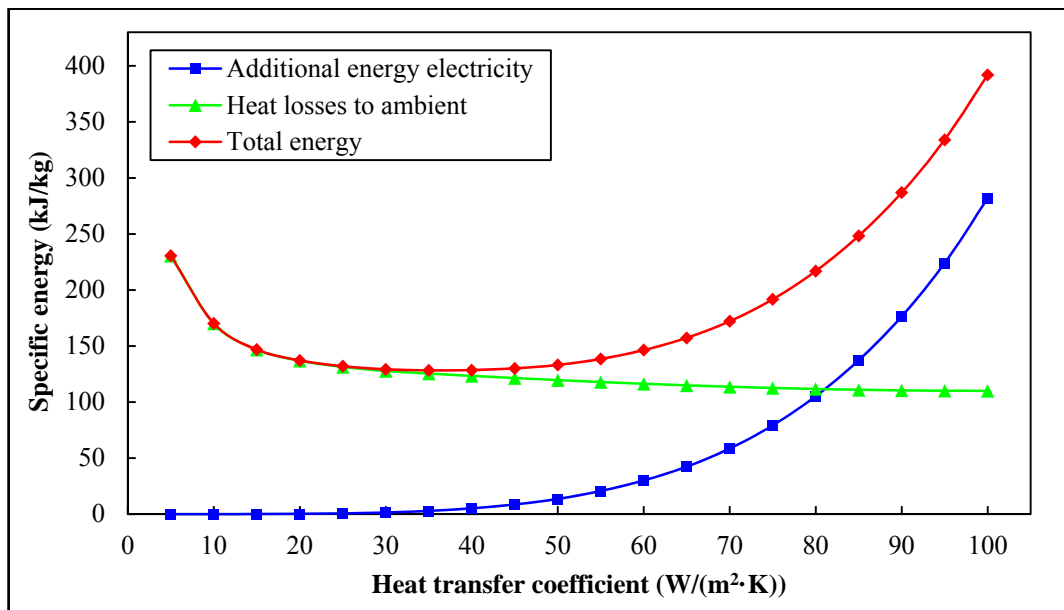


Figure 7.23 – Predicted specific oven gas and electricity use as a function of heat transfer coefficient

In terms of total specific energy in kJ/kg, the optimum value for heat transfer coefficient occurs for $h_c = 35$ W/(m²·K). Using these conditions, the energy model gives specific energy savings based on using the reported value of $h_c = 10$ W/(m²·K) (Rohsenow *et al.*, 1998) of 41.8 kJ/kg, which is composed of using an extra 2.9 kJ/kg of electricity in the fans to save 44.7 kJ/kg of heat losses to ambient. The total energy saving is 5.20 % based on the fact that the energy needed to bake

bread under typical operating conditions is at least 804 kJ/kg – as seen in section 6.7. Depending on whether bakeries wish to prioritise reducing their energy use, financial cost of energy or carbon emissions may influence the measure used for energy efficiency. The carbon and financial cost penalties for electricity are currently greater than gas, meaning a lower value for heat transfer coefficient may be preferable. The carbon dioxide equivalent emissions per kg production graph, as shown in Figure 7.24, indicates an optimum value for lowering carbon emissions of 30 W/(m²·K), i.e. 5 W/(m²·K) lower than optimising for energy consumption.

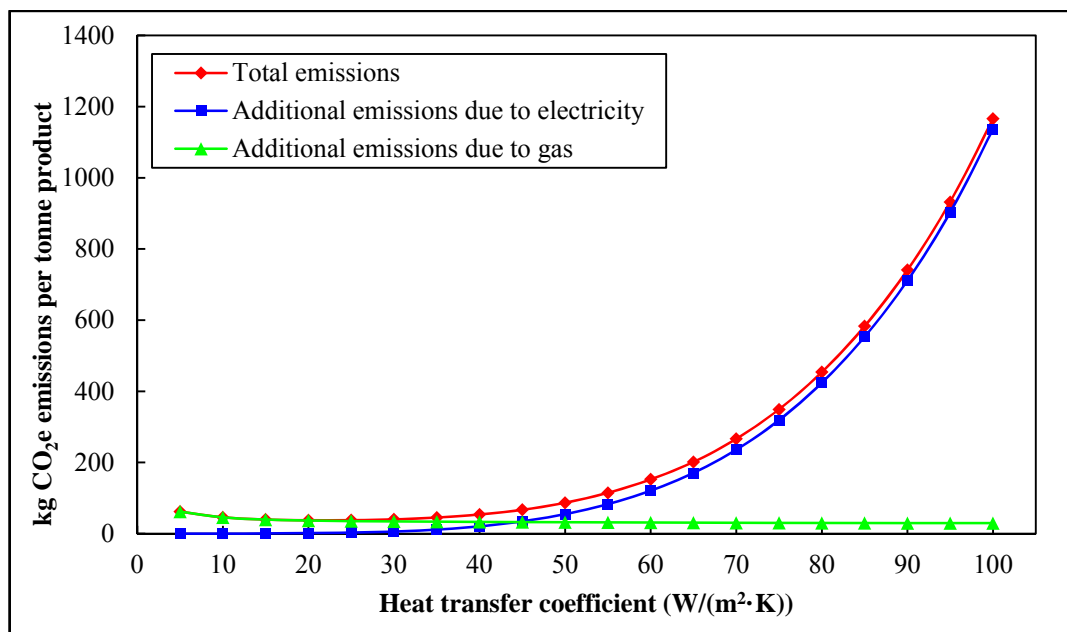


Figure 7.24 – Predicted bread baking carbon emissions equivalent per kg as a function of heat transfer coefficient

7.8 Summary

The methods used in this study give a new approach for measuring heat transfer in the baking industry, with both global and local heat transfer coefficients being determined for a number of conditions relevant to direct-fired jet impingement baking ovens. The careful specification and use of heat flux sensors has made it possible to conduct these experiments.

The results show interesting findings that correlate well with previous literature relating to air jet impingement heat transfer. The mean heat transfer results for

ASN match closely with correlations proposed by Das *et al.* (1985) and Martin (1977). The ARN configuration was unique because of the asymmetric distribution of nozzles. The heat transfer characteristics were similar to the equivalent ASN correlations but not the symmetric ARN correlations proposed by (Martin, 1977).

The mean dimensionless heat transfer coefficient (Nu) varies considerably under different regimes. This demonstrates the importance of experimental measurements to compare a specific regime to one of the many mean Nusselt number correlations that exist in literature. Interestingly, the ARN configuration, where there is a large degree of asymmetry of hole distribution can be effectively correlated as an ASN by using the relative nozzle area, f , to calculate the equivalent slot width.

Local heat flux variations also exhibit interesting behaviours that should be understood when designing commercial bread baking ovens. The effect of variation in nozzle-to-surface distance can have little effect on the mean heat transfer, but locally the effect across the profile of a nozzle can be of importance. Local heat flux profiles also showed the prevalence of secondary peaks in a number of cases. The magnitude of these secondary peaks was greater for high air velocities and low H/d ratios

Using the experimental results, it was possible to estimate the optimum value for heat transfer coefficient with relation to energy usage. It was found that by using $h_c = 35 \text{ W}/(\text{m}^2 \cdot \text{K})$, energy use could be reduced by over 5 %. The results presented in this chapter may be of use to oven designers and bakery operators when selecting conditions for bread baking to maximise heat transfer. Increasing the rate of heat transfer could have a direct effect on lowering the baking time and therefore improving plant efficiency and reducing energy usage and carbon emissions.

Chapter 8

Conclusions and Further Work

This thesis presents research focussed on analysing energy utilisation in commercial bread baking – a manufacturing process that is responsible for significant carbon emissions and environmental impact – with yearly energy usage totalling 2,000 GWh and carbon emissions of 570,000 TCO₂/year in the UK alone. This research has been conducted in collaboration with industrial partners Warburtons Limited, Spooner Industries Ltd. and SKM Enviros. Prior to the commencement of this research, comparatively few studies have addressed end-use energy demand and carbon emissions in the bread industry. Reasons for this include: the relatively low cost of energy supply until recent times, food quality/hygiene concerns of changing the production process and the traditional nature of the industry.

This thesis challenges some of the ingrained and inherently inefficient commercial practices used in the manufacture of bread. It provides rigorous scientific justification and analysis tools to drive change in an important and large-scale industry. These analysis tools have been actively used by industry in an attempt to reduce energy use in the bread industry. This chapter provides a summary of the contributions to new scientific understanding, methodologies, findings and key conclusions that this research has provided.

8.1 Conclusions and Main Contributions to Scientific Understanding

8.1.1 Computational Fluid Dynamic Analysis of Bread Provers

This study is the first attempt to analyse airflow within industrial bread provers with the aim to reduce energy usage. Non-invasive measurement and predictive techniques, such as CFD, are particularly pertinent when assessing bakery

equipment, as disruption to the manufacturing processes can be financially expensive and leave the potential to cause food quality/ safety breaches. CFD has been used for the first time to mitigate the detrimental impact that direct measurements have to improve the energy efficiency of the bread proving phase. The number of air changes is the practical parameter bakeries use to ensure important food safety criteria are adhered to. A parametric study using ten different cases for air changes between 10/hr and 100/hr was used to predict airflow within the prover. Residence time analysis has shown the time taken for each individual particle out of 2,000 injected to leave the prover cavity. Experimental measurements of air velocity at the vent exits were obtained to validate the CFD predictions, providing the validation and credibility needed to encourage commercial bakeries to reduce the number of air changes.

It has been shown that for the proving process, the number of air changes can be reduced by at least a third, from the previous level of 90/hr to 60/hr, without breaching any current legislative or quality-driven standards. This reduction will reduce the electricity demand of the prover air handling units by over 70 %. In addition, it is anticipated that fewer air changes will mean the prover retains heat and humidity, leading to reductions in the steam and gas burner energy demand. The results of the CFD simulations have been used by bread manufacturers to benchmark the number of air changes in industrial provers across a number of UK bakeries. Furthermore, it has been suggested that the results could be used to formulate a universal standard that would encourage bakeries to operate provers under more energy efficient conditions.

8.1.2 System-Level Modelling of Industrial Bread Baking Ovens

Energy system modelling is a well-documented methodology that is used to predict and measure energy streams. System models can lead to improvements in process efficiency since they take into account the key influences affecting energy. Initially, a system diagram of energy and material flows into and out of the oven

was generated, with reference to several different oven types, both indirect-fired and direct-fired. Measurements of fundamental flow characteristics in a baking oven, such as air velocity and temperature, were conducted to characterise oven behaviour and provide parameters to be input into the system model. This facilitated the formulation of the governing equations necessary to drive the system-level model.

Thermal imaging, another form of non-invasive measurement, enabled surface temperature profiles to be established at places that were difficult to access. Careful configuration of the thermal imaging devices and software allowed reliable surface plots of temperature distribution to be generated, which were then used to estimate energy losses from the oven.

The results were verified by performing a sensitivity analysis on the model, which used two separate scenarios to calculate the potential error. Firstly, each input to the model was varied by $\pm 10\%$ to show the effect this had on the output results and it was found that the variation of the majority of the outputs were within the range expected for a model of this type. Secondly, each input was varied by the expected accuracy of the measurement/ equipment used; again this showed accuracy to be sufficient to allow reliable interpretation of the results. The results of the analysis showed that energy use in bread baking can be reduced by 1.9%. This energy saving on a large scale is significant, as explained in Paton *et al.* (2012b) the annual cost saving is estimated to be at least £0.5 million and carbon savings of more than 5,000 tonnes CO₂ equivalent for UK industry.

Energy system modelling is an increasingly popular technique that can be used to flexibly analyse energy flow streams. The work presented here uses a system model encompassed into a software framework that aims to provide direct benefit to the bread industry as well as unique contributions to the scientific community. The combination of novel measurement techniques to assess heat losses in

conjunction with a set of equations that can analyse the oven as a system has never been done before for the bread industry, and builds upon previous studies in other industries, both food and otherwise. The model has been used widely in industry to benchmark and predict energy utilisation of commercial ovens, and by equipment designers to identify opportunities for manufacturing the next generation of energy efficient baking ovens.

8.1.3 Experimental Measurements for Air Jet Impingement Heat Transfer for Regimes Relevant to Bread Baking

The novel experimental results showing mean and local heat transfer characteristics for jet impingement nozzles under conditions applicable to the baking industry are a valuable contribution of knowledge in the field of jet impingement heat transfer. Furthermore, the correlations developed can prove useful to commercial oven designers for developing a new generation of bread ovens where heat transfer can be optimised in terms of jet velocity and nozzle dimensions. Much of the previous experimental work carried out in this field was of little relevance to process engineers, largely due to the types of nozzles used. Consequently, the experiments described in this thesis intentionally used scaled-down industrially relevant apparatus, which has enhanced the applicability of the methodologies and results. The pilot oven facility enabled a wide range of conditions to be tested. The apparatus ensured the flow represented conditions commonly experienced in industrial baking and a turbulent regime under steady state conditions could be maintained. A commercially available heat flux sensor was used for this, which could measure convective and total heat transfer for typical conditions experienced in bread baking ovens.

The mean heat transfer results agreed well with the seminal correlations of Martin (1977), which give credibility and validation to the results. The experimental evidence substantiates the assumption of the industry that asymmetric banks of round nozzles can be approximated as slot nozzles. This insight could prove

especially significant as it means that mean heat transfer rates for arrays of both round and slot nozzles can be modelled in two-dimensions, thereby reducing the complexity of analysis and the corresponding computational requirements.

Theoretical optimisation of the heat transfer coefficient was conducted by balancing the additional electricity load required to increase air velocity with the subsequent reduction in baking time (and thus ambient heat losses per kg of bread) made possible as a result of higher heat transfer rates. It was found that increasing h_c from the industry standard value of 10 to 35 W/(m²·K) resulted in energy savings of over 5 %. This saving equates to over 75,000 tonnes CO₂ equivalent per year worldwide. This is a key finding that can help encourage the bread industry to increase air velocity, depending on the effect on the product, in order to reduce overall energy consumption. A further efficiency gain could be made if local cogeneration (combined heat and power) could be made feasible to meet bakery energy demand.

8.2 Future Work

The work presented in this thesis is not only relevant to the baking industry, but covers technologies that are used in a number of other drying industries. The future work that has been identified in this section reflects the adaptability of some of the analysis techniques to identify energy savings in the bread industry.

8.2.1 Prover

In order to measure the energy savings that have been made possible as a result of the CFD analysis presented in this thesis, a regression analysis of year-on-year energy use would be necessary. This would help to substantiate the scale of energy savings that have been estimated. Based on the magnitude of the energy savings for using a lower number of air changes, it may be advisable to rethink prover design and/ or retrofit technology in order to downsize the prover heating system (gas burners) and review the sizing of air handling units based on worst-case scenarios.

Further optimisation of airflow within the prover could be conducted using a CFD design optimisation study. Formal design optimisation, using methods such as genetic programming, is a computational approach used to find an optimal solution to an engineering problem. For multi-objective design optimisation, design variables are identified, which in the case of the prover could be factors such as: the number of air changes, the pitch between outlet vents, the size or shape of the outlet vents, the distribution of tins within the prover, positioning of inlet/ outlet ducts, air humidity etc. With current techniques, it is usually feasible to have no more than 3-4 design variables, therefore the specification of the problem would need to identify which variables are most practically varied and that are going to have the greatest impact on energy usage. The objective function should define the parameter to be maximised or minimised. For the prover, minimising the energy use would be the objective function, but with a set of critical quality objectives that would be required to ensure product quality and food safety. A simple graph shown by Figure 8.1 characterises a Pareto front, where a trade-off between two variables can be made. For this application, quality is a non-negotiable variable, therefore the critical value must be maintained – the related costs can then be estimated. Such approaches have been carried out in bread ovens.

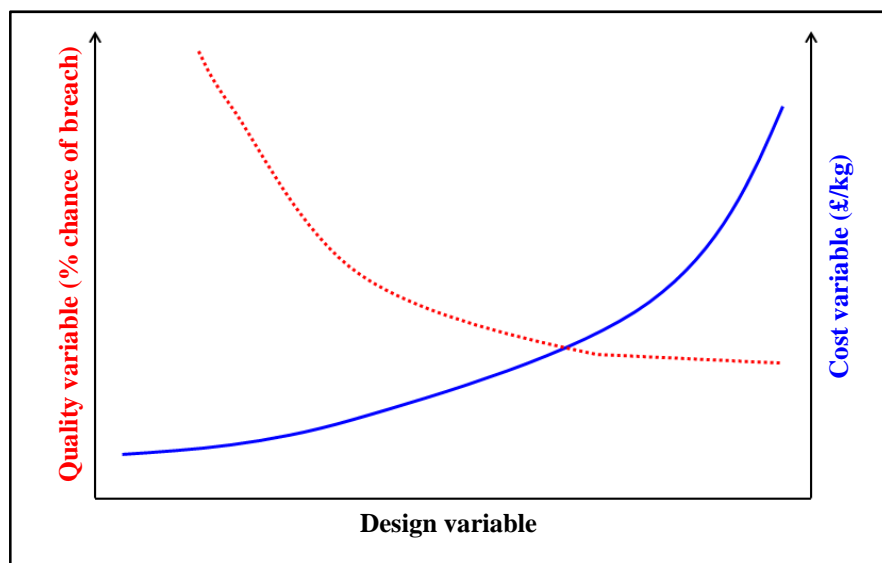


Figure 8.1 – Example of a Pareto front showing competing objectives: the objective function, minimising cost (blue) and a critical quality objective (red)

Figure 8.2 displays the three-dimensional surface response of the impact of two design variables, H/d and u_{noz} , on the objective function, temperature uniformity (σ_T), for an industrial bread oven (Khatir *et al.*, 2011b).

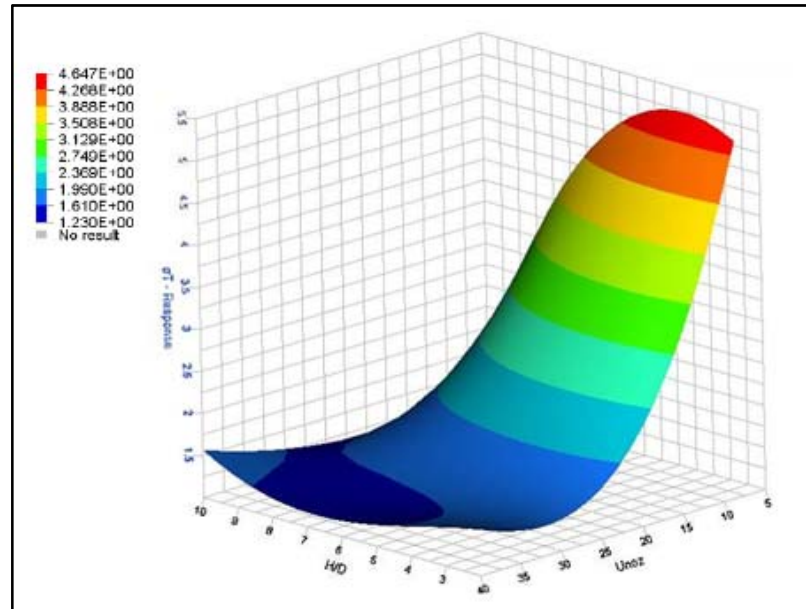


Figure 8.2 – Surface response of CFD optimisation study for optimising airflow in and industrial bread oven (Khatir *et al.*, 2013, Khatir *et al.*, 2012d)

8.2.2 Oven

The thermodynamic system-level model has been distributed and widely used in Warburtons' bakeries, the second largest grocery brand in the UK after Coca-Cola (Phillips, 2011). Whilst the fundamental principles behind the analysis does not change, as the software has evolved slight modifications have been made to the governing equations – either to improve the accuracy, increase the ease of operation or to simplify the methodology. It will be important for the legacy of the model to continue maintenance on the software. The model could also be expanded to form a life cycle assessment framework, where the cradle-to-grave environmental impact of bread production could be assessed by a bakery operator in a straightforward manner. The model will help industry to track improvements in energy efficiency as advances are made to baking oven technology, therefore continual use will help to highlight the change in energy utilisation as a result of process enhancements.

One particular area for improvement identified as a result of the aforementioned model, is in reducing the amount of heat being exhausted to atmosphere in flue gases. There are three ways to increase efficiency in this area. Firstly, reducing the flow rate of flue gases exhausted – this has been dismissed by industry, as a minimum portion of combustion products need to be removed from the oven to maintain safe manufacturing conditions. Secondly, reusing the heat for another process by directly pumping exhaust gases to another process – for example in the sugar industry waste heat from CHP incinerators is used to help grow tomatoes (Stark and Jarvis, 2009). Thirdly, using heat exchangers to transfer the energy from the waste flue gases to another form (solid, liquid or gas) to be used in another operation – for example in washing tins. None of these options have been implemented successfully despite numerous attempts over the years. However, advances in heat exchanger efficiency and reliability mean there is increased optimism that a commercially viable heat exchanger may be manufactured to recover heat from oven exhausts in the short-term future.

Experimentation on heat transfer is a subject that can never be exhausted. The range of different operating conditions that are possible is virtually limitless. Although the subject of jet impingement heat transfer has been extensively covered by literature, there is no method that is totally reliable for assessing heat transfer, other than direct experimental measurement. Despite this, due to the expense of preparing meticulous experimental setups and conducting careful measurements, it is often more effective to use heat transfer correlations. Though it is clear that some of the correlations are applicable, it has also been found correlations are lacking in certain areas of parameter space – such as those used in bread baking. There has been little experimentation relating to analysing the proportion of convection and radiation with respect to air velocity based on measurements. This is a correlation that could be developed but would potentially be highly dependent on the apparatus used. Further studies could assess this by using different oven materials and

geometries to identify the relative ratio of convective to radiative heat transfer for different systems. Further investigation into how rows of asymmetric round nozzles can be approximated as slot nozzles would formulate completely novel research. Deeper understanding of this phenomenon would add to scientific knowledge and help designers of jet impingement systems to engineer nozzles that are both energy efficient and practical.

Design of a completely new generation of baking ovens that are energy efficient is a current priority for the baking industry. To minimise the energy consumption of a new design of oven, it will be important for the previous work on heat transfer (such as that presented in this thesis) along with the practical design experience of those in the industry to be considered.

8.2.3 Other Bakery Equipment

Due to the large energy requirement of dough mixing since the advent of the Chorleywood Bread Process, there are significant challenges relating to minimising the mechanical energy used in dough mixers. Mixing using this method uses approximately 5 % of the bakery energy load – in terms of financial cost this figure is greater due to the relative costs of electricity in comparison to other primary energy sources. As stated in the introduction to this thesis, some computational modelling work has been carried out in an attempt to optimise the mixing process, but further work can be done. A number of factors affect the mixing process (Frank, 2009), including: ingredients, dough rheology and temperature. Measuring the impact of these variables to produce dough with the same product characteristics would form an interesting piece of research.

Formation of the dough into a loaf shape is another area where research can help to drive forward innovation in the bread manufacturing process. Dough-pieces are currently formed by flattening the dough into a thin sheet and rolling into a cylinder, before folding this into two or four sections. Little investigation has been

conducted to experiment with different ways of shaping the dough. The benefits of the technique described over shaping the dough into a sphere and stretching into a loaf shape have not been scientifically justified. Likewise, inventive solutions such as: layering thin sheets of dough into a loaf shaped stack, joining multiple cylinders or forcing the dough through a nozzle are all possibilities for modernising the dough formation phase of bread baking. The energy impact of dough formation is relatively low compared to the baking, proving and mixing stages; however, the way in which the dough is formed can also have an impact on other stages of the bread-making process.

As discussed previously, there are several cooling technologies available in the food industry, many of which have been trialled to varying extents in bread-making. It is important to fully understand the comparative benefits of different coolers in terms of: energy impact/ life cycle assessment, capital investment, operating costs, product quality (for example moisture loss), reliability, space requirements and ease of operation. Ideally this multi-objective trade-off analysis would be conducted on a commercial scale, to present the strongest possible case for the best technology to be universally adopted. However, it is unlikely that commercial bakeries would be willing to take the financial and operational risk necessary to acquire unproven equipment on a large scale. It would be more realistic to work with cooler manufacturers to understand the bakery requirements, optimise design and trial innovative technologies on a pilot-scale with the aim to revolutionise the cooling process.

8.3 Summary

The bread manufacturing process is traditional by nature, and as such it has been observed in literature and through collaboration with industry, that innovation has been limited over the past half-century. Carbon emission legislation and spiralling energy costs have encouraged bakeries and equipment suppliers to reduce the

environmental impact of their products. There is a significant challenge to do this whilst maintaining the product characteristics that have made bread a staple food in a modern society. Despite these barriers, opportunities for reducing energy utilisation are plentiful. The main challenge is to take theoretical performance gains and transform them into commercially viable opportunities for investment.

Operational changes to the bread proving process have been suggested, with scientific substantiation obtained through CFD modelling techniques. Using residence time theory to analyse ten cases for different numbers of air changes has shown that bakeries can reduce prover AHU electricity consumption by an estimated 70 % whilst maintaining critical food safety and performance characteristics. Additional savings in natural gas and steam consumption will follow from this and can be quantified retrospectively.

System-level energy analysis of bread ovens has analysed the heat streams within commercial bread ovens, showing that around 40 to 50 % of heat in the oven is wasted in losses to atmosphere. This novel approach has made benchmarking possible for both direct and indirect-fired ovens to compare energy efficiency using a scientifically rigorous framework. Furthermore, the results highlight opportunities for energy savings to be made – most notably in recovering waste heat from exhaust gases, improving oven insulation to reduce the wall/ roof losses and reducing energy losses from the conveyor.

Experimental measurements of heat flux for nozzles and temperature/ velocity conditions relevant to the baking industry have corroborated many of the previously published correlations. Unique data on the proportion of convection and radiation shows, as expected, that the degree of convection is proportional to the jet velocity. Furthermore, local heat flux profiles of air jets have shown interesting behaviours that can be useful for oven designers. The prevalence of secondary peaks, which were more noticeable for round nozzles than slots, is an interesting

result and can be explained by the effect of a decrease in nozzle-to-surface distance due to the way the airflow develops for impinging jets.

As bread is a staple food product across most of the globe it is important to keep availability high and retail prices low. The future prosperity of the bread baking industry is increasingly dependent on lowering the cost of manufacture. Recent years have seen the price of raw ingredients (in particular wheat) escalate rapidly, due to poor harvests in the UK, Canada and USA, squeezing profit margins of commercial bakers. Moreover, the fact that raw ingredients can be bought and sold as stocks in a commodities market can have a further negative impact when there are shortages of these ingredients.

The main costs in an industrial bakery aside from raw materials are: capital expenditure, maintenance, staffing and energy. Of these four factors, capital expenditure is often necessary to improve process efficiency, maintenance is essential to avoid undue downtime and staffing levels have been reduced to an absolute minimum through increased automation. Energy is the last remaining cost that bakeries have largely neglected to address. The research presented here explores energy utilisation in the commercial baking industry in order to help mitigate the environmental impact and financial cost of bread manufacture. It is envisaged that this research will help secure the long-term commercial and environmental viability of one of the most historic and important of all industries.

References

- AHRNE, L., ANDERSSON, C. G., FLOBERG, P., ROSEN, J. & LINGNERT, H. 2007. Effect of Crust Temperature and Water Content on Acrylamide Formation During Baking of White Bread: Steam and Falling Temperature Baking. *LWT - Food Science and Technology*. **40**(10), pp. 1708-1715.
- AIAA. 1998. *Guide for the Verification and Validation of Computational Fluid Dynamics Simulations (G-077-1998e)*. Washington D.C.: American Institute of Aeronautics and Astronautics.
- AKSYUTOV, L. N. 1974. Normal Spectral Emissivity of Gold, Platinum, and Tungsten. *Journal of Engineering Physics and Thermophysics*. **27**(2), pp. 913-917.
- ALTAMIRANO-FORTOUL, R., LE-BAIL, A., CHEVALLIER, S. & ROSELL, C. M. 2012. Effect of the Amount of Steam During Baking on Bread Crust Features and Water Diffusion. *Journal of Food Engineering*. **108**(1), pp. 128-134.
- ANDERSSON, B. J. 2012. *Computational Fluid Dynamics for Engineers*. Cambridge: Cambridge University Press.
- ANDERSSON, K. & OHLSSON, T. 1999. Life Cycle Assessment of Bread Produced on Different Scales. *The International Journal of Life Cycle Assessment*. **4**(1), pp. 25-40.
- ANSYS INC. 2009. *Ansys Fluent 12.0 in Workbench User's Guide*. Canonsburg: ANSYS.
- AUGUSTO, P. E. D., PINHEIRO, T. F. & CRISTIANINI, M. 2010. Using Computational Fluid-Dynamics (Cfd) for the Evaluation of Beer Pasteurization: Effect of Orientation of Cans. *Ciência e Tecnologia de Alimentos*. **30**(4), pp. 980-986.
- AZAR, K., ENGELBERTS, N., GOODMAN, C. W., HASKELL, M., LEI, N., JEGGEIS, Y., POURVASH, M. & TAVASSOLI, B. 2009. *Qpedia Thermal Magazine*. Norwood: Advanced Thermal Solutions.
- BACON, D. H. 1989. *Basic Heat Transfer*. London: Butterworth-Heinemann.
- BAEHR, H. D. & STEPHAN, K. 1998. *Heat and Mass Transfer*. New York: Springer.
- BAIK, O. D., GRABOWSKI, S., TRIGUI, M., MARCOTTE, M. & CASTAIGNE, F. 1999. Heat Transfer Coefficients on Cakes Baked in a Tunnel Type Industrial Oven. *Journal of Food Science*. **64**(4), pp. 688-694.
- BARDINA, J. E., HUANG, P. G. & COAKLEY, T. J. 1997. Turbulence Modeling Validation, Testing, and Development. *NASA Technical Memorandum T110446*. Moffett Field: Ames Research Center
- BEECH, G. A. 1980. Energy Use in Bread Baking. *Journal of the Science of Food and Agriculture*. **31**(3), pp. 289-298.
- BEGGS, C. 2002. *Energy: Management, Supply and Conservation*. Oxford: Butterworth-Heinemann.

- BENDING, R. & EDEN, R. J. 1984. *Uk Energy: Structure, Prospects and Policies*. Cambridge: Cambridge University Press.
- BIRD, J. O. & ROSS, C. T. F. 2012. *Mechanical Engineering Principles*. New York, NY: Routledge.
- BLANCHARD, G. H. 1965. The Blanchard Batter Process. *Milling*. **147** pp. 519-521.
- BOULET, M., MARCOS, B., DOSTIE, M. & MORESOLI, C. 2010. Cfd Modeling of Heat Transfer and Flow Field in a Bakery Pilot Oven. *Journal of Food Engineering*. **97**(3), pp. 393-402.
- BRASCHKAT, J., PATYK, A., QUIRIN, M. & REINHARDT, G. A. 2003. Life Cycle Assessment of Bread Production - a Comparison of Eight Different Scenarios. In: *Life Cycle Assessment in the Agri-food sector, 6-8 October 2003, Horsens, Denmark*.
- BREWSTER, M. Q. 1992. *Thermal Radiative Transfer and Properties*. Indianapolis: Wiley.
- BRUMBAUGH, J. E. 2011. *Audel Hvac Fundamentals Volume 3: Air Conditioning, Heat Pumps and Distribution Systems*. Indianapolis: Wiley.
- CAMPDEN & CHORLEYWOOD FOOD RESEARCH ASSOCIATION (CCFRA) & BRISTOL UNIVERSITY 2008. Utilisation of Waste Heat from Food Factories - Afm248br. CCFRA.
- CARBON TRUST 2009. Conversion Factors: Energy and Carbon Conversions. London: Carbon Trust.
- CARBON TRUST 2010. Industrial Energy Efficiency Accelerator: Guide to the Industrial Bakery Sector. London: Carbon Trust.
- CARBON TRUST 2012a. Steam and High Temperature Hot Water Boilers: Introducing Energy Saving Opportunities for Business. London: Carbon Trust.
- CARBON TRUST 2012b. Prices of Fuels Purchased by Manufacturing Industry. London: Department of Energy and Climate Change (DECC).
- CARVALHO, M. D. & NOGUEIRA, M. 1997. Improvement of Energy Efficiency in Glass-Melting Furnaces, Cement Kilns and Baking Ovens. *Applied Thermal Engineering*. **17**(8-10), pp. 921-933.
- CASEY, M. & WINTERGERSTE, T. 2000. *Best Practice Guidelines: Special Interest Group on "Quality and Trust in Industrial Cfd"*. London: European Research Community on Flow Turbulence and Combustion (ERCOFTAC).
- CASPER, M. E. 1977. *Energy-Saving Techniques for the Food Industry*. Park Ridge: Noyes Data Corporation.
- CAUVAIN, S. P. & YOUNG, L. S. 1998. *Technology of Breadmaking*. New York: Springer.
- CAUVAIN, S. P. & YOUNG, L. S. 2006. *The Chorleywood Bread Process*. Boca Raton: CRC Press.

CHAPMAN, P. F. 1975. *Fuel's Paradise: Energy Options for Britain*. Harmondsworth: Penguin.

CHEVALLIER, S., ZUNIGA, R. & LE-BAIL, A. 2012. Assessment of Bread Dough Expansion During Fermentation. *Food and Bioprocess Technology*. **5**(2), pp. 609-617.

CHILDS, P. R. N., GREENWOOD, J. R. & LONG, C. A. 1999. Heat Flux Measurement Techniques. *Proceedings of the Institution of Mechanical Engineers, Part C*. **213**(7), pp. 655-677.

CHIOTELLIS, E. & CAMPBELL, G. M. 2003a. Proving of Bread Dough II - Measurement of Gas Production and Retention. *Food and Bioprocess Technology*. **81**(3), pp. 207-216.

CHIOTELLIS, E. & CAMPBELL, G. M. 2003b. Proving of Bread Dough I - Modelling the Evolution of the Bubble Size Distribution. *Food and Bioprocess Technology*. **81**(3), pp. 194-206.

CHRISTENSEN, A. & SINGH, R. P. 1984. Energy Consumption in the Baking Industry. *In: Third International Congress on Engineering and Food, 26-28 September 1983, Dublin, Republic of Ireland*.

COKER, A. K. 2001. *Modeling of Chemical Kinetics and Reactor Design*. Boston: Gulf Professional Publishing.

COLUCCI, D. W. & VISKANTA, R. 1996. Effect of Nozzle Geometry on Local Convective Heat Transfer to a Confined Impinging Air Jet. *Experimental Thermal and Fluid Science*. **13**(1), pp. 71-80.

COMSOL. 2012. *Comsol Multiphysics Installation and Operations Guide*. Burlington: COMSOL AB.

CORDOBA, A. 2010. Quantitative Fit of a Model for Proving of Bread Dough and Determination of Dough Properties. *Journal of Food Engineering*. **96**(3), pp. 440-448.

CVERNA, F. 2002. *Thermal Properties of Metals*. Ohio: ASM International.

DANCKWERTS, P. V. 1953. Continuous Flow Systems. Distribution of Residence Times. *Chemical Engineering Science*. **2**(1), pp. 1-13.

DAS, D., DOUGLAS, W. J. M. & CROTOGINO, R. H. 1985. Convective Heat Transfer under Turbulent Impinging Slot Jet Nozzles at Large Temperature Differences. *In: TOEI, R. & MAJUMDAR, A. S., (eds.). Drying '85*. New York: Hemisphere.

DATAMONITOR 2011a. Bread & Rolls Industry Profile: United Kingdom. *Bread & Rolls Industry Profile: United Kingdom*. London: Datamonitor.

DATAMONITOR 2011b. Bread & Rolls Industry Profile: Global. *Bread & Rolls Industry Profile: Global*. London: Datamonitor.

DEPARTMENT OF ENERGY AND CLIMATE CHANGE 2012. Uk Emissions Statistics - 2011 Provisional Uk Figures: Data Tables. London: Department of Energy and Climate Change (DECC).

DILLER, T. E. 1993. Advances in Heat Flux Measurements. *In*: HARTNETT, J. P., IRVINE, T. F. & CHO, Y. I., (eds.). *Advances in Heat Transfer*. San Diego: Academic Press.

DONALD F. YOUNG, BRUCE R. MUNSON, THEODORE H. OKIISHI & HUEBSCH, W. W. 2010. *A Brief Introduction to Fluid Mechanics, 5th Edition*. Hoboken: Wiley.

DURBIN, P. A. 1996. On the K-E Stagnation Point Anomaly. *International Journal of Heat and Fluid Flow*. **17**(1), pp. 89-90.

EARLE, R. L. 2004. *Unit Operations in Food Processing: Web Edition*. Palmerston North: The New Zealand Institute of Food Science & Technology.

ECKERT, E. R. G. 1959. *Heat and Mass Transfer*. New York: McGraw-Hill.

ERDOĞDU, F. & ANDERSON, B. 2010. Impingement Thermal Processing. *In*: FARID, M. M., (ed.) *Mathematical Modeling of Food Processing*. Boca Raton: CRC Press.

EUROPEAN COMMISSION JOINT RESEARCH CENTRE: INSTITUTE FOR ENVIRONMENT AND SUSTAINABILITY. 2010. *International Reference Life Cycle Data System (Ilcd) Handbook - General Guide for Life Cycle Assessment - Detailed Guidance (Eur 24708 En)*. Luxembourg: Publications Office of the European Union.

FALKOVICH, G. 2011. *Fluid Mechanics: A Short Course for Physicists*. Cambridge: Cambridge University Press.

FELLOWS, P. J. 2009. *Food Processing Technology Principles and Practice*. Boca Raton: Woodhead Publishing.

FESSAS, D. & SCHIRALDI, A. 2000. Starch Gelatinization Kinetics in Bread Dough - Dsc Investigations on 'Simulated' Baking Processes. *Journal of Thermal Analysis and Calorimetry*. **61**(2), pp. 411-423.

FITZGERALD, J. A. & GARIMELLA, S. V. 1998. A Study of the Flow Field of a Confined and Submerged Impinging Jet. *International Journal of Heat and Mass Transfer*. **41**(8-9), pp. 1025-1034.

FRANK, P. 2009. Energy Efficiency Yields High Return on Investment. *Baking Management [online]* 1 June 2009. <http://baking-management.com> [Accessed on: 30 October 2012].

FUHRMANN, E., SOCKEL, H. & STEINRUCK, P. 1984. Improvement of Continuous Baking Ovens Efficiency. *Journal of Wind Engineering and Industrial Aerodynamics*. **16**(2-3), pp. 201-212.

GARDON, R. & AKFIRAT, J. C. 1966. Heat Transfer Characteristics of Impinging Two-Dimensional Air Jets. *Journal of Heat Transfer*. **88**(1), pp. 101-107.

GEERS, L. F. G., TUMMERS, M. J. & HANJALIC, K. 2004. Experimental Investigation of Impinging Jet Arrays. *Experiments in Fluids*. **36**(6), pp. 946-958.

GELINAS, P. 2006. Yeast. *In*: HUI, Y. H., (ed.) *Bakery Products: Science and Technology*. Ames: Blackwell.

- GHANI, A. G. A., FARID, M. M., CHEN, X. D. & RICHARDS, P. 1999a. Numerical Simulation of Natural Convection Heating of Canned Food by Computational Fluid Dynamics. *Journal of Food Engineering*. **41**(1), pp. 55-64.
- GHANI, A. G. A., FARID, M. M., CHEN, X. D. & RICHARDS, P. 1999b. An Investigation of Deactivation of Bacteria in a Canned Liquid Food During Sterilization Using Computational Fluid Dynamics (Cfd). *Journal of Food Engineering*. **42**(4), pp. 207-214.
- GOTTSCHALK, C. M. 1996. *Industrial Energy Conservation*. Chichester: Wiley.
- GRENIER, A., LUCAS, T., COLLEWET, G. & LE BAIL, A. 2003. Assessment by Mri of Local Porosity in Dough During Proving. Theoretical Considerations and Experimental Validation Using a Spin-Echo Sequence. *Magnetic Resonance Imaging*. **21**(9), pp. 1071-1086.
- GRENIER, A., LUCAS, T., DAVENEL, A., COLLEWET, G. & LE BAIL, A. 2006. Comparison of Two Sequences: Spin-Echo and Gradient Echo for the Assessment of Dough Porosity During Proving. In: BELTON, P. S., GIL, A. M., WEBB, G. A. & RUTLEDGE, D., (eds.). *Magnetic Resonance in Food Science: Latest Developments*. Cambridge: The Royal Society of Chemistry.
- GRENIER, D., LUCAS, T. & LE RAY, D. 2010. Measurement of Local Pressure During Proving of Bread Dough Sticks: Contribution of Surface Tension and Dough Viscosity to Gas Pressure in Bubbles. *Journal of Cereal Science*. **52**(3), pp. 373-377.
- GUPTA, T. R. 2001. Individual Heat Transfer Modes During Contact Baking of Indian Unleavened Flat Bread (Chapati) in a Continuous Oven. *Journal of Food Engineering*. **47**(4), pp. 313-319.
- HAMDAMI, N., MONTEAU, J. Y. & LE BAIL, A. 2004. Heat and Mass Transfer in Par-Baked Bread During Freezing. *Food Research International*. **37**(5), pp. 477-488.
- HANSEN, S. J. & BROWN, J. W. 2004. *Investment Grade Energy Audit: Making Smart Energy Choices*. Lilburn: Fairmont Press.
- HARDISTY, H. & CAN, M. 1983. An Experimental Investigation into the Effect of Changes in the Geometry of a Slot Nozzle on the Heat-Transfer Characteristics of an Impinging Air Jet. *Proceedings of the Institution of Mechanical Engineers, Part C*. **197** pp. 7-15.
- HARLOW, F. H. & WELCH, J. E. 1965. Numerical Calculation of Time-Dependent Viscous Incompressible Flow of Fluid with Free Surface. *Physics of Fluids*. **8**(12), pp. 2182-2189.
- HARLOW, F. H. & NAKAYAMA, P. I. 1967. Turbulence Transport Equations. *Physics of Fluids*. **10**(11), pp. 2323-2332.
- HOLDERBEKE, M. V., SANJUÁN, N., GEERKEN, T. & VOOGHT, D. D. 2003. The History of Bread Production: Using Lca in the Past. In: *Life Cycle Assessment in the Agri-food sector, 6-8 October 2003, Horsens, Denmark*.
- HOLMAN, J. P. 2002. *Heat Transfer*. Boston: McGraw-Hill.
- HUKSEFLUX THERMAL SENSORS c. 2010. Rc01 Manual V1004.

IBARRA-CASTANEDO, C., GONZALEZ, D., KLEIN, M., PILLA, M., VALLERAND, S. & MALDAGUE, X. 2004. Infrared Image Processing and Data Analysis. *Infrared Physics & Technology*. **46**(1-2), pp. 75-83.

INCROPERA, F. P. & DEWITT, D. P. 2007. *Fundamentals of Heat and Mass Transfer*. Hoboken: Wiley.

INGOLD, B. J. 2008. Selecting a Nondestructive Testing Method, Part Vi: Thermal/Infrared Inspection Techniques – Thermography. *Advanced Materials, Manufacturing, and Testing Information Analysis Center Quarterly*. **3**(2), pp. 9-12.

INTERNATIONAL ORGANIZATION FOR STANDARDIZATION. 2006a. *Environmental Management - Life Cycle Assessment - Requirements and Guidelines*. ISO 14044:2006.

INTERNATIONAL ORGANIZATION FOR STANDARDIZATION. 2006b. *Environmental Management - Life Cycle Assessment - Principles and Framework*. ISO 14040:2006.

JACOB, H. E., WINSTON, R. & WINSTON, C. 1944. *Six Thousand Years of Bread, Its Holy and Unholy History*. Garden City: Doubleday, Doran and Company.

JAHNKE, J. A. 2000. *Continuous Emission Monitoring*. New York: Wiley.

JAMES, S. J. & JAMES, C. 2011. The Potential of Ambient Cooling Systems for Reducing Refrigeration Loads and Saving Energy. *In: International Congress on Engineering and Food, May 22-26 2011, Athens, Greece*.

JOHNSON, L. A. & HOOVER, W. J. 1977. Energy Use in Baking Bread. *Bakers Digest*. **51** pp. 58-65.

KADISH, A. 1996. *The Corn Laws: The Formation of Popular Economics in Britain*. London: Pickering and Chatto.

KANNAN, R. & BOIE, W. 2003. Energy Management Practices in Sme - Case Study of a Bakery in Germany. *Energy Conversion and Management*. **44**(6), pp. 945-959.

KAUSHAL, P. & SHARMA, H. K. 2012. Concept of Computational Fluid Dynamics (Cfd) and Its Applications in Food Processing Equipment Design *Journal of Food Processing and Technology*. **3**(1), pp. 1-7.

KAWAGUTI, M. 1953. Numerical Solution of the Navier-Stokes Equations for the Flow around a Circular Cylinder at Reynolds Number = 40. *Journal of the Physical Society of Japan*. **8**(6), pp. 747-757.

KENT, J. 2012. *Our Daily Bread: A Half-Baked History*. BBC Radio 4. 21 May 2012.

KHATIR, Z., PATON, J. B., THOMPSON, H. M., KAPUR, N., TOROPOV, V. V., LAWES, M. & KIRK, D. 2010. Computational Fluid Dynamics (Cfd) Investigation of Air Flow and Temperature Distribution in a Small Scale Bread-Baking Oven. *In: Sustainable Thermal Energy Management Conference (SusTEM2010), 3-4 November 2010, Newcastle, UK*.

KHATIR, Z., THOMPSON, H. M., KAPUR, N., TOROPOV, V. V. & PATON, J. B. 2011a. The Application of Computational Fluid Dynamics and Design

Optimisation in the British Bread-Baking Industry. *In: The 8th International Conference on CFD in Oil & Gas, Metallurgical and Process Industries (SINTEF/NTNU), 21-23 June 2011, Trondheim, Norway.*

KHATIR, Z., THOMPSON, H. M., KAPUR, N., TOROPOV, V. V. & PATON, J. B. 2011b. Multi-Objective Computational Fluid Dynamics (Cfd) Design Optimisation in Commercial Bread-Baking. *In: The Twelfth UK National Heat Transfer Conference (UKHTC 2011), 30 Aug-1 Sept 2011, Leeds, UK.*

KHATIR, Z., PATON, J. B., THOMPSON, H. M., KAPUR, N. & TOROPOV, V. V. 2012a. A Multi-Objective Design Methodology to Improve Energy Efficiency in the Bread-Baking Industry. *In: 2012 EFFoST Annual Meeting, 20-23 November 2012, Montpellier, France.*

KHATIR, Z., PATON, J. B., THOMPSON, H. M., KAPUR, N. & TOROPOV, V. V. 2012b. Opportunities for Energy Savings by Experimental and Numerical Analysis of the Bread Baking Process. *In: The 4th International Conference on Applied Energy (ICAE 2012), 5-8 July 2012, Suzhou, China.*

KHATIR, Z., PATON, J. B., THOMPSON, H. M., KAPUR, N., TOROPOV, V. V., LAWES, M. & KIRK, D. 2012c. Computational Fluid Dynamics (Cfd) Investigation of Air Flow and Temperature Distribution in a Small Scale Bread-Baking Oven. *Applied Energy*. **89**(1), pp. 89-96.

KHATIR, Z., THOMPSON, H. M., KAPUR, N., TOROPOV, V. V. & PATON, J. B. 2012d. Multi-Objective Computational Fluid Dynamics (Cfd) Design Optimisation in Commercial Bread-Baking. *Applied Thermal Engineering*. DOI: 10.1016/j.applthermaleng.2012.08.011.

KHATIR, Z., PATON, J. B., THOMPSON, H. M., KAPUR, N. & TOROPOV, V. V. 2013. Optimisation of the Energy Efficiency of Bread-Baking Ovens Using a Combined Experimental and Computational Approach. *Applied Energy*. DOI: 10.1016/j.apenergy.2013.02.034.

KIRK, D. 2011. *Spooner Industries Ltd.*, Personal communication.

KLEMES, J., SMITH, R. & KIM, J.-K. 2008. *Handbook of Water and Energy Management in Food Processing*. Boca Raton: Woodhead Publishing.

KONDJOYAN, A. & DAUDIN, J. D. 1997. Optimisation of Air-Flow Conditions During the Chilling and Storage of Carcasses and Meat Products. *Journal of Food Engineering*. **34**(3), pp. 243-258.

KREITH, F. & GOSWAMI, Y. 2008. *Energy Management and Conservation Handbook*. Boca Raton: Taylor & Francis.

KREITH, F., MANGLIK, R. M., BOHN, M. & TIWARI, S. 2011. *Principles of Heat Transfer*. Stamford: Cengage Learning.

KRESS-ROGERS, E. & BRIMELOW, C. J. B. 2001. *Instrumentation and Sensors for the Food Industry*. Boca Raton: CRC Press.

LAUKKANEN, M. 1984. Improving Energy Use in Finnish Bakeries. *In: Third International Congress on Engineering and Food, 26-28 September 1983, Dublin.*

LAUNDER, B. E. & SPALDING, D. B. 1974. The Numerical Computation of Turbulent Flows. *Computer Methods in Applied Mechanics and Engineering* **3**(2), pp. 269-289.

- LE-BAIL, A., DESSEV, T., JURY, V., ZUNIGA, R., PARK, T. & PITROFF, M. 2010. Energy Demand for Selected Bread Making Processes: Conventional Versus Part Baked Frozen Technologies. *Journal of Food Engineering*. **96**(4), pp. 510-519.
- LEACH, G. 1975. Energy and Food Production. *Food Policy*. **1**(1), pp. 62-73.
- LI, A. & WALKER, C. E. 1996. Cake Baking in Conventional, Impingement and Hybrid Ovens. *Journal of Food Science*. **61**(1), pp. 188-197.
- LUCAS, T., GRENIER, D., BORNERT, M., CHALLOIS, S. & QUELLEC, S. 2010. Bubble Growth and Collapse in Pre-Fermented Doughs During Freezing, Thawing and Final Proving. *Food Research International*. **43**(4), pp. 1041-1048.
- LYTLE, D. & WEBB, B. W. 1994. Air Jet Impingement Heat Transfer at Low Nozzle-Plate Spacings. *International Journal of Heat and Mass Transfer*. **37**(12), pp. 1687-1697.
- MALDAGUE, X. 2001. *Theory and Practice of Infrared Technology for Nondestructive Testing*. New York: Wiley.
- MARCOTTE, M. & GRABOWSKI, S. 2008. Minimising Energy Consumption Associated with Drying, Baking and Evaporation. In: KLEMES, J., SMITH, R. & KIM, J.-K., (eds.). *Handbook of Water and Energy Management in Food Processing*. Cambridge: Woodhead Publishing.
- MARSON, A. D. 1999. *Air Flotation Drying of Paper Pulp*. Engineering Doctorate, University of Manchester.
- MARTIN, H. 1977. Heat and Mass Transfer between Impinging Gas Jets and Solid Surfaces. *Advances in Heat Transfer*. **13** pp. 1-60.
- MATTSSON, B. & SONESSON, U. 2003. *Environmentally-Friendly Food Processing*. Boca Raton: Woodhead Publishing.
- MCADAMS, W. H. 1954. *Heat Transmission*. London: McGraw-Hill.
- MCDONALD, K. & SUN, D. W. 2000. Vacuum Cooling Technology for the Food Processing Industry: A Review. *Journal of Food Engineering*. **45**(2), pp. 55-65.
- MENTER, F. R. 1994. Two-Equation Eddy-Viscosity Turbulence Models for Engineering Applications. *AIAA Journal*. **32**(8), pp. 1598-1605.
- MIDDEN, T. M. 1995. Impingement Air Baking for Snack Foods. *Cereal Foods World*. **40**(8), pp. 532-535.
- MIRADE, P. S. & DAUDIN, J. D. 2000. A Numerical Study of the Airflow Patterns in a Sausage Dryer. *Drying Technology*. **18**(1-2), pp. 81-97.
- MIRADE, P. S., DAUDIN, J. D., DUCEPT, F., TRYSTRAM, G. & CLEMENT, J. 2004. Characterization and Cfd Modelling of Air Temperature and Velocity Profiles in an Industrial Biscuit Baking Tunnel Oven. *Food Research International*. **37**(10), pp. 1031-1039.
- MISTRY, H., GANAPATHI-SUBBU, DEY, S., BISHNOI, P. & CASTILLO, J. L. 2006. Modeling of Transient Natural Convection Heat Transfer in Electric Ovens. *Applied Thermal Engineering*. **26**(17-18), pp. 2448-2456.

- MONTEAU, J. Y. 2008. Estimation of Thermal Conductivity of Sandwich Bread Using an Inverse Method. *Journal of Food Engineering*. **85**(1), pp. 132-140.
- MOREIRA, R. G. 2002. Impingement Drying Applications to Foods. *In: 2002 IFT Annual Meeting & Food Expo, 16-19 June 2002, Anaheim, California*.
- MUJUMDAR, A. S. 2007. *Handbook of Industrial Drying*. Boca Raton: Taylor & Francis.
- NAVANEETHAKRISHNAN, P., SRINIVASAN, P. S. S. & DHANDAPANI, S. 2007. Heat Transfer and Heating Rate of Food Stuffs in Commercial Shop Ovens. *Sadhana*. **32**(5), pp. 535-544.
- NELLIS, G. & KLEIN, S. A. 2009. *Heat Transfer*. Cambridge: Cambridge University Press.
- NITIN, N. & KARWE, M. V. 2001. Heat Transfer Coefficient for Cookie Shaped Objects in a Hot Air Jet Impingement Oven. *Journal of Food Process Engineering*. **24**(1), pp. 51-69.
- NORRIS, J. R., ABBOTT, M. T. & DOBIE, M. 2002. High Performance Air Impingement/Microwave Cooking Systems. *In: 2002 IFT Annual Meeting & Food Expo, 16-19 June 2002, Anaheim, California*.
- NORTON, T. & SUN, D.-W. 2006. Computational Fluid Dynamics (Cfd) - an Effective and Efficient Design and Analysis Tool for the Food Industry: A Review. *Trends in Food Science & Technology*. **17**(11), pp. 600-620.
- NORTON, T. & SUN, D.-W. 2007. An Overview of Cfd Applications in the Food Industry. *In: SUN, D.-W., (ed.) Computational Fluid Dynamics in Food Processing*. Boca Raton: Taylor & Francis.
- O'DONOVAN, T. S. & MURRAY, D. B. 2007. Jet Impingement Heat Transfer - Part I: Mean and Root-Mean-Square Heat Transfer and Velocity Distributions. *International Journal of Heat and Mass Transfer*. **50**(17-18), pp. 3291-3301.
- OAKLEY, T. 2009. *Warburtons Limited*, Personal communication.
- OBBERKAMPF, W. L. & TRUCANO, T. G. 2002. Verification and Validation in Computational Fluid Dynamics. *Progress in Aerospace Sciences*. **38**(3), pp. 209-272.
- OLSSON, E. E. M., AHRNE, L. M. & TRÄGÅRDH, A. C. 2004. Heat Transfer from a Slot Air Jet Impinging on a Circular Cylinder. *Journal of Food Engineering*. **63**(4), pp. 393-401.
- OLSSON, E. E. M., AHRNE, L. M. & TRÄGÅRDH, A. C. 2005. Flow and Heat Transfer from Multiple Slot Air Jets Impinging on Circular Cylinders. *Journal of Food Engineering*. **67**(3), pp. 273-280.
- OLSSON, E. E. M. & TRÄGÅRDH, A. C. 2007. Cfd Modeling of Jet Impingement During Heating and Cooling of Foods. *In: SUN, D.-W., (ed.) Computational Fluid Dynamics in Food Processing*. Boca Raton: Taylor & Francis.
- OPENCFD LTD. 2012. *Openfoam - the Open Source Cfd Toolbox: User Guide*. Bracknell: OpenFOAM Foundation.

- OUSEGUI, A., MORESOLI, C., DOSTIE, M. & MARCOS, B. 2010. Porous Multiphase Approach for Baking Process - Explicit Formulation of Evaporation Rate. *Journal of Food Engineering*. **100**(3), pp. 535-544.
- OVADIA, D. Z. & WALKER, C. E. 1998. Impingement in Food Processing. *Food Technology*. **52**(4), pp. 46-50.
- OWEN, J. 2012. Passion for Artisan Bread Puts Wind in the Sails of Britain's Mills. *The Independent [online]* 13 May 2012. <http://www.independent.co.uk> [Accessed on: 30 October 2012].
- PARK, J. & MACKAY, S. 2003. *Practical Data Acquisition for Instrumentation and Control Systems*. Oxford: Elsevier.
- PATANKAR, S. V. & SPALDING, D. B. 1972. Calculation Procedure for Heat, Mass and Momentum-Transfer in Three-Dimensional Parabolic Flows. *International Journal of Heat and Mass Transfer*. **15**(10), pp. 1787-1806.
- PATON, J. B., KHATIR, Z., THOMPSON, H. M., KAPUR, N. & TOROPOV, V. V. 2011. Thermal Energy Management in the Bread-Baking Industry Using a System Modelling Approach. In: *Sustainable Thermal Energy Management International Conference (SusTEM 2011), 25-26 Oct 2011, Newcastle upon Tyne, UK*.
- PATON, J. B., KHATIR, Z., KAPUR, N., THOMPSON, H. M. & TOROPOV, V. V. 2012a. An Experimental and Numerical Investigation of Industrial Bread Proving. In: *2012 EFFoST Annual Meeting, 20-23 November 2012, Montpellier, France*.
- PATON, J. B., KHATIR, Z., THOMPSON, H. M., KAPUR, N. & TOROPOV, V. V. 2012b. Thermal Energy Management in the Bread Baking Industry Using a System Modelling Approach. *Applied Thermal Engineering*. DOI: 10.1016/j.applthermaleng.2012.03.036.
- PHILLIPS, B. 2011. *The 100 Biggest Grocery Retailers in Britain*. London: The Grocer.
- PIMENTEL, D. & PIMENTEL, M. H. 2008. *Food, Energy, and Society*. Boca Raton: CRC Press.
- POPE, S. B. 2000. *Turbulent Flows*. Cambridge: Cambridge University Press.
- PRICE, I. 2012. *Warburtons Limited*, Personal communication.
- PROBERT, D. & NEWBOROUGH, M. 1985. Designs, Thermal Performances and Other Factors Concerning Cooking Equipment and Associated Facilities. *Applied Energy*. **21**(2-3), pp. 81-222.
- PURLIS, E. & SALVADORI, V. O. 2009a. Bread Baking as a Moving Boundary Problem. Part 1: Mathematical Modelling. *Journal of Food Engineering*. **91**(3), pp. 428-433.
- PURLIS, E. & SALVADORI, V. O. 2009b. Bread Baking as a Moving Boundary Problem. Part 2: Model Validation and Numerical Simulation. *Journal of Food Engineering*. **91**(3), pp. 434-442.
- PURLIS, E. 2011. Bread Baking: Technological Considerations Based on Process Modelling and Simulation. *Journal of Food Engineering*. **103**(1), pp. 92-102.

REBITZER, G., EKVALL, T., FRISCHKNECHT, R., HUNKELER, D., NORRIS, G., RYDBERG, T., SCHMIDT, W. P., SUH, S., WEIDEMA, B. P. & PENNINGTON, D. W. 2004. Life Cycle Assessment: Part 1: Framework, Goal and Scope Definition, Inventory Analysis, and Applications. *Environment International*. **30**(5), pp. 701-720.

REVEDIN, A., ARANGUREN, B., BECATTINI, R., LONGO, L., MARCONI, E., LIPPI, M. M., SKAKUN, N., SINITSYN, A., SPIRIDONOVA, E. & SVOBODA, J. 2010. Thirty Thousand-Year-Old Evidence of Plant Food Processing. *Proceedings of the National Academy of Sciences of the United States of America*. **107**(44), pp. 18815-18819.

RIBOTTA, P. D., LEON, A. E. & AÑÓN, M. C. 2001. Effect of Freezing and Frozen Storage of Doughs on Bread Quality. *Journal of Agricultural and Food Chemistry*. **49**(2), pp. 913-918.

RICHARDSON, L. F. 1910. On the Approximate Arithmetical Solution by Finite Differences of Physical Problems Involving Differential Equations, with an Application to the Stresses in a Masonry Dam. *Philosophical Transactions of the Royal Society of London Series A - Containing Papers of a Mathematical or Physical Character*. **83**(563), pp. 335-336.

RICHARDSON, L. F. 1922. *Weather Prediction by Numerical Process*. Cambridge: Cambridge University Press.

ROACHE, P. J. 1994. Perspective: A Method for Uniform Reporting of Grid Refinement Studies. *Journal of Fluids Engineering*. **116**(3), pp. 405-413.

ROACHE, P. J. 1998. *Verification and Validation in Computational Science and Engineering*. Socorro: Hermosa.

ROBERTS, J. S., TONG, C. H. & LUND, D. B. 2002. Drying Kinetics and Time-Temperature Distribution of Pregelatinized Bread. *Journal of Food Science*. **67**(3), pp. 1080-1087.

ROGERS, G. F. C. & MAYHEW, Y. R. 1988. *Thermodynamic and Transport Properties of Fluids, Si Units*. Oxford: Blackwell.

ROHSENOW, W. M., HARTNETT, J. P. & CHO, Y. I. 1998. *Handbook of Heat Transfer*. London: McGraw-Hill.

ROSING, L. & NIELSEN, A. M. 2003. When a Hole Matters - the Story of the Hole in a Bread for French Hotdog. In: *Life Cycle Assessment in the Agri-food sector, 6-8 Oct 2003, Horsens, Denmark*.

RUSSELL, T. W. F., ROBINSON, A. S. & WAGNER, N. J. 2008. *Mass and Heat Transfer: Analysis of Mass Contactors and Heat Exchangers*. Cambridge: Cambridge University Press.

SABLANI, S. S., MARCOTTE, M., BAIK, O. D. & CASTAIGNE, F. 1998. Modeling of Simultaneous Heat and Water Transport in the Baking Process. *LWT - Food Science and Technology*. **31**(3), pp. 201-209.

SARKAR, A. & SINGH, R. P. 2004. Air Impingement Technology for Food Processing: Visualization Studies. *LWT - Food Science and Technology*. **37**(8), pp. 873-879.

SATO, H., MATSUMURA, T. & SHIBUKAWA, S. 1987. Apparent Heat Transfer in a Forced Convection Oven and Properties of Baked Food. *Journal of Food Science*. **52**(1), pp. 185-193.

SCOTT, G. & RICHARDSON, P. 1997. The Application of Computational Fluid Dynamics in the Food Industry. *Trends in Food Science & Technology*. **8**(4), pp. 119-124.

ŠERUGA, B., BUDŽAKI, S. & UGARČIĆ-HARDI, Ž. 2007. Individual Heat Transfer Modes During Baking of “Mlinici” Dough. *Agriculturae Conspectus Scientificus*. **72**(3), pp. 257-263.

SERWAY, R. A. & JEWETT, J. W. 2010. *Physics for Scientists and Engineers, Volume 1*. Pacific Grove: Brooks/Cole.

SHAH, P., CAMPBELL, G. M., MCKEE, S. L. & RIELLY, C. D. 1998. Proving of Bread Dough: Modelling the Growth of Individual Bubbles. *Food and Bioproducts Processing*. **76**(2), pp. 73-79.

SHIBUKAWA, S., SUGIYAMA, K. & YANO, T. 1989. Effects of Heat Transfer by Radiation and Convection on Browning of Cookies at Baking. *Journal of Food Science*. **54**(3), pp. 621-624.

SHIH, T. H., LIOU, W. W., SHABBIR, A., YANG, Z. G. & ZHU, J. 1995. A New K-E Eddy Viscosity Model for High Reynolds-Number Turbulent Flows. *Computers & Fluids*. **24**(3), pp. 227-238.

SØRENSEN, B. 2011. *Life-Cycle Analysis of Energy Systems: From Methodology to Applications*. Cambridge: RSC Publishing.

STAFFORD, J., WALSH, E. & EGAN, V. 2009. Characterizing Convective Heat Transfer Using Infrared Thermography and the Heated-Thin-Foil Technique. *Measurement Science & Technology*. **20**(10), pp. 1-11.

STARK, R. & JARVIS, P. 2009. Bioethanol from Sugar Beet and Horticultural Use of Surplus Process Heat. In: *Meeting of the International Fertiliser Society, 2 April 2009, London, UK*.

STEAR, C. A. 1990. *Handbook of Breadmaking Technology*. London: Elsevier.

STEPHAN, P. 1993. *Vdi Heat Atlas*. Dusseldorf: Springer.

SUMNU, S. G. & SAHIN, S. 2008. *Food Engineering Aspects of Baking Sweet Goods*. Boca Raton: CRC Press.

SUN, D.-W. 2007. *Computational Fluid Dynamics in Food Processing*. Boca Raton: Taylor & Francis.

TANNAHILL, R. 2002. *Food in History*. London: Broadway.

THE FEDERATION OF BAKERS 2010. Annual Report and List of Members 2010. London: The Federation of Bakers.

THERDTHAI, N., ZHOU, W. B. & ADAMCZAK, T. 2002. Optimisation of the Temperature Profile in Bread Baking. *Journal of Food Engineering*. **55**(1), pp. 41-48.

THERDTHAI, N., ZHOU, W. B. & ADAMCZAK, T. 2003. Two-Dimensional Cfd Modelling and Simulation of an Industrial Continuous Bread Baking Oven. *Journal of Food Engineering*. **60**(2), pp. 211-217.

THERDTHAI, N., ZHOU, W. B. & ADAMCZAK, T. 2004a. Three-Dimensional Cfd Modelling and Simulation of the Temperature Profiles and Airflow Patterns During a Continuous Industrial Baking Process. *Journal of Food Engineering*. **65**(4), pp. 599-608.

THERDTHAI, N., ZHOU, W. B. & ADAMCZAK, T. 2004b. The Development of an Anemometer for Industrial Bread Baking. *Journal of Food Engineering*. **63**(3), pp. 329-334.

THOM, A. 1933. The Flow Past Circular Cylinders at Low Speeds. *Proceedings of the Royal Society of London Series A - Containing Papers of a Mathematical and Physical Character*. **141**(844), pp. 651-669.

THOMPSON, J. F., SONI, B. K. & WEATHERILL, N. P. 1999. *Handbook of Grid Generation*. London: CRC Press.

THUMANN, A. & YOUNGER, W. J. 2003. *Handbook of Energy Audits*. Lilburn: Fairmont Press.

THUMANN, A. & MEHTA, D. P. 2008. *Handbook of Energy Engineering*. Lilburn: Fairmont Press.

TU, J., YEOH, G. H. & LIU, C. 2008. *Computational Fluid Dynamics: A Practical Approach*. Oxford: Butterworth-Heinemann.

TURNER, W. C. 1993. *Energy Management Handbook*. Lilburn: Fairmont Press.

UNKLESBAY, N., UNKLESBAY, K., NAHAISI, M. & KRAUSE, G. 1981. Thermal Conductivity of White Bread During Convective Heat Processing. *Journal of Food Science*. **47** pp. 249-259.

VERBOVEN, P., SCHEERLINCK, N., DE BAERDEMAEKER, J. & NICOLAI, B. M. 2000a. Computational Fluid Dynamics Modelling and Validation of the Isothermal Airflow in a Forced Convection Oven. *Journal of Food Engineering*. **43**(1), pp. 41-53.

VERBOVEN, P., SCHEERLINCK, N., DE BAERDEMAEKER, J. & NICOLAI, B. M. 2000b. Computational Fluid Dynamics Modelling and Validation of the Temperature Distribution in a Forced Convection Oven. *Journal of Food Engineering*. **43**(2), pp. 61-73.

VERSTEEG, H. K. & MALALASEKERA, W. 2007. *An Introduction to Computational Fluid Dynamics: The Finite Volume Method*. Harlow: Prentice Hall.

WANG, L. & SUN, D.-W. 2003. Recent Developments in Numerical Modelling of Heating and Cooling Processes in the Food Industry: A Review. *Trends in Food Science & Technology*. **14**(10), pp. 408-423.

WANG, L. J. & SUN, D. W. 2001. Rapid Cooling of Porous and Moisture Foods by Using Vacuum Cooling Technology. *Trends in Food Science & Technology*. **12**(5-6), pp. 174-184.

WARD, I. 2010. *Warburtons Limited*, Personal communication.

- WHITESIDE, R. L. 1982. Energy Use in the Baking Industry. *Bakers Digest*. **56**(4), pp. 30-34.
- WILCOX, D. C. 1988. Reassessment of the Scale-Determining Equation for Advanced Turbulence Models. *AIAA Journal*. **26**(11), pp. 1299-1310.
- WILLIAMSON, M. E. & WILSON, D. I. 2009. Development of an Improved Heating System for Industrial Tunnel Baking Ovens. *Journal of Food Engineering*. **91**(1), pp. 64-71.
- WIMBERGER, R. J. 1999. Convection Air Dryer Sizing and Section of Nozzle Design/ Spacing. In: *TAPPI Polymers, Laminations & Coatings Conference, 22-26 Aug 1999, Atlanta, GA*.
- WONG, S. Y., ZHOU, W. B. & HUA, J. S. 2007. Cfd Modeling of an Industrial Continuous Bread-Baking Process Involving U-Movement. *Journal of Food Engineering*. **78**(3), pp. 888-896.
- WU, H., JOUHARA, H., TASSOU, S. A. & KARAYIANNIS, T. G. 2010. Modelling of Energy Flows in Potato Crisp Frying Processes. In: *Sustainable Thermal Energy Management Conference (SusTEM2010), 3-4 Nov 2010, Newcastle, UK*.
- WU, H., JOUHARA, H., TASSOU, S. A. & KARAYIANNIS, T. G. 2012. Modelling of Energy Flows in Potato Crisp Frying Processes. *Applied Energy*. **89**(1), pp. 81-88.
- YAKHOT, V., ORSZAG, S. A., THANGAM, S., GATSKI, T. B. & SPEZIALE, C. G. 1992. Development of Turbulence Models for Shear Flows by a Double Expansion Technique. *Physics of Fluids a-Fluid Dynamics*. **4**(7), pp. 1510-1520.
- YANNIOTIS, S. 2008. *Solving Problems in Food Engineering*. New York: Springer.
- YASUNAGA, T., BUSHUK, W. & IRVINE, G. N. 1968. Gelatinization of Starch During Bread-Baking. *Cereal Chemistry*. **45**(3), pp. 269-279.
- ZANONI, B., PERI, C. & BRUNO, D. 1995a. Modeling of Starch Gelatinization Kinetics of Bread Crumb During Baking. *LWT - Food Science and Technology*. **28**(3), pp. 314-318.
- ZANONI, B., SCHIRALDI, A. & SIMONETTA, R. 1995b. Naive Model of Starch Gelatinization Kinetics. *Journal of Food Engineering*. **24**(1), pp. 25-33.
- ZHANG, J. & DATTA, A. K. 2006. Mathematical Modeling of Bread Baking Process. *Journal of Food Engineering*. **75**(1), pp. 78-89.
- ZHOU, W. & THERDTHAI, N. 2007. Three-Dimensional Modeling of a Continuous Industrial Baking Process. In: SUN, D.-W., (ed.) *Computational Fluid Dynamics in Food Processing*. Boca Raton: Taylor & Francis.
- ZIENKIEWICZ, O. C., TAYLOR, R. L. & ZHU, J. Z. 2005. *The Finite Element Method Its Basis and Fundamentals*. Oxford: Butterworth-Heinemann.
- ZUCKERMAN, N. & LIOR, N. 2006. Jet Impingement Heat Transfer: Physics, Correlations, and Numerical Modeling. In: GREENE, G. A., CHO, Y. I., HARTNETT, J. P. & BAR-COHEN, A., (eds.). *Advances in Heat Transfer Volume 39*. London: Elsevier.